PREPARATION AND CHARACTERIZATION OF AND INTRAMOLECULAR ELECTRON TRANSFER IN A PENTAAMMINERUTHENIUM DERIVATIVE OF *CANDIDA KRUSEI* CYTOCHROME *c*

Thesis by

Mary Selman

In Partial Fulfillment of the Requirements

for the Degree of

Doctor of Philosophy

California Institute of Technology

Pasadena, California

1989

(Submitted March 1, 1989)

Acknowledgments

First and foremost, I would like to thank my research advisor, Harry B. Gray, for his support and encouragement over these several years. I am especially grateful to him for allowing me to set my own pace and standards for the work presented here.

The collaboration of Cindy St. Clair in the initial stages of development of the FMOC amino acid analysis method is gratefully acknowledged. I would also like to thank Cindy, and many other women at Caltech, especially Emily Carter, Adel Naylor, and Kathy Kanes, for their friendship and encouragement. Adel also deserves mention for helping me understand the ins and outs of Biograf, and for proofreading much of this thesis.

I am grateful to Walther Ellis for introducing me to the techniques of electrochemistry.

Certain members of the support staff deserve special mention: I am indebted to Tom Dunn and Dave Malerba for their patience and expertise in answering numerous questions related to electronics and computers, respectively.

I would also like to thank my parents and friends, especially Bernhard, Monica, Susan, Keith, and Sunny and Jim for their encouragement over the years. I thank Tio Antonio and Tia Rebeca for their generous hospitality and love, and for providing us with some semblance of family in Southern California.

And finally, I thank my husband, Fernando. As a scientist, he has generously shared his knowledge of computers, programming, physics, mathematics, and electronics. As a friend, he has given me support,

encouragement, and love. Thanks, chum!

This work was supported by grants from the National Science Foundation. An Earle C. Anthony Graduate Fellowship for the 1982-1983 academic year is gratefully acknowledged.

Abstract

A semisynthetic binuclear metalloprotein has been prepared by appending the pentaammineruthenium moiety to histidine 39 of the cytochrome *c* from the yeast *Candida krusei.* The site of ruthenium binding was identified by peptide mapping. Spectroscopic and electrochemical properties of the derivative indicate the protein conformation is unperturbed by the modification. A preliminary (minimum) rate constant of $170s^{-1}$ has been determined for the intramolecular electron transfer from ruthenium(II) to iron(III), which occurs over a distance of at least 13Å (barring major conformational changes). Electrochemical studies indicate that this reaction should proceed with a driving force of ~170mV. The rate constant is an order of magnitude faster than that observed in horse heart cytochrome *c* for intramolecular electron transfer from pentaammineruthenium(II)(histidine 33) to iron(III) (over a similar distance, and with a similar driving force), suggesting a medium or orientation effect makes the *Candida* intramolecular electron transfer more favorable.

Table of Contents

Acknowledgments ii

Abstract iv

List of Figures vii

List of Tables xii

List of Abbreviations xiv

Chapter 1. Introduction 1

1. Introduction 2

1.1 Theoretical Background 4

1.2 Experimental Approaches to the Study of Electron Transfer 6

2. Covalent Labeling 10

2.1. The Experimental System 10

2.2. Results to Date from Covalent Labeling Experiments 16

2.3. Aim of this Project 17

3. Previous Investigations of Medium and Orientation Effects 26

Chapter 2. Preparation and Isolation of the Cytochrome Derivative 29

Materials and Instrumentation 30

Methods 32

Results 37

Chapter 3. Characterization of the Derivative 47

Materials and Instrumentation 48

Methods 53

Results 66

EPR Spectroscopy 66

NMR Spectroscopy 68

UV-visible Difference Spectroscopy 77

Peptide Mapping 80

Spectroelectrochemistry 90

Differential Pulse Polarography 98

Discussion 104

Chapter 4. Electron Transfer Studies 116

Materials and Instrumentation 117

Methods 120

Results and Discussion 124

Chapter 5. Discussion and Conclusion 140

Appendix 1. Amino Acid Analysis Method Development 156

Appendix 2. Tryptic Digestion of the Modified Derivative and Related Studies 184

Appendix 3. Spectroelectrochemical Data 195

Appendix 4. Problems with the Flash Photolysis Instrumentation 200

Appendix 5. Programs for Fitting Kinetic Data 209

Appendix 6. Characterization of the Second Modified Product 225

List of Figures

Chapter 1

Figure 1.1.	Energy diagram for photosynthesis	3
Figure 1.2.	Potential reactions of the $[A_5Ru(OH_2)]^{2+}$ complex with common amino acid side chains	11
Figure 1.3.	Cytochrome prosthetic group, protoporphyrin IX	19
Figure 1.4.	Cytochrome *c* prosthetic group (Biograf photo)	20
Figure 1.5.	Sequences of the cytochromes *c* from *C. krusei* and horse heart	22
Figure 1.6.	Histidine residues of interest for modification in *C. krusei* cytochrome *c*	24
Figure 1.7.	Cytochrome *c* fold	24

Chapter 2

Figure 2.1.	Elution profiles of commercial *C. krusei* cytochrome *c* from (a) Amberlite CG-50, and (b) CM-52	39
Figure 2.2.	Time analyses of the *C. krusei* cytochrome *c* modification reaction by polyacrylamide gel electrophoresis	42
Figure 2.3.	Chromatogram for the elution of the products of the reaction of pentaammineruthenium(II)aquo and *C. krusei* cytochrome *c* from CM-52	44
Figure 2.4.	Chromatogram for the analytical FPLC separation of the oxidized modification reaction mixture	46

Chapter 3

Figure 3.1.	Front and side view of an optically transparent thin layer spectroelectrochemistry cell	51
Figure 3.2.	Dual-jacketed electrochemical cell for differential pulse polarography	51
Figure 3.3.	Schematic representation of the role of $[A_5Rupy]^{2+/3+}$ as a redox mediator	59
Figure 3.4.	EPR spectra of native cytochrome *c*, $[A_5RuHis^{3+}]$, and modified cytochrome *c*	67

Figure 3.5.	NMR spectra of native and A_5Ru-modified *C. krusei* cytochrome *c*, δ6.5-9.5ppm	70
Figure 3.6.	Titrating resonances of native *C. krusei* ferricytochrome *c*	73
Figure 3.7.	NMR spectra of native and modified *C. krusei* cytochrome *c*, δ-38 to -22ppm	76
Figure 3.8.	Clarification of the discrepancy in histidine C-2 proton resonance chemical shifts	78
Figure 3.9.	UV-visible difference spectrum of A_5Ru-modified *C. krusei* cytochrome *c* minus native cytochrome *c*	79
Figure 3.10.	Peptides expected upon digestion of *C. krusei* cytochrome *c* by submaxillaris protease	81
Figure 3.11.	HPLC chromatograms of SMP peptides with 220nm detection	82
Figure 3.12.	HPLC chromatograms of SMP peptides with 300nm detection	85
Figure 3.13.	HPLC chromatogram of SMP peptides of ruthenium-modified derivative with 400nm detection	86
Figure 3.14.	UV-visible spectrum of ruthenium-containing peptide recovered from the SMP digest	87
Figure 3.15.	Family of visible spectra recorded during a spectroelectrochemistry experiment on native *C. krusei* cytochrome *c*, 24.4°C.	91
Figure 3.16.	Nernst plot for spectroelectrochemistry data on native *C. krusei* cytochrome *c*, 24.4°C	94
Figure 3.17.	Temperature dependence of the reduction potential of the iron site in native and A_5Ru-modified *C. krusei* cytochrome *c*	96
Figure 3.18.	DPP traces for native and A_5Ru-modified *C. krusei* cytochrome	100
Figure 3.19.	Temperature dependence of the ruthenium reduction potential in A_5Ru-*C. krusei* cytochrome *c*	102
Figure 3.20.	Residues which are potential ligands to pentaammineruthenium in *C. krusei* cytochrome *c*	106
Figure 3.21.	His26 hydrogen-bonding network	109

Figure 3.22. Local environments of histidine residues of interest in *C. krusei* and horse cytochromes *c* 112

Chapter 4

Figure 4.1. Schematic diagram of the flash photolysis instrument 119

Figure 4.2. Flow chart for kinetic data collection and fitting 125

Figure 4.3. Sequence of reactions initiated by a microsecond pulse of 450nm light in the electron transfer experiment 127

Figure 4.4. Stern-Volmer plot for the quenching of $[Ru(bpy)_3]^{2+*}$ by *C. krusei* cytochrome *c* 128

Figure 4.5. Postulated mechanism of action of Na_2EDTA in the flash photolysis experiment 130

Figure 4.6. Flash photolysis data for native *C. krusei* cytochrome *c* 133

Figure 4.7. Flash photolysis of modified *C. krusei* cytochrome *c* (112s) 135

Figure 4.8. Flash photolysis of modified *C. krusei* cytochrome *c* (12ms; fit to all data) 136

Figure 4.9. Flash photolysis of modified *C. krusei* cytochrome *c* (12ms; fit to 7-12ms range) 138

Chapter 5

Figure 5.1. Possible pathways of electron transfer in A_5Ru-(His39)-*C. krusei* cytochrome *c* 144

Figure 5.2. Reaction of imidazole with diethylpyrocarbonate 150

Figure 5.3. Sequences of cytochromes *c* from the yeasts *C. krusei* and *S. cerevisiae* 154

Appendix 1

Figure A1.1. Elution profile for the derivatized amino acid standard 168

Figure A1.2. Peak area as a function of the pH of the derivatization reaction 173

Figure A1.3. Area counts as a function of derivatization reaction time 175

Figure A1.4. Calibration data for FMOC-amino acid derivatives 178

Appendix 2

Figure A2.1. Peptides expected upon digestion of *C. krusei* cytochrome *c* with trypsin 186

Figure A2.2. UV-visible spectrum of a modified peptide recovered from a tryptic digest of A_5Ru(His39)-*C. krusei* cytochrome *c* 189

Figure A2.3. DPP traces for odd peptide recovered from A_5Ru(His39)-*C. krusei* cytochrome *c* tryptic digest and tyrosine 192

Appendix 4

Figure A4.1. Signal resulting from cessation of air flow cooling probe lamp 203

Figure A4.2. Relationship of output-to-bleeder chain current ratio and light intensity for a typical Hamamatsu photomultiplier tube 203

Figure A4.3. Signal resulting from flashing a blank sample, with detection at 549nm 205

Figure A4.4. Signal resulting from flashing a blank sample after the installation of capacitors in the PMT housing to maintain the voltage difference between the final dynodes 205

Figure A4.5. Signal resulting from flashing a blank sample using 450nm bandpass filters 206

Appendix 6

Figure A6.1. Chromatogram for the analytical FPLC elution of oxidized product 2 228

Figure A6.2. EPR spectra of $[A_5RuHis]Cl_3$, native *C. krusei* cytochrome *c*, A_5Ru(His39)-*C. krusei* cytochrome *c*, and the second A_5Ru-cytochrome modification product 229

Figure A6.3. NMR ^{1}H spectra for native, A_5Ru(His39)-modified, and A_5Ru-modified (product 2) *C. krusei* ferricytochromes *c*, δ6-10ppm 232

Figure A6.4. NMR ^{1}H spectra for native, A_5Ru(His39)-modified, and A_5Ru-modified (product 2) *C. krusei* ferricytochromes *c*, δ-22 to -38 ppm 233

Figure A6.5. UV-visible difference spectrum: A_5Ru-modified *C. krusei* cytochrome *c* (product 2) minus native *C. krusei* cytochrome *c* 234

List of Tables

Chapter 1

Table 1.1 Results of covalent labeling experiments to date (native prosthetic groups) 13

Chapter 2

Table 2.1. FPLC programs for analytical and preparative separation of the oxidized reaction mixture 38

Chapter 3

Table 3.1. Chemical shifts of titrating histidine C-2 protons 72

Table 3.2. Parameters for least-squares fit of NMR titration data 72

Table 3.3. Total amino acid analyses of native *C. krusei* cytochrome *c* SMP peptides 83

Table 3.4. Amino acid analysis of a ruthenium-containing peptide from the SMP digest of A_5Ru-*C. krusei* cytochrome *c* 89

Table 3.5. Reduction potentials of the iron site in native and A_5Ru-modified *C. krusei* cytochromes *c* 95

Table 3.6. Thermodynamic parameters for the reduction of the iron site in native and A_5Ru-modified *C. krusei* cytochrome *c* 97

Table 3.7. Differential pulse polarography data 101

Table 3.8. Thermodynamic parameters for the reduction of the ruthenium site in A_5Ru-*C. krusei* cytochrome *c* and other environments 103

Table 3.9. Surface areas of tuna cytochrome residue side chains which are potential pentaammineruthenium ligands in *C. krusei* cytochrome *c* 108

Chapter 4

Table 4.1. $[Ru(bpy)_3]^{2+*}$ lifetimes in the presence and absence of tryptophan 131

Table 4.2. Monoexponential fits to the kinetic data of modified cytochrome *c* 139

Appendix 1

Table A1.1.	Gradient program for FMOC-AA elution and column reequilibration	162
Table A1.2.	Retention times and standard deviations for FMOC amino acid derivatives	170
Table A1.3.	Area counts as a function of derivatization pH	172
Table A1.4.	Area counts as a function of derivatization reaction time	174
Table A1.5.	Calibration data - peak area as a function of concentration	179
Table A1.6.	Coefficients for calibration data analysis	180
Table A1.7.	Analyses of known peptides	182

Appendix 2

Table A2.1.	Gradient program for the separation of tryptic peptides	188

Appendix 3

Table A3.1.	Native *C. krusei* cytochrome *c* spectroelectrochemistry data	196
Table A3.2.	Fitted parameters to spectroelectrochemical Nernst plots for native *C. krusei* cytochrome *c*	197
Table A3.3.	Modified A_5Ru(His39)-*C. krusei* cytochrome *c* spectroelectrochemistry data	198
Table A3.4.	Fitted parameters to spectroelectrochemical Nernst plots for modified A_5Ru(His39)-*C. krusei* cytochrome *c*	199

List of Abbreviations

A_5Ru	pentaammineruthenium
ASCII	American standard code for information interchange
bpy	bipyridine
CM	carboxymethylcellulose
DEPC	diethylpyrocarbonate
DPP	differential pulse polarography
DSS	2,2'-dimethyl-2-silapentane-5-sulfonate
EDTA	ethylenediaminetetraacetic acid
FID	free induction decay
FMOC-Cl	9-fluorenylmethoxycarbonyl chloride
FPLC	fast protein liquid chromatography
FWHM	full width half maximum
HEPES	N-2-hydroxyethylpiperazine-N'-2-ethanesulfonic acid
HPLC	high performance liquid chromatography
ID	inner diameter
NaAc	sodium acetate buffer
NaP_i	sodium phosphate buffer
NHE	normal hydrogen electrode
OD	outer diameter
OTTLE	optically transparent thin layer electrochemistry
PAGE	polyacrylamide gel electrophoresis
PMT	photomultiplier tube
py	pyridine
SCE	saturated calomel electrode
SMP	submaxillaris protease

TEA	triethylamine
TEMED	N,N,N',N'-tetramethylethylenediamine
TFA	trifluoroacetic acid
TMK	trimethyllysine
TMS	tetramethylsilane
TPCK	L-1-tosylamido-2-phenylethyl chloromethyl ketone
Tris	tris(hydroxymethyl)aminomethane

Standard three letter abbreviations are used for the amino acids (*Pure Appl. Chem.* **56**, 595 (1984)).

CHAPTER 1

INTRODUCTION

1. Introduction

Electron transfer is the elementary reaction underlying such fundamental processes as respiration, photosynthesis, and nitrogen fixation.[1] Energy released in the transfer of electrons from one redox protein to another of higher reduction potential is harnessed in the production of adenosine triphosphate (ATP), which is then utilized for cellular processes (figure 1.1). Protein electron transfer is also of interest with regard to other biological processes, *e.g.*, protein[2] and nucleic acid[3] degradation caused by free radicals and ionizing radiation.

Photosynthetic and respiratory chain redox proteins generally contain one or more redox-active prosthetic groups, which may be metal ions (*e.g.*, copper in azurins and plastocyanins, iron in iron-sulfur proteins), metalloporphyrins (*e.g.*, cytochromes, chlorophyll), or organic moieties (*e.g.*, flavins).[4] Structural studies of numerous redox proteins have revealed that these prosthetic groups are often not exposed at the protein surface. This suggests that electrons must travel across large distances (*e.g.*, 10Å), barring large protein conformational changes, in order to migrate between redox centers.

It is of interest to understand those factors which govern electron transfer rates, as controlled charge separation is the key to

[1] (a) Hatefi, Y. *Ann. Rev. Biochem.* **54**, 1015 (1985); (b) Foyer, C. *Photosynthesis*, J. Wiley (New York), 1984.

[2] Henriksen, T., Melo, T., Saxebol, G. in *Free Radicals in Biology*, W. Pryor, ed., vol. 2, Academic Press (New York), 1976, p. 213.

[3] Myers, L. in *Free Radicals in Biology*, W. Pryor, ed., vol. 4, Academic Press (New York), 1980, p. 95.

[4] Dreyer, J. *Experentia* **40**, 653 (1984).

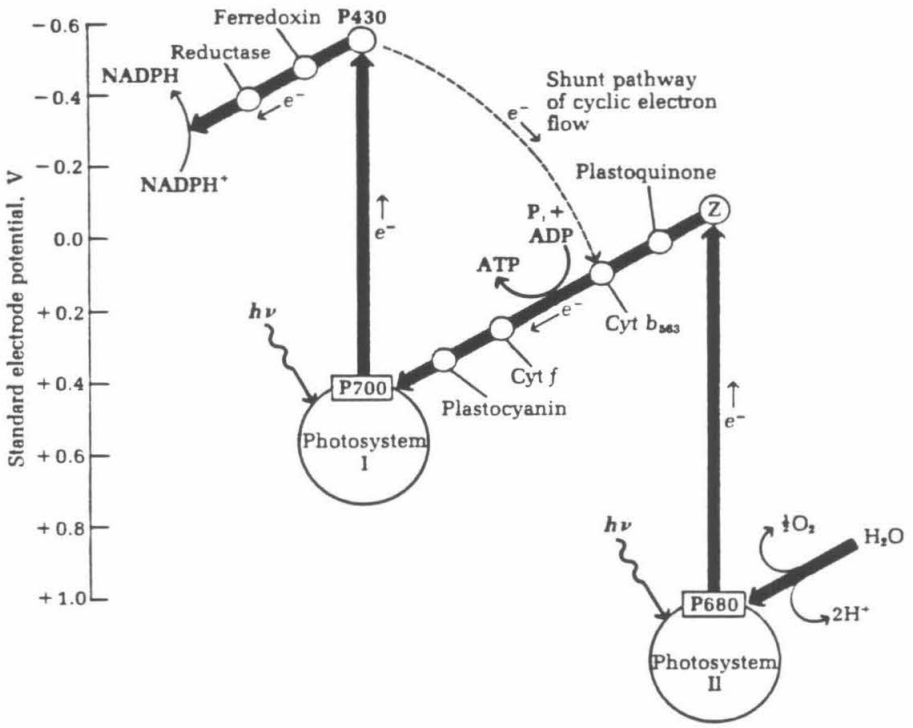

Figure 1.1. Energy diagram for photosynthesis. Absorption of light results in charge separation which leads to redox protein reduction. As electrons are transferred to proteins of higher reduction potential, the released energy is coupled to ATP production (figure 23-12 from A. Lehninger, *Principles of Biochemistry*, Worth Publishing Co. (New York), 1982, p. 657).

photochemical energy storage and utilization. Ultimately, a thorough understanding of Nature's exquisite control of the highly exoergic oxygen reduction reaction may provide guidelines for the design of devices to efficiently derive energy from exceedingly exothermic reactions.

1.1. Theoretical background

Marcus theory[5] has been reasonably successful in predicting the rates of intermolecular outer-sphere[6] electron transfer for many inorganic coordination complexes from self-exchange rate constants.[7] This theory predicts that rates of electron transfer will be dependent on the following factors:

-nuclear frequency, ν

-free energy of activation, ΔG^*

-donor and acceptor electronic coupling, β

-distance of donor-acceptor separation, d.

The relevant equation is

$$k_{et} = \nu \exp(-\beta d) \exp(-\Delta G^*/RT)$$

where k_{et} is the electron transfer rate. These influences can be classified into contributions of either an electronic ($\exp(-\beta d)$) or

[5] (a) Marcus, R. *J. Chem. Phys.* **43**, 679 (1965); (b) Marcus, R. *J. Chem. Phys.* **24**, 966 (1956).

[6] Outer sphere electron transfer is defined as electron transfer between complexes with no change in ligation, as opposed to inner sphere electron transfer, in which donor and acceptor are linked by a bridging ligand prior to electron transfer.

[7] (a) Siders, P., Marcus, R. *J. Amer. Chem. Soc.* **103**, 741 (1981); (b) Chou, M., Creutz, C., Sutin, N. *J. Amer. Chem. Soc.* **99**, 5615 (1977).

nuclear (ν exp($-\Delta G^*/RT$)) nature. The free energy of activation, ΔG^*, can be expressed in terms of the free energy of the reaction, ΔG^o, and the reorganization energy λ:

$$\Delta G^* = (\Delta G^o + \lambda)^2/4\lambda$$

The reorganization energy is that energy required for changes in geometry accompanying the redox process at the donor and acceptor sites (inner-sphere reorganization) and in the surrounding solvent molecules (outer-sphere reorganization). Several other theories have been developed which differ from Marcus theory in that they treat nuclear motion in a semi-classical or quantum mechanical manner, rather than in a classical sense.[8]

Predictions of Marcus theory and experimental results for biological systems have been compared in a review by Marcus and Sutin.[9] At present, there are insufficient data to determine whether this theory is applicable to biological electron transfer,[10] and if so, how the parameters ν, β, and λ will vary from protein to protein (or even within a single protein).

One outstanding question is the mechanism of the electron transfer, *i.e.*, the path through which the electron (or hole) travels. The electron may migrate through "space", in which case the coupling is expected to be related to the overlap of only the participating donor and acceptor orbitals, which is, of course, critically dependent on donor-

[8] DeVault, D. *Quantum-Mechanical Tunneling in Biological Systems*, Cambridge University Press (New York), 1984, and references therein.

[9] Marcus, R., Sutin, N. *Biochem. Biophys. Acta* **811**, 265 (1985).

[10] in terms of absolute rate predictions; some aspects of Marcus theory seem to apply (*vide infra*).

acceptor orientation. While the likely dependence of electron transfer rates on orientation is generally recognized, few theories have treated this variable explicitly.[11] Alternatively, the electron may travel through bonds, making use of orbitals of the intervening medium, in which case the electron transfer distance is likely to be greater than the distance of closest donor-acceptor approach. A combination of these two mechanisms, which are probably of different efficiency, are likely to be required in proteins. Hence, more than a single value of β would be necessary to describe the rate theoretically.

1.2 Experimental approaches to the study of electron transfer

Until recently, investigations of protein electron transfer were predominantly studies of bimolecular reactions, either between redox proteins or between a single metal complex and a single redox protein,[12] and investigations of this sort continue.[13] One difficulty

[11] (a) Cave, Robert J., "A Theoretical Model for Orientation Effects in Electron Transfer Reactions.", Ph.D. Dissertation, California Institute of Technology, 1986; (b) Cave, R., Siders, P., Marcus, R., *J. Phys. Chem.* **90**, 1436 (1986); (c) Cave, R., Klippenstein, S., Marcus, R. *J. Chem. Phys.* **84**, 3089 (1986); (d) Siders, P., Cave, R., Marcus, R. *J. Chem. Phys.*, **81**, 5613 (1984); (e) Siders, Paul, "Theory of Outer Sphere Electron Transfer Reactions.", Ph.D. Dissertation, California Institute of Technology, 1983, ch. 5.

[12] (a) Brunschwig, B., DeLaive, P., English, A., Goldberg, M., Gray, H., Mayo, S., Sutin, N. *Inorg. Chem.* **24**, 3743 (1985); (b) Mauk, A., Bordignon, E., Gray, H. *J. Amer. Chem. Soc.* **104**, 7654 (1982); (c) English, A., Lum, V., DeLaive, P., Gray, H. *J. Amer. Chem. Soc.* **104**, 870 (1982); (d) Schichman, S., Gray, H. *J. Amer. Chem. Soc.* **103**, 7794 (1981); (e) McArdle, J., Yocom, K., Gray, H. *J. Amer. Chem. Soc.* **99**, 4141 (1977); (f) Wherland, S., Gray, H. *Proc. Natl. Acad. Sci.* **73**, 2950 (1976); (g) Coyle, C., Gray, H. *Biochem. Biophys. Res. Comm.*, **73**, 1122 (1976); (h) McArdle, J., Gray, H., Creutz, C., Sutin, N. *J. Amer. Chem. Soc.* **96**, 5737 (1974).

[13] (a) Reid, L., Dalvit, G., Wright, C., Saltman, P. *Biochemistry* **26**, 7102 (1987); (b) McGinnis, J., Sinclair-Day, J., Sykes, A., Powls,

encountered in these studies lies in defining the nature of the complex(es) in which the electron transfer event takes place. Evidence has recently been obtained which suggests that several possible orientations of a single protein pair, differing in subtle ways, may result in electron transfer (as opposed to there being one unique orientation).[14] In the case of small molecule-protein electron transfer, there may be several sites of interaction, and some experiments have suggested that the ligands of metal complexes may intercalate into the protein structure, making definition of the electron transfer distance difficult.[15]

To avoid the difficulties of bimolecular reactions, researchers have resorted to using more well-defined donor-acceptor complexes, particularly those involving covalent linkage of the donor and acceptor.[16] Numerous organic model systems have been synthesized with various donors, acceptors, and bridges.[17] To evaluate amino acids as mediators of electron transport, inorganic complexes bridged by peptides have also been synthesized, but those containing two or more amino acid residues are sufficiently flexible to allow close approach of the donor and acceptor, and direct outer-sphere electron transfer.[18] Poly-

R., Moore, J., Wright, P. *Inorg. Chem.* **27**, 2306 (1988).

14 Poulos, T., Sheriff, S., Howard, A. *J. Biol. Chem.* **262**, 13881 (1987).

15 Mauk, A., Scott, R., Gray, H. *J. Amer. Chem. Soc.* **102**, 4360 (1980).

16 (a) Closs, G., Miller, J. *Science* **240**, 440 (1988); (b) Scott, R., Mauk, A., Gray, H. *J. Chem. Ed.* **62**, 932 (1985).

17 (a) Miller, J., Calceterra, L., Closs, G. *J. Amer. Chem. Soc.* **106**, 3047 (1984); (b) Joran, A., Leland, B., Geller, G., Hopfield, J., Dervan, P. *J. Amer. Chem. Soc.* **106**, 6090 (1984).

proline isomerization is sufficiently slow to allow measurement of fast intramolecular electron transfer in these complexes (in an extended conformation) under conditions of high driving force,[19] but such experiments do not permit the study of medium effects. Electron transfer has also been studied in bimetallic complexes with other types of bridges.[20]

Another approach has been to work with redox protein partners, *i.e.*, proteins between which electron transfer occurs *in vivo*, or other pairs of redox proteins (nonphysiological) whose interactions have been modeled and/or defined experimentally.[21]

Yet another tack has been taken by Hoffman *et al.* in the preparation of "hybrid hemoglobins", where zinc or magnesium is substituted for iron in either hemoglobin subunit, and the product reconstituted with the other native subunit to study photoinduced intramolecular electron transfer.[22] Because the donor and acceptor sites are fixed,

[18] (a) Isied, S., Vassilian, A., Magnuson, R., Schwarz, H. *J. Amer. Chem. Soc.* **107**, 7432 (1985); (b) Isied, S., Vassilian, A. *J. Amer. Chem. Soc.* **106**, 1732 (1984); (c) Isied, S., Vassilian, A. *J. Amer. Chem. Soc.* **106**, 1726 (1984).

[19] By high driving force is meant a reaction which is strongly favored thermodynamically.

[20] (a) Kendrick Geno, M., Dawson, J. *Inorg. Chem.* **24**, 1731 (1985); (b) Anderes, B., Lavallee, D. *Inorg. Chem.* **22**, 2665 (1983).

[21] (a) Liang, N., Kang, C., Ho, P., Margoliash, E., Hoffman, B. *J. Amer. Chem. Soc.* **108**, 4665 (1986); (b) Cheung, E., Taylor, K., Kornblatt, J., English, A., McLendon, G., Miller, J. *Proc. Natl. Acad. Sci.* **83**, 1330 (1986); (c) Simolo, K., McLendon, G., Mauk, M., Mauk, A. *J. Amer. Chem. Soc.* **106**, 5012 (1984).

[22] (a) Natan, M., Hoffman, B. Book of Abstracts, 196th American Chemical Society National Meeting, Inorganic Abstract #357, Los Angeles, CA, September 25-30, 1988; (b) Peterson-Kennedy, S., McGourty, J., Kalweit, J., Hoffman, B. *J. Amer. Chem. Soc.* **108**, 1739 (1986); (c) Peterson-Kennedy, S., McGourty, J., Hoffman, B. *J. Amer. Chem. Soc.*

this native hemoglobin system does not provide a means of studying orientation and medium effects.[23] Metal-substituted porphyrin systems introduce uncertainty with regard to protein structure, as the substitution may involve changes in ligation and secondary effects. Also, the electron transfer distance is uncertain, not only because of possible perturbations in the polypeptide chain, but also because the extent of electron delocalization is often unknown for radical cation porphyrins.[24] Systems involving excited state or high driving force electron transfer may involve different mechanisms of electron transfer not accessible in reactions of low driving force, *e.g.*, aromatic moiety participation, and it is believed that the absolute redox level of the transferring electron may affect the donor-acceptor coupling.[25] One great advantage of these systems is the ability to study intramolecular electron transfer in the solid state, *i.e.*, at subzero temperatures, as initiation of the reaction does not involve any bimolecular process.

Finally, single-site metalloproteins have been covalently modified with a single organic[26] or inorganic moiety, which then serves as the counterpart of the prosthetic group in forming a donor-acceptor

106, 5010 (1984); (d) McGourty, J., Blough, N., Hoffman, B. *J. Amer. Chem. Soc.* **105**, 4470 (1983).

[23] Site-directed mutagenesis would be one way to overcome this problem, and has been demonstrated in the β chain of human hemoglobin. Nagai, K., Perutz, M., Poyart, C. *Philos. Trans. R. Soc. London A*, **317**, 443 (1986).

[24] Atamian, M., Wagner, R., Lindsey, J., Bocian, D. *Inorg. Chem.* **27**, 1510 (1988).

[25] Beratan, D. *J. Amer. Chem. Soc.* **108**, 4321 (1986).

[26] Faraggi, M., Klapper, M. *J. Amer. Chem. Soc.* **110**, 5753 (1988).

pair. It is a modification of the latter type which is the basis of this work.

2. Covalent Labeling

2.1 The experimental system

The approach taken in this work involves the covalent binding of an inert ruthenium complex to a defined amino acid side chain of a well-characterized single-site metalloprotein, to create a donor-acceptor complex bridged by a known medium at a defined distance and orientation. Thermodynamic parameters, which are expected to be similar to those of biological electron transfer reactions, can be determined from electrochemical studies of the metal sites.

Aquopentaammineruthenium(II), $[A_5Ru(OH_2)]^{2+}$, is known from model studies to react with imidazole,[27] thiols,[28] and thioethers,[29] the functional moieties of the side chains of the amino acids histidine, cysteine, and methionine, respectively (see figure 1.2). Cysteine is a rare residue in globular proteins of single polypeptide chains, while methionine is more frequently encountered, but it is often found in the protein interior. Modification of these amino acids is undesirable, as the pentaammineruthenium complexes are rather labile.[28,29] The histidine complex of pentaammineruthenium is expected to be inert in both the +2 and +3 oxidation states.[27] Carboxylato- complexes of

[27] Sundberg, R., Bryan, R., Taylor, I., Taube, H. *J. Amer. Chem. Soc.* **96**, 381 (1974).

[28] Kuehn, C., Taube, H. *J. Amer. Chem. Soc.* **98**, 689 (1976).

[29] Stein, C., Taube, H. *Inorg. Chem.* **18**, 1168 (1979).

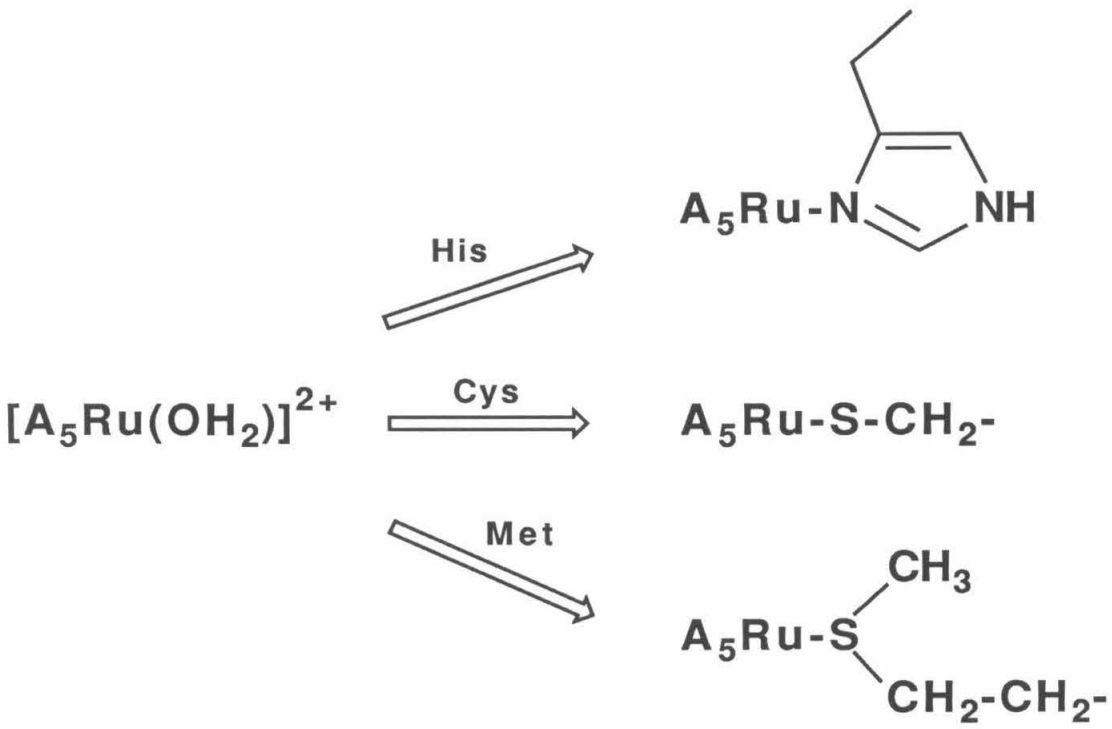

Figure 1.2. Potential reactions of the aquopentaammineruthenium(II) complex with common amino acid side chains.

pentaammineruthenium(III) are also known, but neither their synthesis nor stability at neutral pH has been demonstrated.[30] Reaction with lysine to form hexammine complexes can be discouraged by the appropriate choice of reaction pH.

Modification of proteins by the pentaammineruthenium moiety was first demonstrated with ribonuclease;[31] the chromophore was utilized to monitor conformational changes,[32] to aid in the assignment of NMR resonances,[33] and to perform distance measurements by fluorescence energy transfer.[34]

Proteins in which electron transfer has been studied to date (table 1.1) using this procedure include sperm whale[35] and human[36] myoglobin, horse heart cytochrome *c*,[37] *Pseudomonas aeruginosa* azurin,[38]

[30] Stritar, J., Taube, H. *Inorg. Chem.* **8**, 2281 (1969).

[31] Matthews, C., Erickson, P., Van Vliet, D., Petersheim, M. *J. Am. Chem. Soc.* **100**, 2260 (1978).

[32] Matthews, C., Erickson, P., Froebe, C. *Biochim. Biophys. Acta* **624**, 499 (1980).

[33] Matthews, C., Recchia, J., Froebe, C. *Anal. Biochem.* **112**, 329 (1981).

[34] Recchia, J., Matthews, C., Rhee, M., Horrocks, W. *Biochim. Biophys. Acta* **702**, 105 (1982).

[35] (a) Cowan, J., Gray, H. *Chem. Scripta* **28A**, 21 (1988); (b) Karas, J., Lieber, C., Gray, H. *J. Amer. Chem. Soc.* **110**, 599 (1988); (c) Crutchley, R., Ellis, W., Gray, H. in *Frontiers in Bioinorganic Chemistry*, A. Xavier, ed., VCH Verlagsgesellschaft (Weinheim, Fed. Rep. Germ.), 1986, p. 679; (d) Crutchley, R., Ellis, W., Gray, H. *J. Am. Chem. Soc.* **107**, 5002 (1985).

[36] Zewert, T., unpublished

[37] (a) Elias, H., Chou, M., Winkler, J. *J. Amer. Chem. Soc.* **110**, 429 (1988); (b) Bechtold, R., Kuehn, C., Lepre, C., Isied, S. *Nature* **322**, 286 (1986); (c) Bechtold, R., Gardineer, M., Kazmi, A., van Hemelryck, B., Isied, S. *J. Phys. Chem.* **90**, 3800 (1986); (d) Nocera, D., Winkler, J., Yocom, K., Bordignon, E., Gray, H. *J. Amer. Chem.*

Table 1.1. Results of covalent labeling experiments to date (native prosthetic groups)[a]

Protein	Species	His	Label[b]	Prosthetic Group	ΔE^{o}(mV)	d(Å)	$k(s^{-1})$	ref.
myoglobin	sperm whale[c]	48	(D) A_5Ru^{2+}	Fe(heme)	-20	12	0.019 (0.002)	g
	"	"	(A) A_5Ru^{3+}	"	20	"	0.041(0.003)	g
	"	"	(A) A_4pyRu^{3+}	"	275	"	2.5(0.5)	h
cytochrome *c*	horse heart	33	(D) A_5Ru^{2+}	"	170	11.8	30(3)	i
	"	"	(A) A_4pyRu^{3+}	"	~90-100	"	2[e]	j
	"	"	(A) A_4isnRu^{3+}	"	~160	"	11[e]	j
	C. krusei	39	(D) A_5Ru^{2+}	"	170	~13.0	>170[e]	k
cyt. c_{551}	*P. stutzeri*	47	"	"	~200[f]	7.9	13(2)	l
azurin	*P. aeruginosa*	83	"	Cu	280	11.8	1.9(0.4)	m
	"	"	"	"	"	"	2.5(0.8)	n

Table 1.1 continued

Protein	Species	His	Label	Prosthetic Group	ΔE^{o}(mV)	d(Å)	$k(s^{-1})$	ref.
plastocyanin	*A. variabilis*	59	(D) A_5Ru^{2+}	Cu	~260[f]	~11.9	0.024(0.058)	l, n
	S. obliquus	"	"	"	~300[f]	10-12	0.04 (0.22)	l, n
HiPIP[d]	*C. vinosum*	20	"	4Fe-4S	258(7)	9.2	14(2)[e]	o
	"	42	"	"	289(7)	6.9	14(2)[e]	o
	"	"	"	"	270[f]	7.9	18	p

a. only 1:1 (Ru:M) derivatives are included;

b. D or A preceding label indicates whether electron donor or acceptor; py=pyridyl, isn=isonicotinamide;

c. His18-, His112-, and His116-A_5Ru myoglobin derivatives have been prepared. No electron transfer is observed at room temperature for these systems. Distances are in the 19-22Å range. Driving force is expected to be similar to that of the His48 derivative.

d. HiPIP = high potential iron-sulfur protein

e. tentative; measured under conditions described in appendix 4

f. assuming a reduction potential of 80mV for the pentaammineruthenium histidine

g. Crutchley, R., Ellis, W., Gray, H. *J. Amer. Chem. Soc.* **110**, 599 (1988).

h. Karas, J., "Long Range Electron Transfer in Ruthenium-Labelled Myoglobin.", Ph.D. Dissertation, California Institute of Technology (1989).

i. Nocera, D., Winkler, J., Yocom, K., Bordignon, E., Gray, H. *J. Amer. Chem. Soc.* **106**, 5145 (1984).

j. Meade, T., unpublished results
k. this work
l. Osvath, P., Salmon, G., Sykes, A. *J. Amer. Chem. Soc.* **110**, 7114 (1988).
m. Kostic, N., Margalit, R., Che, C., Gray, H. *J. Amer. Chem. Soc.* **105**, 7765 (1983).
n. Jackman, M., McGinnis, J., Powls, R., Salmon, G., Sykes, A. *J. Amer. Chem. Soc.* **110**, 5880 (1988).
o. Cowan, J., unpublished results
p. Jackman, M., Lim, M.-C., Salmon, G., Sykes, A. *J.C.S. Chem. Comm.* 179 (1988).

two algal plastocyanins,[39] *Rhus vernicifera* stellacyanin,[40] and the high potential iron-sulfur protein (HiPIP) from *Chromatium vinosum.*[41] In addition to the results presented in table 1.1, many studies have been done with the same modifications using nonnative, photoactive prosthetic groups.

2.2 Results to date from covalent labeling experiments

Studies of intramolecular electron transfer in ruthenium-modified proteins have yielded some important results. Results from penta-ammineruthenium-modified horse heart cytochrome *c* were the first to demonstrate that electron transfer can occur over large distances at a measurable rate and biologically relevant driving force. Rates of electron transfer in zinc-substituted ruthenium-modified sperm whale myoglobin derivatives strongly support the view of electron transfer as occurring by a "through space" rather than a "through bond" pathway,[42]

Soc. **106**, 5145 (1984); (e) Isied, S., Kuehn, C., Worosila, G. *J. Amer. Chem. Soc.* **106**, 1722 (1984); (f) Yocom, K., Winkler, J., Nocera, D., Bordignon, E., Gray, H. *Chem. Scripta* **21**, 29 (1983); (g) Isied, S., Worosila, G., Atherton, S. *J. Amer. Chem. Soc.* **104**, 7659 (1982); (h) Yocom, K., Shelton, J. B., Shelton, J. R., Schroeder, W., Worosila, G., Isied, S., Bordignon, E., Gray, H. *Proc. Natl. Acad. Sci.* **79**, 7052 (1982).

38 (a) Margalit, R., Kostić, N., Che, C.-M., Blair, D., Chiang, H., Pecht, I., Shelton, J. B., Shelton, J. R., Schroeder, W., Gray, H. *Proc. Natl. Acad. Sci.* **81**, 6554 (1984); (b) Kostić, N., Margalit, R., Che, C.-M., Gray, H. *J. Amer. Chem. Soc.* **105**, 7765 (1983).

39 Jackman, M., McGinnis, J., Powls, R., Salmon, G., Sykes, A. *J. Amer. Chem. Soc.* **110**, 5880 (1988).

40 Farver, O., Pecht, I., submitted for publication

41 Jackman, M., Lim, M., Salmon, G., Sykes, A. *J.C.S. Chem. Comm.* 179 (1988).

42 By "through space" it is not meant without orbital participation,

and have provided an estimate of 0.9Å^{-1} for β, assuming an exponential distance dependence of the rates.[43]

Using two derivatives of sperm whale myoglobin modified at His48, it was demonstrated that the driving force dependence of electron transfer rates predicted by Marcus theory is obeyed in proteins.[44] More extensive driving force dependence curves have been obtained with data on metal-substituted A_5RuHis48 sperm whale myoglobin[45] and zinc-substituted ruthenium-modified His33 horse heart cytochrome *c*[46] derivatives. The rates exhibit the predicted dependence on driving force, but the "inverted region" has yet to be found in these systems.[47]

2.3 Aim of this project

In this project, the modification of yeast cytochrome *c* was undertaken to investigate medium and orientation effects on electron

but rather a relatively direct (*i.e.*, shortest distance) pathway. "Through bond" is used here to denote participation of all residues as they occur in the peptide chain between the modified histidine and and the point of ligation or covalent attachment of the prosthetic group.

43 (a) Axup, A., Albin, M., Mayo, S., Crutchley, R., Gray, H. *J. Amer. Chem. Soc.* **110**, 435 (1988); (b) Axup, Andrew W. "Laser Flash Spectroscopy of Zinc/Ruthenium Myoglobins: An Investigation of Distance and Medium Effects of Photoinduced Long-Range Intraprotein Electron Transfers.", Ph.D. Dissertation, California Institute of Technology, 1987.

44 Karas, J., Lieber, C., Gray, H. *J. Amer. Chem. Soc.* **110**, 599 (1988).

45 Cowan, J., Gray, H., *Chem. Scripta* **28A**, 21 (1988).

46 Meade, T., Gray, H., Winkler, J., unpublished.

47 The "inverted region" is that regime in which electron transfer rates are predicted by Marcus theory to decrease with increasing exothermicity, *i.e.*, $-\Delta G^{o} > \lambda$.

transfer rates.

Cytochrome *c* is a member of the respiratory chain, and is the protein responsible for the reduction of cytochrome *c* oxidase, the terminal electron transfer protein and the enzyme which effects the reduction of oxygen to water. Studies of long-range electron transfer involving cytochrome *c* have recently been reviewed by Pielak *et al.*[48]

Cytochromes *c* are monomeric proteins of 103-111 residues, containing a single protoporphyrin IX heme per molecule. The prosthetic group is covalently bound at the 1-vinyl positions via thioether linkages formed by cysteine residues 14 and 17 (figures 1.3 and 1.4). His18 and Met80 serve as ligands in both the 2+ and 3+ oxidation states in the pH 4-8 range, resulting in a low-spin electronic configuration. The structural aspects of cytochromes have been reviewed.[49]

Cytochromes from the yeasts *Saccharomyces cerevisiae* and *Candida krusei* both have histidine residues at positions 33 and 39.[50] Horse heart cytochrome c has been modified with the pentaammineruthenium(III) moiety at His33, and an intramolecular electron transfer rate of $30s^{-1}$ has been observed for this derivative (the horse protein lacks histidine at position 39).[37d] A comparison of this rate with that of a

[48] Pielak, G., Concar, D., Moore, G., Williams, R. *Protein Eng.* **1**, 83 (1987).

[49] (a) Mathews, F., *Prog. Biophys. Molec. Biol.* **45**, 1 (1985); (b) Timkovich, R. in *The Porphyrins*, D. Dolphin, ed., vol. 7, Biochemistry, part B, Academic Press (San Francisco), 1979, p. 241; (c) Dickerson, R., Timkovich, R. in *The Enzymes*, P. Boyer, ed., vol. XI, part A, 3rd ed., Academic Press (New York), 1975.

[50] numbering used is that based on the horse heart cytochrome sequence

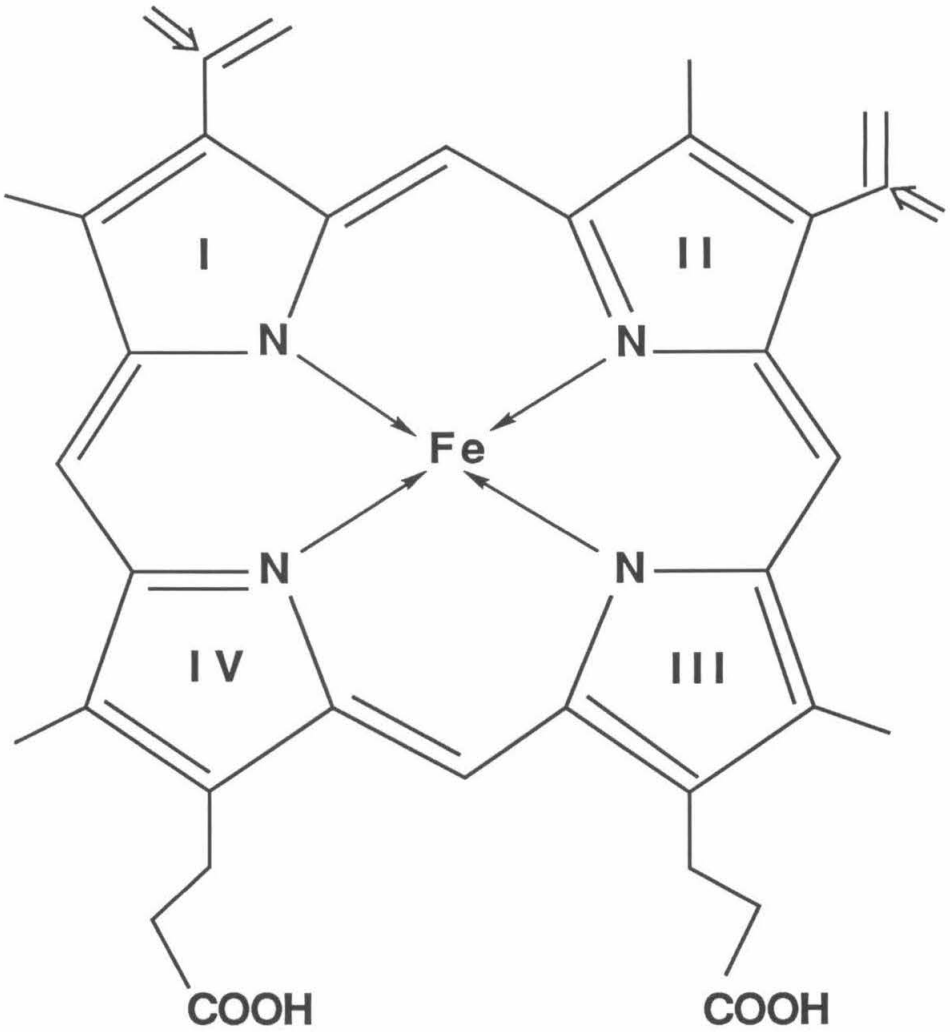

Figure 1.3. Cytochrome prosthetic group, protoporphyrin IX. Vinyl side chains are actually saturated, and form thioether linkages with Cys14 and Cys17 side chains (at the 1 positions, indicated by the arrows). The iron is ligated by the protein residues His18 and Met80 (not shown).

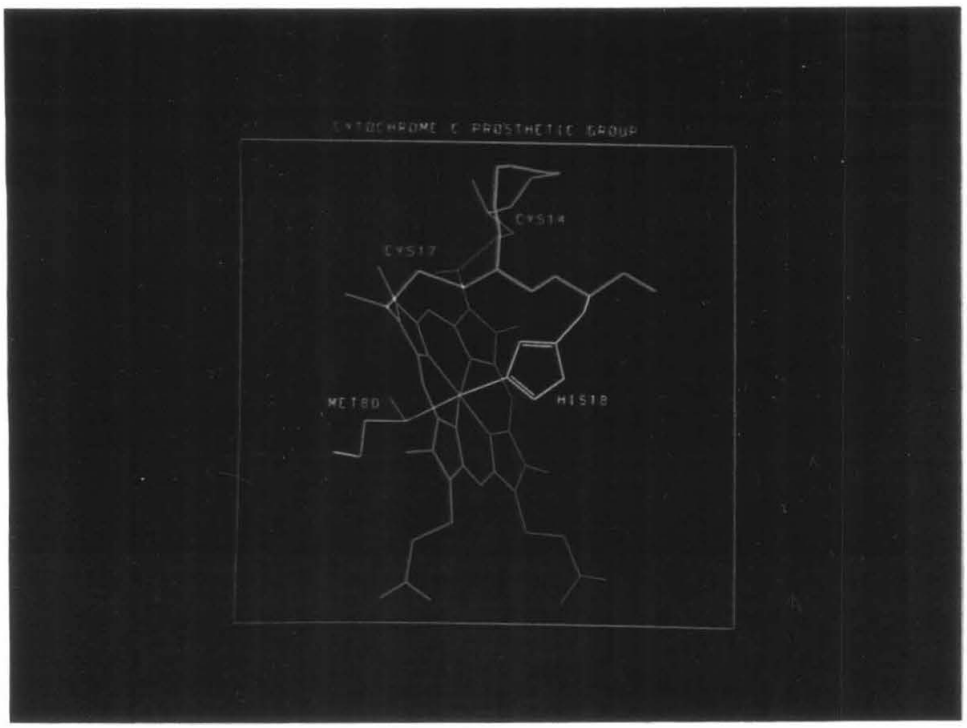

Figure 1.4. The cytochrome *c* prosthetic group is a protoporphyrin IX (red) with a central iron ion. The polypeptide anchors the prosthetic group by both ligation to the iron via His18 and Met80 (yellow), and by bonds to the 1-vinyl side chains via the Cys14 and Cys17 (green) side chains.

yeast cytochrome *c*, singly-modified at this same residue, might reveal medium dependence, as the proteins are ~50% identical in amino acid sequence (see figure 1.5). A second derivative of a yeast cytochrome, singly-modified at His39, might allow for comment on the role of donor-acceptor orientation in governing electron transfer rates, as the two histidines are in dramatically different orientations with respect to the heme. His33 lies ~11.7Å in front of the His18-ligated face of the heme,[51] while His39 is ~13Å below the heme edge, in the plane of the porphyrin ring (see figure 1.6).[52] Medium effects might be expected to be similar, as the intervening protein (in a through space pathway) contains no aromatic residues in both cases.

Initial work was begun on the cytochrome *c* from *S. cerevisiae*, as its gene has been cloned[53] and mutagenesis experiments (to selectively delete and insert histidine residues) were planned. However, the presence of a cysteine residue introduced complications, *e.g.*, dimerization, and commercial supplies of the protein were unreliable. The work reported here was done exclusively on the *Candida* cytochrome.

Although a crystal structure of the *Candida* cytochrome has not been determined, that of the *iso-1* cytochrome from *S. cerevisiae*[54] con-

[51] The triad of the Cα of residue 33, the heme iron atom, and the pyrrole ring IV nitrogen (the nearest porphyrin atom) form an angle of 51.7° in the reduced tuna cytochrome crystal structure.

[52] distances are measured from the C_γ of the residue to the heme or ligand atom of closest approach; there is some uncertainty as to what distance to consider, but the heme is generally thought of as an extended donor/acceptor due to mixing of the porphyrin molecular orbitals with the iron d orbitals.

[53] Montgomery, D., Hall, B., Gillam, S., Smith, M. *Cell* **14**, 673 (1978).

[54] Louie, G., Hutcheon, W., Brayer, G. *J. Mol. Biol.* **199**, 295 (1988).

```
                                1                                   10
Pro-Ala-Pro-Phe-Glu-Gln-Gly-Ser-Ala-Lys-Lys-Gly-Ala-Thr-Leu-Phe-
                    acetyl-   -Asp-Val-Glu-          -Lys -Lys- Ile-

                                           20
Lys-Thr-Arg-Cys-Ala-Gln-Cys-His-Thr-Ile-Glu-Ala-Gly-Gly-Pro-His-
Val- Gln - Lys-                          -Val-    -Lys-        -Lys-

              30                                            40
Lys-Val-Gly-Pro-Asn-Leu-His-Gly-Ile-Phe-Ser-Arg-His-Ser-Gly-Gln-
   -Thr-                          -Leu-   -Gly-    -Lys-Thr-

                                50
Ala-Glu-Gly-Tyr-Ser-Tyr-Thr-Asp-Ala-Asn-Lys-Arg-Ala-Gly-Val-Glu-
   -Pro-    -Phe -Thr-                        -Asn- Lys-      -Ile - Thr-

    60                                                  70
Trp-Ala-Glu-Pro-Thr-Met-Ser-Asp-Tyr-Leu-Glu-Asn-Pro-TMK-Lys-
   -Lys-    -Glu-    -Leu- Met-Glu-                      -Lys-

                           80
Tyr-Ile-Pro-Gly-Thr-Lys-Met-Ala-Phe-Gly-Gly-Leu-Lys-Lys-Ala-Lys-
                          -Ile-    -Ala-    -Ile-          -Lys-Thr-

 90                                          100
Asp-Arg-Asn-Asp-Leu-Val-Thr-Tyr-Met-Leu-Glu-Ala-Ser-Lys
Glu-     -Glu-          -Ile- Ala-     -Leu -Lys- Lys-    -Thr-Asn-Glu
```

Figure 1.5. Sequences of the cytochromes *c* from ***Candida krusei***[a] and horse heart[b] (the horse heart residues are identical to those of yeast unless specified). The residue numbers are assigned according to the horse sequence. The two proteins have 59 identical residues; approximately half of the 44 substitutions are conservative.

a. Lederer, F. *Eur. J. Biochem.* **31,** 144 (1972); Narita, K., Titani, K. *J. Biochem.* **63**, 226 (1968).
b. Margoliash, E., Smith, E., Kreil, G., Tuppy, H. *Nature* **192**, 1125 (1962).

Figure 1.6. Histidine residues (yellow) of interest for modification in *C. krusei* cytochrome *c*. His33 is located at 11.7Å from the heme (red), as measured from the C_γ atom to the N_δ of His18. His 39 is located at 13.0Å from the heme, as measured from the C_γ atom to the C atom of pyrrole ring IV to which the propionic acid is bound.

Figure 1.7. The cytochrome *c* fold. The polypeptide backbone $(\text{-N-C-C-})_n$ is shown here in blue. Cytochrome *c* is a globular protein with no β-sheet, and several stretches of α-helix.

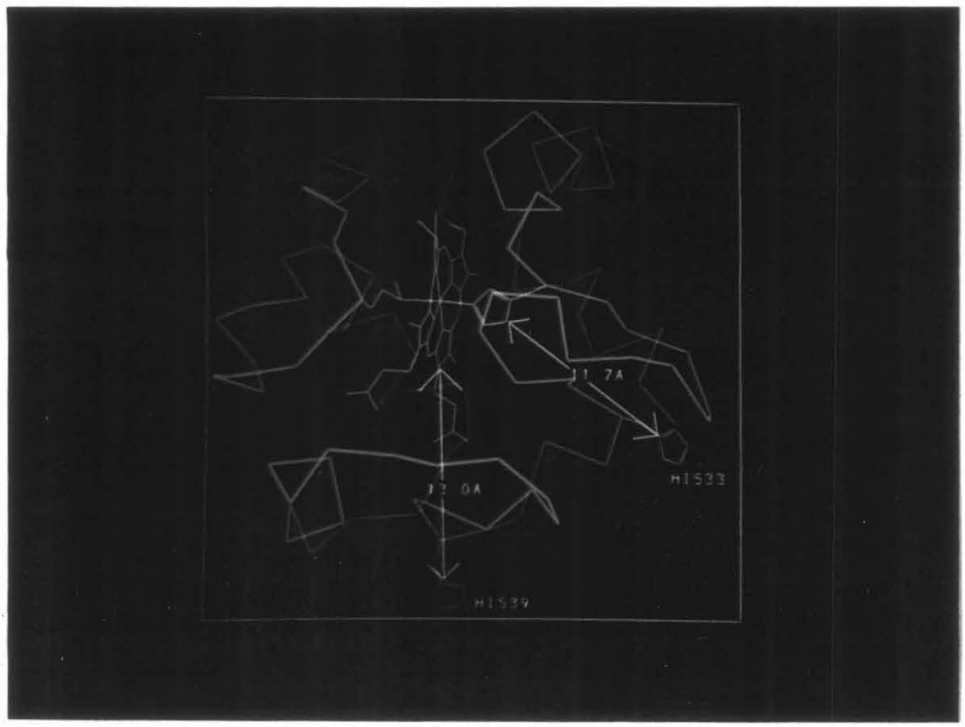

Figure 1.6

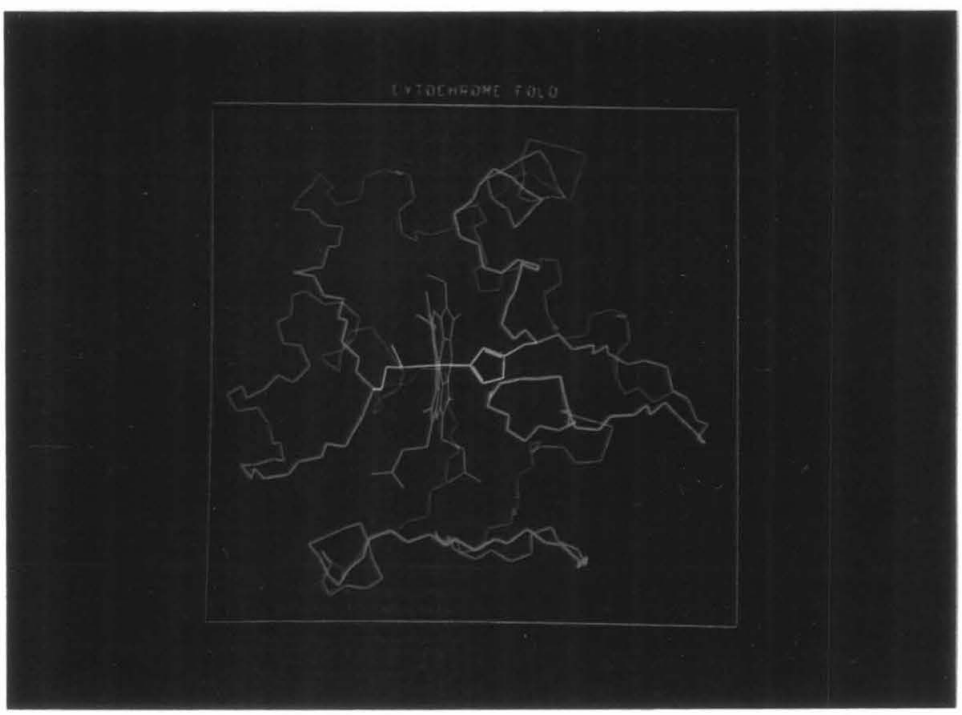

Figure 1.7

firms the general trend found for cytochromes *c*, *i.e.*, the conformation and fold are similar for all species investigated thus far (five species of cytochrome have been characterized crystallographically: tuna [reduced[55] and oxidized[56]], horse,[57] rice,[58] bonito,[57a] and *Saccharomyces cerevisiae*, see figure 1.7). Furthermore, NMR studies utilizing nuclear Overhauser enhancement have demonstrated the similarity of the crystal and solution cytochrome structures.[59]

Studies of the intramolecular electron transfer between the native iron site and the ruthenium label in modified cytochromes c are not necessarily expected to provide new insight into the mechanism of electron transfer in this protein. It is known from numerous studies that cytochrome *c* reacts with its physiological partners, cytochrome c_1 and cytochrome *c* oxidase, through its exposed heme edge, seemingly bypassing the protein medium altogether.[60] These experiments have some

[55] (a) Takano, T., Dickerson, R. *J. Mol. Biol.* **153**, 79 (1981); (b) Takano, T., Kallai, O., Swanson, R., Dickerson, R. *J. Chem. Biol.* **248**, 5234 (1973).

[56] Takano, T., Dickerson, R. *J. Mol. Biol.* **153**, 95 (1981).

[57] (a) Dickerson, R., Takano, T., Eisenberg, D., Kallai, O., Samson, L., Cooper, A., Margoliash, E. *J. Biol. Chem.* **246**, 1511 (1971); (b) Dickerson, R., Kopka, M., Borders, C., Varnum, J., Weinzierl, J. *J. Mol. Biol.* **29**, 77 (1967).

[58] Ochi, H., Hata, Y., Tanaka, N., Kakudo, M., Sakurai, T., Aihara, S., Morita, Y. *J. Mol. Biol.* **166**, 407 (1983).

[59] (a) Feng, Y., Roder, H., Englander, S., Wand, A., DiStefano, D. *Biochemistry* **28**, 195 (1989); (b) Pielak, G., Boyd, J., Moore, G., Williams, R. *Eur. J. Biochem.* **177**, 167 (1988).

[60] Rieder, R., Bosshard, H. *J. Biol. Chem.* **255**, 4732 (1980). However, evidence has recently been obtained to suggest that electrostatically-stabilized protein complexes are not necessarily optimum for electron transfer efficiency: Hazzard, J., McLendon, G., Cusanovich, M., Das, G., Sherman, F., Tollin, G. *Biochemistry* **27**, 4445 (1988). Furthermore, electron transfer through the heme edge is

bearing, however, on the mechanism of intramolecular electron transfer in other proteins whose redox centers are separated by tens of angstroms (*e.g.*, cytochrome *c* oxidase).[61]

3. Previous investigations of medium and orientation effects

A number of organic model systems have been developed to study intramolecular electron transfer, and several have suggested that the rate depends on the electronic structure of the medium bridging the donor and acceptor. For example, Heitele *et al.* found electron transfer from dimethylaniline to excited pyrene is ~25% faster in compounds whose bridge includes a 1,4-naphthyl as opposed to a phenyl moiety.[62] A similar 1,5-naphthyl-bridged compound undergoes electron transfer at a rate ~60% of that of the phenyl-bridged compound.

The electron transfer rates of a series of *S. cerevisiae* iso-1 cytochrome (cyt) *c* mutants with zinc-substituted cytochrome *c* peroxidase (Zn-CCP) appear to display significant medium dependence.[63] The photoactivated electron transfer from ^{3}ZnCCP to Fe^{3+}cyt proceeds at a similar rate (~200s^{-1}) for the native protein (Phe) and the mutants containing Tyr or Ser at residue position 82, but falls to ~10% of this value when Gly is substituted. Intermediate values are observed for

not necessarily expected to be adiabatic, as the heme is recessed (see Marcus and Sutin, p. 265).

61 Brudvig, G., Blair, D., Chan, S. *J. Biol. Chem.* **259**, 11001 (1984).

62 Heitele, H., Michel-Beyerle, M., Finckh, P. *Chem. Phys. Lett.* **134**, 273 (1987).

63 (a) Liang, N., Mauk, A., Pielak, G., Johnson, J., Smith, M., Hoffman, B. *Science* **240**, 311 (1988); (b) Liang, N., Pielak, G., Mauk, A., Smith, M., Hoffman, B. *Proc. Natl. Acad. Sci.* **84**, 1249 (1987).

Leu and *Ile* mutants. In contrast, the thermal back electron transfer ($Fe^{2+}cyt \rightarrow Zn^{+}CCP$) is much faster ($k_{et} \sim 10^{4} s^{-1}$) in the wild type (WT) cytochrome and Tyr mutant than in those mutants containing aliphatic residues (Ser, Leu, Ile or Gly; $k_{et} \sim 2s^{-1}$). These results are at variance with what one predict on the basis of reduction potentials: the Ser and Gly mutants have a reduction potential ~50mV less than that of the WT and the Tyr mutant. One possible interpretation of these results is that the aromatic residues mediate electron transfer by a superexchange mechanism.[64]

While the recent x-ray structural analyses of the reaction centers of the photosynthetic bacteria *Rhodopseudomonas viridis*[65] and *R. sphaeroides* R-26[66] have revealed the exact orientation of donor and acceptor pairs, it is not evident at this point to what extent this geometric arrangement serves to facilitate "forward" electron transfer *vis-a-vis* preventing charge recombination.

Relatively few of the numerous model systems featuring covalently bound donor and acceptor moieties that have been synthesized contain the redox participants in a rigid, defined geometry. However, studies of those that do have demonstrated how critical orientation may be in determining electron transfer rates. The rate of electron transfer between a stacked porphyrin dimer and a cofacial pyromellitimide acceptor has been found to be one thousand times faster than that from

[64] Miller, J., Beitz, J. *J. Chem. Phys.* **74**, 6746 (1981).

[65] (a) Deisenhofer, J., Epp, O., Miki, K., Huber, R., Michel, H. *Nature* **318**, 618 (1985); (b) *idem*, *J. Mol. Biol.* **180**, 385 (1984).

[66] Chang, C., Tiede, D., Tang, J., Smith, U., Norris, J., Schiffer, M. *FEBS Lett.* **205**, 82 (1986).

a side-by-side isomeric dimer to the same acceptor in a perpendicular orientation.[67]

The project reported on here is an attempt to investigate these two influences, donor-acceptor orientation and medium effects, by making use of what is expected to be a minor perturbation to a native biological system.

[67] Cowan, J., Sanders, J., Beddard, G., Harrison, R. *J.C.S. Chem. Comm.* 55 (1987).

CHAPTER 2

PREPARATION AND ISOLATION OF THE CYTOCHROME DERIVATIVE

MATERIALS and INSTRUMENTATION

All buffers and solutions were prepared with distilled water that was further purified by passage through a Barnstead Nanopure system (model D2794). The specific resistance of the water was greater than 18MΩ-cm.

Candida krusei cytochrome *c* was purchased from Sigma (Type VII).

Chloropentaammineruthenium(III) chloride ($[Ru(NH_3)_5Cl]Cl_2$) was used as supplied by Strem Chemicals, Inc.

Mossy zinc, mercuric oxide, sulfuric acid, ethanol, and diethyl ether were of reagent grade. Ammonium hexafluorophosphate (NH_4PF_6) was obtained from Pennwalt.

All buffer salts (Na_2HPO_4, $NaH_2PO_4 \cdot H_2O$, Tris, Tris·HCl, glycine, and HEPES acid and sodium salt) were reagent grade.

CM-52 carboxymethylcellulose cation-exchange resin was obtained from Whatman. Amberlite CG-50, 100-200 mesh, was purchased from Alfa Products.

Biorad Econocolumns (2.5cm ID) were utilized for separations and purifications involving less than 100mg protein. All other columns, made in the Caltech glass shop, were glass tubes fitted with medium sintered glass frits and Teflon stopcocks.

Flow rates were usually maintained with either a Gilson Minipuls 2 model R1 or a Pharmacia model P-1 peristaltic pump fitted with polyvinylchloride manifold tubing.

Fractions were collected with a Gilson model FC-80 Micro-Fractionator in 13mm x 100mm Pyrex glass test tubes. Elution profiles were recorded using a Gilson Model HM Holochrome and Gilson model N2 DC recorder, or constructed by plotting the absorbance reading (λ=410nm) of

(at least) every third fraction during apparent band elution and (at least) every fifth fraction otherwise.

pH measurements were made with a Brinkmann Instruments model pH-101 or Beckman model Φ32 pH meter, using a combination microelectrode. Beckman buffer standards were used for calibration. The pH values quoted for buffer solutions are those measured at room temperature.

Conductivity measurements were made with a Markson model 10 portable conductivity meter. Beckman 0.01N KCl calibrating solution (1410μMHO/cm) was used.

Ultrafiltration cells, type YM-5 membranes (5000 molecular weight cutoff), and Centricon-10 microconcentrators (10000 molecular weight cutoff) were purchased from the Amicon Corporation.

UV-visible spectra were recorded on either a Cary 219, Cary 17, or Shimadzu UV-260 spectrophotometer.

Solutions were degassed on a vacuum-argon dual-manifold line. Argon was scrubbed of oxygen by passage through a manganese oxide tower. Solutions were transferred anaerobically by means of a cannula fitted at each end with a 6" stainless steel 20-gauge deflected-tip needle.

BioRad or LKB acrylamide and EM Reagents N,N'-methylenediacrylamide were used to prepare electrophoresis gels. Acrylamide solutions were filtered and stored in amber bottles at $4^{o}C$ up to two weeks. N,N,N',N'-tetramethylethylenediamine (TEMED) was obtained in 1 ml ampules from LKB. Solutions of ammonium peroxydisulfate (EM Reagents) were prepared immediately prior to gel polymerization. Trichloroacetic acid was obtained from Sigma, and 5-sulfosalicylic acid from Kodak. Coomassie Blue R250 was supplied by

Scientific Chemical Company. All other chemicals were reagent grade. Analytical horizontal electrophoresis was carried out using an LKB 2117 Multiphor and 2197 DC power supply. Glass supports and paper wicks were obtained from LKB. Water cooled by a Brinkmann RM3 bath was circulated within a support plate to maintain the gel temperature below $10^{o}C$.

The fast protein liquid chromatography (FPLC) instrumentation, manufactured by Pharmacia, included two P-500 pumps, a UV-M UV-visible detector (Hg lamp), and an LCC-500 controller. Elution profiles were recorded simultaneously on a two-channel strip chart recorder (Pharmacia REC-482) and the LCC-500 integrator. Separations were carried out on Pharmacia cation exchange Mono S columns, either size 5/5 or 10/10, for analytical and preparative runs, respectively. Fractions were collected during preparative runs using a Pharmacia FRAC-100 instrument in a time-based peak-only mode.

METHODS

Na[Co(EDTA)] was prepared by the method of Kirschner,[1] substituting sodium carbonate for barium carbonate.

The hexafluorophosphate salt of aquopentaammineruthenium(II) was prepared by the method of Callahan *et al.*[2] The compound was stored under vacuum and used within one week of preparation.

CM-52 resin was removed from each column after a single use and suspended in 1M NaCl for a minimum of 24 hours. If the supernatant was

[1] Kirschner, S. *Inorg. Syntheses* **5**, 186 (1957).

[2] Callahan, R., Brown, G., Meyer, T. *Inorg. Chem.* **14**, 1443 (1975).

especially dirty, it was decanted off and the resin was resuspended in 1M NaCl. The resin was rinsed by repeated decanting of the supernatant and resuspension in water. Once the ionic strength was reduced sufficiently, the resin was suspended in the buffer to be used.

Chromatography

All columns were packed with a slurry of resin while flowing. All chromatography was performed at $4^{o}C$, unless stated otherwise. Columns were considered equilibrated when the pH and conductivity of the reservoir and effluent buffers were identical.

Purification of commercial Candida krusei cytochrome c

The protein was dissolved in a minimum of pH 7 sodium phosphate buffer (<100mM), and an aliquot of a concentrated Na[Co(EDTA)] solution was added. The cytochrome solution was stored at $4^{o}C$ for several hours to insure that all the protein was oxidized, and thus avoid complications from redox isomers in subsequent chromatography. Excess oxidant was sometimes removed by ultrafiltration, or if the sample was of sufficiently low ionic strength, the cytochrome was loaded onto the column directly (the negatively charged $CoEDTA^{-}$ does not bind to cation-exchange resins, but elutes immediately in the void volume).

The cytochrome was routinely purified by elution from CM-52 with 85mM, pH 7 sodium phosphate (NaP_i) buffer.[3] However, before deciding upon this method, a comparison was made with a second method, which had

[3] Brautigan, D., Ferguson-Miller, S., Margoliash, E. *Meth. Enzym.* **53**, 128 (1978).

been reported specifically for the purification of the cytochrome *c* from *Candida krusei.*[4] This method involved the elution of 100mg cytochrome *c* from a 4cm x 23cm column of 100-200 mesh Amberlite CG-50, equilibrated in pH 7 100mM NaP_i, with a linear gradient from 50mM to 250mM NaCl in the same buffer (1280mL each), at a flow rate of 52mL/hr.

Concentration of protein solutions

Concentration of protein solutions was achieved by ultrafiltration in an Amicon apparatus with YM-5 membranes. When small volumes were required, Amicon YM-10 Centricons were utilized. New membranes were soaked several hours prior to use to remove preservatives. Membranes were stored in 10% ethanol at 4°C to prevent bacterial growth.

Estimates of protein concentration

An aliquot of cytochrome solution was diluted with a known volume of buffer, and its absorbance was read at 410nm (cytochrome isosbestic; ε=106100$M^{-1}cm^{-1}$ for horse heart cytochrome *c*) against the appropriate blank.[5]

Optimization of the reaction conditions to achieve a 1:1 derivative

Polyacrylamide gel electrophoresis (PAGE) was utilized to determine the reaction time for optimum production of a 1:1 ruthenium:cytochrome derivative. 3.5% polyacrylamide gels (1.5mm x 125mm x 250mm; T=3.6%, C=2.6%)[6] with 5µl sample wells were prepared according

[4] Lederer, F. *Eur. J. Biochem.* **31**, 144 (1972).

[5] Margoliash, E., Frohwirt, N. *Biochem. J.* **71**, 570 (1959).

to LKB Application Note 306 using pH 7 100mM imidazole (titrated with phosphoric acid) or pH 8.9 Tris-Gly buffer and were stored at 4°C for at least 12 hours prior to use. Imidazole-buffered gels were preelectrophoresed at least one half hour at 80mA; samples were concentrated for 10 minutes at 20mA, and run for 2 hours, 50 minutes at 80mA. Tris-Gly gels were preelectrophoresed 1.5 hours at 38mA; samples were concentrated for 5 minutes at 20mA, and run for 1 hour 45 minutes at 38mA.

A solution of *Candida krusei* cytochrome *c* (>0.2mM) in 100mM pH 7.5 HEPES buffer was degassed in a serum bottle at room temperature. Care was taken to avoid foaming of the solution, which is known to result in protein denaturation.[7] Meanwhile, a volume of buffer sufficient to result in a protein concentration of 0.2mM when combined with the cytochrome solution was degassed also. Once thoroughly degassed by several cycles of evacuation and saturation with argon, thirty equivalents of $[Ru(NH_3)_5OH_2](PF_6)_2 \cdot H_2O$ were added to the degassed buffer and the serum bottle was again evacuated. After several more cycles of saturation with argon and evacuation, the solution of the ruthenium complex was transferred anaerobically to the bottle containing the cytochrome. As the reaction proceeded, 1.2ml aliquots were removed via syringe and diluted to approximately 10ml with pH 5 sodium acetate (NaAc) buffer. Ultrafiltration of the reaction mixture was begun immediately upon removal, and was carried out for at least three cycles of concentration, dilution, and reconcentration. An aliquot of $CoEDTA^-$

[6] T=total acrylamide concentration (w/w), C=crosslinker concentration as a percentage of the total acrylamide

[7] Henson, A., Mitchell, J., Mussellwhite, P. *J. Colloid Interfac. Sci.* **32**, 162 (1970).

solution was added to the concentrated protein to oxidize the ruthenium label. Removal of the oxidant and exchange of the buffer were accomplished by repeated ultrafiltration and dilution with 10mM electrophoresis buffer in Centricons.

Aliquots were removed at the following time points: 17 min., 34 min., 50 min., 1 hr., 1.5 hr., 2 hr., 3 hr., and 4 hr. A second reaction run under similar conditions was also monitored by electrophoresis, with time points of 15 min., 1 hr., 2 hr., 4 hr., 6 hr., 8 hr., 12 hr., 18 hr. and 24 hr. Proteins were fixed and stained and the gels preserved according to the instructions of LKB Application Note 306.

Modification of Candida krusei cytochrome c on a preparative scale

The reaction was carried out as described above, for a period of thirty minutes, usually on the scale of 50-100mg cytochrome. The solution of the ruthenium complex was often turbid, in which case the vessel was filled with argon and the solid was allowed to settle. Several milliliters of the supernatant were transferred anaerobically to a spectrophotometric cell which had been flushed with argon, and the absorbance of the solution at 414nm was measured (*versus* buffer blank). An extinction coefficient of $44M^{-1}cm^{-1}$ was used to calculate the ruthenium concentration, which generally was such that the molar ratio was 23:1 [Ru]:[cyt], after dissolving a mass equal to ~30 equivalents.[8] As the supernatant ruthenium solution was transferred anaerobically to the protein solution, the cytochrome changed from red to orange, an

[8] Ford, P., Kuempel, J., Taube, H. *Inorg. Chem.* 7, 1976 (1968).

indication of its reduction.

Separation of the pentaammineruthenium modification reaction products

The oxidized reaction mixture was applied to a column of CM-52 equilibrated in 100mM pH 7 sodium phosphate, and eluted with same.

The programs for control of FPLC functions and the solvent gradient for analytical and preparative runs are presented in table 2.1. The binary solvent system included 50mM pH 7 NaP_i ("A") and 50mM pH 7 NaP_i, 1M in NaCl ("B").[9] Product elution was monitored by absorption at either 280nm or 405nm.

RESULTS

Purification

Purification of the commercial cytochrome product is required to remove deamidated protein, *i.e.*, protein in which amide side chains (of asparagine and glutamine) have been hydrolyzed to the corresponding acid (Asp or Glu).[10]

The purification achieved on CM-52 was judged to be superior to that obtained with Amberlite CG-50, as the former resulted in more numerous and better resolved bands for cytochrome of identical lot (figure 2.1).

Although the number of bands and the elution pattern of the product on CM-52 varied from lot to lot, a minimum of four bands was

[9] the method of preparation took into account the ionic strength dependence of the sodium phosphate ionization constant; Gutfreund, H. *Enzymes: Physical Principles*, Wiley (New York), 1972, p. 34.

[10] Harding, J. *Adv. Prot. Chem.* **37**, 247 (1985).

Table 2.1. FPLC programs for analytical (a) and preparative (b) separation of the oxidized reaction mixture.

a.

volume (mL)	**instruction**
0	%B = 0
	1mL/min
	0.2cm/mL
	valve position = 1.1
2	2mL/mark
	monitor
	clear data
	level % = 3
	integration on
	valve position = 1.2
32	%B=50
34	%B=100
	integration off
36	%B = 100
38	%B = 0
42	%B = 0
	valve position = 1.1

b.

volume (mL)	**instruction**
0	%B = 0
	4mL/min
	0.05cm/mL
	valve position = 1.1
40	8mL/mark
	monitor
	clear data
	level % = 4
	integration on
	valve position = 1.2
	%B = 0
	port open
296	%B=50
312	%B=100
	integration off
	port closed
328	%B = 100
344	%B = 0
360	%B = 0
	valve position = 1.1

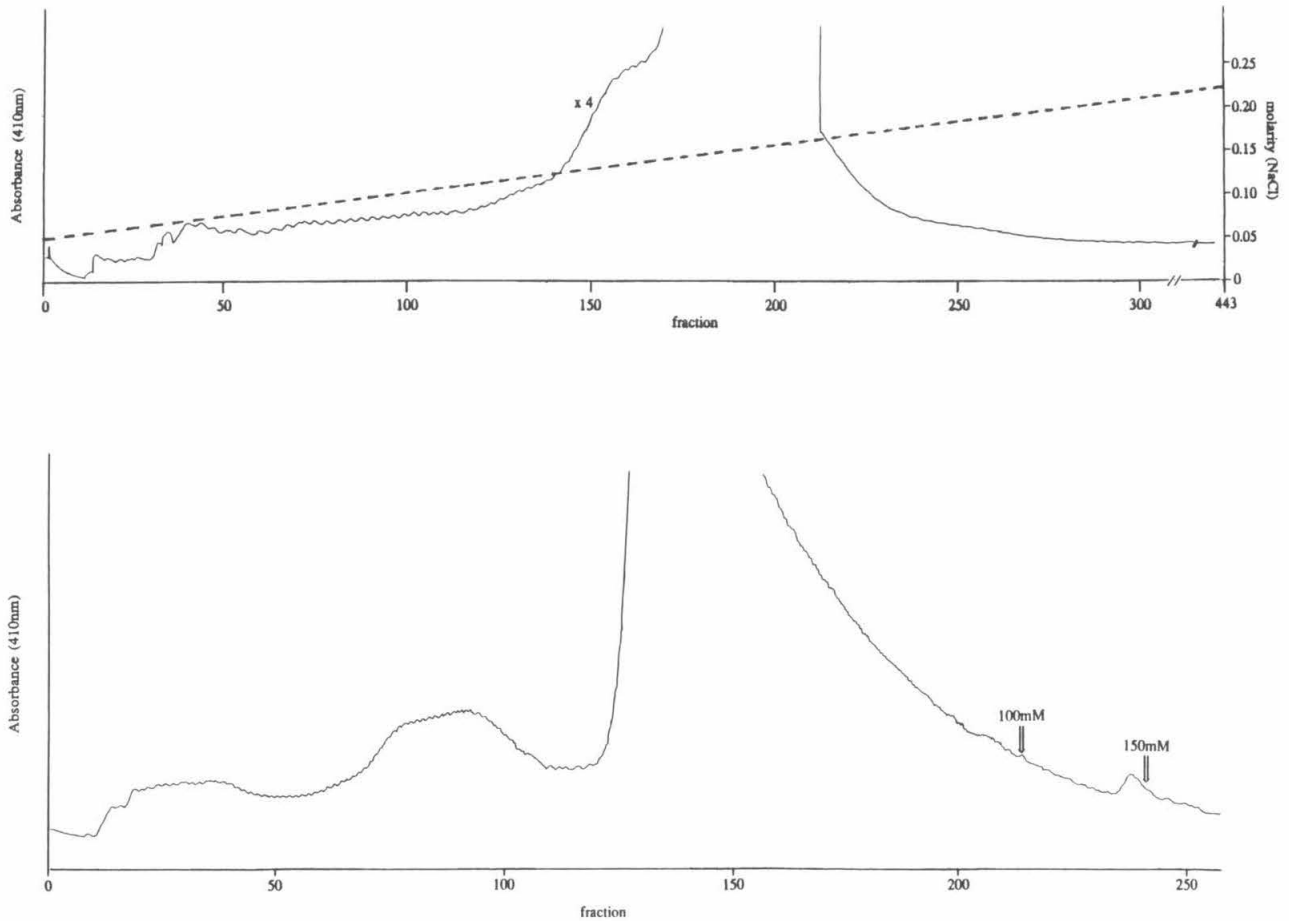

Figure 2.1. Elution profiles of commercial *C. krusei* cytochrome *c* from (a) Amberlite CG-50, and (b) CM-52. See text for conditions.

always seen: the major component was usually immediately preceded by two bands, one brown, and the other pinkish-orange (the latter is likely to be reduced protein). A fourth reddish-pink band remained at the top of the resin bed, but could be eluted with 150mM NaP_i. The great affinity of this material for the anionic support suggests this band may be polymeric cytochrome.[11] In more impure lots, and in cases where aged cytochrome samples were repurified, an additional unretained band was observed. The purified cytochrome was found to be homogeneous by PAGE and FPLC.

Time analyses

In the electrophoresis sample taken immediately after mixing, a product of mobility higher than that of native cytochrome *c* is evident. After one half hour (figure 2.2a, lane 8), most of the native cytochrome has reacted to form this product. At longer reaction times (figure 2.2b), products of even greater mobility are observed, and a concommitant decrease of the initial product is observed.

Interpretation of electrophoretic results is not without ambiguity. What appears to be a single band may be one or more species. Electrophoretic mobility may be more a function of the molecular dipole moment or perhaps sample-gel interactions, rather than the absolute charge, as demonstrated by the resolution of singly-modified pentaammineruthenium myoglobin derivatives (A_5RuHis12-Mb and A_5Ru-His116-Mb) under conditions identical to those described in figure 2.2b (data not shown).

[11] Margoliash, E., Lustgarten, J. *J. Biol. Chem.* **237**, 3397 (1962).

Figure 2.2. Time analyses of the *C. krusei* cytochrome *c* modification reaction by polyacrylamide gel electrophoresis. Migration is from top to bottom, towards the (negative) cathode.

(a) *Upper*: pH 8.9 Tris-glycine buffer, 5 hr. reaction

Lanes 1-4: native *C. krusei* cytochrome *c*, 3mg/ml, 10mg/ml, 20 mg/ml, 12mg/ml, respectively; **Lane 5**: modified product from a previous experiment;

Reaction time points:

Lanes 6, 7, 8, 9: 0, 17, 34, and 50 min., respectively;

Lanes 10, 11, 12, 14, 15, 16: 1, 1.5, 2, 3, 4, and 5 hours, respectively;

Lane 17: as for lane 4

No sample was applied to the defective slot of lane 13. Splotchiness of the lane 9 sample is due to overfilling of the slot.

(b) *Lower*: pH 7 imidazole-phosphate buffer, 24 hr. reaction

Lane 1: native *C. krusei* cytochrome *c*, reduced;

Lanes 2, 8, 15: native *C. krusei* cytochrome *c*, oxidized;

Reaction time points:

Lanes 3, 4, 5, 6, 7: 15 min., 1 hr., 2 hr., 4 hr., 6 hr., respectively;

Lanes 10, 11, 12, 13: 8, 12, 18, and 24 hours, respectively;

Lanes 9, 16: product from previous experiments (thought to be singly modified)

Lane 14: mixture, native and modified cytochromes

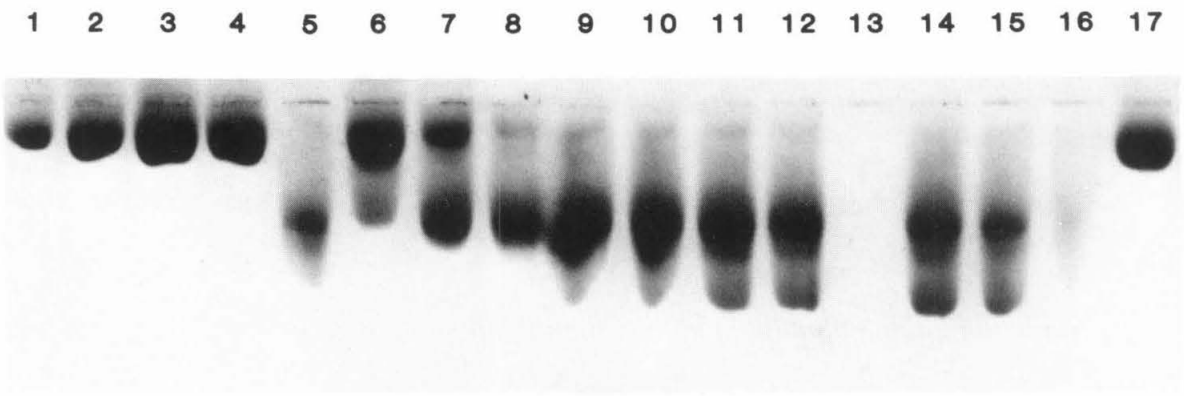
1 2 3 4 5 6 7 8 9 10 11 12 13 14 15 16 17

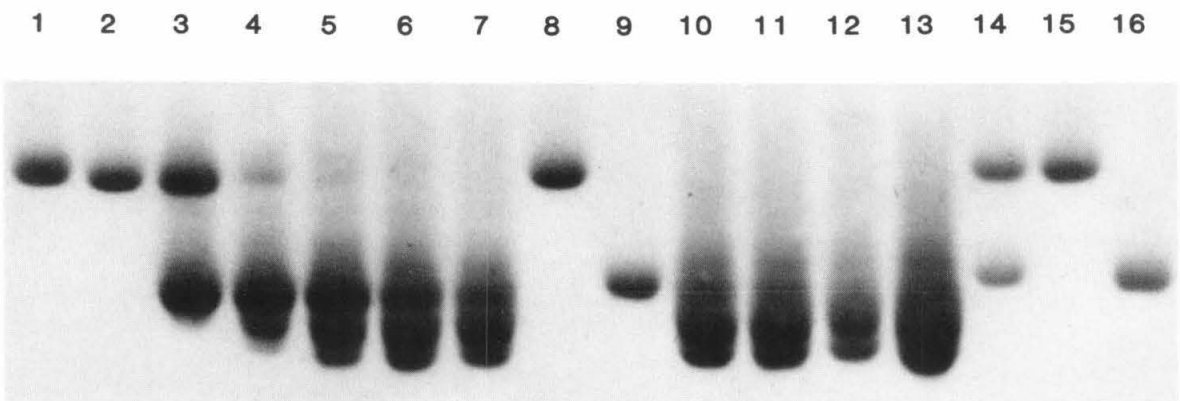
1 2 3 4 5 6 7 8 9 10 11 12 13 14 15 16

Modification of the *C. krusei* cytochrome *c* is rapid, despite the fact that the protein molecule has a high net positive charge,[12] which might be expected to repel the positively charged ruthenium complex. While protein charge has been suggested to account for the slow modification of horse heart cytochrome *c*, and for the relative rates of reaction of two species of plastocyanin,[13] this result demonstrates that local factors, including charge as well as steric constraints, figure prominently in determining the rate with which modification progresses (*vide infra*).

Chromatography

Typically, three bands were evident upon elution of the half-hour reaction mixture (figure 2.3). Additional bands were occasionally observed, particularly when the period of oxidation was short, and were presumed to be redox isomers. Elution volumes were ~3.7 and ~7.8 column volumes for the first two components. The third band was slow to elute with 100mM buffer, and was often removed with a stronger buffer solution once elution of the second component was complete. Typical yields of the three components were 12%, 50%, and 12% (total recovery was as high as 95%, but tails of bands were excluded from determinations of yield).

An elution profile for separation of the products by FPLC is

[12] estimated to be +6 at pH 7 for the reduced form on the basis of the amino acid sequence, assuming all Lys and Arg are protonated, all Glu and Asp are deprotonated, and a pK_a of 7 for all His (*i.e.*, half are protonated at pH 7)

[13] Jackman, M., McGinnis, J., Powls, R., Salmon, G., Sykes, A. *J. Amer. Chem. Soc.* **110**, 5880 (1988).

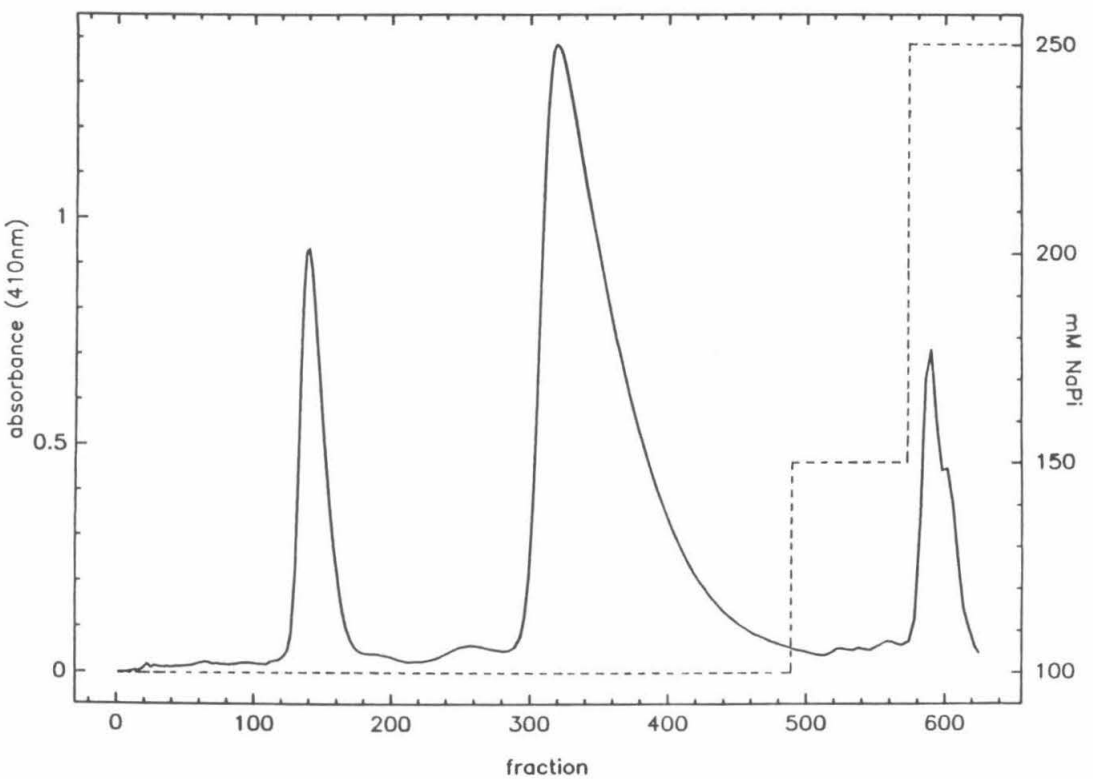

Figure 2.3. Chromatogram for the elution of the products of the reaction of pentaammineruthenium(II)aquo and *C. krusei* cytochrome *c* from CM-52.

shown in figure 2.4. Individual FPLC runs of each product recovered from CM-52 confirmed that the order of elution is identical for conventional and fast protein chromatography. Reduced native protein is also resolved by FPLC, and elutes prior to the oxidized form (as expected on the basis of total protein charge). Redox isomers of the modified products are resolved also, but coelute with the native cytochrome. Retention times for the four species are 12.8, 14.6, 15.9, and 19.3 minutes. *Baseline* resolution of the native and first modified derivative could be achieved under other conditions (elution at 18%B, retention volumes of 9.5mL and 15mL, respectively). However, bands were broad and resolution was compromised when the procedure was attempted on a preparative basis. No evidence was obtained from FPLC for significant amounts of additional products.

Efforts toward characterization were focused on the first two bands eluted from CM-52. The first band was shown by electrophoresis, NMR, and EPR to be native cytochrome *c*. Characterization experiments for the second band are described in chapter 3, and this product may be referred to as <u>the</u> modified cytochrome. The third band has been partially characterized, and this work is described in appendix 6.

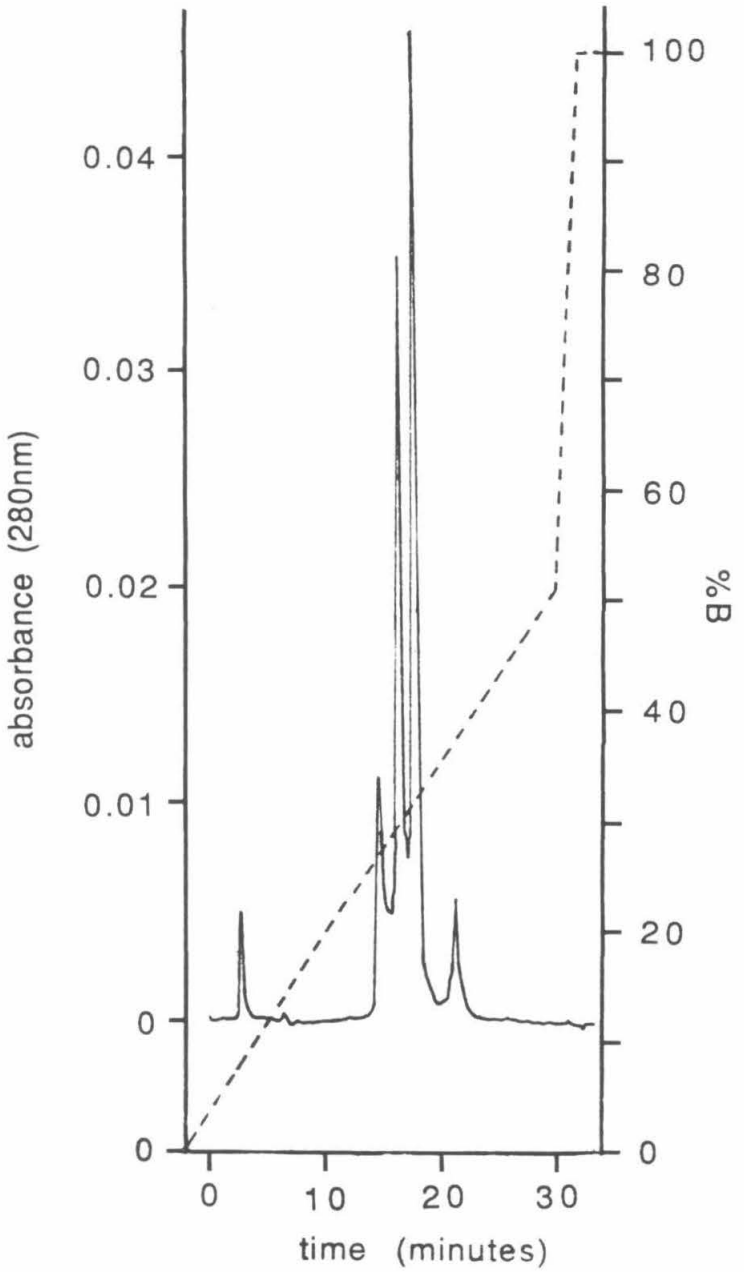

Figure 2.4. Chromatogram for the analytical FPLC separation of the oxidized modification reaction mixture (--- gradient, 0-50%B in 32 minutes at 1mL/min; injection at 2 minutes; unretained product is $CoEDTA^-$; other products in order of elution are reduced native cytochrome *c*, oxidized native cytochrome *c*, and the two modified products).

CHAPTER 3

CHARACTERIZATION OF THE DERIVATIVE

MATERIALS and INSTRUMENTATION

Protein

All of the native protein samples used were purified as described in chapter 2. The modified cytochrome was used as recovered from the CM-52 column, except for peptide mapping, in which case the derivative was further purified by FPLC (see chapter 2 for details).

Electron Paramagnetic Resonance Spectroscopy

EPR spectra were recorded on a Varian E-line Century series X-Band spectrometer operating in the absorption mode. Sample temperature was maintained with an Air Products Heli-Tran cryostat.

The chloride salt of the pentaammineruthenium(III)histidine complex, $[A_5Ru(His)]Cl_3 \cdot H_2O$, was prepared by Kathy Yocom by the method of Sundberg and Gupta.[1]

Nuclear Magnetic Resonance Spectroscopy

^1H NMR spectra were recorded at 25°C on a Bruker AM-500 instrument operating at 500.13MHz. Typically, 128 transients were acquired and stored as 16000 (pH 5.2 samples) or 32000 sampled points of the FID.

UV-visible Difference Spectroscopy

Spectra were recorded on a Shimadzu UV-260 spectrophotometer. Quartz cuvettes (1cm pathlength) were obtained from NSG Precision Cells.

[1] Sundberg, R., Gupta, G. *Bioinorg. Chem.* **3**, 39 (1973).

Peptide Mapping

Submaxillaris protease (SMP) was obtained from the Pierce Chemical Company.

The ReactiTherm heating module was purchased from the Pierce Chemical Company.

The chromatograph consists of two Altex 110A solvent metering pumps controlled by a Model 420 Microprocessor controller/programmer, an Altex mixer, and several columns connected in parallel and selected by two Rheodyne 7060 switching valves. Effluent was monitored with an Altex/Hitachi Model 110-10 variable wavelength detector fitted with a 20μL standard analytical flow cell (model 155-00). An Upchurch Scientific flow restrictor, part U-444, is placed after the detector to maintain the effluent under pressure (40 psi), and prevent degassing in the detector cell.

All tubing is type 316, 1/16" O.D. stainless steel, of internal diameter 0.02" prior to the injector and 0.01" after the injector. The system is also equipped with a Rheodyne model 7037 pressure relief valve, an Alltech #9299 in-line pressure gauge, and an SSI Prime/Purge Valve (#02-0292).

Column temperature was maintained constant ($\pm 0.5^{o}C$) by a Waters temperature control system. Samples were injected manually via a Rheodyne model 7125 syringe loading sample injector, which accommodated loops up to 200μL in volume. A Hitachi/EM Science integrator or Shimadzu C-R5A Chromatopac was used to record and integrate peaks. Sample injection and activation of the recorder were synchronized manually.

Acetonitrile, methanol, triethylamine (TEA), and trifluoroacetic

acid (TFA) were *HPLC* grade. Water was purified as described previously. 4mm Millipore type HV 0.45μ filter units, and 45mm Millipore type HA filters held in a glass filtration apparatus, were used for samples and aqueous solvent mixtures, respectively.

The HPLC column utilized was a 4.5mm x 15cm silica-based reverse phase C4 type, manufactured by Vydac (catalog no. 214TP5415, no. 270028, #21).

A Savant SpeedVac, model SVC100H, containing a RH40-11 rotor, was attached to a vacuum pump via a liquid nitrogen trap, and was always operated with the sample compartment maintained at 40°C.

Spectroelectrochemistry

Optically-transparent thin-layer electrochemistry (OTTLE) cells were constructed by Walther R. Ellis using two 17mm x 35mm rectangles of fine gold mesh (500 lines/inch; 60% transmittance; Interconics, St. Paul, MN) as the working electrode (figure 3.1).[2] The cell was constructed with a copper-constantan microthermocouple (Omega Engineering) which protruded into the sample compartment and, in conjunction with a Fluke 2175A digital thermometer (±0.2°C), allowed for the monitoring of sample temperature. Platinum wire was used as the counter electrode, and the reference electrode was a miniature saturated calomel electrode (SCE) obtained from Sargent-Welch.

The assembled electrochemical cell was held in the cell compartment of a Cary 219 spectrophotometer by a special mount built in the

[2] Ellis, Walther Robert Jr., "Spectroelectrochemical Studies of Heme and Copper Proteins.", Ph.D. Dissertation, California Institute of Technology, 1986.

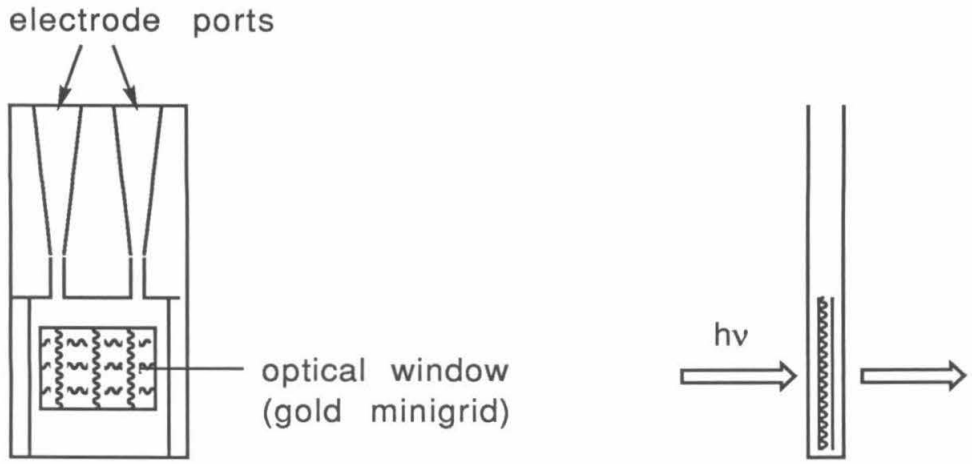

Figure 3.1. Front *(left)* and side *(right)* view of an optically transparent thin layer spectroelectrochemistry cell.

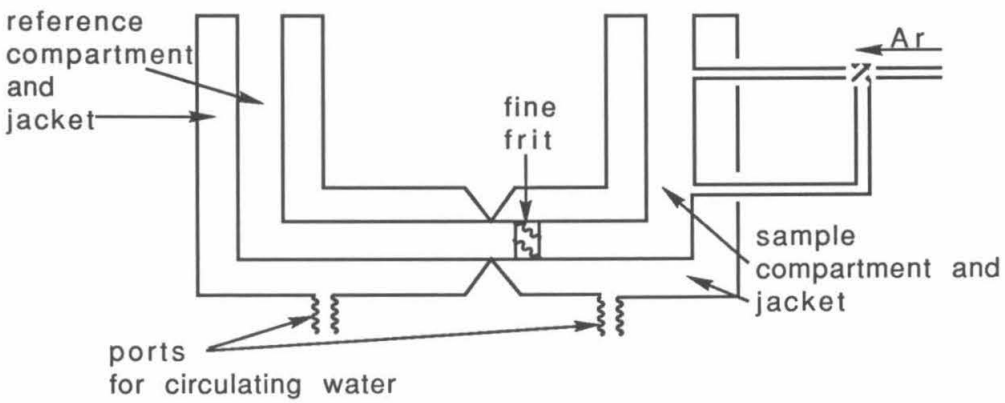

Figure 3.2. Dual-jacketed electrochemical cell for differential pulse polarography.

Caltech machine shop. Sample temperature was maintained by water from a constant-temperature bath which circulated through this cell holder. The reference electrode (SCE) was maintained at ambient temperature, which was measured with an ordinary mercury thermometer (graduated in $0.2^{o}C$).

The cell potential was controlled with a Princeton Applied Research Model 174A polarographic analyzer, and was measured to 0.1mV with a Keithley 177 digital voltmeter.

The cytochrome, 0.4mM in μ=0.1M, pH 7.0 sodium phosphate, had been purified twice by cation exchange chromatography. A "pinch" of pentaammineruthenium(III)pyridine perchlorate, $[Ru(NH_3)_5py](ClO_4)_3$, prepared by Walther R. Ellis,[3] was added as a mediator (E^{o} = 298 mV).[4]

Differential Pulse Polarography

The electrochemical cell was manufactured in the Caltech Glass shop, and consists of two compartments which are connected by a fine sintered frit (figure 3.2). The compartments have independent water jackets. Each compartment contains a port to allow for the insertion of a thermocouple, and the sample compartment can be connected via a Teflon stopcock to a line of nitrogen or argon for degassing. Incubation of the two compartments was achieved with Forma Scientific models 2095 and 2132 circulating baths.

A 4mm gold button electrode was purchased from Bioanalytical Systems. Miniature saturated calomel electrodes were obtained from

[3] Cummins, D., Gray, H. *J. Amer. Chem. Soc.* **99**, 5158 (1977).

[4] Matsubara, T., Ford, P. *Inorg. Chem.* **15**, 1107 (1976).

Sargent Welch. Platinum wire was used as the counter electrode.

Equipment to scan the potential and record the current included a Princeton Applied Research Model 174A Polarographic Analyzer and a Houston Instrument 2000 XY recorder. Temperature and potential were monitored by a Fluke 2175A digital thermometer and 8010A digital multimeter, respectively. Thermocouples, catalog number 5TC-TT-T-36-36-STD (type T copper-constantan) were obtained from Omega Engineering.

Aldrithiol-4 (4,4'-dipyridyl disulfide) was used as supplied by Aldrich.

Modeling Studies

All modeling and calculations of distances and surface areas were conducted using the program Biograf (Biodesign, Pasadena, CA), version 1.5.

METHODS

Electron Paramagnetic Resonance Spectroscopy

EPR spectra were recorded with a modulation amplitude of 16G, a modulation frequency of 100KHz, and a microwave power of 0.2mW.

The temperature at the sample position was measured before and after the spectra were acquired using a gold-chromel thermocouple. Spectra were recorded at ~12K.

NMR Spectroscopy

pH 5.2 NMR samples were prepared by subjecting cytochrome (lyophilized from water) to two cycles of dissolution in D_2O and lyophilization. Other samples were exchanged into D_2O by diafiltration

in Centricon-10 units. Solution pH was adjusted using solutions of NaOD and DCl in D_2O. pH values quoted are direct meter readings, as measured with a micro-combination electrode within one hour after the spectra were recorded.

The sodium salt of 2,2'-dimethyl-2-silapentane-5-sulfonate (DSS) was present in samples at concentrations of ~1-2mM. Chemical shift values are quoted in parts per million (ppm) downfield of the methyl resonance of DSS.

Titration data were fit by a least-squares analysis to the expression

$$pH = pK_a + log\ [(\delta^+ - \delta)/(\delta - \delta^o)]$$

where δ^o and δ^+ are the chemical shifts of the proton of interest for the deprotonated and protonated species, respectively, and δ is the observed chemical shift for the proton at a pH where both forms are in equilibrium.

The derivation of the above expression is as follows. The assumption is made that the chemical shift is a linear function of concentration, *i.e.*,

$$\delta = \delta^o + ([His^+]/[His])(\delta^+ - \delta^o)$$

where $[His^+]$ is the concentration of the protonated histidine residue, and [His] is the total histidine concentration. Letting x and y represent the fractions of histidine protonated ($[His^+]/[His]$) and deprotonated ($[His^o]/[His]$) (where $[His^o]$ is the concentration of the deprotonated form of the histidine residue), respectively, any observed chemical shift can be expressed as follows:

$$\delta = \delta^+(x) + \delta^o(y)$$

Since $x + y = 1$,

$$\delta = \delta^{+}(x) + \delta^{o}(1-x) = \delta^{+}(1-y) + \delta^{o}(y)$$

Solving for each variable,

$$x = (\delta-\delta^{o})/(\delta^{+}-\delta^{o})$$

and

$$y = (\delta-\delta^{+})/(\delta^{o}-\delta^{+})$$

Therefore, using the Henderson-Hasselbalch equation,[5]

$$pH = pK_a + log\ [His^{o}]/[His^{+}] = pK_a + log\ (y/x)$$

$$pH = pK_a + log\ [(\delta^{+}-\delta)/(\delta-\delta^{o})]$$

UV-visible Difference Spectroscopy

Water or buffer was used to record a baseline, which was automatically subtracted from the spectra recorded thereafter. Solutions of ~1.7mM of the native cytochrome and modified product (to correspond to a maximum absorbance of 2) were prepared, and their 450-250nm spectra were recorded into separate channels of the spectrophotometer memory. Digital absorbance readings at 410nm (an isosbestic point) were noted for each. The spectrum of the native protein was multiplied by A_{410}(modified)/A_{410}(native) to correct for slight differences in concentration. The corrected spectrum of the native cytochrome was subtracted from the spectrum of the derivative, and the result recorded. Any absorbance at 416nm in the difference spectrum, indicative of different proportions of oxidized and reduced cytochrome in each sample, was used to correct the 300nm reading,[6] as follows:[7]

[5] Boikess, R., Edelson, E. *Chemical Principles*, Harper and Row (New York), 1978, p. 481.

[6] this neglects any contribution from the ruthenium absorbance at 416nm

[7] Margoliash, E., Frohwirt, N. *Biochemical J.* **71**, 570 (1959).

$$c = \Delta A_{416} \div (129100 - 88800)\ M^{-1}cm^{-1}$$

$$\Delta A_{300}(\text{corrected}) = \Delta A_{300}(\text{observed}) - c(21000 - 13000)M^{-1}cm^{-1}$$

where c is the concentration of the reduced species in the modified cytochrome minus that in the native protein. An extinction coefficient of $2000M^{-1}cm^{-1}$ was used to estimate the ruthenium concentration.[8]

Peptide Mapping

The strategy of the peptide mapping experiments is as follows. Both the native and modified proteins are digested with a protease of known and highly selective specificity, to produce two sets of peptides, each of which can be separated by reverse phase HPLC.[9] The enzymatic reaction is carried out under very mild conditions, and the A_5Ru moiety remains bound. A comparison of the peptide chromatograms should reveal peptides which are shifted in retention (in either direction, depending on the net charge of the peptide) due to the presence of trivalent ruthenium. Confirmation of the presence of ruthenium on a peptide depends upon UV-visible spectral characterization. The peptide(s) can then be identified (*i.e.*, related to a specific sequence of the protein) by total amino acid analysis (the A_5RuHis complex is destroyed in the course of acid hydrolysis).[10] It is important that no

[8] An extinction coefficient of $1880M^{-1}cm^{-1}$ has been reported for the pentaammineruthenium imidazole complex: Sundberg, R., Bryan, R., Taylor, I., Taube, H. *J. Amer. Chem. Soc.* **96**, 381 (1974). An extinction coefficient of $2100M^{-1}cm^{-1}$ has been reported for the pentaammineruthenium histidine complex: Sundberg & Gupta, p. 39.

[9] Hermodson, M., Mahoney, W. *Meth. Enzym.* **91**, 352 (1983).

[10] Matthews, C., Recchia, J., Froebe, J. *Anal. Biochem.* **112**, 329 (1981).

more than *one potential* site of modification (of each ligand type) be present on a single peptide. In principle, if the protein cleavage is complete, and the peptides are well-resolved, only the shifted peptides need be analyzed.

250 units (~1mg) SMP were dissolved in 2.5mL 1mM HCl, and stored in 500μL aliquots in liquid nitrogen until needed.

A 25μL aliquot of SMP solution was added to each of eight micro-centrifuge tubes containing 500μL of a ~2mg/mL cytochrome solution in 1%(w/v) $NaHCO_3$ (~pH 8.3). A second 25μL aliquot of SMP was added after 6 hours. The reaction mixtures were incubated at ~37°C for a period of 32 hours; 33μL 2M HCl were added to halt the digestion. Samples were then frozen until analyzed.

The reaction mixtures were analyzed by HPLC. The peptide products were separated on a C4 column, maintained at 27°C, at a flow rate of 1 mL/min., using the following elution method: 5 minute hold at 0%B, 0-10%B in 12 min., 10-15%B in 18 min., 5 min. hold at 15%B, 15-40%B in 64 min., 40-100%B in 10 min., where A = 0.1%TFA, 0.1%TEA in H_2O, and B = 0.1%TFA, 0.1%TEA, 10%H_2O in CH_3CN (mobile phase was prepared fresh daily). Samples were thawed and filtered, and an aliquot of at least 100μL was used to flush and fill the 20μL loop. Peptides were detected by their absorption at 220nm, and those containing ruthenium were identified as such by their absorption at 300nm (λ_{max}) and lack of absorption at 400nm.

For preparative runs, the 32-hour digest of an entire milligram of cytochrome was taken to dryness in the SpeedVac, and then dissolved in 125μL of solvent "A". Following filtration (by centrifugation through a 4mm type HV 0.45μ Millipore filter in a microcentrifuge tube)

the entire sample was loaded into a 200μL loop, and eluted as described above. The effluent was typically collected in 1mL fractions, with a delay of 500μL to allow for the dead volume between the detector cell and tubing outlet.

UV-visible spectra of peptides suspected of containing ruthenium were recorded. Spectra were also recorded of the peptide solutions made basic by the addition of 0.1% (v/v) triethylamine.

Fractions including peptides of interest were pooled as appropriate and concentrated in the SpeedVac. The peptides were further purified by elution from the same C4 column, using elution conditions similar to the original. Pooling of fractions, concentration, and purification were repeated until a single, symmetric peak was evident in the chromatogram.

The peptide solution, as eluted from the HPLC, was transferred to a hydrolysis tube and lyophilized. The residue was dissolved in one milliliter of constant-boiling HCl (Pierce), and the solution was subjected to at least three freeze-pump-thaw cycles. The tube was closed off under vacuum, and placed in a Reacti-Therm block maintained at 110^{o}C. After 24 hours, the sample was removed from the block and taken to dryness on a vacline or in the SpeedVac. 1mL H_2O was added to the residue, and this was again taken to dryness. Dissolution and drying were repeated. The residue was dissolved in borate/CH_3CN and aliquots were derivatized in the presence of at least five equivalents of FMOC-Cl. Amino acid analyses were carried out as described in appendix 1.

A peptide mixture resulting from a 32 hour SMP digestion of native *C. krusei* cytochrome *c* was utilized to optimize the separation of the digestion products. An initial five minute hold at 0%B was

chosen to permit preparative samples to be washed free of salt which might otherwise interfere with the peptide resolution (better resolution, however, can be obtained without this hold in the absence of large quantities of salt).

Spectroelectrochemistry

Spectroelectrochemistry of *C. krusei* cytochrome *c* requires the presence of a mediator, a redox active species of reduction potential similar to that of the protein under study. The $[A_5Rupy]^{2+/3+}$ used in this case serves to interact with the electrode, and shuttles electrons to the protein, which itself is slow to transfer electrons with the electrode.

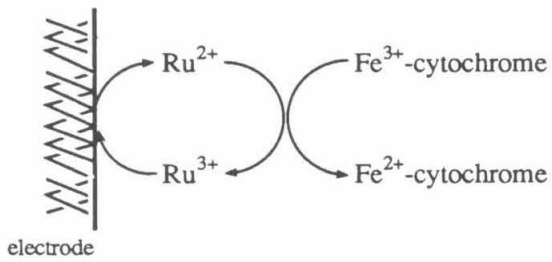

Figure 3.3. Schematic representation of the role of $[A_5Rupy]^{2+/3+}$ (="$Ru^{2+/3+}$") as a redox mediator.

The spectroelectrochemical studies were performed using a non-isothermal configuration, in which the working electrode and the reference electrode are maintained at different temperatures. This is done for convenience, as the reference electrodes are very slow to equilibrate following changes in temperature. The formal potential of the reference electrode was corrected for slight fluctuations in the

room temperature using the following equation:[11]

$$E^{o}(T) = 0.2444 - 0.00066\ (T - 25^{o}C)$$

A description of a typical spectroelectrochemistry experiment follows. The potential of the working electrode ($E_{applied}$) is stepped (in either direction) through a range which covers both electrochemical extremes, *i.e.*, total oxidation and total reduction of the protein, in eight to ten increments. The protein is monitored optically as a function of time, at a wavelength where its absorbance is redox-sensitive, commencing with the potential step. Once a constant absorbance (indicative of protein, mediator, and electrode equilibration) is obtained, as large a portion of the UV-visible spectrum as is feasible is recorded to check for the presence of isosbestic points. Using the final absorbance reading for each potential, the relative amounts of reduced and oxidized cytochrome can be calculated. The relevant expression is:

$$[ox]/[red] = (A_r - A_i)/(A_i - A_o)$$

where A_r and A_o are the absorbances of the totally reduced (red) and totally oxidized (ox) protein, and A_i is the absorbance at the individual potential of interest. For systems obeying the Nernst equation, a plot of the applied potential versus the logarithm (base 10) of the molar ratio of reduced to oxidized species yields a line of slope $2.303RT/n\mathcal{F}$ and an intercept equal to the formal reduction potential of the redox couple of interest:[12]

[11] Ives, D., Janz, G. in *Reference Electrodes*, Academic Press (New York), 1961, p. 161, cited by Lin, J., Breck, W. *Can. J. Chem.* **43**, 1766 (1965).

[12] Bard, A., Faulkner, L. *Electrochemical Methods*, J. Wiley (New York), 1980, p. 51.

$$E = E^{o} - (RT/n\mathcal{F}) \ln ([red]/[ox])$$

where R, T, n, and $\mathcal{F}$ are the universal gas constant, temperature, the number of equivalents of electrons involved in the redox process, and the Faraday constant, respectively.

The temperature dependence of the formal reduction potential yields information regarding the thermodynamics of the reduction process:

$$\Delta G^{o} = -n\mathcal{F}E^{o} = \Delta H^{o} - T\Delta S^{o}$$

$$E^{o} = (\Delta S^{o}/n\mathcal{F})T - (\Delta H^{o}/n\mathcal{F})$$

For a nonisothermal cell arrangement in which the effects of temperature gradients can be neglected, the value of the entropy difference derived from a temperature dependence study is that of the redox couple only, ΔS_{rc}.[13] Using the value of 15.6eu for the hydrogen half reaction,

$$\Delta S^{o}_{cell} = \Delta S^{o}_{rc} + (nS^{o}_{H+} - (n/2)S^{o}_{H_2})$$

$$\Delta S^{o}_{cell} = \Delta S_{rc} - 15.6eu$$

a value for the complete reaction (*vs.* NHE) can be obtained.[14]

The visible lamp of the spectrophotometer was lit for at least one hour prior to commencement of the experiment. A baseline was recorded (*i.e.*, automatically subtracted from subsequent scans) with the OTTLE cell filled with water. *C. krusei* cytochrome *c* was monitored at 548nm; the analogous band in horse heart cytochrome *c* (λ_{max}=550nm) has

[13] Yee, E., Cave, R., Guyer, K., Tyma, P., Weaver, M. *J. Amer. Chem. Soc.* **101**, 1131 (1979).

[14] Taniguchi, V., Ellis, W., Cammarata, V., Webb, J., Anson, F., Gray, H. *Adv. Chem. Ser.* **201**, 51 (1982), K. Kadish, ed., *Electrochemical and Spectrochemical Studies of Biological Redox Components*, American Chemical Society, Washington D.C., and references therein.

a difference of $18500 M^{-1} cm^{-1}$ in extinction for the two redox states at this wavelength.[15] The mediator has negligible absorption at this wavelength.[16] The 600-500nm range of the visible spectrum was scanned (0.5nm/second) after equilibration at each potential step; the strong Soret absorption at 409nm prevented the recording of meaningful spectra at higher energies. The direction of the potential steps was alternated with each temperature. The data for the native cytochrome was recorded with a single sample, starting from the lowest temperature and working upward to prolong the "life" of the protein. Two samples (of the same preparative batch) were required to obtain all data for the modified derivative.

The symbol $E^{o'}$ is used to denote reduction potentials determined at pH 7, as per convention.

Differential Pulse Polarography

Spectroelectrochemistry cannot be used to determine the reduction potential of the ruthenium site in the modified protein, as absorption by the heme dominates at all wavelengths of absorbance of the ruthenium chromophore. Differential pulse polarography (DPP) has been used instead.

In DPP, the potential range of interest is scanned while the current is monitored. Hence, a mediator cannot be employed, as it would produce signals which would obscure the data. Some success has

15 ε(oxidized)=$9100 M^{-1} cm^{-1}$; ε(reduced)=$27600 M^{-1} cm^{-1}$; Margoliash & Frohwirt, p. 570.

16 Ford, P., Rudd D., Gaunder, R., Taube, H. *J. Amer. Chem. Soc.* 90, 1187 (1968).

been achieved in the use of promoters, redox inactive molecules which facilitate electron transfer between protein and electrode, and horse heart cytochrome *c* has been reported on extensively in this regard.[17] It has been postulated that 4,4'-bipyridine enhances the rate of electron transfer by adsorbing to the electrode while also hydrogen-bonding the cytochrome via its surface lysine residues.[18] A similar molecule, 4,4'-dipyridyl disulfide (Aldrithiol-4), is required in the case of *C. krusei* cytochrome *c*, as the yeast protein tends to denature on the electrode surface more readily than the horse cytochrome. This process is delayed somewhat by Aldrithiol, which seems to have a greater affinity for the electrode by virtue of its disulfide moiety.[19]

Like the spectroelectrochemical experiments, DPP was performed in a nonisothermal arrangement. The button electrode was cleaned manually by polishing the gold surface on a piece of felt moistened with a slurry of fine alumina, and then thoroughly rinsing it with water. The electrode was then electrochemically cleaned by sweeping (20mV/s) twice through the -1.0 to +1.3V (*vs.* SCE) potential range in μ=0.1M pH 7 NaP_i. This process was repeated for each complete scan.

Samples were 0.25mM in cytochrome and approximately 0.3mM in Aldrithiol-4 in μ=0.1M pH 7 NaP_i. Samples were continuously purged with a gentle stream of argon, except while scanning the potential. The potential range of -0.4V to 0.35V was scanned at a rate of 2mV/s

[17] Eddowes, M., Hill, H. *J. Amer. Chem. Soc.* **101**, 4461 (1979).

[18] Eddowes, M., Hill, H., Uosaki, K. *J. Amer. Chem. Soc.* **101**, 7113 (1979).

[19] Niwa, K., Furukawa, M., Niki, K. *J. Electroanal. Chem.* **245**, 275 (1988).

using a drop time of 0.5s and a pulse amplitude (ΔE) of 25mV. For a reversible system, Parry and Osteryoung have shown that the peak potential, E_p, is related to the half-wave potential, $E_{1/2}$, by the following expression:[20]

$$E_{1/2} = E_p + (1/2)\Delta E$$

for a cathodic wave. Rather than apply this correction, the reduction potentials were determined to be the average of the potentials of maximum current from forward (anodic) and backward (cathodic) scans. The diffusion coefficients of the reduced and oxidized species are assumed to be equal, hence $E_{1/2}=E^{o'}$, *i.e.*, the half-wave potential is equal to the formal reduction potential.[21]

Three determinations of reduction potential were made at each temperature and averaged. Temperature was measured at the beginning and end of each scan, and upon reversing the scan direction, but the thermocouple was never present in solution while scanning, as its presence gave rise to disturbances in the signal. Data was collected approximately every five degrees, from 5 to 40°C.

Modeling Studies

The starting point for both horse and *C. krusei* model cytochrome structures was the reduced tuna cytochrome crystal structure[22] (1.5Å resolution) coordinates data set, as obtained from the Brookhaven Data

[20] Parry, E., Osteryoung, R. *Anal. Chem.* **37**, 1634 (1965).

[21] Bard and Faulkner, p. 160.

[22] Takano, T., Dickerson, R. *J. Mol. Biol.* **153**, 79 (1981), and references therein.

Bank.[23] The reduced state was used for the study of histidine accessibility, as this is the redox state in which the modification reaction occurs. The portions of polypeptide which extend beyond the 103 residues of tuna were excluded (residue 104 of horse cytochrome, and the six-residue N-terminal extension of *C. krusei* cytochrome). Inclusion of the *C. krusei* N-terminal extension in the surface area calculations is not expected to alter the result: both residues 33 and 39 are at least 17Å from the closest N-terminal residue (residues -6 through -1). Residue 103 of cytochrome *c* resides within 5Å of residue 33; residue 104 is further removed, but its exclusion may result in an overestimation of the His33 accessibility in horse heart cytochrome.

To construct cytochrome of another species from tuna cytochrome, the appropriate residue substitutions were made, and each new side chain was then aligned as well as possible with that which it replaced.[24] No solvation or energy minimization of the resultant structures was performed.

Surface areas of particular residues were determined by the method of Connolly[25] using all atoms (except water molecules) within 7Å to define the local topology. Probe radii of 1.4Å and 3.5Å were used to define the solvent-accessible and reagent-accessible surfaces, respectively.[26]

[23] Bernstein, F., Koetzle, T., Williams, G., Meyer, E., Brice, M., Rodgers, J., Kennard, O., Shimanouchi, T., Tasumi, M. *J. Mol. Biol.* **112**, 535 (1977).

[24] A recent survey of homologous proteins has found this to be a valid assumption: Summers, N., Carlson, W., Karplus, M. *J. Mol. Biol.* **196**, 175 (1987).

[25] Connolly, M. *Science* **221**, 709 (1983).

RESULTS

Electron Paramagnetic Resonance Spectroscopy

EPR spectra for the model complex, $[A_5RuHis]^{3+}$, and native and modified *C. krusei* cytochromes *c* are presented in figure 3.4. Two signals are evident in the native spectrum, and correspond to g values of 3.12 and 2.2. The third, high field signal was not observed, and is reported to be broad and evident only in spectra of highly concentrated solutions.[27] These results are in fair agreement with those of Brautigan *et al.*,[28] who found cytochromes *c* could be grouped into two distinct classes characterized by g values of 3.06, 2.26, & 1.25, and 3.2, 2.05, & 1.39. The former class includes horse, tuna and *S. cerevisiae* iso-1 cytochromes, while the latter includes *S. cerevisiae* iso-2 cytochrome *c* and cytochromes c_2 and c_{550}. The difference was suggested to result from differences in the hydrogen bonding or protonation of the His18 ligand. The author could find no previously reported EPR data for the *Candida* cytochrome.

The low field signal at a g value of 2.89 for the ruthenium model compound, $[A_5RuHis]^{3+}$ is similar to that observed by Margalit *et al.* (g=2.95).[29] These workers did not report any higher field signals.

[26] The Ru-N bond length in hexaammineruthenium(II), $[Ru(NH_3)_6]^{3+}$, is 2.1Å: Stynes, H., Ibers, J. *Inorg. Chem.* **10**, 2304 (1971). Ru-N bond lengths of 2.07-2.12Å have been reported for (L-histidinato)pentaammineruthenium(III) chloride: Krogh-Jesperson, K., Westbrook, J., Potenza, J., Schugar, H. *J. Amer. Chem. Soc.* **109**, 7025 (1987).

[27] Palmer, G. in *The Porphyrins*, D. Dolphin, ed., vol. IV, Physical Chemistry, Part B, Academic Press (San Francisco), 1979, p. 313.

[28] Brautigan, D., Feinberg, B., Hoffman, B., Margoliash, E., Peisach, J., Blumberg, W. *J. Biol. Chem.* **252**, 574 (1977).

[29] Margalit, R., Kostić, N., Che, C.-M., Blair, D., Chiang, H.-J.,

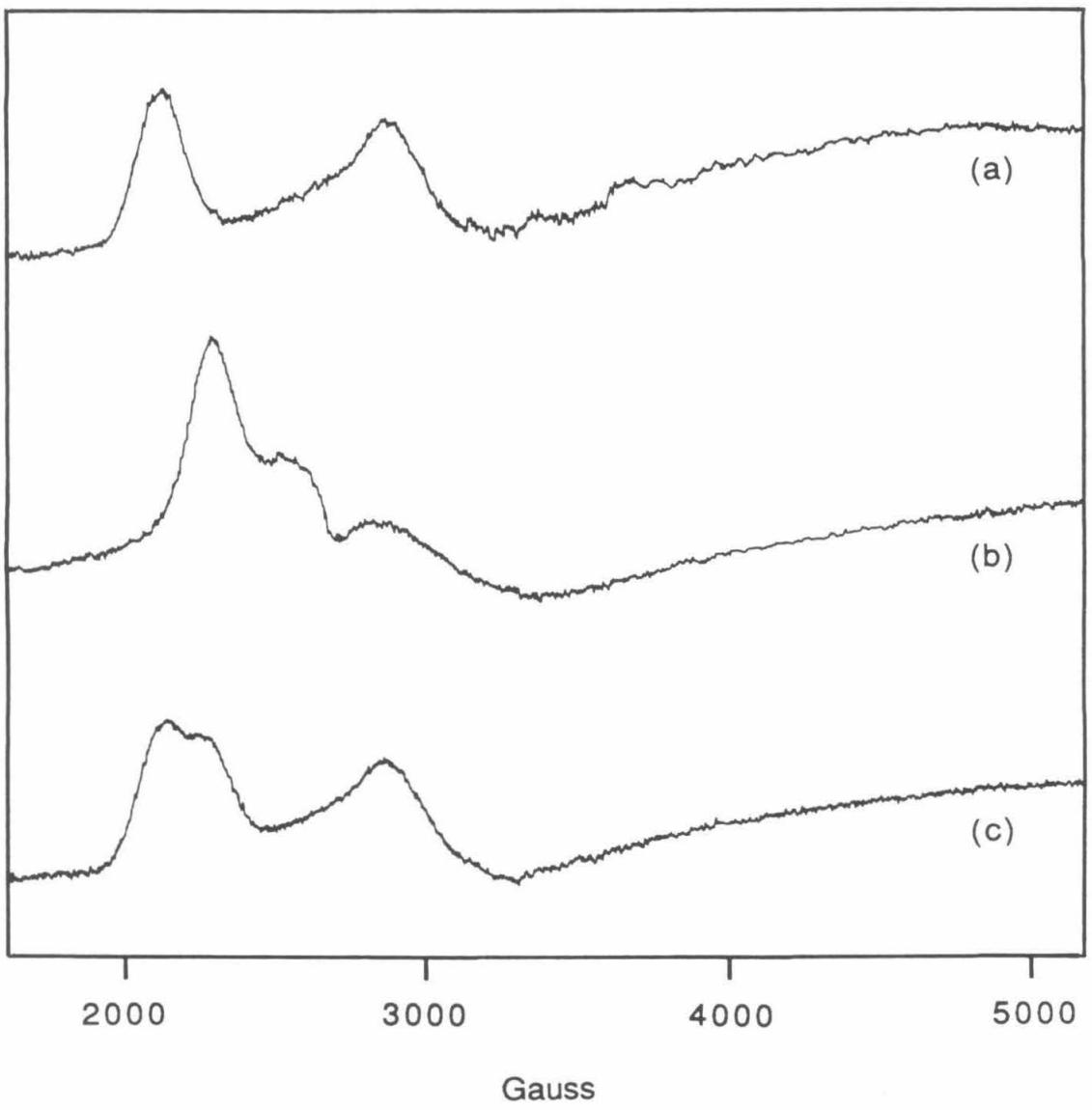

Figure 3.4. EPR spectra of (a) 2mM native *C. krusei* cytochrome *c*, (b) 7.73mM $[A_5RuHis]Cl_3$, (c) 1.85 mM A_5Ru-modified *C. krusei* cytochrome *c*. Protein samples in μ=0.1M pH 7 NaP_i, complex in 0.1M NaAc, pH 5. Initial sample temperatures (rose as much as 0.5K during a run): (a) 12.6K, (b) 12.8K, (c) 13.3K. Other conditions: modulation amplitude, 16G; power, 0.2mW; gain 1.6 x 10^4; frequency: (a) 9.245GHz, (b) 9.25GHz, (c) 9.247GHz.

The spectrum of the modified cytochrome derivative appears to be a superposition of the native cytochrome *c* and model complex spectra, suggesting modification at a histidine residue has occurred. Furthermore, it confirms that the integrity of the cytochrome fold and iron coordination sphere are maintained after modification.

This EPR spectrum does not rule out methionine modification, as a pentaammineruthenium complex would be expected to have a reduction potential of ~500mV, and therefore would not be oxidized by the $CoEDTA^-$ complex employed. The low spin d^6 ruthenium(II) configuration would be EPR silent.

NMR Spectroscopy

Two sharp resonances are evident in the NMR spectrum of native *C. krusei* ferricytochrome *c*, at δ8.62 and δ8.76 (ppm *vs.* DSS), and are presumed to be the signals of the C-2 protons of His33 and His39 (figure 3.5a). The pH dependence of these resonances support their assignment to histidine residues: both titrate with pK_a's of ~6.4 (*vide infra*). The His18 resonances are not found in this region of the spectrum, as they are contact-shifted due to the proximity of these protons to the iron ion.[30] By analogy to the horse and tuna ferricytochromes, the resonances of the highly conserved His26 are expected to be found upfield (δ6.8-7.8) due to ring current or pseudocontact shifts,[31] and are expected not to titrate in the pH 5-8

Pecht, I., Shelton, J., Shelton, R., Schroeder, W., Gray, H. *Proc. Natl. Acad. Sci.* **81**, 6554 (1984).

[30] Senn, H., Eugster, A., Wüthrich, K. *Biochem. Biophys. Acta* **743**, 58 (1983).

Figure 3.5. NMR spectra of (a) native and (b) A_5Ru-modified *C. krusei* ferricytochrome *c*, δ6.5-9.5ppm (*vs.* DSS). Conditions: pH 5.2, 25°C. Note that the sharp native resonance at δ8.62 is absent in the spectrum of the modified protein.

(a) native

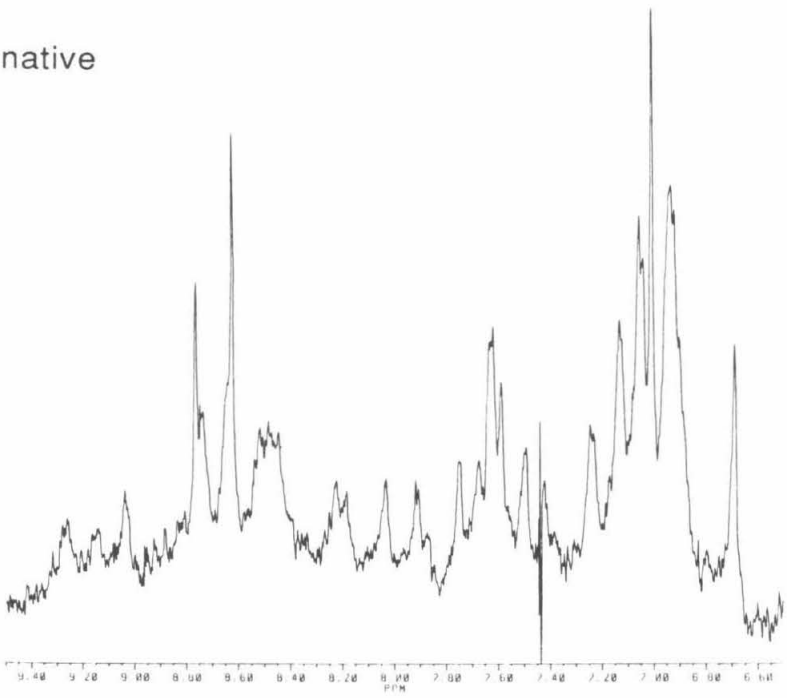

(b) modified

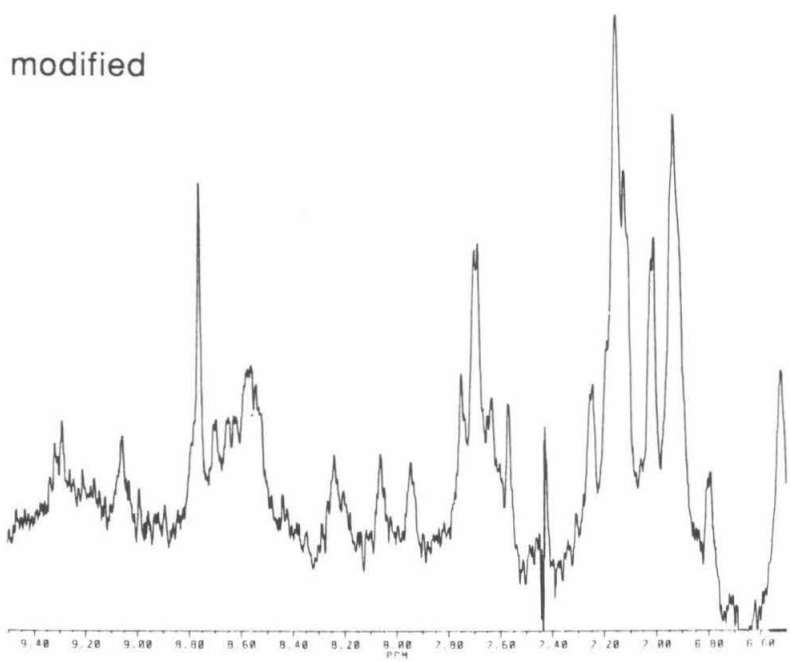

range.

NMR spectra were recorded for the native *C. krusei* ferricytochrome *c* at six pH values. This number is insufficient to correlate the high and low pH data (table 3.1), but does allow for the estimation of pK_a values. Data and possible titration curves are plotted for the two histidine resonances in figure 3.6 (for each curve, a second can be drawn through the remaining data points). In the δ6.7-9.1 region, only these two resonances were seen to shift and could be cleanly followed throughout the pH 4.2→8 range.

Data analysis does not allow for the correlation of the high and low pH data. While both curves 1 and 2 give good fits to the data in terms of correlation coefficients (table 3.2), curves 3 and 4 are best fit to lines with slopes more closely approaching the theoretical value of one. The results in any case are similar: pK_a values for the two histidines are approximately 6.55 and 6.33.

The observed chemical shifts, however, are in conflict with those values reported by Cohen and Hayes.[32] These workers reported C-2 histidine resonances at δ8.48 and δ8.62 relative to TMS for the same protein under identical conditions,[33] values which are both 0.14ppm upfield of the chemical shift values observed. This suggests the possibility of a systematic error, which might arise from using an inappropriate peak as the standard. There is, however, no resonance evident at δ0.14ppm *vs.* DSS which might be mistaken for the standard in

[31] Dobson, C., Moore, G., Williams, R. *FEBS Lett.* **51**, 60 (1975).

[32] Cohen, J., Hayes, M. *J. Biol. Chem.* **249**, 5472 (1974).

[33] Chemical shifts are as read from figure 6 of reference 32.

Table 3.1. Chemical shifts[a] of titrating histidine C-2 protons

pH	upfield	downfield
4.2	8.6430	8.75680
4.9	8.6110	8.74850
6.1	8.4043	8.47490
6.7	8.1340	8.33216
7.1	7.8977	8.28370
7.9	7.6570	8.19930

a. parts per million downfield of the methyl resonance of 2,2'-dimethyl-2-silapentane-5-sulfonate

Table 3.2. Parameters for least-squares fit of NMR titration data[a]

	Upfield[b]			**Downfield**		
Curve	m	pK_a	r^2	m	pK_a	r^2
1	1.212	6.337	0.995	0.8844	6.542	0.993
2	1.236	6.266	0.986	0.8859	6.562	0.996
3	0.9600	6.574	0.969	0.9425	6.335	0.973
4	0.9858	6.537	0.979	0.9555	6.371	0.987

[a] For curves 1 and 2, δ^+=8.643 and δ^o=8.18 for the upfield resonance, and δ^+=8.76 and δ^o=7.63 for the downfield resonance. The fits to curves 3 and 4 were evaluated using δ^+=8.643 and δ^o=7.630 for the upfield resonance, and δ^+=8.76 and δ^o=8.18 for the downfield resonance.

[b] Labels describe resonances according to their relative positions at pH 5.2.

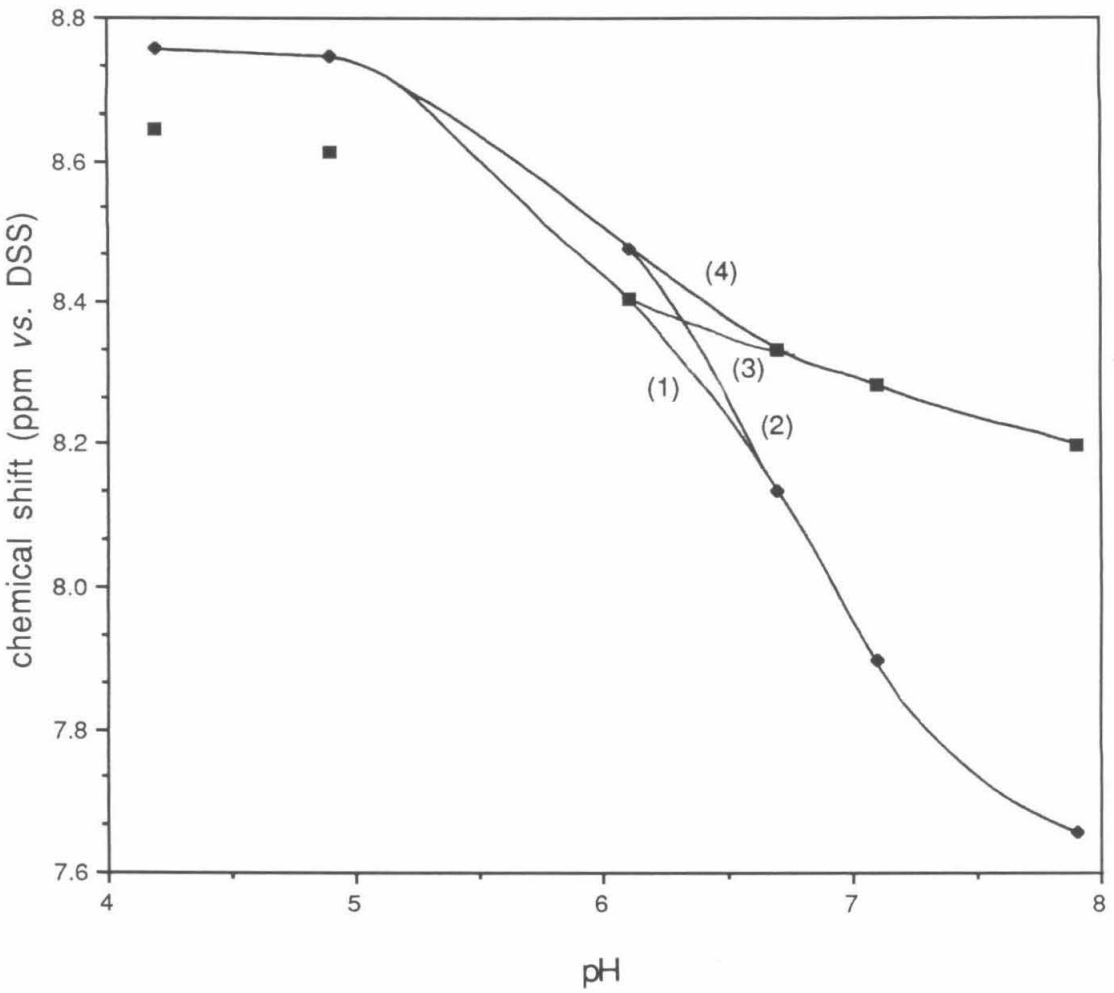

Figure 3.6. Titrating resonances of native *C. krusei* ferricytochrome *c*. Four possible titration curves are shown (to delineate what points were included in each fit); complementary curves can be drawn through the remaining points.

the cytochrome spectrum (TMS has a chemical shift identical to DSS; the former is soluble in organic solvent, while the latter is soluble in aqueous solution). The workers may actually have used a different internal standard, and incorrectly adjusted the chemical shift values to refer them to DSS. Resonances of residual water (δ4.8) and of the methylene protons (adjacent to the sulfonate moiety) of DSS (δ4.67)[34] in the samples in this work served as reference points in identifying the DSS methyl resonance.

Alternatively, one might consider that one chemical shift value is identical to that reported in the literature (δ8.62), and the other is in disagreement, but it is difficult to imagine how such a situation would result.

The sharp signal at δ8.62 found in the native cytochrome NMR spectrum is abolished in that of the modified cytochrome (figure 3.5b), indicating that the residue responsible for that resonance is a site of ruthenium modification. The paramagnetic and quadrupolar nature of the bound ruthenium (^{99}Ru: 12.7% abundant, I=3/2; ^{101}Ru: 17.1% abundant, I=5/2)[35] is expected to broaden and split the proton resonances of adjacent histidine residues. The second C-2 proton resonance appears to be unaffected by the reaction with the ruthenium reagent. A new resonance is evident at ~δ-32.5ppm in the spectrum of the modified protein (figure 3.7). It is likely to be a contact-shifted histidine resonance, as reported by Toi *et al.* for pentaammineruthenium(III)

[34] Pouchert, C., ed. *Aldrich Library of NMR Spectra*, vol. 2, Aldrich Chemical Co. (Milwaukee), 1983, p. 1003.

[35] Becker, E. *High Resolution Nuclear Magnetic Resonance*, Academic Press (New York), 1980, p. 285.

Figure 3.7. NMR spectra of (a) native and (b) A_5Ru-modified *C. krusei* ferricytochrome *c*, δ-22 to -38 ppm (*vs.* DSS). Conditions: pH 5.0, 25°C. A new resonance is evident at δ–32.5 in the spectrum of the modified protein.

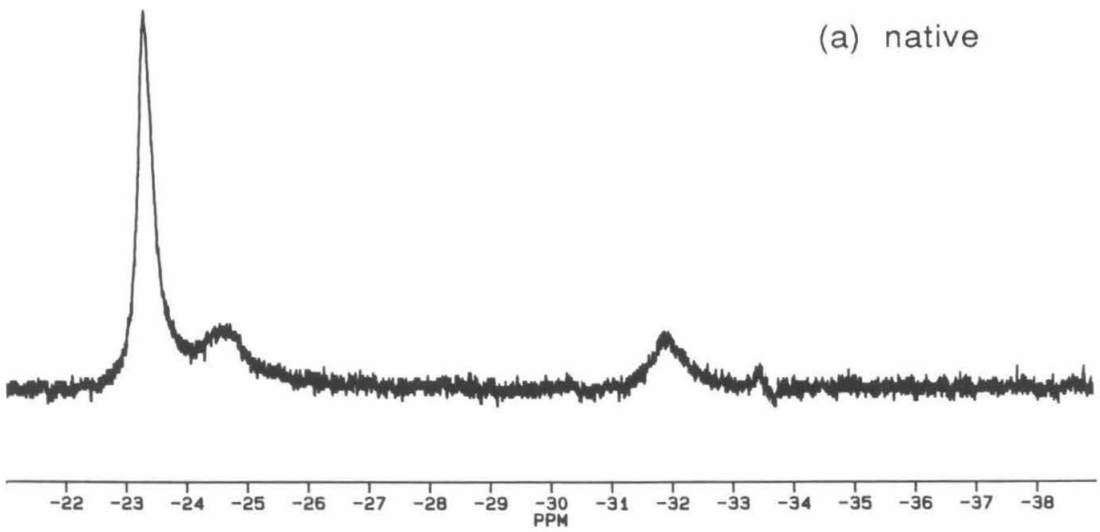
(a) native
-22 -23 -24 -25 -26 -27 -28 -29 -30 -31 -32 -33 -34 -35 -36 -37 -38
PPM

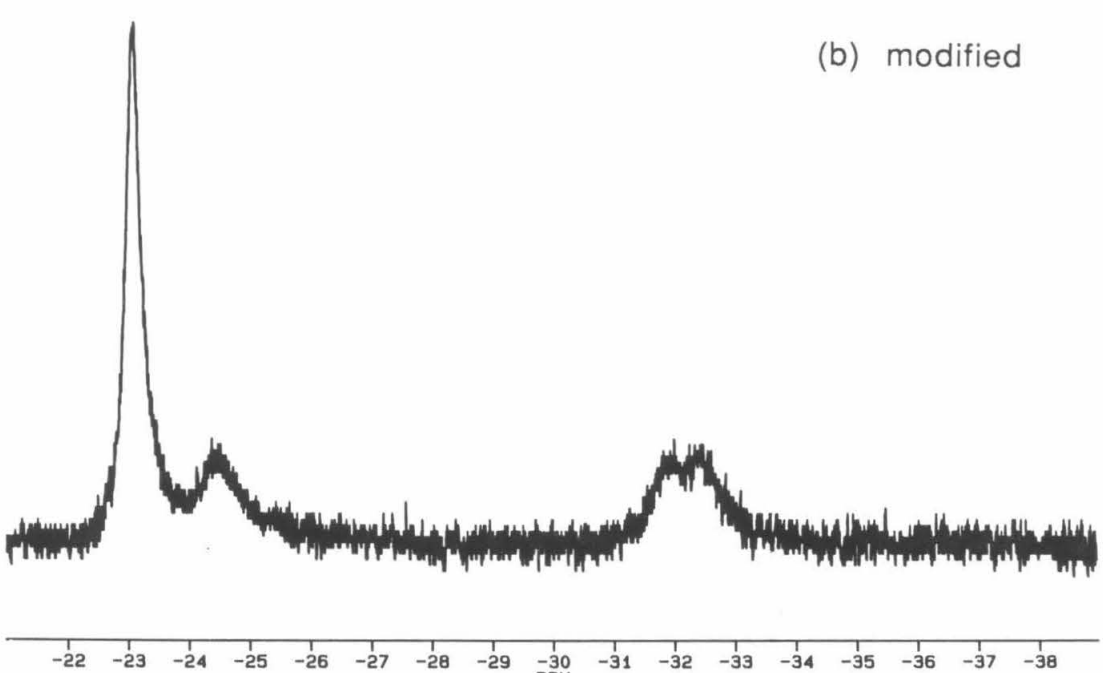
(b) modified
-22 -23 -24 -25 -26 -27 -28 -29 -30 -31 -32 -33 -34 -35 -36 -37 -38
PPM

derivatives of sperm whale myoglobin.[36]

Robinson *et al.* have assigned the upfield resonance to His33 and the other to His39 in the very similar *S. cerevisiae* cytochrome in the reduced state.[37] No chemical shift values for the ferricytochrome resonances were reported. Assuming the resonances maintain their relative positions between oxidation states, and assuming the disagreement between chemical shift values from the work of Cohen and Hayes and this work arises from a systematic error in the former (*vide supra*), one would interpret the spectrum of the modified cytochrome as an indication of modification at His33. Alternatively, the spectrum could be taken as evidence for His39 modification (see figure 3.8). Regardless of the assignment, it is clear from the NMR spectrum that one histidine is extensively modified by the A_5Ru moiety, while the other is not.

UV-visible Difference Spectroscopy

The UV-visible absorption spectra of native and A_5Ru-modified *C. krusei* ferricytochromes *c* are exceedingly similar, with maxima at 696, 528.5, 409, 360, and 280 nm. UV-visible difference spectroscopy reveals a chromophore with a wavelength of maximal absorbance at 300nm (figure 3.9), consistent with the spectral properties of the $[A_5RuHis]^{3+}$ model complex. The intensity of this absorption is such that a 1:1 [ruthenium]:[cytochrome] ratio is indicated. Differences in

[36] Toi, H., LaMar, G., Margalit, R., Che, C.-M., Gray, H. *J. Amer. Chem. Soc.* **106**, 6213 (1984).

[37] Robinson, M., Boswell, A., Huang, Z., Eley, C., Moore, G. *Biochemical J.* **213**, 687 (1983).

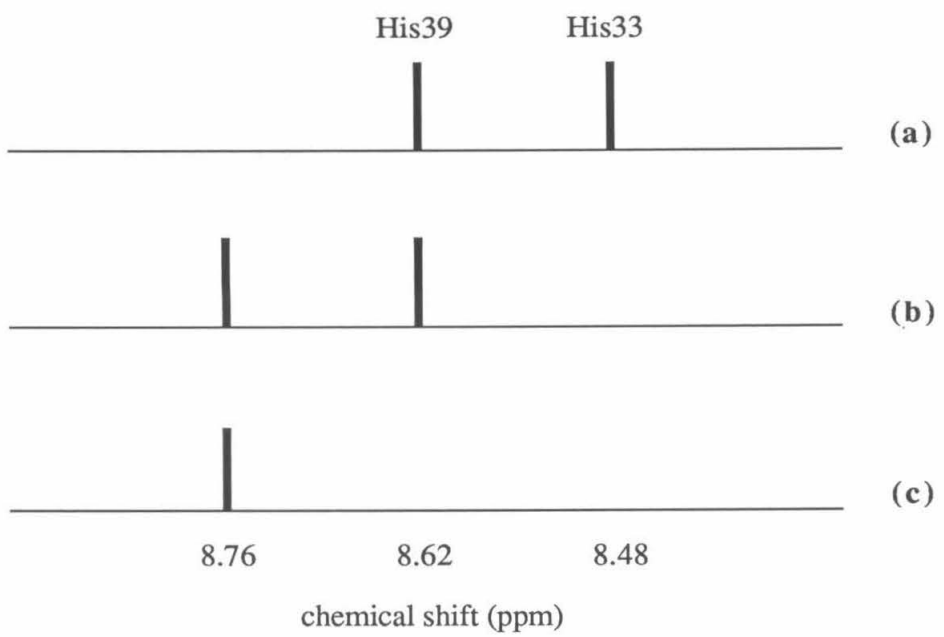

Figure 3.8. Clarification of discrepancy in histidine C-2 proton resonance chemical shifts: (a) as read from figure 6 of reference 32, with assignments given by Robinson *et al.* for *S. cerevisiae* ferrocytochrome above; (b) this work, as observed for native *C. krusei* ferricytochrome *c* at pH 5.2; (c) this work, as observed for A_5Ru-*C. krusei* ferricytochrome at pH 5.2. An assumption could be made that a systematic error is the cause of the discrepancy between (a) and (b), in which case one would assign the modification site to the residue responsible for the upfield resonance, His33. Alternatively, one could assume δ8.62 corresponds to the His39 proton, with no explanation for the discrepancy of the second resonances. One would then conclude His39 had been modified.

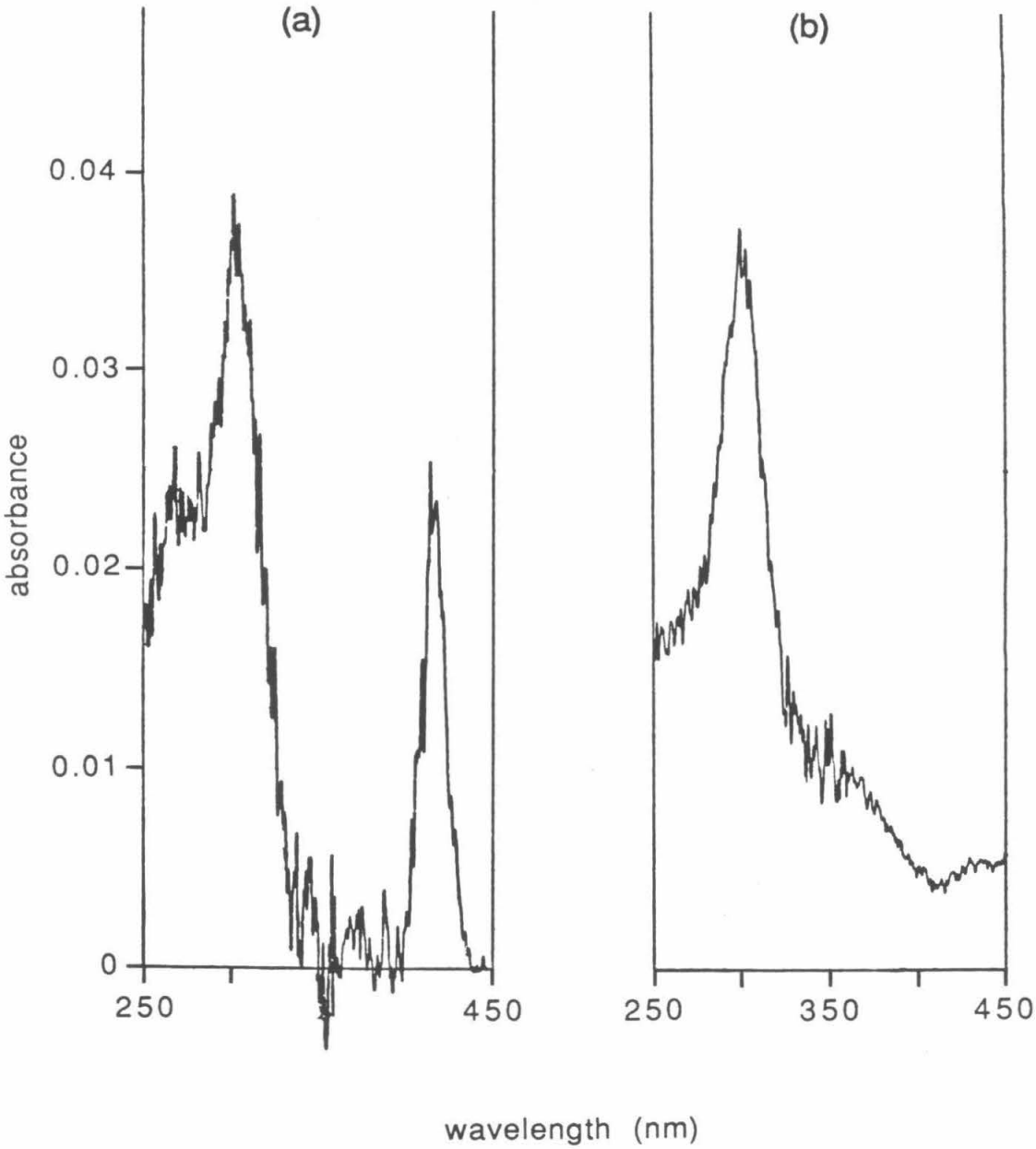

Figure 3.9. (a) UV-visible difference spectrum of A_5Ru-modified *C. krusei* cytochrome *c* minus native cytochrome *c* (~18μM); (b) UV-visible spectrum of ~18μM $[A_5RuHis]Cl_3$.

absorption between the difference spectrum and a spectrum of the model complex can be attributed to differences in the proportions of redox states in the native and modified cytochrome samples, *e.g.*, the spectrum in figure 3.9(a) indicates the modified sample contained 3.5% more of the reduced form than the native sample, and hence higher absorption is observed below 280nm and in the ~410-440nm region (horse cytochrome isosbestic points occur at 339, 410, and 434nm).[38]

Peptide Mapping

Because of the uncertainty in the NMR histidine C2-^{1}H assignments, peptide mapping was undertaken to obtain definitive evidence as to which histidine residue is modified in the derivative of interest. The submaxillaris protease (SMP) is reported to be very specific, cleaving peptide bonds involving the carboxyl group of arginine residues.[39] Five peptide products are expected (see figure 3.10), and His33 and His39 should reside on different peptides due to the presence of a cleavage site at residue (Arg) 38. However, the presence of numerous peptides in the native cytochrome 32-hour SMP digest (figure 3.11) suggested incomplete or excessive cleavage had occurred. Cleavage at sites other than arginine was confirmed by analysis of two native peptides. Peptides of ~4 and ~7 minutes retention were found to correspond to residues Tyr46-Arg54 and His39-Tyr48 (table 3.3), revealing unexpected cleavage after Gly45 and Tyr48, respectively. Such

[38] Margoliash & Frohwirt, p. 570.

[39] Schenkein, I., Levy, M., Franklin, E., Frangione, B. *Arch. Biochem. Biophys.* **182**, 64 (1977).

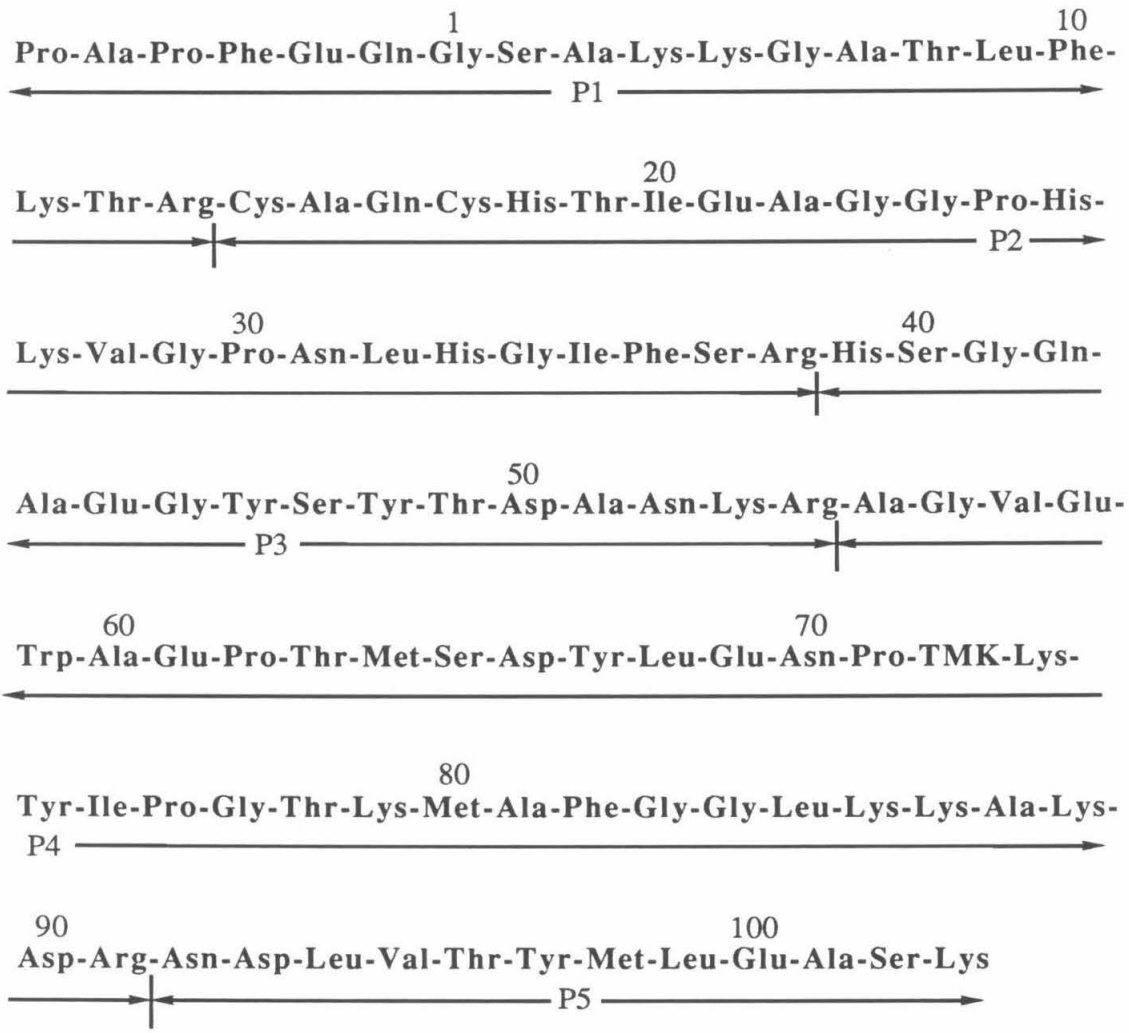

Figure 3.10. Peptides expected upon digestion of *C. krusei* cytochrome *c* by submaxillaris protease. The points of cleavage (after Arg residues) are indicated by vertical lines.

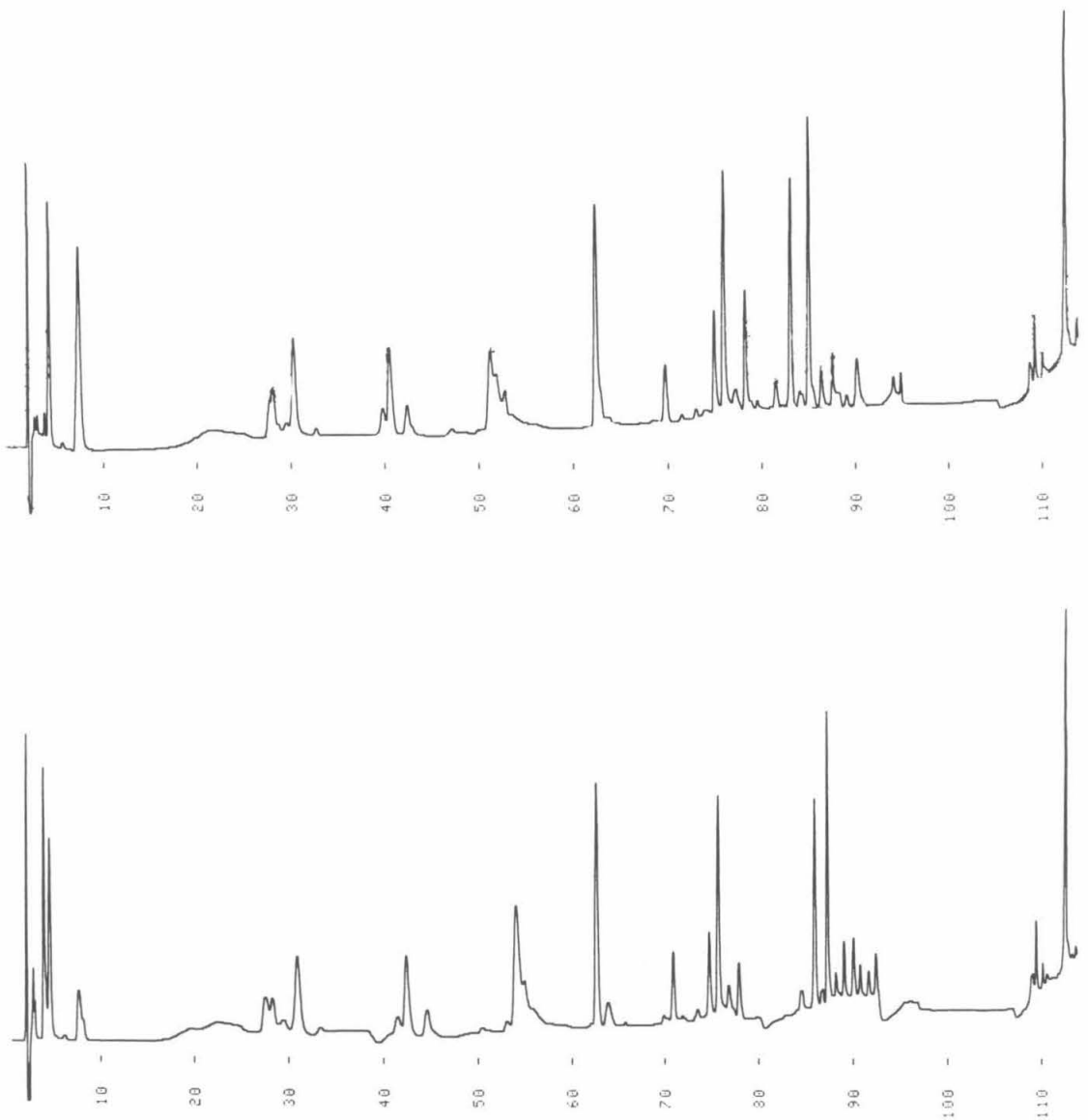

Figure 3.11. HPLC chromatograms of SMP peptides with 220nm detection. Elution profiles of ~40µg SMP digest of native *(upper)* and ruthenium-modified *(lower) C. krusei* cytochrome *c*, as monitored at 220nm (x axis is time, in minutes).

Table 3.3. Total amino acid analyses of native *C. krusei* cytochrome *c* SMP peptides

	peptide 1[a]		**peptide 2**[b]	
Amino acid	Found	Expected[c]	Found	Expected[d]
Arg	1.07	1	-	-
Ser	1.03	1	1.40	2
Asp	1.89	2	-	-
Glu	-	-	1.97	2
Thr	1.14	1	-	-
Gly	-	-	2.18	2
Ala	1.07	1	0.84	1
His/Lys[e]	+	-/1	+	1/-
Tyr[e]	+	2	+	2

a. retention time of ~4 minutes

b. retention time of ~7 minutes

c. on the basis of the peptide being Tyr46-Arg54 (Tyr-Ser-Tyr-Thr-Asp-Ala-Asn-Lys-Arg)

d. on the basis of the peptide being His39-Tyr48 (His-Ser-Gly-Gln-Ala-Glu-Gly-Tyr-Ser-Tyr)

e. + indicates that the presence of these amino acids was confirmed by HPLC resolution of their FMOC derivatives, but their amounts could not be quantified (see appendix 1)

adventitious cleavage may have resulted from contamination of the SMP with another protease.

The most dramatic difference between the chromatograms of the SMP digests of the native and ruthenium-modified *C. krusei* cytochromes *c* is the significant reduction in a native peptide with ~7 minutes retention, and the appearance of a new peak of 3-4 minutes retention in the digest of the modified protein (figure 3.11).

Chromatograms of the peptide mixtures with detection at 300nm (figure 3.12) indicate that there are several components in the modified cytochrome digest that absorb at this wavelength and which are absent in the native cytochrome digest. The 400nm elution profile (figure 3.13) of the ruthenium-modified cytochrome digest indicates that the 300nm-absorbing components common to both digests are probably heme fragments (native cytochrome *c* is retained at least 90 minutes).

The peptide of ~3-4 minutes retention was observed to have a 300nm absorption, which shifted to ~365nm upon the addition of base to the sample (figure 3.14). These spectral features are identical to those reported for the model $[A_5RuHis]^{3+}$ complex; upon deprotonation of the coordinated imidazole moiety (pK_a=8.9),[40] the ligand-to-metal charge transfer (LMCT) bands[41] are shifted to lower energy. In addition, upon alkalinization the absorbance at 300nm increased, presumably due to the presence of tyrosine; the ~275nm absorption of this amino acid shifts to ~295nm upon deprotonation of the phenolic side chain.[42]

[40] Sundberg, R., Bryan, R., Taylor, I., Taube, H. *J. Amer. Chem. Soc.* **96**, 381 (1974).

[41] Johnson, C., Henderson, W., Shepherd, R. *Inorg. Chem.* **23**, 2754 (1984).

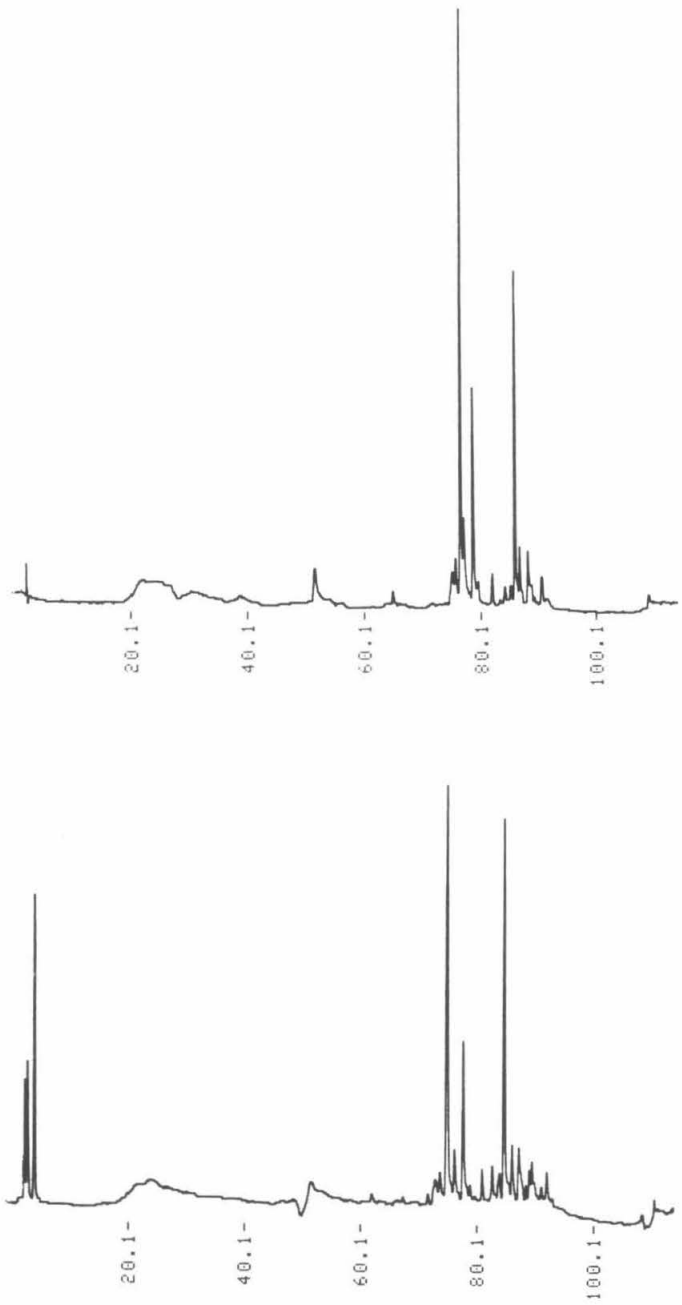

Figure 3.12. HPLC chromatograms of SMP peptides with 300nm detection. Elution profiles of ~40μg SMP digest of native *(upper)* and ruthenium-modified *(lower)* *C. krusei* cytochrome *c*, as monitored at 300nm (x axis is time, in minutes).

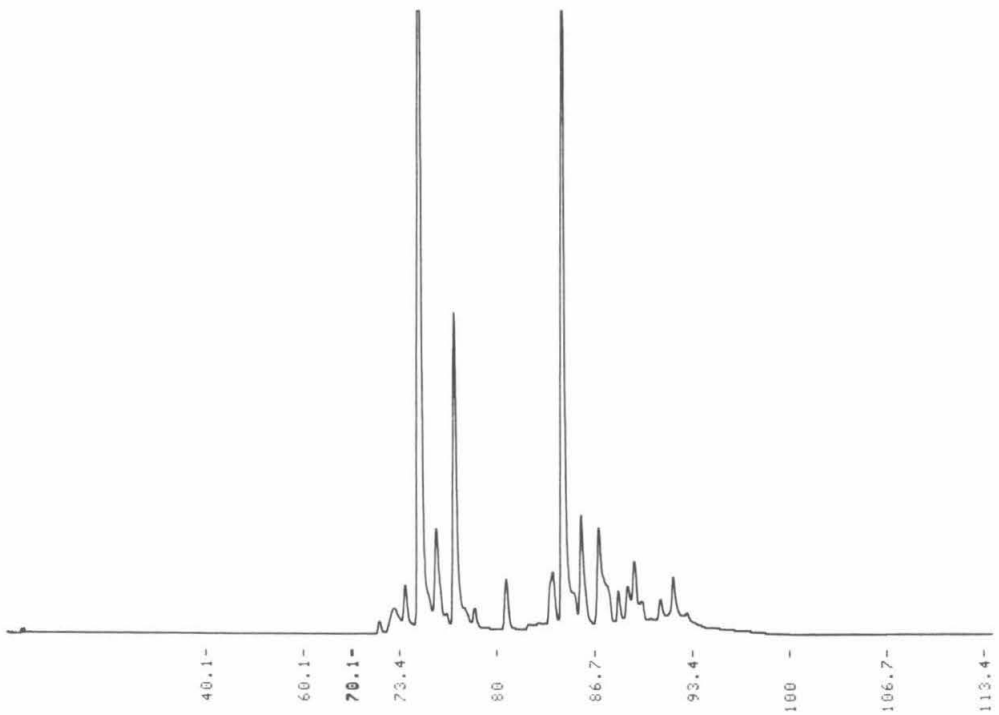

Figure 3.13. HPLC chromatogram of SMP peptides with 400nm detection. Elution profile of ~40μg SMP digest of ruthenium-modified *C. krusei* cytochrome *c*, as monitored at 400nm (x axis is time, in minutes). These fragments also absorb at 300nm (figure 3.12) due to their heme content.

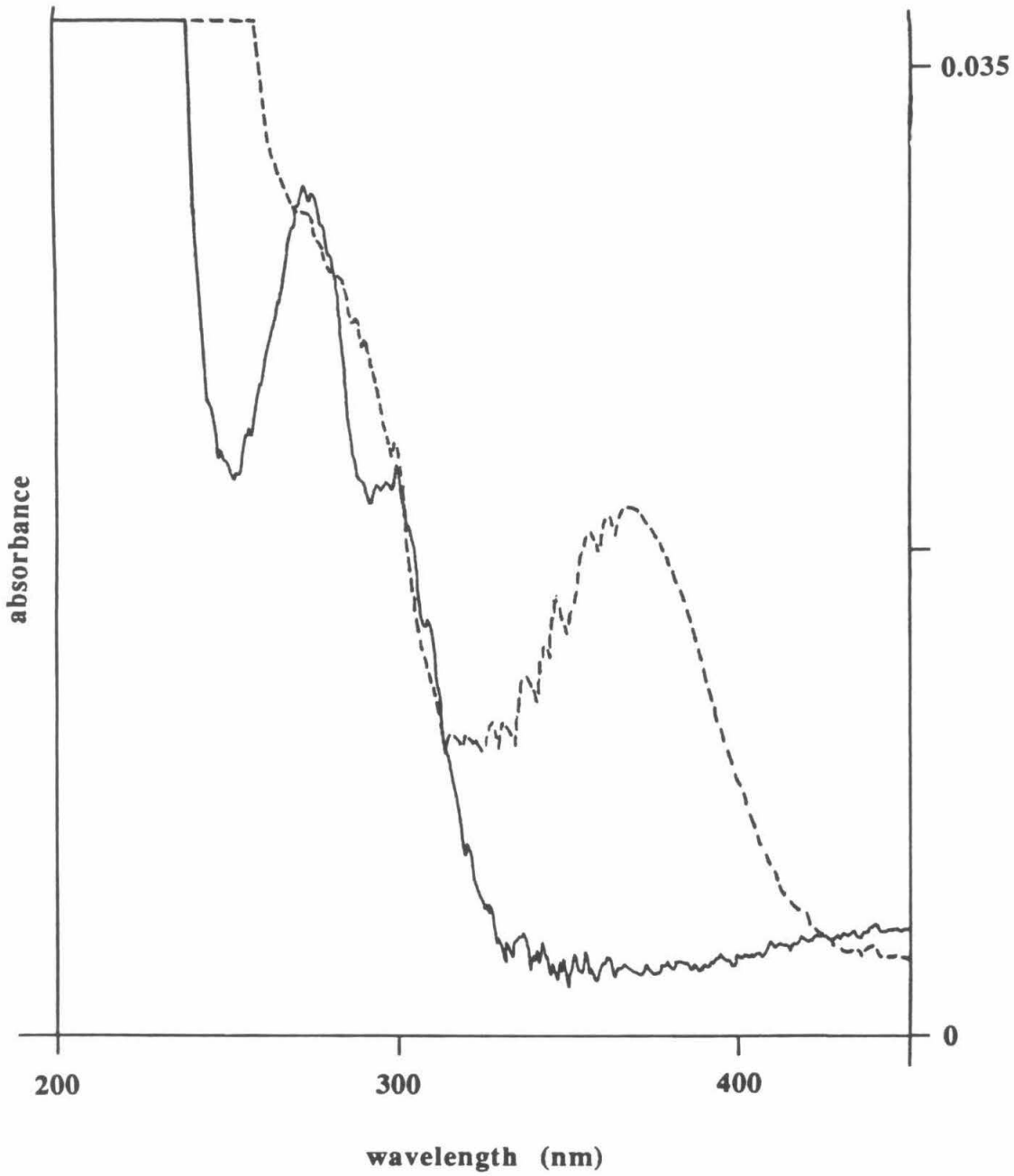

Figure 3.14. UV-visible spectrum of the ruthenium-containing peptide recovered from the SMP digest of the modified protein: — as eluted from the HPLC column; - - - after being made basic by the addition of TEA.

The composition of this new peptide, as determined by total amino acid analysis (table 3.4), uniquely defines the site of modification, as it corresponds to only one portion of the *C. krusei* cytochrome *c* sequence, *i.e.*, His39 through Tyr46.

The additional peaks eluting near the void volume had intense UV absorption below 250nm, but lacked the characteristic bands of the pentaammineruthenium histidine complex. A general red shift of 10-25nm was observed upon alkalinization, but no maximum emerged at ~365nm. The spectrum (in 0.1% TFA) is similar to that reported for the pentaammineruthenium(III) methionine complex (in 4N HCl),[43] but it is difficult to understand how this species might have formed, as $CoEDTA^-$ is not a sufficiently strong oxidant to oxidize pentaammineruthenium(II) methionine (E^o=380 *vs.* 500mV, respectively).[44] Electrochemical studies provide no evidence to support modification at a methionine residue in the intact protein (*vide infra*). The early-eluting components may have been decomposition products of some sort (see appendix 2). Upon attempting to repurify the components for amino acid analysis, retention volumes and peak areas were found to be irreproducible, suggesting the peaks were to some extent artifacts related to the high salt concentration of the samples.

The components of seven-minute retention remaining in the modified cytochrome digest may be unmodified His39-Tyr46 (resulting from decomposition of the ruthenium complex) or another peptide (analysis of

[42] Cantor, C., Schimmel, P. *Biophysical Chemistry*, Part 2, W. H. Freeman (San Francisco), 1980, p. 377.

[43] Stein, C., Taube, H. *Inorg. Chem.* **18**, 1168 (1979).

[44] Hin-Fat, L., Higginson, W. *J. Chem. Soc. A* 298 (1967).

Table 3.4. Amino acid analysis of the ruthenium-containing peptide recovered from the SMP digest of A_5Ru-modified *C. krusei* cytochrome *c* (3.9 minutes retention)

	Found	Expected[a]
Tyr[b]	+	1
Gly	1.88	2
Glu	1.49	2
Ala	1.14	1
Ser	0.91	1
His[b]	+	1

a. on the basis of the sequence of the peptide being that of residues 39 through 46: His-Ser-Gly-Gln-Ala-Glu-Gly-Tyr

b. + indicates that the presence of these amino acids was confirmed by UV spectroscopy of the peptide and by HPLC resolution of their FMOC derivatives, but their amounts could not be quantified (see appendix 1).

the seven-minute fraction of the native digest suggested it contained two peptides, only one of which was identified). It is interesting to note that His39 was found on different peptides in the native (His39-Tyr48) and modified (His39-Tyr46) digests, suggesting that the presence of the ruthenium label alters the site of cleavage, though not the protease specificity.

Spectroelectrochemistry

Determination of the heme reduction potential serves two purposes: it not only allows for the characterization of the redox thermodynamics, but also is a sensitive indicator of changes in the heme environment.[45] Hence, any major disruption of the native polypeptide fold in the modified protein is expected to result in an alteration of the cytochrome reduction potential.

Knowledge of the temperature dependence of the reduction potentials of the donor and acceptor are critical in understanding the temperature dependence of electron transfer rates.

Equilibration of the cytochrome with the electrode was rapid, and was usually attained within five minutes of setting the potential. Four isosbestic points were observed for the native cytochrome in the 600-500nm region; their positions fell in the ranges of 503-505, 523.5-525, 540-541, and 554-556 nm (figure 3.15). Isosbestic points of the modified protein were observed in the same ranges as three of the four

[45] (a) Varadarajan, R., Zewert, T., Boxer, S., Gray, H. *Science* **243**, 69 (1989); (b) Santucci, R., Reinhard, H., Brunori, M. *J. Amer. Chem. Soc.* **110**, 8536 (1988); (c) Walker, F., Emrick, D., Rivera, J., Hanquet, B., Buttlaire, D. *J. Amer. Chem. Soc.*, **110**, 6234 (1988); (d) Pielak, G., Mauk, A., Smith, M. *Nature* **313**, 152 (1985).

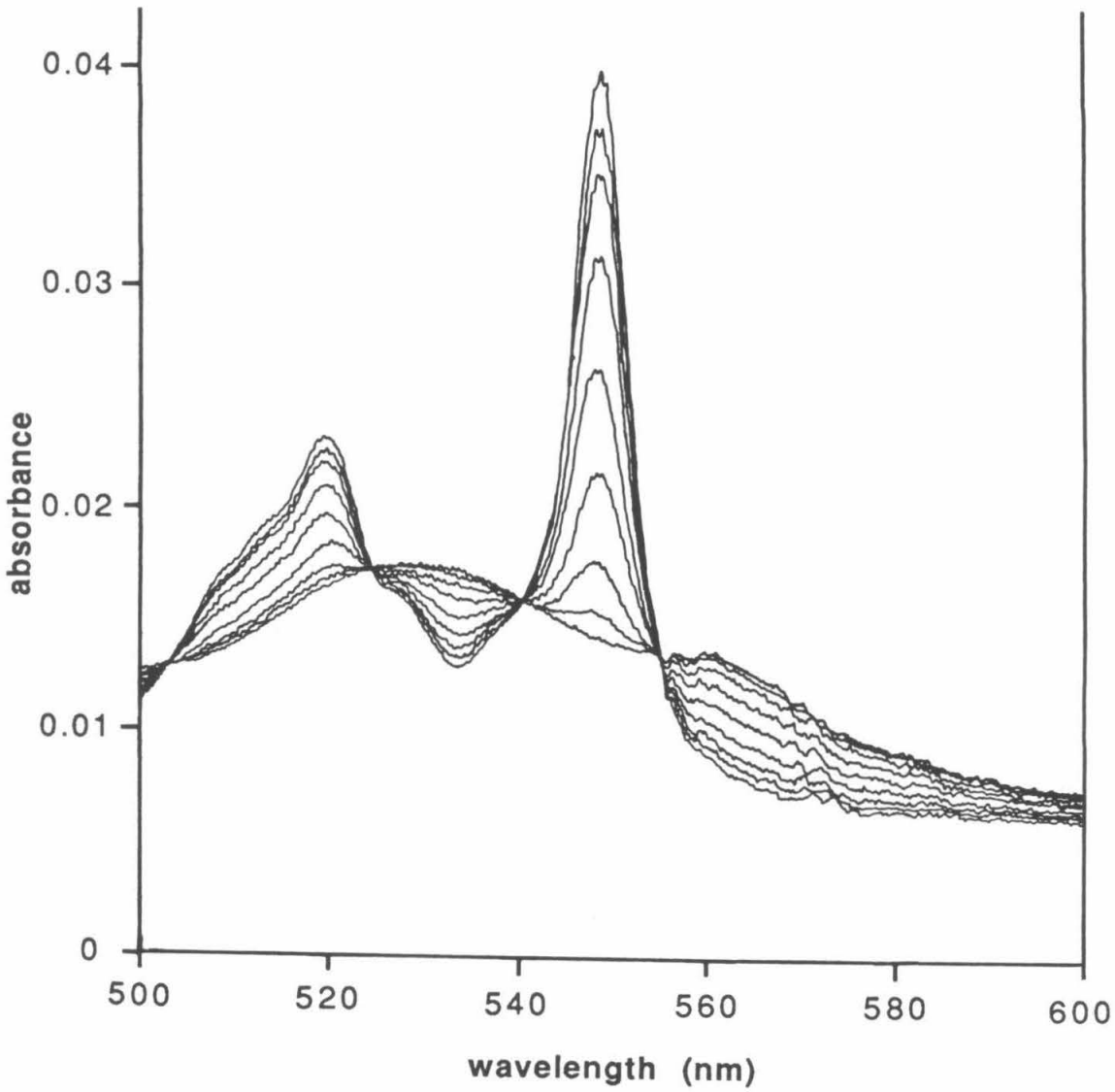

Figure 3.15. Family of visible spectra recorded during a spectroelectrochemistry experiment on native *C. krusei* cytochrome *c*, 24.4°C. Spectra were recorded at applied potentials of -230.9, -25.5, -6.1, 14.0, 34.8, 55.0, 79.9, 109.8, and 230.7 mV (*vs.* SCE), which correspond to the curves of the most to the least absorbance at ~550nm.

native points; the fourth, of highest energy, was observed at 502-503nm.[46] Isosbestic points were maintained throughout the potential steps for native samples maintained at 55°C or less, indicating no gross alteration of the protein conformation had occurred. Despite the presence of isosbestic points, results at 54.8°C indicate some thermal denaturation of the protein was occurring. The potential dropped precipitously (226.6mV *vs.* 247.3mV (*vs.* NHE) predicted by the lower temperature data), and the fit to the Nernst relation was poor (see appendix 3). This temperature is similar to that which has been reported to result in the partial denaturation of horse ferricytochrome *c*.[47]

At elevated temperatures, isosbestic points of the modified cytochrome were lost, suggesting an unfolding of the protein. The exact temperature varied from 36.6°C upward, depending on the history of the sample. The recovery of the isosbestic points upon reducing the temperature suggests that the denaturation process is a reversible one. The inability to obtain data for the modified protein at temperatures as high as those utilized for the native cytochrome suggests the cytochrome is somewhat destabilized by the modification.

The data for the spectroelectrochemical experiments are tabulated in appendix 3. The total change in absorbance for a sample typically fell to 80% of its original value by the completion of the experiment. The minimum absorbance observed, however, increased. Both may be attributed to denaturation and precipitation of the protein: should the protein precipitate onto the gold minigrid, the transmittance of the

[46] The significance of this difference is questionable, as the spectrophotometer chart drive was not working properly at times.

[47] Myer, Y. *Biochemistry* 7, 765 (1968).

electrochemical compartment might be reduced, thus giving rise to an apparent increase in absorption for the fully oxidized protein.

A typical Nernst plot is shown in figure 3.16. Data correlation is excellent, with r^2 values of 0.9994 or greater for the native cytochrome. The slopes of most of the Nernst plots agree well with the theoretical values (<4% error in most cases).

The reduction potentials determined in the range of 5-60^{o}C are tabulated in table 3.5 and plotted in figure 3.17. The derived thermodynamic parameters are presented in table 3.6. The values for the native protein ($E^{o'}$=276mV (*vs.* NHE), $\Delta G^{o'}$=-6.36kcal/mol, $\Delta H^{o'}$=-17.6 kcal/mol, $\Delta S^{o'}$=-37.8eu) are in good agreement with those reported by Margalit and Schejter ($E^{o'}$=264mV, $\Delta G^{o'}$=-6.0kcal/mol, $\Delta H^{o'}$=-17.8 kcal/mol, $\Delta S^{o'}$=-39eu, μ=0.01M).[48]

The parallel nature of the temperature-dependence plots for the native and modified cytochromes *c* is an indication of the similarity of $\Delta S^{o'}_{rc}$ for each. The large negative ΔS^{o} found for many protein reduction processes has been attributed to redox-linked conformational changes. The slight displacement of the temperature dependence plots is indicative of the modest increase in reduction potential for the modified cytochrome. This increase of 13mV can be rationalized on the basis of electrostatics: reduction is more favorable in the modified cytochrome due to the presence of additional positive charge provided by the trivalent ruthenium. Increases of 6-12mV in reduction potential have been observed for other singly-modified A_5Ru-protein derivatives.[49] It can be concluded that no major alteration of the heme

[48] Margalit, R., Schejter, A. *Eur. J. Biochem.* **32**, 492 (1973).

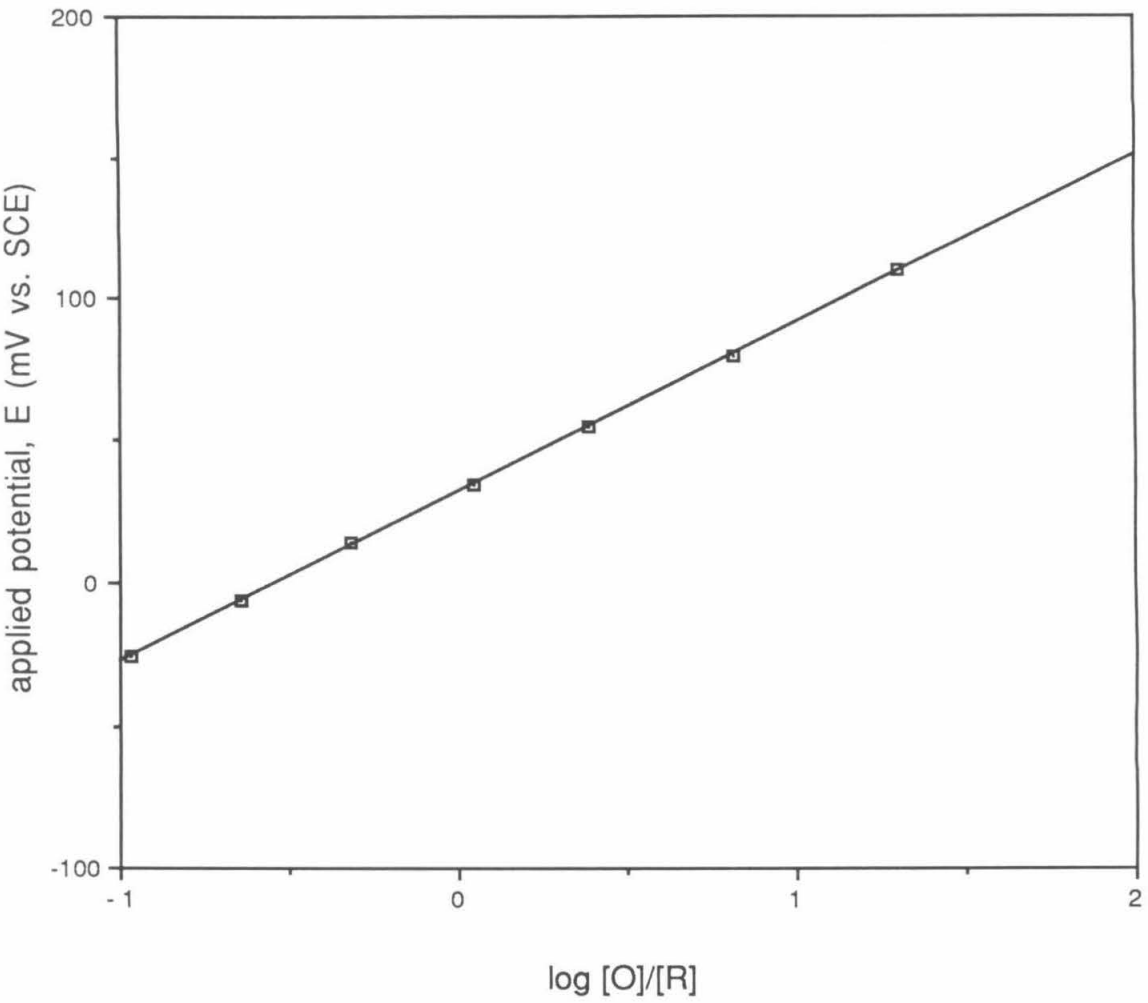

Figure 3.16. Nernst plot for spectroelectrochemical data on native *C. krusei* cytochrome *c*, 24.4°C. The data is best fit to the equation $y = 59.3x + 32.15$, $r^2 = 0.9999$.

Table 3.5. Reduction potentials of the iron site in native and A_5Ru-modified *C. krusei* cytochromes *c* as determined by variable temperature spectroelectrochemical studies

(a) native

temperature (°C)	$E^{o'}$ (mV *vs.* NHE)
9.1	290.1
15.2	285.9
19.8	281.8
24.4	275.8
29.6	271.4
34.2	269.1
39.8	262.3
44.8	256.7
50.2	250.4
54.8	226.5

(b) modified

temperature (°C)	$E^{o'}$ (mV *vs.* NHE)
6.8 [a]	304.7
7.6	307.2
12.6	300.5
19.6	294.2
26.4	287.5
31.0	282.6
36.6	277.2
36.6 [a]	273.7
40.6 [a]	271.0
47.0 [a]	258.6

a. sample 2 of same preparative batch

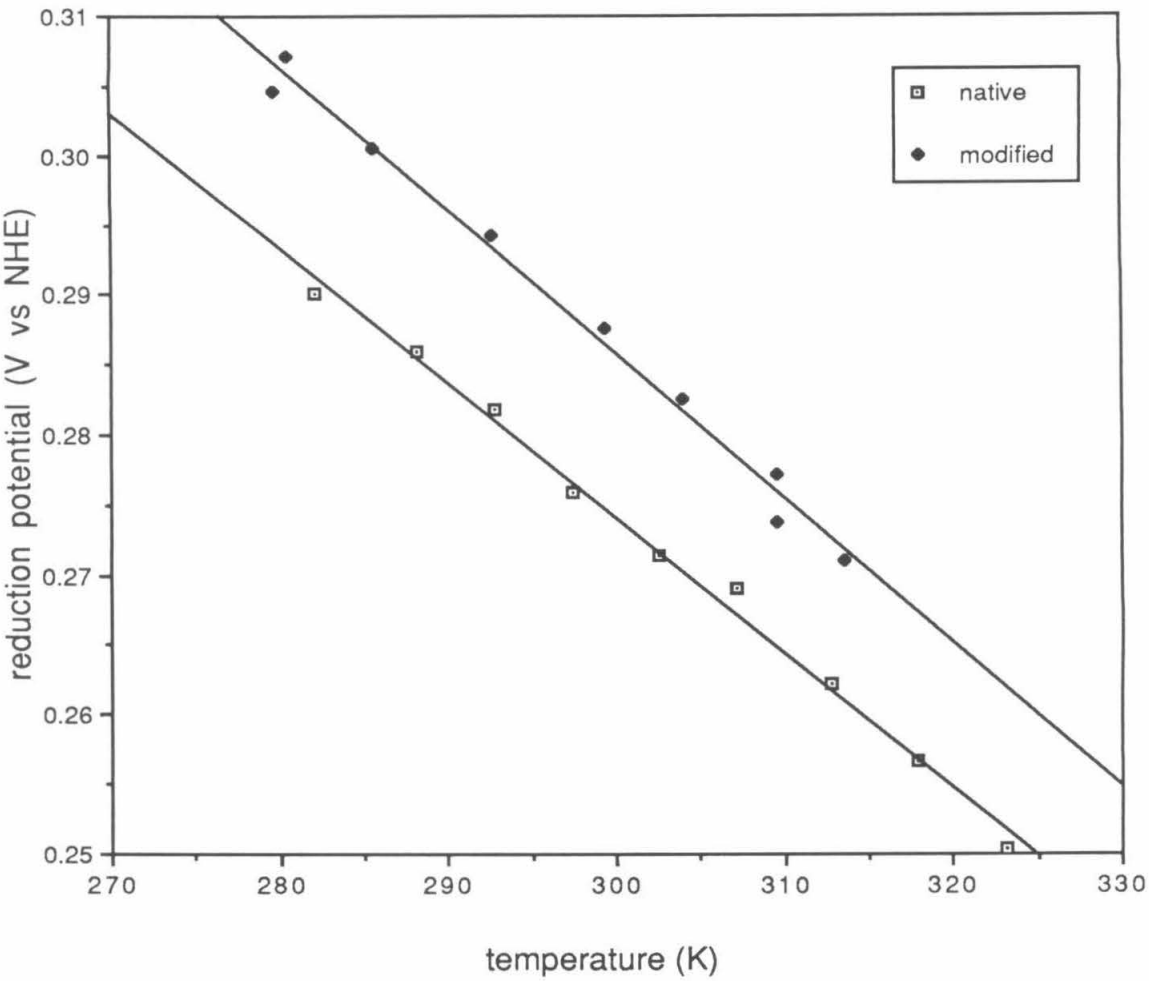

Figure 3.17. Temperature dependence of the reduction potentials of the iron site in native and A_5Ru-modified *C. krusei* cytochromes *c*, as determined by spectroelectrochemistry. The data are best fit by the equations $y = -0.964 \times 10^{-4}x + 0.5634$ for the native cytochrome, and $y = -1.04 \times 10^{-3}x + 0.5967$ for the modified.

Table 3.6. Thermodynamic parameters for the reduction of the iron site in native and A_5Ru-modified *C. krusei* cytochromes *c*, as determined from variable temperature spectroelectrochemical studies

	native	A_5Ru-modified
$E^{o'}$ (25°C, mV *vs.* NHE)	276.0 ± 0.4	287.9 ± 0.4
$\Delta G^{o'}$ (kcal/mol, 25°C)	-6.36 ± 0.01	-6.60 ± 0.01
$\Delta S_{rc}^{o'}$ (eu)	-22.2 ± 0.2	-23.9 ± 0.2
$\Delta S^{o'}$ (eu)	-37.8 ± 0.2	-39.5 ± 0.2
$\Delta H^{o'}$ (kcal/mol, 25°C)	-17.6 ± 0.1	-18.4 ± 0.1

environment occurs in this derivative as a result of appending the pentaammineruthenium moiety to the *C. krusei* cytochrome molecule.

Differential Pulse Polarography

Typical traces recorded in differential pulse polarography experiments on the native and modified *C. krusei* cytochrome *c* are shown in figure 3.18. A single peak is observed for the native protein at a potential of ~290mV (*vs.* NHE), and corresponds to the oxidation/reduction of the heme iron. A new signal evident in the modified derivative at ~120mV (*vs.* NHE) suggests that the site of modification is a histidine residue, as the reduction potential is similar to the 106mV reported for the model compound $[A_5RuHis]^{2+/3+}$.[50] The absence of signals in the 500mV (*vs.* NHE) region demonstrates the lack of modification at methionine.

Reduction potentials determined from DPP studies of the native and modified protein are presented in table 3.7 and plotted in figure 3.19. Using the best-fit parameters for the ruthenium site, a value of 119mV (*vs.* NHE) is obtained for the reduction potential at 25°C. Deviation of this value from that reported for the model compound, and from reduction potentials found for other A_5Ru-modified proteins (table 3.8), is not necessarily an indication of error, but may reflect the

[49] (a) Crutchley, R., Ellis, W., Gray, H. *J. Amer. Chem. Soc.* **107**, 5002 (1985); (b) Margalit, R., Kostić, N., Che, C.-M., Blair, D., Chiang, H.-J., Pecht, I., Shelton, J., Shelton, R., Schroeder, W., Gray, H. *Proc. Natl. Acad. Sci.* **81**, 6554 (1984); (c) Nocera, D., Winkler, J., Yocom, K., Bordignon, E., Gray, H. *J. Amer. Chem Soc.* **106**, 5145 (1984).

[50] Yocom, K., Winkler, J., Nocera, D., Bordignon, E., Gray, H. *Chem. Scripta* **21**, 29 (1983).

Figure 3.18. Differential pulse polarography traces (current *vs*. potential) for anodic scans of (a) native and (b) A_5Ru-modified *C. krusei* cytochromes *c*. Conditions: 0.25mM cytochrome in pH 7 μ=0.1M NaP_i, ~0.3mM in Aldrithiol-4; (a) 26.3°C, (b) 20.0°C.

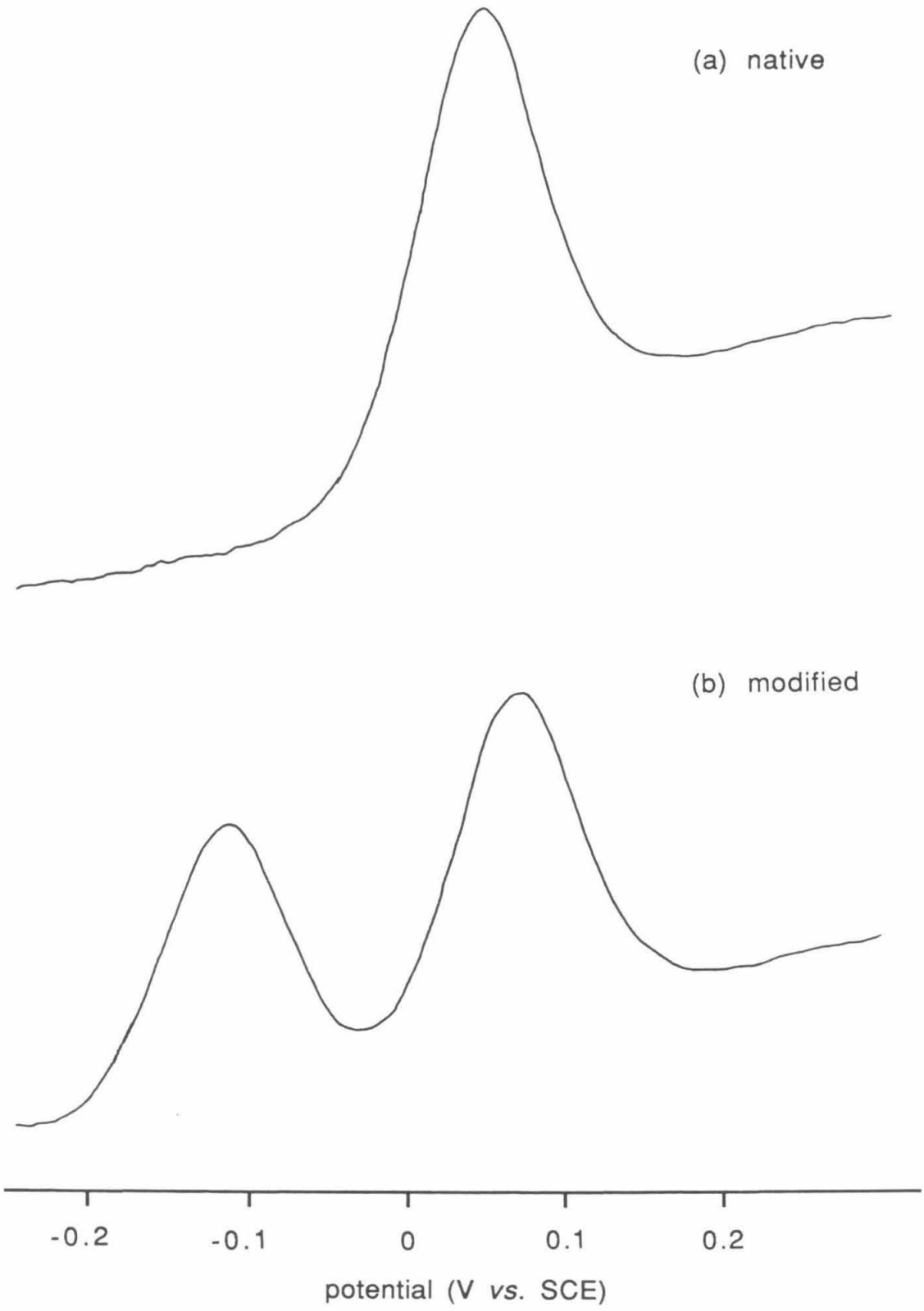
(a) native
(b) modified
-0.2
-0.1
0
0.1
0.2
potential (V vs. SCE)

Table 3.7. Differential pulse polarography data

Native *C. krusei* cytochrome *c*[a]

T (°C)	$E^{o'}$ (mV *vs.* NHE)
6.6	302.1 ± 1.4
10.1	297.1 ± 1.4
15.1	295.0 ± 1.4
21.2	290.4 ± 1.4
26.2	283.5 ± 2.2
31.0	282.9 ± 2.0

Modified (A_5RuHis39) *C. krusei* cytochrome *c*[b]

T (°C)	$E^{o'}$ (Ru, mV *vs.* NHE)	$E^{o'}$ (Fe, mV *vs.* NHE)
6.4	96.5 ± 1.9	300.5 ± 1.9
10.2[c]	112.3 ± 1.5	310.6 ± 1.5
14.2	103.9 ± 1.4	308.6 ± 1.4
20.4[c]	117.7 ± 1.4	303.7 ± 1.4
24.0	119.0 ± 1.4	299.3 ± 1.4
35.6	129.4 ± 2.1	291.7 ± 2.1
40.4	132.8 ± 3.6	289.4 ± 3.6

a. Linear regression of the data results in a fit to the equation $y = -0.799x + 306.5$ with correlation coefficient $r^2=0.97$.
b. Linear regression of the data for the ruthenium site results in a fit to the equation $y = 0.963x + 95.1$ with correlation coefficient $r^2=0.89$. The data for the iron site is best fit to the line $y=0.528x + 312.0$ with correlation coefficient $r^2=0.71$.
c. sample 2 of same preparative batch

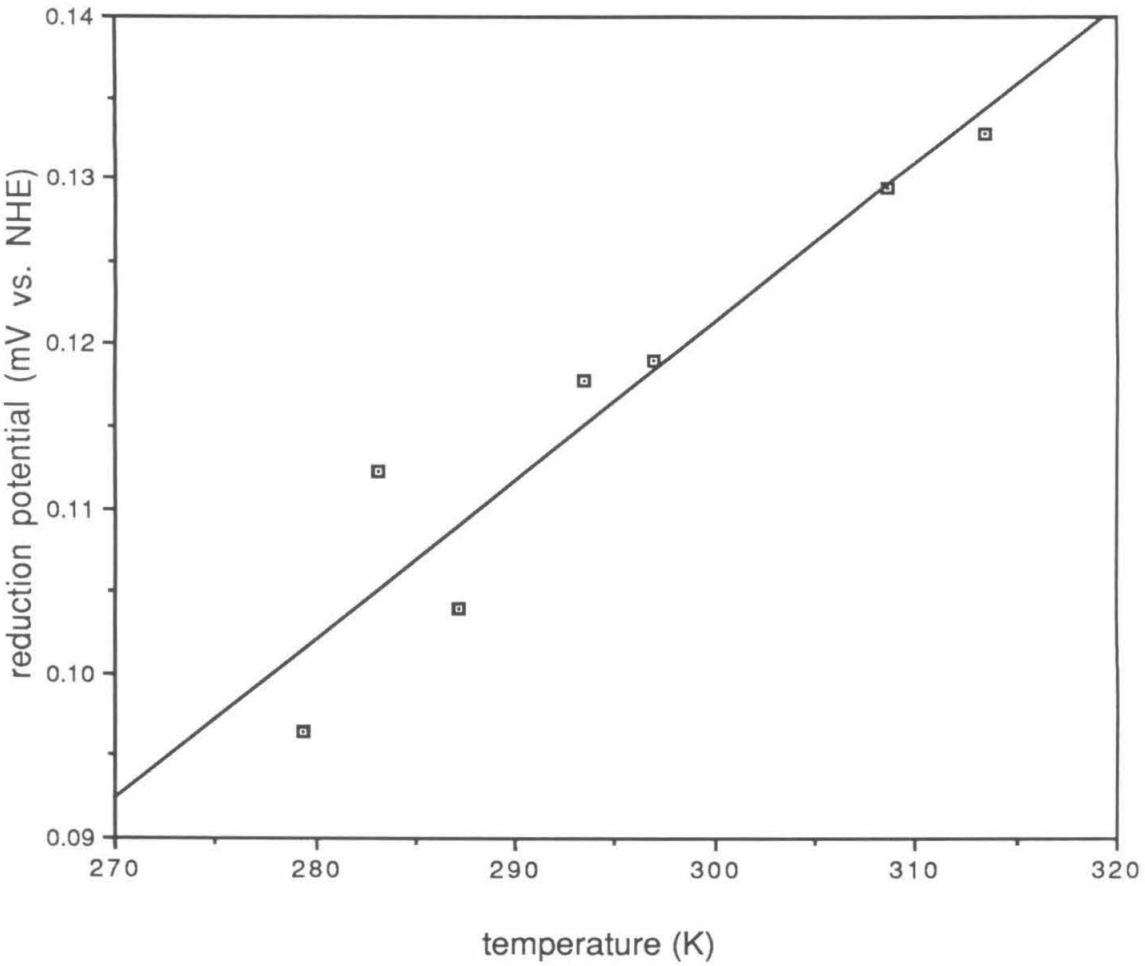

Figure 3.19. Temperature dependence of the ruthenium reduction potential in A_5Ru-modified *C. krusei* cytochrome *c*, as determined by differential pulse polarography. The data are best fit by the equation y=9.63e-4x - 0.168.

Table 3.8. Thermodynamic parameters for the reduction of the pentaammineruthenium histidine site (as determined by DPP or CV) in *C. krusei* cytochrome *c* and other environments[a]

	A_5Ru-*C.k.* cytochrome	A_5Ru-myoglobin	$[A_5RuHis]^{2+/3+}$
$E^{o'}$ (mV *vs.* NHE)	119.2 ±21	85.8 ±2.0	80.0 ±5
$\Delta G^{o'}$ (kcal/mol, 25°C)	-2.75 ±0.48	-1.98 ±0.05	-1.96 ±0.12
$\Delta S^{o'}$ (eu)	6.6 ±1.6	4.2 ± 1.2	-3.4 ±2.0
$\Delta H^{o'}$ (kcal/mol, 25°C)	-0.78 ±0.95	-0.7 ± 0.4	-3.0 ±0.8

a. Data for myoglobin from Crutchley, R., Ellis, W., Gray, H. *J. Amer. Chem. Soc.* **107**, 5002 (1985). Data for the model compound were recorded in 0.1M $NaClO_4$ using cyclic voltammetry(CV); Nocera, D., Winkler, J., Yocom, K., Bordignon, E., Gray, H. *J. Amer. Chem. Soc.* **106**, 5145 (1984).

influence of the local protein environment in stabilizing one oxidation state over the other.

The DPP data is used only to derive the thermodynamic parameters for the ruthenium site, as the technique is inferior to spectroelectrochemistry. The use of promoters results in quasi-reversible electrode kinetics, whereas mediators allow for fully reversible electron exchange between the protein and the electrode. Additional error in the DPP results from the design of the electrochemical cell: due to technical difficulties in constructing a glass cell with multiple coincident junctions, the interface of the sample and reference compartments is displaced from the point where the independent water jackets meet (see figure 3.2). The slight overlap of the sample jacket onto the reference compartment gives rise to fluctuations in the temperature of the latter, to which the reference electrode is slow to respond.

DISCUSSION

C. krusei cytochrome *c* has numerous sites which can potentially react with the aquopentaammineruthenium(II) reagent. Attempts to modify tuna cytochrome *c* were unsuccessful (100mM NaAc, pH5, 0.2mM cytochrome, 30:1 [ruthenium]:[cytochrome], for reaction times up to 10 hours) as determined by gel electrophoresis (data not shown). Thus, routine modification of carboxylate and amine moieties (of Asp, Glu, and Lys side chains) can be ruled out.

The only cysteine residues present in *C. krusei* cytochrome *c* (figure 3.20a) are those involved in the covalent binding of the heme, Cys14 and Cys17, and these therefore contain thioether rather than sulfhydryl moieties. Other amino acids which are potential sites of

Figure 3.20. Residues which are potential ligands to pentaammineruthenium in *C. krusei* cytochrome *c* (in addition to the His33 and His39 targets). Dotted regions are matched in color to the line drawing of the residues whose side chain surface they represent (3.5Å probe; 8 dots/Å^2).

(a) Cys14 and Cys17 (green) are the sites of covalent linkage of the porphyrin to the polypeptide. Only the latter (forward) is exposed. Histidine residues (pink) are present at positions 18 and 26. The former serves as a ligand to the iron, and is buried within the protein.

(b) Methionine residues in *C. krusei* cytochrome *c*. Three methionine (yellow) residues are present, Met64, Met80 (the sixth ligand), and Met98, none of which are expected to be solvent-accessible.

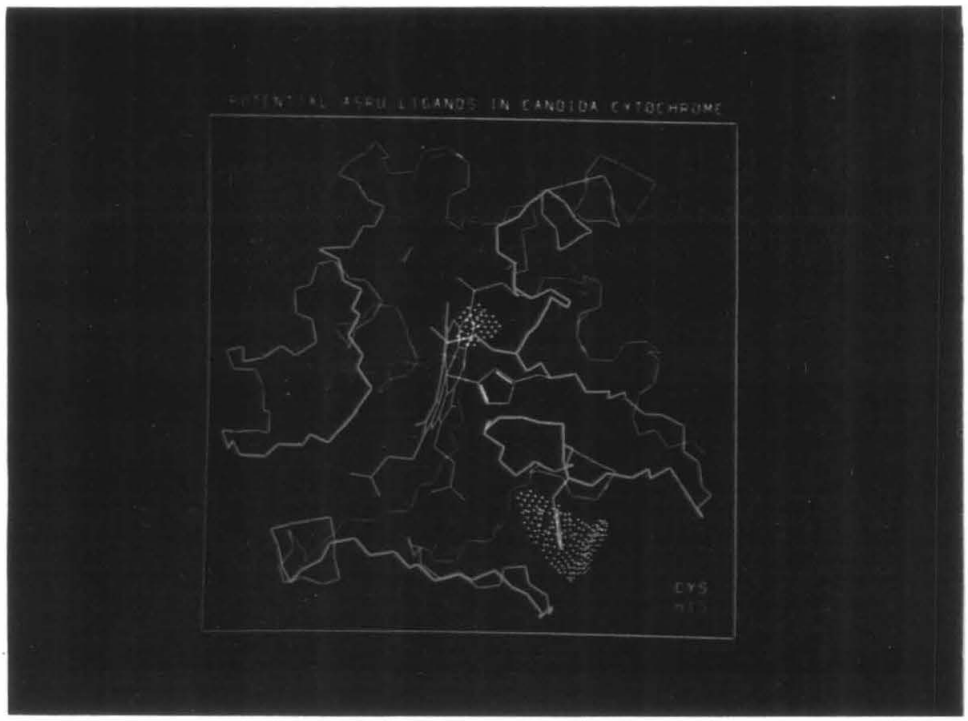

Figure 3.20 (a)

Figure 3.20 (b)

modification are the histidine and methionine residues (figure 3.20a & b, respectively). *C. krusei* has three methionine residues, Met64, Met80, and Met98, and four histidine residues, His18, His26, His33, and His39. His18 and Met80 are ligands to the iron and are not expected to react as long as the protein conformation is maintained.

The accessibility of these residues in reduced tuna cytochrome *c* was evaluated using Biograf. The results are presented in table 3.9. Aside from His33 and His39, none of the residues except Cys17 and His26 are of concern, as they are internal and are inaccessible to solvent. Cys17 modification can be ruled out, as it was not observed to occur in tuna cytochrome *c*. His26, though solvent-accessible, is involved in an extensive hydrogen-bonding network (figure 3.21), and should this residue be modified, a substantial change in the polypeptide conformation is likely to result.

Thus, one might predict histidine residues would be the only potential sites of modification. Indeed, all of the spectroscopic studies of the modified derivative suggest a pentaammineruthenium histidine complex has been formed. NMR data support the conclusion that one of the two normally-titrating histidine (His33 or His39) residues is modified. The number of sites of modification is narrowed by UV-visible difference spectroscopy, which reveals a [Ru]:[Fe] ratio of 1:1 in the modified derivative. Peptide mapping assigns the site of modification definitively to His39.

The lack of modification at His33 is consistent with the horse heart cytochrome reaction kinetics: after allowing the horse protein to react with the aquopentaammineruthenium(II) reagent (0.2mM cytochrome, 10mM $[A_5Ru(OH_2)]^{2+}$, 100mM HEPES buffer, pH 7.0) for twenty four hours,

Table 3.9. Surface areas of tuna cytochrome residues which are potential penta-ammineruthenium ligands in *C. krusei* cytochrome *c*.[a]

	PROBE RADIUS	
residue	**1.4Å**	**3.5Å**
Cys14	0	0
Cys17	10.72	5.82
Leu64[b]	0	0
Met80	0	0
Leu98[b]	0	0
His18	0	0
His26	37.28	28.36

a. as defined by Connolly, M. *Science* **221**, 709 (1983); given in $Å^2$; based on the 1.5Å crystal structure of reduced tuna cytochrome *c*: Takano, T., Dickerson, R. *J. Mol. Biol.* **153**, 79 (1981) and Takano, T., Kallai, O., Swanson, R., Dickerson, R. *J. Biol. Chem.* **248**, 5234 (1973). Calculations with the 1.4Å probe radius define the solvent(water)-accessible surface whereas those of radius 3.5Å reveal area accessible to the pentaammineruthenium reagent. Residues 33 and 39 are omitted, as these are known to be at the protein surface, and are not histidine in the tuna cytochrome. See text for further details.

b. Met in *C. krusei* cytochrome *c*

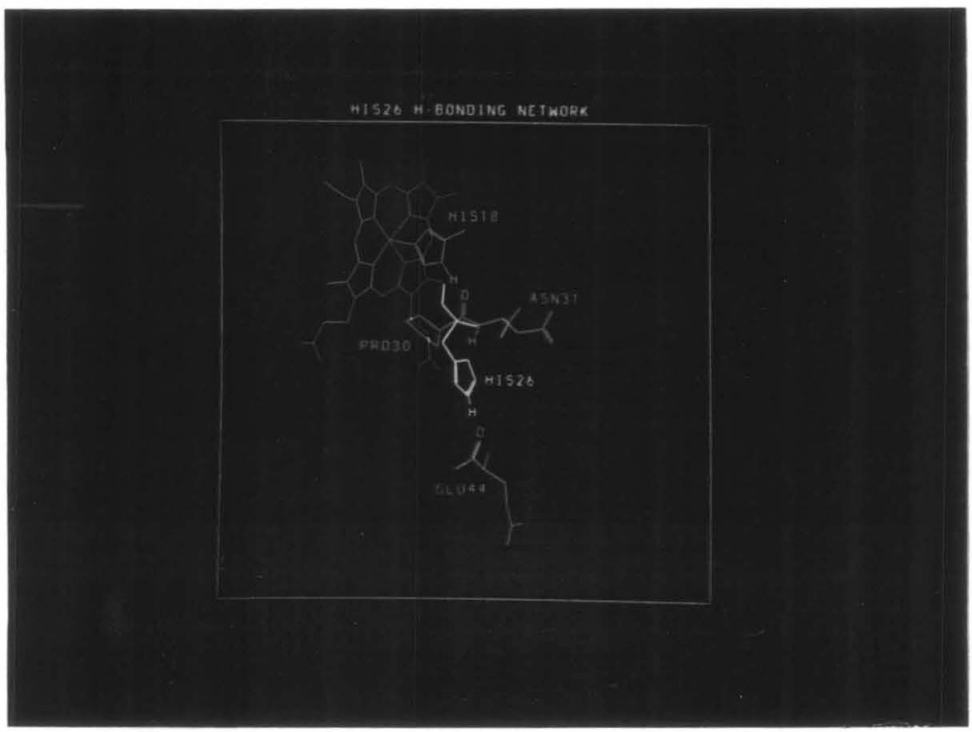

Figure 3.21. His26 hydrogen-bonding network. His26 is hydrogen-bonded through both imidazole nitrogen atoms, and modification of this residue is expected to disrupt the polypeptide conformation. The residue 44 (purple) carbonyl serves as a hydrogen bond acceptor to the N_ε of His26 (yellow). The N_δ of His26 is hydrogen-bonded to the amine of residue 31 (green). The adjacent carbonyl (of the residues 30-31 peptide bond) is hydrogen-bonded to the N_δ of the iron ligand, His18 (red).

a 30% yield of His33-modified product is obtained.[51] A time analysis of this reaction by electrophoresis indicated that no product (of mobility higher than that of the native protein) was observed until the reaction had progressed for four hours (data not shown).

Very recent studies with *S. cerevisiae* cytochrome mutants corroborate the results and interpretation presented here. Attempts to modify His58 in a mutant cytochrome containing His33 but not His39 at pH 7 (30:1 [Ru]:[cytochrome], pH 7, 100mM HEPES) result in little product formation after 45 minutes, as judged by FPLC.[52] Longer reaction times seem to lead to the formation of multiply-modified products. Therefore, the residue which modifies rapidly in the *Candida* cytochrome is likely to be His39.

The reason for the lack of modification at His33, or more appropriately, the slower reaction of His33 relative to His39, appears to be steric hindrance. Modeling of the *C. krusei* cytochrome was conducted to investigate the environment surrounding each residue (figure 3.22a). No evidence was found to suggest that local electrostatic repulsion might be the cause for the discrepancy in the reaction rates: each histidine is surrounded by two or three charged residues, both positive and negative, within a 7Å radius. Inspection of His33 revealed a more constrained environment relative to that of His39: the imidazole ring of His33 is "sandwiched" between two portions of the protein, and is accessible only via the edge. In contrast, the His39 side chain extends freely into solution, and approach by the ruthenium

[51] Nocera, D., Winkler, J., Yocom, K., Bordignon, E., Gray, H. *J. Amer. Chem. Soc.* **106**, 5145 (1984).

[52] Chang, J., personal communication

Figure 3.22. Local environment of histidines of interest in (a) *C. krusei* and (b) horse heart cytochrome *c*. Negatively (Asp, Glu) and positively (Lys, Arg) charged side chains are shown in red and blue, respectively. Histidine side chains are shown in yellow. Dotted regions indicate the surface accessible to a 3.5Å probe for each side chain (8 dots/Å^2), and are colored appropriately.

(a) *C. krusei* cytochrome *c*. Note that there is no preponderance of one type of charge surrounding either histidine. Lys103 provides additional negative charge, as it is the C-terminal residue. Note the greater surface area of the His39 residue (71.7Å^2) as opposed to His33 (43.4Å^2).

(b) Horse heart cytochrome *c*. There are no indications of excessive positive charge surrounding His33 which would slow the modification reaction. Note that the imidazole side chain is accessible only at the edge (33.7Å^2 total surface area).

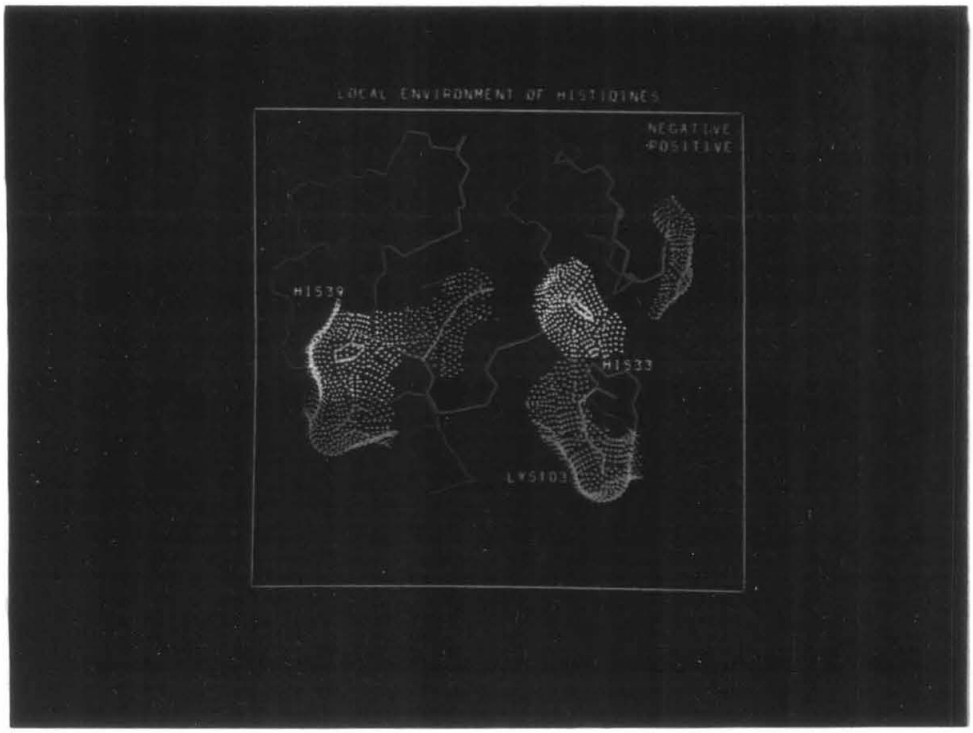

Figure 3.22 (a)

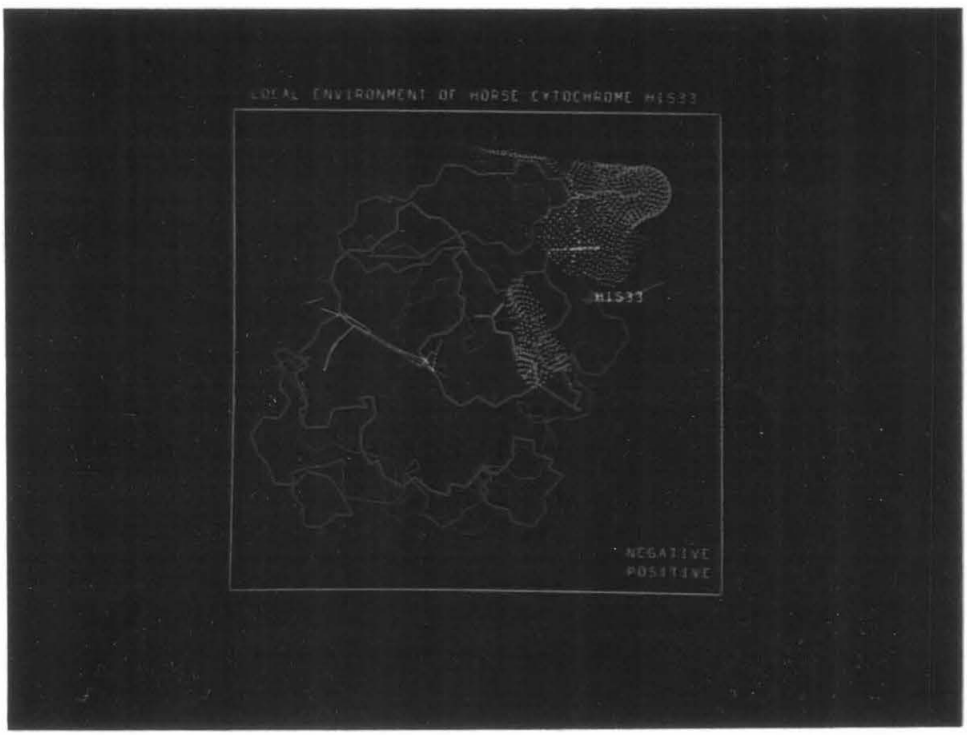

Figure 3.22 (b)

complex is possible from the edge and either face of the imidazole ring. Calculated surface areas for His33 and His39 are 43.4 and 71.7Å^2, respectively (3.5Å probe).[53]

The relative rates of modification of horse and yeast His33 may also be explained by steric hindrance. Some reaction of His33[54] is observed in *C. krusei* cytochrome *c* within one half hour, while horse cytochrome *c* shows no evidence of modification (by electrophoresis) before four hours (under similar conditions). Modeling suggests His33 is less exposed to solvent in the horse cytochrome than in the yeast protein (surface areas of 33.7 and 43.4Å^2, respectively, were calculated (see figure 3.22b)).

The results of this inorganic modification can be contrasted with previous investigations of histidine modification in yeast cytochrome *c*. Brothers and Kostić found *C. krusei* cytochrome *c* to be labeled readily at both His33 and His39 by a terpyridylplatinum(II) reagent, and isolated two singly-modified derivatives in equal yield.[55] Horinishi *et al.* found horse and yeast (Bakers') cytochromes were modified by diazonium-1-H-tetrazole in three steps, with His33 and His39 reacting most readily, followed by His26, and then His18.[56] The second

[53] For comparison: an unencumbered histidine side chain has an area of 82.9Å^2 accessible to a 3.5Å probe.

[54] Reaction at His33 is inferred from the further reaction of the major *C. krusei* cytochrome *c* A_5Ru-derivatization product with time (as observed by electrophoresis), and the recovery of a minor product after one half hour which seems to be modified at two histidine residues (see appendix 6).

[55] Brothers, H., Kostić, N. *Inorg. Chem.* **27**, 1761 (1988).

[56] Horinishi, H., Kurihara, K., Shibata, K. *Arch. Biochem. Biophys.* **111**, 520 (1965).

and third steps were accompanied by changes in the visible spectrum, supporting the assumption that the His26 hydrogen-bonding network is integral to maintaining the cytochrome fold. His33 may be more readily modified by these reagents than by aquopentaammineruthenium(II) because of reduced steric hindrance.

Preliminary characterization of the second *Candida* pentaammineruthenium-modified product suggests it is a doubly-modified derivative, and is discussed in appendix 6.

The results reported here allow for unambiguous assignment of the C-2 ^{1}H NMR resonances for histidines 33 and 39 in *C. krusei* ferricytochrome *c*. The upfield resonance (δ8.62) at pH 5, which is absent in the spectrum of the modified product, can be assigned to His39, the residue demonstrated to be the site of pentaammineruthenium modification by peptide mapping. There is evidence to suggest that the pH dependence of the yeast cytochrome reduction potential is related to the ionization of His39.[57] This may be readily confirmed by the use of the A_5Ru(His39)-cytochrome derivative: the heme reduction potential is expected to be pH-independent in the pH 5 to 8 range, as the modified histidine would not undergo any ionization.

Taken together, the electrochemical studies indicate that reduction of the iron site is favored over that of the ruthenium center. Hence, preparation of a Ru^{2+}-Fe^{3+} intermediate should result in electron transfer to the iron site, *i.e.*, Ru^{3+}-Fe^{2+} production, which should proceed with a driving force of ~170mV at room temperature. The thermodynamic parameters for the overall reaction (at 25°C) are $\Delta G^{o'}$=

[57] Robinson *et al.*, p. 687.

-3.85(± 0.49)kcal/mol, $\Delta H^{o'}$=-17.6(± 1.1)kcal/mol, $\Delta S^{o'}$=-46.1(± 1.8)eu. As the temperature is increased, the electron transfer reaction will become less exothermic as the gap between the two reduction potentials narrows.

CHAPTER 4

ELECTRON TRANSFER STUDIES

MATERIALS and INSTRUMENTATION

$[Ru(bpy)_3]Cl_2 \cdot 6H_2O$, (2,2'-bipyridyl)ruthenium(II) chloride hexahydrate, was used as supplied by Strem Chemicals Inc. $Na_2EDTA \cdot 2H_2O$ was reagent grade. All manipulations of degassed solutions were conducted in an inert atmosphere box (Vacuum/Atmospheres Co.) filled with argon. Degassing was accomplished on the dual-manifold vacuum-argon line described in chapter 2.

Protein

Native cytochrome *c* was purified as described in chapter 2. The modified cytochrome was used as eluted from CM-52 for quenching studies, and was further purified by FPLC prior to the flash photolysis studies.

$[Ru(bpy)_3]^{2+*}$ lifetime studies

Cells for quenching experiments were test tubes fitted with needle valves to allow for evacuation, and with side arms terminating in 1mm x 10mm x 30mm quartz cells. The narrow side-arm cell was used for lifetime measurements, and also permitted absorbance measurements to be made. Lifetimes were measured at ambient temperature; no special provisions were made to maintain the sample temperature constant.

The excitation source was a Quanta Ray DCR-1 Nd:YAG laser frequency-doubled with a Quanta Ray HG-1 harmonic generator, followed by a Quanta Ray PHS-1 prism harmonic separator to produce a 532nm pulse of 8ns (fwhm) duration at 10Hz. Emitted light, monitored at 650nm, was collected at a right angle to the laser beam with a collimating lens (f/1.3), then focused by a second lens (f/6.5) through a Corning 3-67

filter (transmittance<0.5% at λ<524nm) onto the entrance slits of a MacPherson monochromator. The light was detected by a Hamamatsu R928 photomultiplier tube, and the resultant signal was passed through a LeCroy VV101ATM amplifier to the 50Ω impedance input of a Biomation 6500 waveform recorder. A Digital PDP11/03-L computer controlled the firing of the laser and the data acquisition. The data acquired for each sample were averages of at least 200 laser pulses.

Analysis of the data was performed using the BASIC program TOOBIG1, written by Michael Albin. This program allows one to fit data to a mono- or bi-phasic exponential decay.

Flash photolysis

The flash photolysis apparatus (figure 4.1) consisted of a Xenon Corporation N851D flash lamp fired by a Xenon Corporation model 457A micropulser (36-100J/flash; $\tau_{1/2}$~5μs). The flash light was filtered through Corning 3-73 filters (37% transmittance at 416<λ<436nm; >80% transmittance at λ>511 nm) to prevent electronic excitation of the protein by ultraviolet light.

The sample was contained in an evacuated cylindrical cell, ~15cm in length, which fit within an aluminum cavity containing the flash lamp. A constant sample temperature could be maintained by circulating thermostatted water through the cell jacket.

The tungsten probe lamp (Osram HLX64 625) was contained in a Oriel 6324 housing, powered by a PowerMate Corporation power supply, and cooled with a gentle flow of filtered air which was maintained throughout the data collection process. The monitoring beam was filtered through a Corning 15 filter (zero transmittance at λ<523nm to

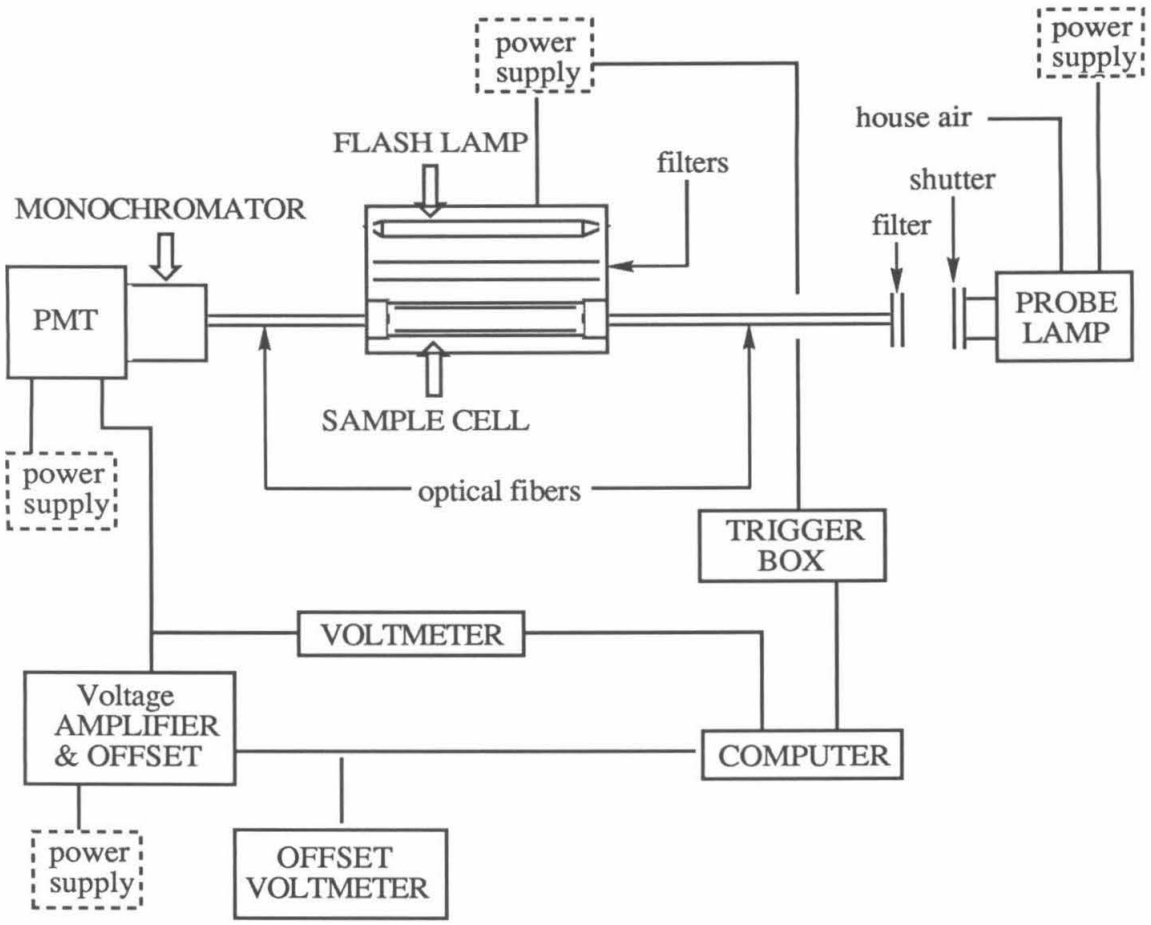

Figure 4.1. Schematic diagram of the flash photolysis instrument.

minimize continuous excitation of the $[Ru(bpy)_3]^{2+}$ complex), and then guided to the cell by optical fibers (Oriel). The light emerging from the far end of the cell was carried by optical fibers to the Oriel 7240 grating monochromator (λ=549 nm). The slit width was typically 2.3mm.

The light was detected by a Hamamatsu R928 photomultiplier tube (PMT), contained in a Pacific Photometric Instruments model 50B housing, and powered by a Pacific Precision Instruments model 204 power supply. The output current of the PMT was fed through a 5KΩ resistor, monitored by a Keithley 177 microvoltmeter, and then fed into a DC voltage offset circuit. The offset voltage was displayed on a Simpson 2865 digital panel. Release 2.25, the 256 Kbyte version of UnkelScope (Unkel Software, Lexington, MA), running on a ATronics ANI 8T computer with a Princeton Graphic System screen, was used to trigger the flash lamp and data collection. For details about the shortcomings of this arrangement, see appendix 4.

METHODS

$[Ru(bpy)_3]^{2+*}$ lifetime measurements

Absorption of visible light (400-580nm; λ_{max}=452nm in H_2O) by $[Ru(bpy)_3]^{2+}$ results in an electronically excited metal-to-ligand charge transfer (MLCT) state.[1] Two competitive pathways of de-excitation are available: the compound may emit light as it returns to the ground state with a rate constant of k_ℓ, or the complex may return to its ground state by nonradiative relaxation with a rate constant of

[1] The photophysical properties of ruthenium(II) polypyridyl complexes have recently been reviewed: Juris, A., Balzani, V., Barigelletti, F., Campagna, S., Belser, P., von Zelewsky, A. *Coord. Chem. Rev.* **84**, 85 (1988).

k_{nr}. The rate expression for the de-excitation process is given by

$$-d[Ru^*]/dt = k_{\ell}[Ru^*] + k_{nr}[Ru^*]$$

where Ru* represents the excited state of the ruthenium complex. The concentration of the excited state will decrease according to the following expression:

$$[Ru^*] = [Ru^*]_o\{\exp -(k_{\ell}+k_{nr})t\}$$

where $[Ru^*]_o$ is the initial concentration of the excited state. The lifetime of the excited state, τ_o, is given by the inverse of the sum of the de-excitation rate constants, *i.e.*, $(k_{\ell}+k_{nr})^{-1}$. Certain molecules react with the excited complex and return it to the ground state; in such cases the excited state is said to be "quenched". If this bimolecular process proceeds with a rate constant of k_q, the rate of de-excitation is given by

$$-d[Ru^*]/dt = k_{\ell}[Ru^*] + k_{nr}[Ru^*] + k_q[Q][Ru^*]$$

and

$$[Ru^*] = [Ru^*]_o\{\exp -(k_{\ell}+k_{nr}+k_q[Q])t\}$$

if $[Q]>>[Ru^*]_o$, where [Q] is the concentration of the quencher. The lifetime in the presence of a quencher of concentration [Q], τ, is $(k_{\ell}+k_{nr}+k_q[Q])^{-1}$. A plot of the ratio of the lifetimes of the excited state in the absence and presence of quencher, τ_o/τ, *versus* the quencher concentration should give a line with an intercept of 1 and a slope of $k_q\tau_o$:

$$\frac{\tau_o}{\tau} = \frac{k_{\ell}+k_{nr}+k_q[Q]}{k_{\ell}+k_{nr}} = 1 + \frac{k_q[Q]}{k_{\ell}+k_{nr}} = 1 + k_q\tau_o[Q]$$

This is known as the Stern-Volmer relation.[2]

[2] Barltrop, J., Coyle, J. *Principles of Photochemistry*, J. Wiley (New York), 1978, p. 110.

All quenching experiments were done with ~65μM $[Ru(bpy)_3]Cl_2$ in μ=0.1M pH 7 sodium phosphate buffer. Quenching rate constants were determined from a series of emission lifetime measurements in the presence of successively lower quencher concentrations. Quencher solutions of the highest (practical) concentrations attainable were maintained in the test tube side of the cell and were degassed and purged with argon for at least three cycles, then sealed. After the lifetime measurement was made, the cell was transferred to an inert atmosphere box, where it was diluted with a known volume of deoxygenated $[Ru(bpy)_3]^{2+}$-buffer solution. This procedure allowed for a more accurate estimation of the quencher concentration by avoiding the reduction in sample volume which would have accompanied evacuation with each dilution.

For tryptophan quenching studies, 51.4mg tryptophan (Pierce amino acid standard kit 22) was added to 10mL 63.2μM $[Ru(bpy)_3]Cl_2$ in 0.1M ionic strength sodium phosphate pH 7 buffer. The mixture was left overnight, protected from light, to allow the solid to dissolve. The tryptophan concentration was estimated to be ~33.5mM from the solution absorbance at 280nm, using an extinction coefficient of $5600M^{-1}cm^{-1}$ (recorded after the lifetime measurement).[3]

Flash photolysis

Flash photolysis is a technique for the study of fast photoactivated reactions.[4] The sample is exposed to a short (μs or ns), intense

[3] Cantor, C., Schimmel, P. in *Biophysical Chemistry*, Part 2, W. H. Freeman (San Francisco), 1980, p. 443.

[4] Norrish, R., Thrush, B. *Q. Rev. Chem. Soc.* **10**, 149 (1956).

flash of light which initiates the reaction by creating a non-equilibrium situation. A probe beam, set at a right angle to the direction of the flash, allows for monitoring of the progress of the reaction by changes in absorbance.

A ~98mM cytochrome solution in μ=0.1M pH 7 NaP_i was thoroughly degassed and saturated with argon on a dual manifold Ar-vacline. A second solution of 65μM $[Ru(bpy)_3]Cl_2$ and 5mM Na_2EDTA in the same buffer was similarly prepared. Both solutions were transferred into an inert atmosphere box along with a dry flash cell. Samples were prepared by pipetting aliquots of each solution into the flash cell; typically 10mL (2 x 5mL) of the $[Ru(bpy)_3]^{2+}$ solution and <200μL of the cytochrome solution were used, to yield a final cytochrome concentration of ~1.05μM.

This procedure was adopted so that the concentration dependence of the electron transfer rate could be investigated without introducing a variation in volume (and therefore concentration) which would arise from degassing each sample. However, rigorous concentration-dependence studies have not been conducted due to problems with the flash instrumentation (see appendix 4). Those reported at cytochrome concentrations above 1μM were conducted on individually degassed, complete reaction mixtures. It is preferable to degas the reactants separately to avoid reduction of the cytochrome by any ambient light present during the sample preparation.

Samples were protected from all light (by wrapping the cells in foil) prior to placing them in the probe beam. A delay of several minutes was required to allow the PMT to stabilize prior to flashing.

Data reported here for native cytochrome were obtained at room

temperature; *no special* provisions were made to maintain the sample temperature constant. Modified cytochrome samples were maintained at 22°C by a circulating water bath.

Data were collected as 1024 points, 64 of which defined the baseline voltage prior to the flash. The data file, recorded by Unkelscope in binary form, was converted to ASCII form using the program BINLOT, also a product of Unkel Software. The intensity (voltage) values of the resulting file were converted into relative absorbance values using the program BLT2DAT, with the baseline (*i.e.*, that before the flash) absorbance being set equal to zero. Data were plotted and estimates were made of the parameters A(x), where x=1,2,3... A parameter file was created, and used as input to the program MEXPFIT_DP. The fit was made to an equation of the form

$$y = A(1) + A(2)[1 - \exp(-A(3)t)]$$

Parameters for the best fit found and the predicted absorbance values were output to separate files. Programs which are not products of Unkel Software can be found in appendix 5. A flow chart for the data analysis procedure can be found in figure 4.2.

Data for the kinetics of the modified cytochrome were fit twice, once using all data above 2ms, and again using data collected beyond 7ms. The latter region is that which should be relatively unaffected by the problem of flash breakthrough (see appendix 4).

RESULTS and DISCUSSION

The result presented here for the intramolecular electron transfer rate constant of the derivative (A_5Ru(His39)-*C. krusei* cytochrome *c*) which is the subject of this thesis is preliminary.

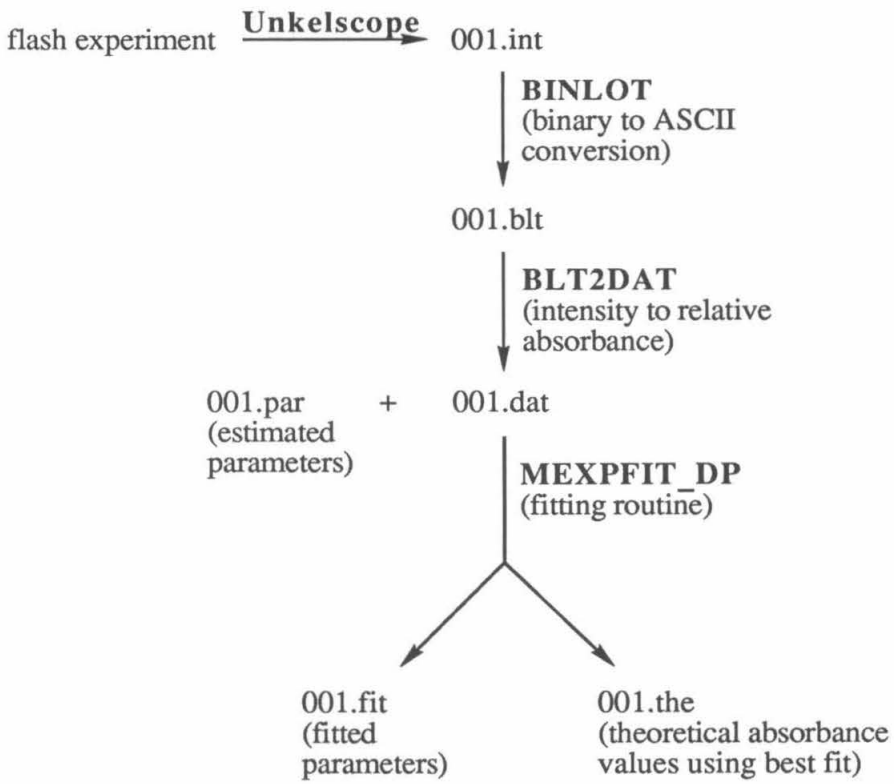

Figure 4.2. Flow chart for kinetic data collection and fitting.

Several problems with the flash photolysis instrument design were discovered by the author, and several changes were made in an attempt to remedy the situation. However, time and politics did not permit all the necessary changes to be made. Therefore, the data is presented with the following caveat: if one can assume the PMT response was linear (although the instrument operation was such that the response would be definitely nonlinear for large changes in light intensity), then the rate presented is likely to be a lower limit. A discussion of the instrumental problems is presented in appendix 4.

Scheme 1 (figure 4.3) delineates the sequence of reactions expected to occur following flashing of the sample at ~450nm. The flash, microseconds in duration, serves to excite the $[Ru(bpy)_3]^{2+}$ complex, inducing the formation of a metal-to-ligand charge transfer (MLCT) state. The longest reported lifetime of $[Ru(bpy)_3]^{2+*}$ in aqueous solution is 685ns,[5] hence after ~2.4μs (five half lives), it should not be able to participate directly in any reaction causing an observed change in absorbance. Implicit is the assumption that the lifetime is not lengthened in the presence of the protein. In fact, the lifetime of the trisbipyridylruthenium(II) excited state is reduced in the presence of cytochrome *c*, as the latter serves as an oxidative quencher (*vide infra*). A rate constant of 4.4 x $10^8 M^{-1}s^{-1}$ has been determined for this quenching reaction (figure 4.4).[6]

[5] Harriman, A. *J.C.S. Chem. Comm.* 777 (1977).

[6] This is somewhat faster than the quenching rate constant of 2.5 x $10^8 M^{-1}s^{-1}$ reported for horse heart cytochrome *c*; Nocera D., Winkler, J., Yocom, K., Bordignon, E., Gray, H. *J. Am. Chem. Soc.* **106**, 5145 (1984).

$$[Ru(bpy)_3]^{2+} \xrightarrow{h\nu} [Ru(bpy)_3]^{2+*}$$

$$2[Ru(bpy)_3]^{2+*} + 2Ru^{3+}\text{-cyt}(Fe^{3+}) \longrightarrow 2[Ru(bpy)_3]^{3+} + Ru^{2+}\text{-cyt}(Fe^{3+}) + Ru^{3+}\text{-cyt}(Fe^{2+})$$

$$Ru^{2+}\text{-cyt}(Fe^{3+}) \longrightarrow Ru^{3+}\text{-cyt}(Fe^{2+})$$

$$2[Ru(bpy)_3]^{3+} + EDTA^{4-} + H_2O \longrightarrow 2[Ru(bpy)_3]^{2+} + HCOH + CO_2 + (CH_2COO^-)_2N(CH_2)_2NHCH_2COO^- + H^+$$

Scheme 1

Figure 4.3. Sequence of reactions initiated by a microsecond pulse of visible (~450nm) light in the electron transfer experiment (the stoichiometry is not necessarily such that the ruthenium and iron sites of the modified protein are reduced in equal proportions).

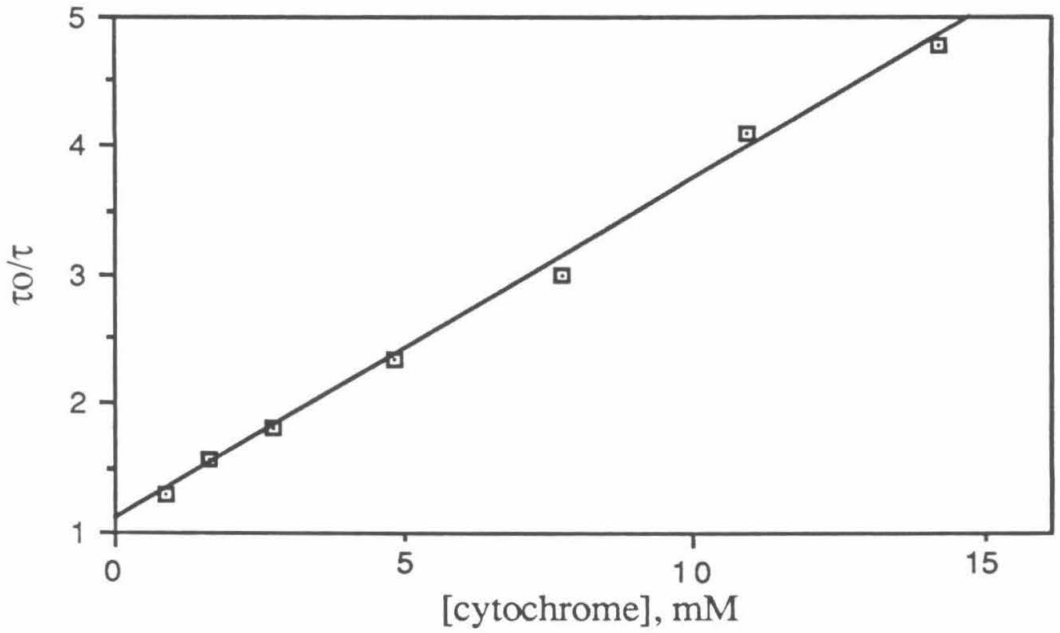

Figure 4.4. Stern-Volmer plot for the quenching of the $[Ru(bpy)_3]^{2+*}$ by *C. krusei* cytochrome *c*. The solid line is the least squares fit to the data: $y = 0.263x + 1.09$ ($r^2 = 0.996$).

When ruthenium is present on the cytochrome, it, as well as the heme iron, may serve as an oxidizing center to $[Ru(bpy)_3]^{2+*}$. Protein molecules reduced at the ruthenium label are expected to undergo intramolecular electron transfer, as the electron is expected to migrate to the iron site to form the thermodynamic product. Ethylenediaminetetraacetic acid (EDTA) present in solution serves as a sacrificial electron donor, reducing the $[Ru(bpy)_3]^{3+}$ before it can undergo back electron transfer with the reduced protein. A mechanism for the EDTA oxidation by $[Ru(bpy)_3]^{3+}$ has been proposed, and is outlined in scheme 2 (figure 4.5).

Ideally, one would like to monitor both the donor oxidation and the acceptor reduction, to verify that no other groups contribute to the observed electron transfer process. Monitoring of the redox activity of the ruthenium center is precluded in this system, as the required wavelength of the probe beam (280-450nm) would result in continuous excitation of the photosensitive $[Ru(bpy)_3]^{2+}$ complex.

The quenching of $[Ru(bpy)_3]^{2+*}$ by tryptophan was studied to investigate the possibility of participation of amino acid radicals in the electron transfer process. Lifetime measurements made for the trisbipyridyl complex of Ru(II) in the presence and absence of tryptophan are presented in table 4.1. No quenching of the excited state was observed, suggesting that the reduction potential of the excited state was too low to allow for tryptophan oxidation. This result is consistent with the value of $0.87(\pm 0.1)$V,[7] and inconsistent with reports[8] of 0.64V for the tryptophan radical ($Trp^{\cdot}$) reduction

[7] Butler, J., Land, E., Prütz, W., Swallow, A. *J.C.S. Chem. Comm.* 348 (1986).

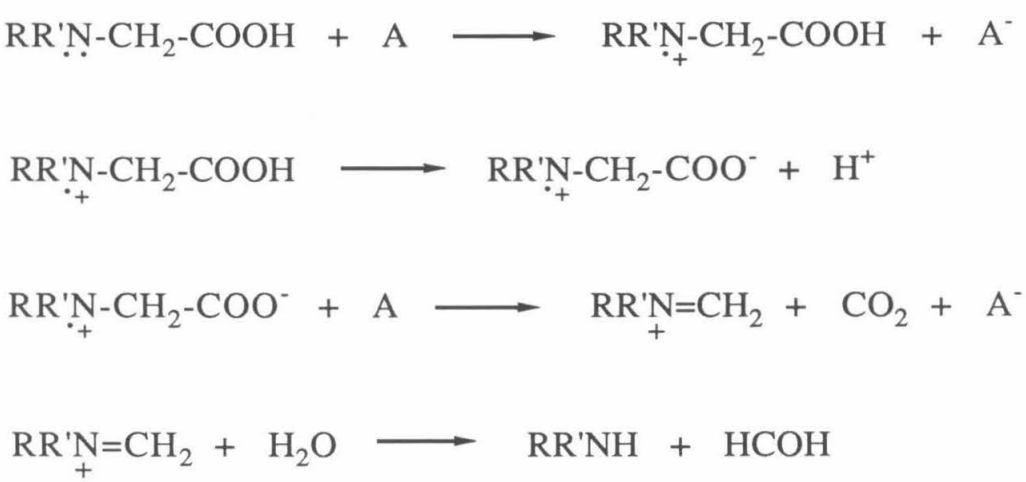

Scheme 2

Figure 4.5. Postulated mechanism of action of Na_2EDTA in the flash photolysis experiment (D. Miller, G. McLendon, *Inorg. Chem.* **20**, 950 (1981)). $EDTA^{2-}$ ($R=CH_2COOH$, $R'=CH_2CH_2N(CH_2COO^-)_2$) acts to reduce $[Ru(bpy)_3]^{3+}$ (A=acceptor) and prevent its reduction by the protein under study. The radical intermediate is believed to be responsible for the slow reduction of the native cytochrome, *i.e.*, the second equivalent of acceptor may be ferricytochrome rather than $[Ru(bpy)_3]^{3+}$.

Table 4.1. $[Ru(bpy)_3]^{2+*}$ lifetimes in the presence and absence of tryptophan

sample	τ (ns)[a]
$[Ru(bpy)_3]^{2+}$	591.5
$[Ru(bpy)_3]^{2+}$	573.7
$[Ru(bpy)_3]^{2+}$ + Trp	581.5

a. average of two values, each determined by fits to averages of at least 200 pulses.

potential,[9] assuming a value of 0.84V[10] for $[Ru(bpy)_3]^{2+*}$ reduction.[11]

Since the reduction potential of a tryptophan residue might be expected to vary depending on its particular protein environment, studies should be conducted to test for the transient formation of the Trp· radical upon $[Ru(bpy)_3]^{2+}$ excitation and subsequent cytochrome reduction. *C. krusei* cytochrome *c* contains a single tryptophan residue (number 59).[12] The absorbance can be monitored at 526.5nm, a

[8] Jovanovic, S., Harriman, A., Simic, M. *J. Phys. Chem.* **90**, 1935 (1986).

[9] Once oxidized, tryptophan may lose a proton, depending on the solution pH. The pK_a has been reported to be 4.3 by Posener, M., Adams, G., Wardman, P., Cundall, R. *J.C.S. Faraday Soc. I* **72**, 2231 (1976).

[10] Creutz, C., Sutin, N. *Inorg. Chem.* **15**, 496 (1976).

[11] Butler, J., Land, E., Swallow, A., Prütz, W. *J. Phys. Chem.* **91**, 3114 (1987).

[12] Narita, K., Titani, K. *J. Biochem.* **63**, 226 (1968).

C. krusei cytochrome *c* isosbestic point, near the 485-510nm absorbance maximum of Trp·.[13]

In an intramolecular electron transfer experiment such as that described above, where the fully oxidized protein is utilized (*i.e.*, $E^{o}(Fe)>E^{o}(Ru)$), formation of Trp· would not interfere with the electron transfer rate constant determination provided no more than one bimolecular redox reaction occurred per cytochrome molecule. However, for other systems, where the fully reduced protein is utilized, Trp· formation and subsequent $Fe^{2+}\rightarrow$Trp· electron transfer might be observed in addition to $Fe^{2+}\rightarrow Ru^{3+}$ electron transfer.

Reduction of amino acid residues was not considered a possibility, as the potentials of the tryptophan, tyrosine, and phenylalanine amino acid/radical anion couples have been estimated from preliminary experiments to be more negative than -1V.[14] A value of -0.84V has been reported for the $[Ru(bpy)_3]^{3+}/[Ru(bpy)_3]^{2+*}$ reduction potential.[15]

Upon flashing the native *C. krusei* cytochrome in the presence of $[Ru(bpy)_3]^{2+}$, a rapid rise in absorbance is observed (figure 4.6). This confirms that the mechanism of $[Ru(bpy)_3]^{2+*}$ quenching by cytochrome is indeed an electron transfer process. Ideally, the excited ruthenium complex would transfer an electron to the heme of native cytochrome *c*, and no further change in absorbance would be observed.

[13] (a) Redpath, J., Santus, R., Ovadia, J., Grossweiner, L. *Int. J. Radiat. Biol.* **27**, 201 (1975); (b) Santus, R., Grossweiner, L. *Photochem. Photobiol.* **15**, 101 (1972).

[14] Butler, J., Land, E., Prütz, W., Swallow, A. *Biochim. Biophys. Acta* **705**, 150 (1982).

[15] Lin, C., Sutin, N. *J. Phys. Chem.* **80**, 97 (1976).

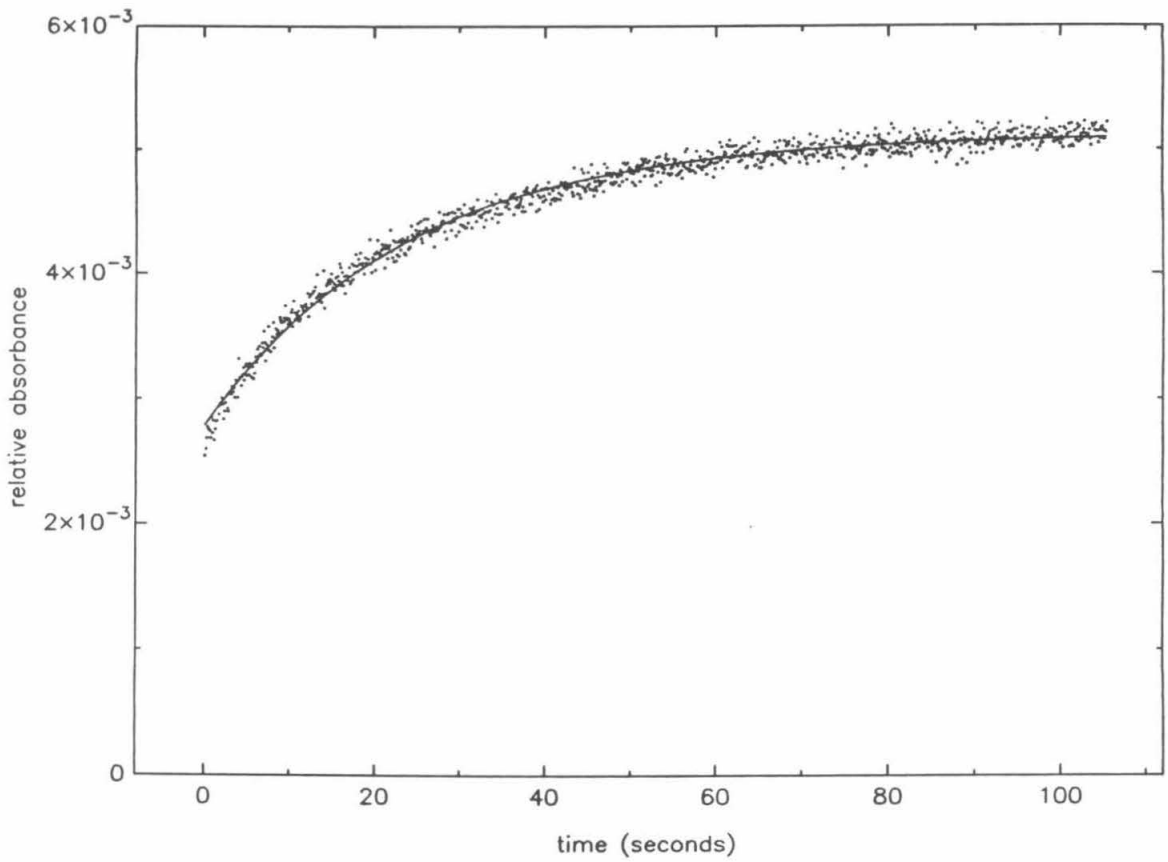

Figure 4.6. Flash photolysis data for native *C. krusei* cytochrome *c* (λ=549nm). The initial jump in absorbance at the time of the flash (0s) is attributed to reduction of the heme iron by the excited ruthenium(II) tris(bipyridyl) complex. The slower reduction is attributed to EDTA radicals which are formed by reaction with the oxidized ruthenium(III) tris(bipyridyl) complex. The data can be approximated by a monoexponential function (k=0.05/s, an average of three experiments).

However, the data reveal a slow process which can be fitted to a mono-exponential function with a rate constant of ~0.05s^{-1} for concentrations identical to those at which the modified protein kinetics were studied. The process is believed to be the reduction of the heme iron by the EDTA radicals which result from the reduction of the $[Ru(bpy)_3]^{3+}$.

On a similar time scale (100s), little absorbance change is observed upon flash photolysis of the modified protein after the initial increase (figure 4.7). Data collected on a much shorter time scale reveal an absorbance increase and leveling after approximately 16ms in addition to the initial jump expected from direct reduction of the iron site (figure 4.8). This process is attributed to the migration of electrons from the ruthenium(II) centers (created upon flashing by oxidation of $[Ru(bpy)_3]^{2+*}$) to the iron(III), and proceeds with a rate constant of ~170s^{-1}. The concentration independence of the observed rate over the 1-6μM range ([cytochrome]) supports the assumption that this is an intramolecular process. Although EDTA radicals may be present, further absorbance changes are minimal because the protein is almost completely reduced.[16]

If the intramolecular electron transfer data is fit beyond 7ms, so as to eliminate that which might be affected by the problem of flash

[16] The similar values of the absorbance change for the native and modified samples suggests that a similar number of bimolecular electron transfer events take place. Hence, the EDTA radical concentration is expected to be similar in each case. Direct EDTA radical reduction of the iron site, or rate-determining radical reduction of the ruthenium site, followed by fast intramolecular electron transfer, may be responsible for the slow rise observed in the 0-5s range following flash photolysis of the modified derivative.

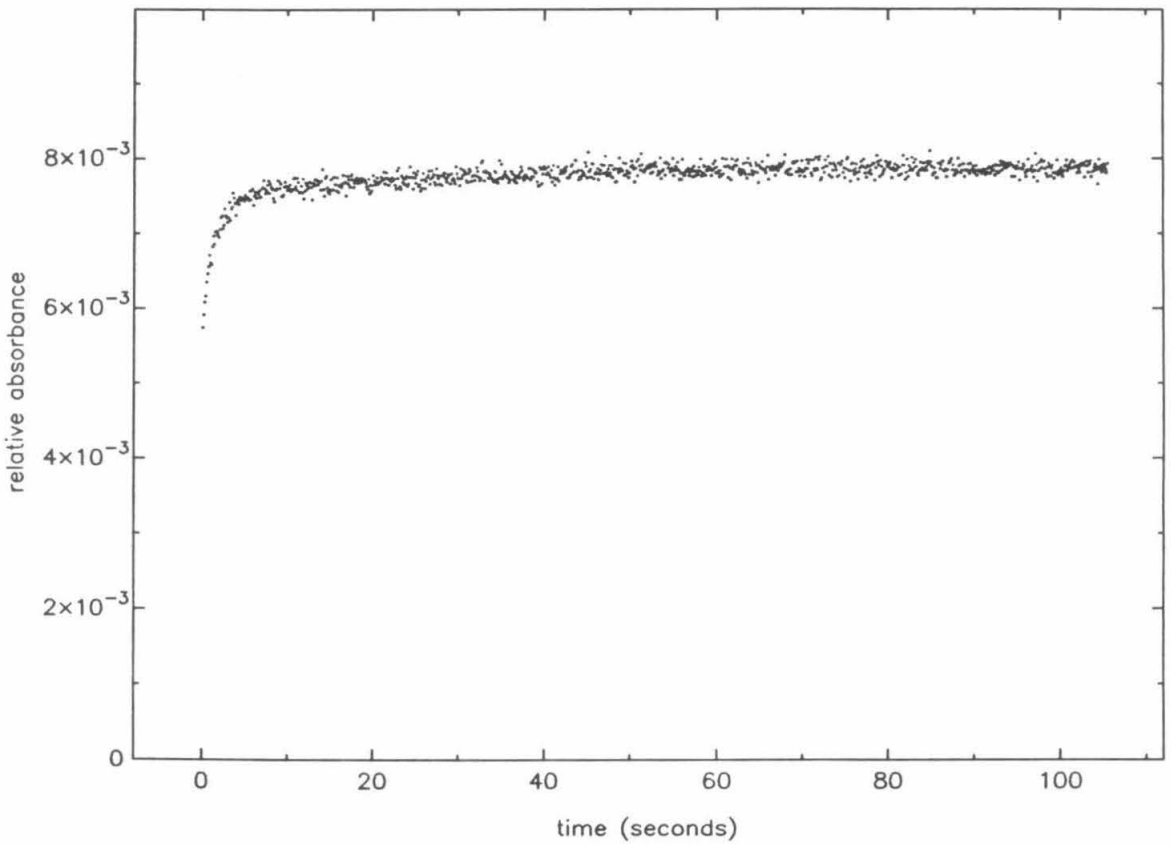

Figure 4.7. Flash photolysis of modified *C. krusei* cytochrome *c* (λ=549nm). Reduction is rapid, and little of the observed signal is due to EDTA radical reduction.

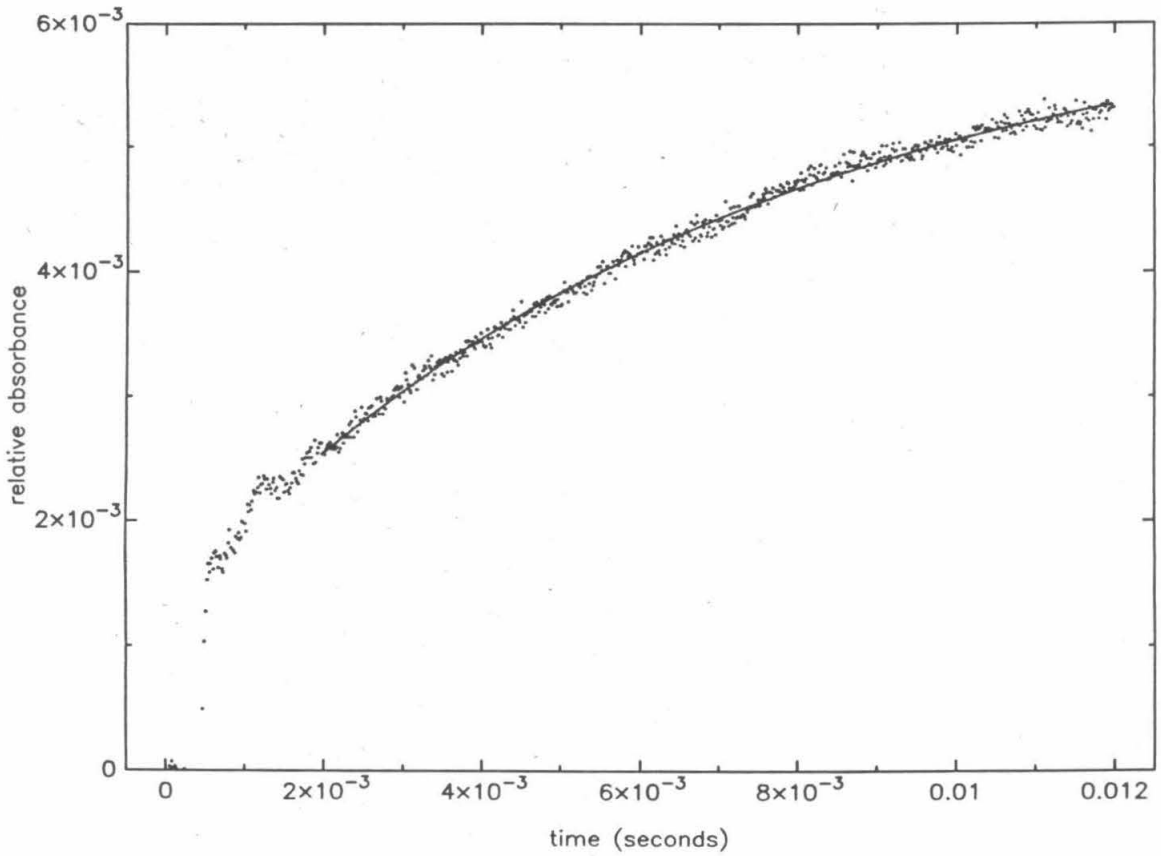

Figure 4.8. Data for flash photolysis of the modified *C. krusei* cytochrome *c*. The average of monoexponential fits to two runs for the 2-12ms range is 170/s.

breakthrough, an average rate of $295s^{-1}$ is obtained (figure 4.9). This value is much more uncertain, but as stated previously, $170s^{-1}$ is probably a lower limit to the actual electron transfer rate constant. Rate constants for the intramolecular electron transfer in the ruthenium-modified protein are tabulated in table 4.2.

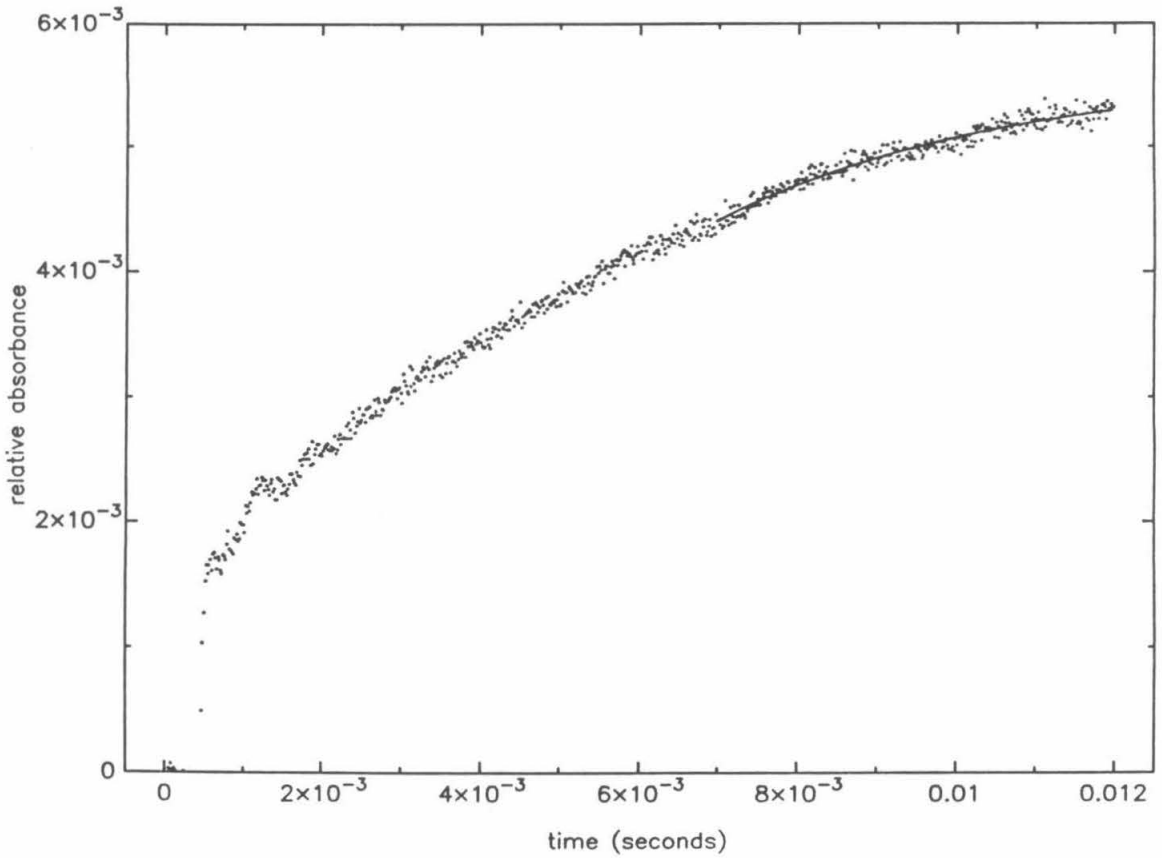

Figure 4.9. Data for flash photolysis of the modified *C. krusei* cytochrome *c*. The average of monoexponential fits to two runs for the 7-12ms range is 295/s.

Table 4.2. Monoexponential fits to the kinetic data of modified cytochrome *c* [a]

A. t>2ms

parameter	Run 1	Run 2
A(1)	0.0096 ± 0.0002	0.0013 ± 0.0001
A(2)	0.0041 ± 0.0001	0.0049 ± 0.0001
k (s^{-1})	194 ± 20	145 ± 16

B. t>7ms

parameter	Run 1	Run 2
A(1)	-0.0027 ± 0.009	-0.0022 ± 0.006
A(2)	0.0075 ± 0.009	0.0078 ± 0.006
k (s^{-1})	320 ± 210	270 ± 139

a. Data were fit to an equation of the form y = A(1) + A(2)[1-exp(-A(3)t)], where A(3) is the rate constant k.

CHAPTER 5

DISCUSSION AND CONCLUSION

The rate constant for intramolecular electron transfer in A_5Ru-(His39)-*C. krusei* cytochrome *c* has been found to be at least $170s^{-1}$. This is the fastest rate measured to date for ground state electron transfer in a ruthenium-modified protein (see table 1.1). To evaluate the significance of this result, it is appropriate to compare this rate with those determined for horse heart A_5Ru(His33)cytochrome *c* (k_{et}= $30s^{-1}$)[1] and *Pseudomonas stutzeri* A_5Ru(His47)cytochrome c_{551} (k_{et}= $13s^{-1}$).[2] In all three cases, the donor and acceptor sites are chemically equivalent, and so are expected to have identical inner sphere reorganization energies. The driving force is equivalent (within experimental error) in each case (~170mV).

These derivatives differ significantly in three respects: distance, medium, and orientation. His39 of *C. krusei* cytochrome *c* is the farthest removed at 13Å from the heme, while His33 and His47[3] are removed 11.7 and 7.9 Å, respectively. Contrary to what is observed, the greater distance in the *Candida* derivative would be expected to result in a diminished electron transfer rate due to decreased electronic coupling of the donor and acceptor. Assuming the values of ν and ΔG^* are identical for both *C. krusei* and horse cytochromes, and using a value of $0.9Å^{-1}$ for β, an electron transfer rate constant of

[1] Nocera, D., Winkler, J., Yocom, K., Bordignon, E., Gray, H. *J. Amer. Chem. Soc.* **106**, 5145 (1984).

[2] Osvath, P., Salmon, G., Sykes, A. *J. Amer. Chem. Soc.* **110**, 7114 (1988).

[3] His47 of cytochrome c_{551} is homologous to residue 67 in horse and yeast cytochrome *c*; (a) de Silva, D., Sykes, A. *Biochim. Biophys. Acta* **952**, 334 (1988); (b) Almassy, R., Dickerson, R. *Proc. Natl. Acad. Sci.* **75**, 2674 (1978).

~$10s^{-1}$ is predicted for the *Candida* derivative (from the k_{et} of the horse cytochrome derivative). Using the same assumptions, and the observed k_{et} of $170s^{-1}$ for the *Candida* derivative, a value of $0.64Å^{-1}$ is estimated for this derivative, *i.e.*, the modified *C. krusei* demonstrates significantly greater donor-acceptor coupling than the the horse heart derivative. Distance cannot explain the rate difference observed if one assumes a through-space mechanism is operative. The actual distance of electron transfer, however, may be shorter in the *C. krusei* derivative (as opposed to the other two) if electron transfer occurs along a through-bond pathway.

When considering the nature of the medium in a "through-space" pathway, none of the three derivatives is significantly different from the others. However, if one considers the possibility of a "through-bond" mechanism, the *Candida* derivative must be singled out for the presence of an aromatic moiety, Trp59, in the vicinity of the path connecting His39 and the heme. The edge of the tryptophan indole ring lies <2Å off the direct line connecting the C_γ of His39 and the closest porphyrin atom, and the ring is inclined at a 70^o angle (relative to the heme plane) toward the heme (figure 5.1a). There is some indication of enhanced donor-acceptor coupling in a zinc-substituted myoglobin derivative, [A_5Ru(His12)-ZnMb], which undergoes intramolecular electron transfer over a ~22Å distance at a rate similar to that of other derivatives involving shorter distances (19-20Å).[4] A tryptophan residue is present in the direct path between His12 and the heme. To

[4] Axup, A., Albin, M., Mayo, S., Crutchley, R., Gray, H. *J. Amer. Chem. Soc.* **110**, 435 (1988).

Figure 5.1. Possible pathways of electron transfer in A_5Ru(His39)-*C. krusei* cytochrome *c*.

(a) Trp59 (green) is located above the plane containing the porphyrin (red) and His39 (yellow), and <2Å from the direct pathway between the C_γ of His39 and the carbon atom of pyrrole ring IV to which the propionate is bound.

(b) A potential through-bond pathway: the amine nitrogen (yellow) of residue 41 forms a hydrogen bond with the propionic side chain of pyrrole ring IV of the heme (red), a possible 13-bond route of electron transfer.

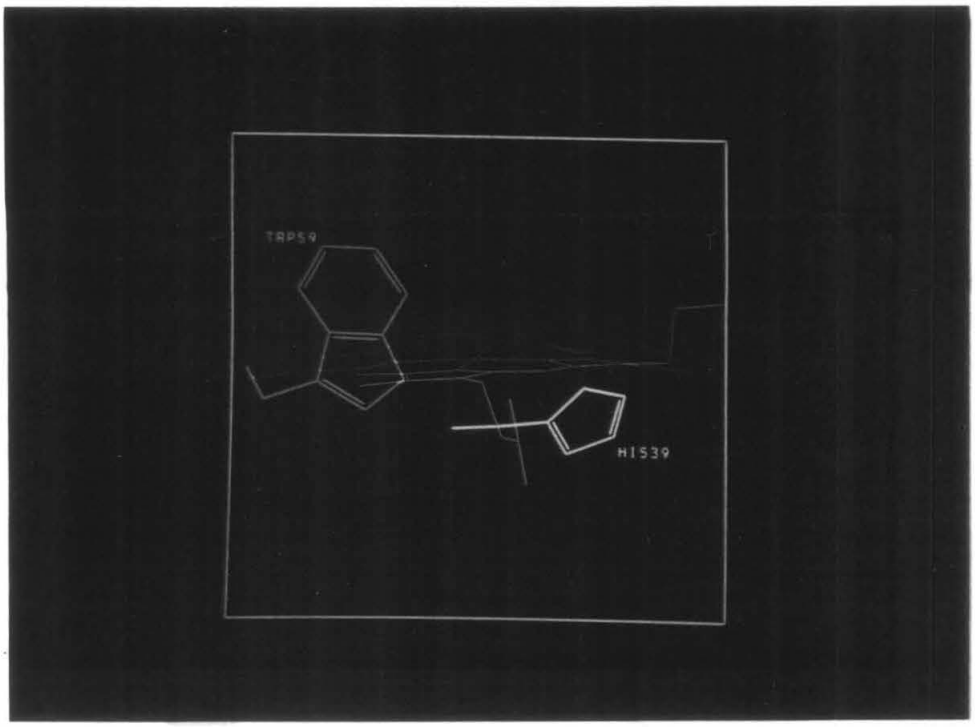

Figure 5.1 (a)

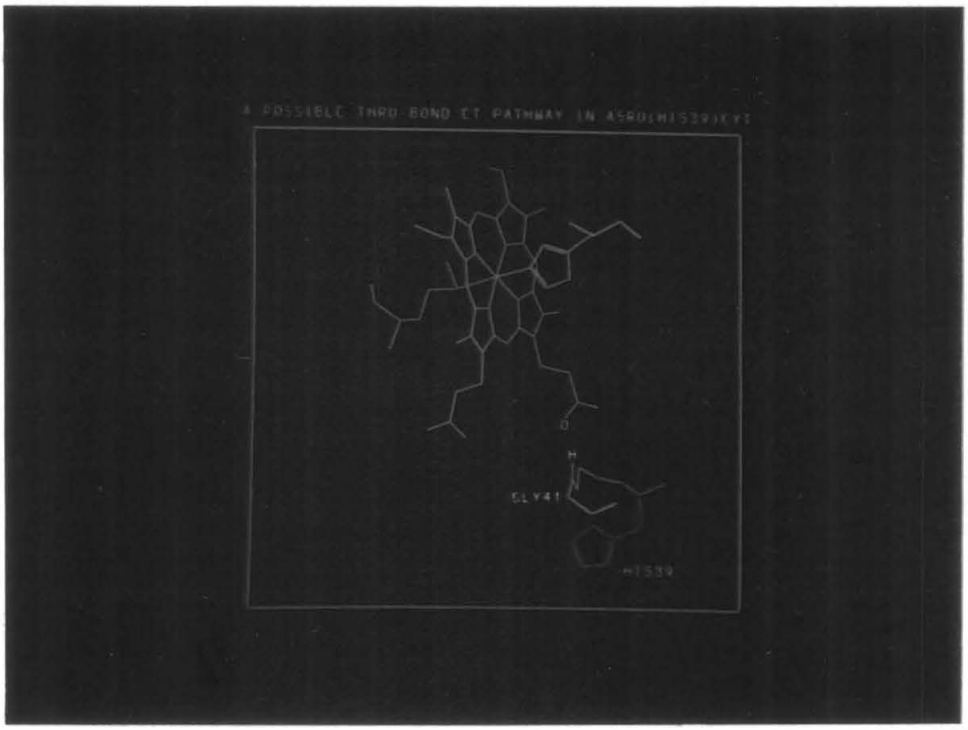

Figure 5.1 (b)

investigate the role of tryptophan in possibly enhanced donor-acceptor coupling via the superexchange mechanism,[5] a mutant cytochrome with another residue substituted at position 59 would be of interest. However, Trp59 is an evolutionarily invariant residue, and replacement of it in *S. cerevisiae* iso-1 cytochrome by even the most similar amino acid, phenylalanine, has been found to lead to instability and reduced biological activity.[6]

If one attempts to delineate specific routes of electron transfer for each derivative, the results do not point to any reason for enhanced electron transfer in the *Candida* cytochrome. A thirteen bond electron transfer pathway may exist in *Candida*, via the peptide backbone to the nitrogen of residue 41, which is hydrogen-bonded to the propionic acid of pyrrole ring IV in tuna and rice cytochromes *c* (figure 5.1b).[7] A thirteen bond pathway has also been proposed for the horse cytochrome electron transfer:[8] electron transfer could occur along the polypeptide backbone from the His33 to residue 30, whose carbonyl is hydrogen-bonded to the His18 ligand (see figure 3.21).

A third factor to consider in comparing these derivatives is donor-acceptor orientation. His33 and His47 are on opposite faces of the heme, the former at an angle of ~52^{o} with respect to the porphyrin

[5] Miller, J., Beitz, J. *J. Chem. Phys.* **74**, 6746 (1981).

[6] Schweingruber, M., Stewart, J., Sherman, F. *J. Mol. Biol.* **118**, 481 (1978).

[7] (a) Ochi, H., Hata, Y., Tanaka, N., Kakudo, M., Sakurai, T., Aihara, S., Morita, Y. *J. Mol. Biol.* **166**, 407 (1983); (b) Takano, T., Dickerson, R. *J. Mol. Biol.* **153**, 79 (1981).

[8] Meade, T., Gray, H., Winkler, J., *in press.*

plane.[9] His39 is situated exactly in the plane of the heme.

With the advent of computer graphics and molecular modeling programs have come several proposals for interactions of physiological protein pairs. Models have been proposed for the complexes of cytochrome *c* and cytochrome *c* peroxidase,[10] cytochrome b_5 and methemoglobin,[11] and cytochrome *c* and cytochrome b_5,[12] and are based to a large extent on optimized electrostatic interactions between complementary charged surface residues. A feature common to them all is the near coplanarity of the hemes, suggesting that coupling is more effective from the heme edge as opposed to the heme face. Conversely, the cytochrome cd_1 contains two pairs of hemes *c* and d_1, with each heme (within a pair) being in a perpendicular orientation with respect to the other, and this protein has been suggested to function to store reducing equivalents.[13]

The discussion thus far has been based on the assumption that the free energy of activation is similar for electron transfer in both cytochromes. While ΔG^o is equivalent (within the uncertainty) for all three derivatives, the reorganization energy, and hence the free energy of activation may not be. As mentioned previously, the similarity of

[9] measured as the angle formed by the pyrrole IV nitrogen, the iron atom, and the C_γ of residue 33 in reduced tuna cytochrome *c*

[10] (a) Poulos, T., Finzel, B. *Pept. Prot. Rev.* **4**, 115 (1984); (b) Poulos, T., Kraut, J. *J. Biol. Chem.* **255**, 10322 (1980).

[11] Poulos, T., Mauk, A. *J. Biol. Chem.* **258**, 7369 (1983).

[12] Salemme, F. *J. Mol. Biol.* **102**, 563 (1976).

[13] Makinen, M., Schichman, S., Hill, S., Gray, H. *Science* **222**, 929 (1983).

the coordination spheres of the donor and acceptor indicate the inner sphere reorganization energy is likely to be similar in each case. The outer sphere reorganization energy can be considered as two separate components: there is the reorganization of solvent molecules around the ruthenium donor and the reorganization of the medium around the heme acceptor. Pielak *et al.* have suggested that the reorganization of the solvent surrounding the ruthenium center may not be identical for each protein, and may vary depending on the local environment.[14] Little of the heme is actually solvent accessible, and the edge that is constitutes about 3% of the total cytochrome surface, so solvent reorganization is expected to be small. In order to rationalize the relative rates of flavinmononucleotide semiquinone reduction of cytochrome *c*, Meyer *et al.* proposed that the *Candida* heme is less recessed (although not necessarily more exposed) than that in horse heart cytochrome *c* on the basis of space-filling models.[15] While the peptide medium surrounding the heme serves to shield it from the polar solvent, thereby reducing outer sphere reorganization, it itself may undergo some relaxation in response to a change in the heme oxidation state.[16] Evidence which suggests the reorganization energy may be different for the two cytochromes comes from measurements of self-exchange rate constants. Even at 1M salt, in which the electrostatic repulsion of the reactants is expected to be suppressed, *Candida* cytochrome exhibits a

[14] Pielak, G., Concar, D., Moore, G., Williams, R. *Prot. Eng.* **1**, 83 (1987).

[15] Meyer, T., Watkins, J., Przysiecki, C., Tollin, G., Cusanovich, M. *Biochemistry* **23**, 4761 (1984).

[16] Churg, A., Weiss, R., Warshel, A., Takano, T. *J. Phys. Chem.* **87**, 1683 (1983).

self-exchange rate an order of magnitude smaller than that of horse heart cytochrome *c*.[17] This would suggest that the reorganization energy is higher for the yeast cytochrome, and would not aid in explaining the anomalously fast rate of intramolecular electron transfer observed.

Studies of reduction of cytochromes by zinc-substituted yeast cytochrome *c* peroxidase have demonstrated how subtle differences, which are not apparent from current thermodynamic and structural information, exist between cytochrome *c* of different species: horse cytochrome *c* is reduced at a rate of $17(\pm 3)s^{-1}$ within the protein complex, while yeast cytochrome is reduced at a rate one order of magnitude faster ($138(\pm 12)s^{-1}$).[18] This trend parallels the one observed for intramolecular electron transfer between the heme site and an appended ruthenium in horse and *Candida* cytochromes *c*.

The foregoing discussion has been predicated on the assumption that electron transfer is the rate-determining step in the observed reaction. It is possible, however, that two (or more) protein conformations exist, each having different donor-acceptor coupling efficiencies. In such a case, the observed rate might be that of a conformational change, necessary to enhance the coupling of the donor and acceptor, which precedes a fast electron transfer.[19] Cytochrome *c* crystallizes in slightly different conformations in the reduced and

[17] Gupta, R. *Biochim. Biophys. Acta* **292**, 291 (1973).

[18] Ho, P., Sutoris, C., Liang, N., Margoliash, M., Hoffman, B. *J. Amer. Chem. Soc.* **107**, 1070 (1985).

[19] Hoffman, B., Ratner, M. *J. Amer. Chem. Soc.* **109**, 6237 (1987).

oxidized state, and is therefore assumed to undergo some motion in the course of reduction.[20] The rate of electron transfer in A_5Ru(His33)-horse heart cytochrome *c* has been demonstrated by Bechtold *et al.* to be independent of the methionine ligand dissociation, which is known to occur on a similar time scale.[21] However, other rate-determining conformational changes cannot be ruled out at present.

Directions for future research

An intramolecular electron transfer rate for a A_5Ru(His33)-*C. krusei* derivative would help to sort out the effects of the variables discussed above. Specifically, if the fast rate observed in A_5Ru-(His39)-*C. krusei* is due to a favorable pathway or medium effect, the A_5Ru(His33)cytochrome may undergo electron transfer at a rate similar to that of the horse heart derivative. To date, only one pair of homologous proteins have been modified at identical residues, that of *A. variabilis* and *S. obliquus* plastocyanin.[22] Each protein has been modified at His59 with a pentaammineruthenium moiety, and each undergoes intramolecular electron transfer (copper reduction) at a rate of ~$0.03s^{-1}$ (ΔE^o=300mV). The slow rate, at a moderate distance (~12Å) and a driving force comparable to that in azurin and cytochrome *c* derivatives, was interpreted as evidence supporting the existence of specific pathways which are more conducive to electron transfer.

[20] Takano, T., Dickerson, R. *J. Mol. Biol.* **153**, 95 (1981).

[21] Bechtold, R., Gardineer, M., Kazmi, A., van Hemelryck, B., Isied, S. *J. Phys. Chem.* **90**, 3800 (1986).

[22] Jackman, M., McGinnis, J., Powls, R., Salmon, G., Sykes, A. *J. Amer. Chem. Soc.* **110**, 5880 (1988).

Several options are available to obtain a rate for the His33 derivative:

(1) a His33-modified derivative might be synthesized by taking advantage of the greater reactivity of His39 to modify His39 with a redox-inactive moiety which would prevent reaction with $[A_5Ru(OH_2)]^{2+}$;

(2) differences in the ionization constants (pK_a values) of the two residues, if significant enough, could be exploited to control the relative proportions of protonated and deprotonated forms of the two residues, and therefore the relative concentrations of the reactive species;

(3) a rate could be obtained for the doubly-modified derivative;

(4) site-directed mutagenesis could be employed to create a protein lacking His39, making modification of the His33 site straightforward.

Each of these options will be discussed in turn.

Option (1) is viable, but the ideal modification reagent is lacking. Currently, the most specific and widely used reagent for modification of histidine residues is diethylpyrocarbonate, DEPC.[23]

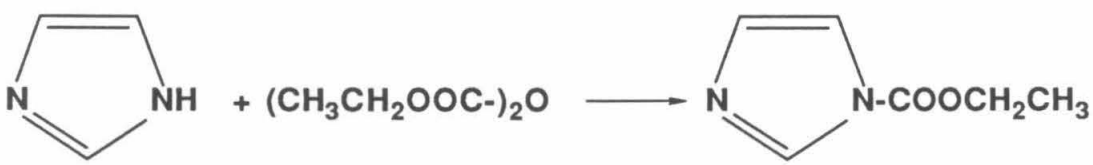

Figure 5.2. Reaction of imidazole with diethylpyrocarbonate.

[23] Miles, E., *Meth. Enzym.* **47**, 431 (1977).

The suitability of this reagent for this application is in doubt, as it may react equally readily with both His33 and His39 due to its small size (see discussion of chapter 3). The modification is attractive, as it is reversible (the model compound decays over a period of several days at pH 7, or the reversal can be induced by hydroxylamine). However, the reagent lacks the desired specificity, and has been found to react with tyrosine, cysteine, and lysine residues as well. Another drawback is that DEPC can react with both imidazole nitrogen atoms to produce a stable product (*i.e.*, the reaction is irreversible).[24] Attempts to use this reagent to quantify histidine before and after reaction of *C. krusei* cytochrome *c* with $[A_5Ru(OH_2)]^{2+}$ were unsuccessful. The usual result indicated a histidine content greater than the known histidine content of the protein, despite the use of small excesses of reagent. This may be attributed to reaction at both nitrogen atoms of each imidazole, or reaction at other sites, leading to protein denaturation and concommitant changes in absorption properties. UV-visible studies suggest that $[A_5RuHis]^{3+}$ is unreactive towards DEPC, but it has not been verified that the product of the reaction of histidine with DEPC is unreactive toward $[A_5Ru(OH_2)]^{2+}$.

NMR studies prior to this work, including determinations of ionization constants and C2-^{1}H assignments for the yeast cytochrome *c* histidine residues, indicated that the His33 pK_a was significantly less than that of His39 in the reduced state of the protein (6.7 *vs.* 7.3, respectively).[25] Hence, at pH 5.3, two full pH units below the His39

[24] A doubly-modified hybrid might be used, *i.e.*, His39 modified with DEPC and His33 with pentaammineruthenium, but it would be preferable to use a protein resembling the native cytochrome as closely as possible.

pK_a, only 1% of this residue would be expected to be unionized. Approximately 4% of His33, in contrast, would exist in the deprotonated form at this pH. Therefore, the effective concentration of His33 could be raised relative to that of His39 by decreasing the pH of the modification reaction mixture.

The third option is the most desirable and feasible. Preliminary evidence indicates that the second product of the $[A_5Ru(OH_2)]^{2+}$ modification reaction is a derivative modified at both His33 and His39 (see appendix 6). The observed rate of iron reduction in such a protein is expected to be biexponential, and should be fitted by the rate constants corresponding to the two intramolecular electron transfer processes.

Finally, a fourth alternative is available which will not produce the exact result desired, but which will allow for the investigation of whether all A_5Ru(His33)-cytochrome *c* derivatives will display similar intramolecular electron transfer kinetics. Work is in progress on site-specific mutants of *S. cerevisiae* cytochrome *c* in the lab of Jack Richards at Caltech, and is being done in collaboration with Harry Gray. A gene in which His39 has been replaced with a glutamine residue has been prepared, and has been used as the basis for further mutations to *introduce* histidines at locations of interest.[26] Protein of this genotype could be prepared and modified to obtain a A_5Ru-His33 derivative. The result would be a better basis for the *Candida* comparison than the horse cytochrome rate, as the two yeast proteins are 77%

[25] Robinson, M., Boswell, A., Huang, Z., Eley, C., Moore, G. *Biochem. J.* **213**, 687 (1983).

[26] Casimiro, D., Richards, J., Gray, H., unpublished results

identical in amino acid composition (figure 5.3),[27] whereas horse cytochrome and *C. krusei* cytochrome *c* have only 50% of their residues in common. The author knows of no report of the isolation of the *C. krusei* cytochrome *c* gene to date.

The dependence of the electron transfer rate on driving force has been studied in a series of A_4RuL(His33)-horse heart cytochrome derivatives. *C. krusei* is a superior candidate for such studies, as His39 reacts readily to give a sizeable yield of modified product. Such studies should be accompanied by detailed spectroscopic and thermodynamic characterization of the protein, as the majority of the voluminous amount of work on cytochrome *c* to date has been done with that of horse heart. Such a study may indicate whether comparisons between the yeast and horse cytochrome are justified, *i.e.*, whether their reorganization energies are similar.

Concluding Remarks

Another number has been added to the growing list of intramolecular electron transfer rates in ruthenium-modified proteins. The unusually fast rate may very well be attributed to enhanced donor-acceptor coupling resulting from their relative orientation and/or the nature of the intervening medium, but a firm interpretation of this number must await further experimentation.

One cannot draw any conclusions about the mechanism of electron transfer from a single intraprotein electron transfer rate, and comparisons with others suffer from a problem which plagues many electron

[27] on a residue-by-residue basis

1 10

Pro-Ala-Pro-Phe-Glu-Gln-Gly-Ser-Ala-Lys-Lys-Gly-Ala-Thr-Leu-Phe-
Thr-Glu- -Lys -Ala-

20

Lys-Thr-Arg-Cys-Ala-Gln-Cys-His-Thr-Ile-Glu-Ala-Gly-Gly-Pro-His-
-Leu- -Val- -Lys-

30 40

Lys-Val-Gly-Pro-Asn-Leu-His-Gly-Ile-Phe-Ser-Arg-His-Ser-Gly-Gln-
-Gly-

50

Ala-Glu-Gly-Tyr-Ser-Tyr-Thr-Asp-Ala-Asn-Lys-Arg-Ala-Gly-Val-Glu-
-Ile -Lys- Lys- Asn - - Leu-

60 70

Trp-Ala-Glu-Pro-Thr-Met-Ser-Asp-Tyr-Leu-Glu-Asn-Pro-TMK-Lys-
-Asp- -Asn-Asn- -Glu- -Thr-

80

Tyr-Ile-Pro-Gly-Thr-Lys-Met-Ala-Phe-Gly-Gly-Leu-Lys-Lys-Ala-Lys-
-Glu-

90 100

Asp-Arg-Asn-Asp-Leu-Val-Thr-Tyr-Met-Leu-Glu-Ala-Ser-Lys
-Ile- -Leu -Lys- Lys- -Cys-Glu

Figure 5.3. Sequences of the cytochromes *c* from the yeasts ***Candida krusei***[a] and *Saccharomyces cerevisiae*[b] (the residues of the latter are identical to those of the former unless specified). The residue numbers are assigned according to the horse sequence. Of the 108 residues the two proteins have in common, 83 are identical.

a. Lederer, F. *Eur. J. Biochem.* **31**, 144 (1972); Narita, K., Titani, K. *J. Biochem.* **63**, 226 (1968).
b. Lederer, F., Simon, A., Verdiere, J. *Biochem. Biophys. Res. Comm.*, **47**, 55 (1972); Narita, K., Titani, K. *J. Biochem.* **65**, 259 (1969); Yaoi, Y. *J. Biochem.* **61**, 54 (1967).

transfer studies: the inability to investigate one variable at a time. In comparing this number to that of horse cytochrome and c_{551}, the non-equivalence of the donor-acceptor coupling (reflected in β), as well as of λ must be borne in mind.

The cytochrome *c* about which the most information is available, horse cytochrome *c*, is of limited use for in-depth electron transfer studies. Mutant *S. cerevisiae* iso-1 cytochromes offer the most versatility in terms of probing distance, medium, and orientation effects, and comparisons between rates of electron transfer in their ruthenium-labeled derivatives may be more appropriate than interspecies comparisons.

Appendix 1

Amino Acid Analysis Method Development

INTRODUCTION

In order to identify proteolytic fragments, a quantitative method for amino acid analysis was developed. The reagent (9-fluorenylmethyl)-chloroformate (FMOC-Cl) reacts rapidly with primary and secondary amines at alkaline pH to form stable derivatives:[1]

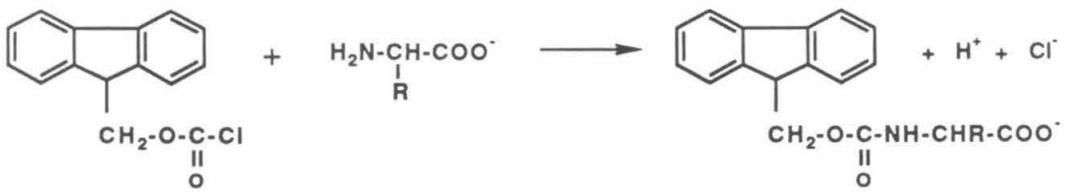

Such derivatization provides a facile means of detection: amino acids derivatized with FMOC-Cl (FMOC-AA's) absorb UV light of 200-300nm (λ_{max} = 300, 289, 265, 227 and 218 nm, with the highest extinction of ~20000-30000 $M^{-1}cm^{-1}$ at 265nm),[2] and have an emission maxima in the region of 310nm.[1a] The derivatives are separated on reverse phase resins, detected by UV absorbance, and quantified.

Precolumn derivatization was chosen over ion-exchange separation with post-column derivatization, as the former method was compatible with available instrumentation. The method involving derivatization with FMOC-Cl was chosen because of its potential sensitivity and the fact that the reagent reacts with both primary and secondary amines to form stable monosubstituted derivatives. Other reagents, such as *o*-phthaldialdehyde, do not react with secondary amines, *i.e.*, quantita-

[1] (a) Einarsson, J., Josefsson, B., Lagerkvist, S. *J. Chromatography* **282**, 609 (1983); (b) Moye, H., Boning, A. *Anal. Lett.* **12**(B1), 25 (1979).

[2] An extinction coefficient of 34000 $M^{-1}cm^{-1}$ is reported in reference 3 for the FMOC derivatives in pentane; values obtained for solutions of both reagent and derivatives in ~40% CH_3CN in this lab were ~18500 $M^{-1}cm^{-1}$.

tion of proline is not possible. Other methods, *e.g.*, reaction with dabsyl chloride or phenylisothiocyanate, result in nonfluorescent derivatives, and so are less sensitive.[3]

The method has been developed to the point of providing relative, but not absolute, amounts of most amino acids. Tryptophan is not distinguished from phenylalanine. The presence of tyrosine can be confirmed but not quantified. The presence of histidine or lysine can be confirmed, but the two are not distinguished from one another, nor quantified.

MATERIALS and INSTRUMENTATION

The chromatographic instrumentation is described in chapter 3. Derivatives were detected by their absorption at 265nm.

n-Pentane was of HPLC grade, and was obtained from Fisher Scientific. Other solvents used are described in chapter 3.

The amino acid derivatives were separated on Vydac 218TPS (4.6mm x 250mm) reverse phase, silica-based C18 columns.

(9-fluorenylmethyl)-chloroformate and 9-fluorenylmethanol were obtained from Fluka; the former was stored at $0^{o}C$ under argon. Solutions of FMOC-Cl in acetonitrile were prepared periodically and used for several weeks. The FMOC derivatives of the L-isomer amino acids glycine, valine, alanine, leucine, isoleucine, phenylalanine, methionine, proline, and tryptophan were obtained from Fluka. N-α-FMOC-L-lysine and N-ε-FMOC-L-lysine were purchased from Chemical Dynamics Corporation. Individual, underivatized amino acids were

[3] Ogden, G., Földi, P. *LC·GC* **5**, 28 (1987), and references therein.

supplied in the Pierce Amino Acid Standard Kit 22. 1-adamantanamine was purchased from Aldrich.

$NaHCO_3$ and $Na_2B_4O_7 \cdot 10H_2O$ were reagent grade. Borate buffer was prepared by titrating a solution of ~50mM $Na_2B_4O_7 \cdot 10H_2O$ to the desired pH with 2N HCl.

Amino acid standards employed in the calibration included Sigma AA-S-18 (two different lots) and Pierce Amino Acid Standard H. Norvaline, β-alanine, norleucine, cysteic acid, bradykinin, angiotensin II, oxidized insulin chain B and hen egg white lysozyme were obtained from Sigma. Sperm whale myoglobin, obtained from Sigma and purified by elution from CM-52 with 50mM pH 7.2 Tris buffer, was kindly provided by Dr. James Cowan. Materials for hydrolyses of test peptides are described in chapter 3.

Filtration materials for solvents and samples are described in chapter 3. The amino acid derivatization and subsequent extractions were carried out in glass, screw-capped vials. Samples were filtered into new 10mm x 75mm borosilicate test tubes. All reagents were dispensed using Gilson Pipetman digital microliter pipets (models P-20, P-200, and P-1000) or an Eppendorf model 4710 pipet, all of which had been recently calibrated. New Becton Dickinson 1cc disposable syringes and a 22G Rheodyne blunt-tipped needle were used to inject calibration samples.

METHODS

Method development was carried out on column #500354 at 25°C. Calibration and actual sample analysis was done on column #60 of lot #870205-10 at 35°C.

When quantitation was important, the needle port was rinsed with 15% (v/v) CH_3CN in H_2O to prevent sample carryover from one injection to the next.

No data was utilized from runs which were the first of the day.

Derivatization

The following procedure was used initially during development of the method to provide samples containing most amino acid derivatives of interest, plus any possible side products, impurities, and excess reagent. An aliquot of known volume (~10μL) of amino acid standard (~2.5μmol/mL of each amino acid dissolved in 0.1N HCl) was added to ~230μL 150mM $NaHCO_3$ (pH>7). An aliquot of ~250μL FMOC-Cl, ~10mM in CH_3CN, was added to give a reagent-to-amino acid ratio of ~5:1. After ten minutes, the reaction mixture was extracted twice with equal volumes of *n*-pentane. An aliquot of the aqueous phase was removed and diluted with sufficient mobile phase "A" to reduce the acetonitrile concentration to 15% (the assumption was made that the acetonitrile concentration was unaffected by the extraction procedure). Derivatizations were performed immediately prior to injection.

Separation

The mobile phase gradient for separation of the amino acid derivatives was developed on a trial-and-error basis, using a standard containing equimolar amounts of all twenty amino acids (except tryptophan, asparagine, and glutamine, the latter two of which are expected to be hydrolyzed to their acid forms during peptide hydrolysis). Cysteine was present as the disulfide, cystine. Assignments of the

peaks were made by spiking the derivatization reaction mixture with a single amino acid, or with the preformed FMOC-AA derivative.

Minor variations in conditions were necessary with new columns.

The mobile phase used is as follows:

"A" = 2.55mL acetic acid was made up to 925mL with water, 1mL triethylamine was added, and the solution was made up to 1 liter with methanol;

"B" = "A", using acetonitrile in place of water (prepared in 500mL batches).

Fresh solutions were prepared daily.

The gradient program used to separate the amino acid derivatives and reequilibrate the column is described in table A1.1.

Standardization of reaction conditions

Several runs were conducted under identical conditions with pH 8.0, 8.4, and 9.0 borate buffer: 210μL 11.7mM FMOC-Cl was added to a solution of 9.6μL standard in 230μL ~50mM borate buffer. The reaction was allowed to proceed for 20 minutes, at which time 125μL of the reaction mixture was removed to a vial containing 938μL H_2O and 275μL CH_3CN. The entire volume, after filtration, was used to flush and fill a 200μL loop.

A time analysis of the derivatization reaction was performed using pH 9 ~50mM borate. Reaction conditions were as follows: 9.6μL amino acid standard was expelled into 230μL pH 9 50mM borate, and a 210μL aliquot of ~11mM FMOC-Cl was added. The reaction was allowed to proceed for a specified time (5, 10, 20, 30, or 40 minutes). 125μL of the reaction mixture was diluted with 275μL CH_3CN and 938μL H_2O. After

Table A1.1. Gradient program for FMOC-AA elution and column re-equilibration

time(minutes)	event
0	flow rate climbs to 1.3 mL/min. in 0.5 min. %B = 15
0.9	alarm sounds signalling beginning of gradient
1.0	%B climbs to 37 in 42.3 min.
43.3	%B climbs to 60 in 17.7 min.
61	%B climbs to 100 in 15.4 min.
76.4	flow rate climbs to 2mL/min. in 1 min.
81.4	flow rate is reduced to 1.3mL/min. in 2 min.
118	flow rate is reduced to 0.3mL/min. in 2 min.

filtration, the entire volume was used to rinse and load a 200μL loop. Four runs were conducted for each reaction time.

Calibration

The following reaction conditions were used for all calibration runs: 225μL 11.2mM FMOC-Cl was added to a solution of 10μL amino acid standard in 225μL pH 9 ~52mM borate. The reaction was allowed to proceed for 45 minutes before the mixture was extracted twice with 460μL aliquots of *n*-pentane. An aliquot of the aqueous layer was removed and diluted with the appropriate volume of CH_3CN and "A" to achieve a final CH_3CN concentration of 15%, and a final volume of ~1250μL. One milliliter of the filtered solution was used to flush and load a 200μL loop.

Three individual runs of derivatized cysteic acid were conducted

to obtain a rough calibration. 91.5mg L-cysteic acid monohydrate was dissolved in 50mL H_2O. A 460μL aliquot of this solution was made up to 2mL to obtain a 2.25mM solution. Aliquots of 10μL of this solution were diluted with 225μL borate and derivatized with 225μL FMOC-Cl. Calibration runs using 200μL and 60μL of the aqueous phase, in total volumes of 1250μL, were conducted. A second solution, 2.5mM in concentration, was prepared by making 980μL of a solution, 0.1192g in 25mL, up to 10mL. A 10μL aliquot of this solution was derivatized and run to give a third calibration point.

Since the extent of extraction of each of the FMOC-AA derivatives is unknown, the concentration was expressed only in a relative fashion, *i.e.*, 200μL aqueous layer = 0.5x, 100μL = 0.25x, *etc.*, where x is the derivative concentration, after extraction and dilution, for a 400μL aliquot of the aqueous layer. At least two runs at each concentration (1x, 0.75x, 0.5x, 0.25x, 0.125x, 0.0625x, and 0.03125x) were performed and average peak areas were used to construct a response curve for each derivative, which were fitted by a least squares linear regression method.

Adjustment of conditions for new column

A new column was obtained for actual sample analysis, as the first was showing signs of deterioration. The new column was washed five hours at 1mL/min with methanol (to react with any chlorosilane), and then washed eleven hours at 0.4mL/min with *i*-propanol (to dissolve any polymerized silanizing reagent).[4]

[4] Hancock, W., Sparrow, J. *HPLC Analysis of Biological Compounds*, Dekker (New York), 1984.

Evaluation of possible internal standards

An aliquot of amino acid standard was derivatized and extracted as usual. ~15mM solutions (in 0.1N HCl) of compounds which were potential internal standards were prepared, and aliquots of these were used in separate derivatization reactions. Equal volumes of the aqueous phases of both the standard and the test compound reaction mixtures were combined, injected, and eluted as usual.

Evaluation of the method

The accuracy of the method was evaluated using sperm whale myoglobin, lysozyme, bradykinin, angiotensin II, and oxidized insulin chain B.

Myoglobin, provided in pH 7.2 50mM Tris buffer, was subjected to several cycles of concentration in Centricons-10 and dilution with water to remove buffer salts. The concentration was determined using an extinction coefficient of $157mM^{-1}cm^{-1}$ at 409.5nm.[5] An aliquot containing 1mg of protein was placed in a clean hydrolysis tube and lyophilized. One milliliter HCl was added to the protein, the solution was frozen in liquid nitrogen, the tube was evacuated, and the solution was then thawed. The sample was subjected to at least two more freeze-pump-thaw cycles before the tube was sealed. The sample was incubated at 155°C for 20 minutes. A second sample was treated in an identical manner, but was stored several days below 0°C after lyophilization, before being subjected to hydrolysis at 110°C for twenty four hours. After digestion, the acid was removed by evaporation under vacuum. The

[5] Rothgeb, T., Gurd, F. *Meth. Enzym.* **50**, 473 (1978).

residue of each sample was dissolved in ~200μL pH 9 borate, then filtered. 9μL and 10μL aliquots, of the 155°C and 110°C digestion hydrolysates, respectively, were diluted with 226μL and 225μL borate, respectively, and derivatized with 225μL FMOC-Cl. Area counts for four and three filled-loop runs (using 200μL of the aqueous layer), for the 155°C and 110°C hydrolysates, respectively, were averaged.

One milligram of bradykinin was dissolved in 0.5mL water, transferred to a hydrolysis tube, and lyophilized. The sample was prepared in 1mL HCl as for myoglobin, and was digested at 110°C 24 hours. The acid was removed on an evacuated line, while the sample was warmed to 45°C with a water bath to speed the evaporation (long drying times are to be avoided, as they result in significant artifact production from side reactions, such as esterification of glutamic acid by serine).[6] The residue was dissolved in 200μL borate and filtered. For the first run, 20μL hydrolysate was diluted with 97μL borate, derivatized with 113μL FMOC-Cl, and extracted twice with 230μL pentane after 45 minutes. 100μL of the aqueous layer was diluted with 140μL CH_3CN and 1010μL "A". The second sample was prepared as follows: 20μL hydrolysate was diluted with 215μL borate, derivatized with 225μL FMOC-Cl, and extracted twice with 460μL pentane after 45 minutes. 200μL of the aqueous layer was diluted with 90μL CH_3CN and 960μL "A".

One milligram samples of angiotensin II, oxidized insulin chain B, and lysozyme were prepared and digested as for bradykinin. 26μL aliquots of the filtered angiotensin II hydrolysate solution were diluted with 209μL borate, and derivatized with 225μL FMOC-Cl. 15μL

[6] Ikawa, M., Snell, E. *J. Biol. Chem.* **236**, 1955 (1961).

aliquots of the filtered insulin chain B hydrolysate solution were diluted with 220μL borate, and derivatized with 225μL FMOC-Cl. Two runs of each hydrolysate were conducted, and peak areas for each amino acid derivative were averaged.

The divisor (to arrive at integer ratios of amino acids) was determined as follows: concentrations for arginine, aspartic acid, glutamic acid, glycine, alanine, proline, methionine, phenylalanine, and leucine were summed, and divided by the total number of equivalents of these amino acids expected. Serine and threonine were omitted, as these residues undergo some decomposition during acid hydrolysis.[7] Valine and isoleucine were omitted, as peptide bonds involving these residues are known to be particularly resistant to acid hydrolysis, and therefore these residues are often underestimated in amino acid analyses.[8] If tryptophan was known to be present, phenylalanine was excluded from the calculation, as derivatives of these amino acids were found to coelute after completion of the development of the method. For samples of unknown composition, integer ratios were derived by visual inspection of the analyses of the above-mentioned amino acids, for which results were the most reliable.

RESULTS

Resolution

Despite numerous variations in the mobile phase composition and gradient, no conditions were found with this column type that would

[7] Osterman, L. *Meth. Protein Nucl. Acid Res.* **3**, 464 (1984).

[8] Hare, P. *Meth. Enzym.* **47**, 3 (1977).

resolve all amino acid derivatives. No other columns were evaluated. FMOC-Ala and FMOC-OH could not be resolved on the original column on which the separation was developed without compromising the resolution of other derivatives, but the partial resolution of these two species was achieved with the second column.[9] A temperature of 35°C was required to resolve $(FMOC)_2$-His and $(FMOC)_2$-Lys with the second column (variations in the gradient alone could not resolve these derivatives), and improved the resolution of the phenylalanine, isoleucine, and leucine derivatives. Higher temperatures resulted in coelution of the threonine and glycine derivatives, and no improvement in the resolution of the lysine and histidine derivatives (for the original gradient program). At 35°C, derivatization of equimolar amounts of histidine and lysine resulted in peaks which were fused to one third the peak height. In actual practice, however, resolution of these derivatives was rarely achieved with samples containing histidine and lysine in unequal amounts.

Figure A1.1 shows the resolution achieved with the second column, *i.e.*, that which had been used for calibration and analyses. Several derivatives eluted consistently as pairs of fused peaks, including serine and aspartic acid, and threonine and glycine. This aided in the assignment of amino acids for real peptides, as retention times were unreliable.

Retention times were highly variable. This is most likely due to the volatile nature of the mobile phase components (and therefore con-

[9] The lack of reproducibility from one column to the next, of the same type and manufacturer, is not unusual; Dolan, J. *LC Magazine* **3**, 316 (1985); *Ibid.*, p. 422.

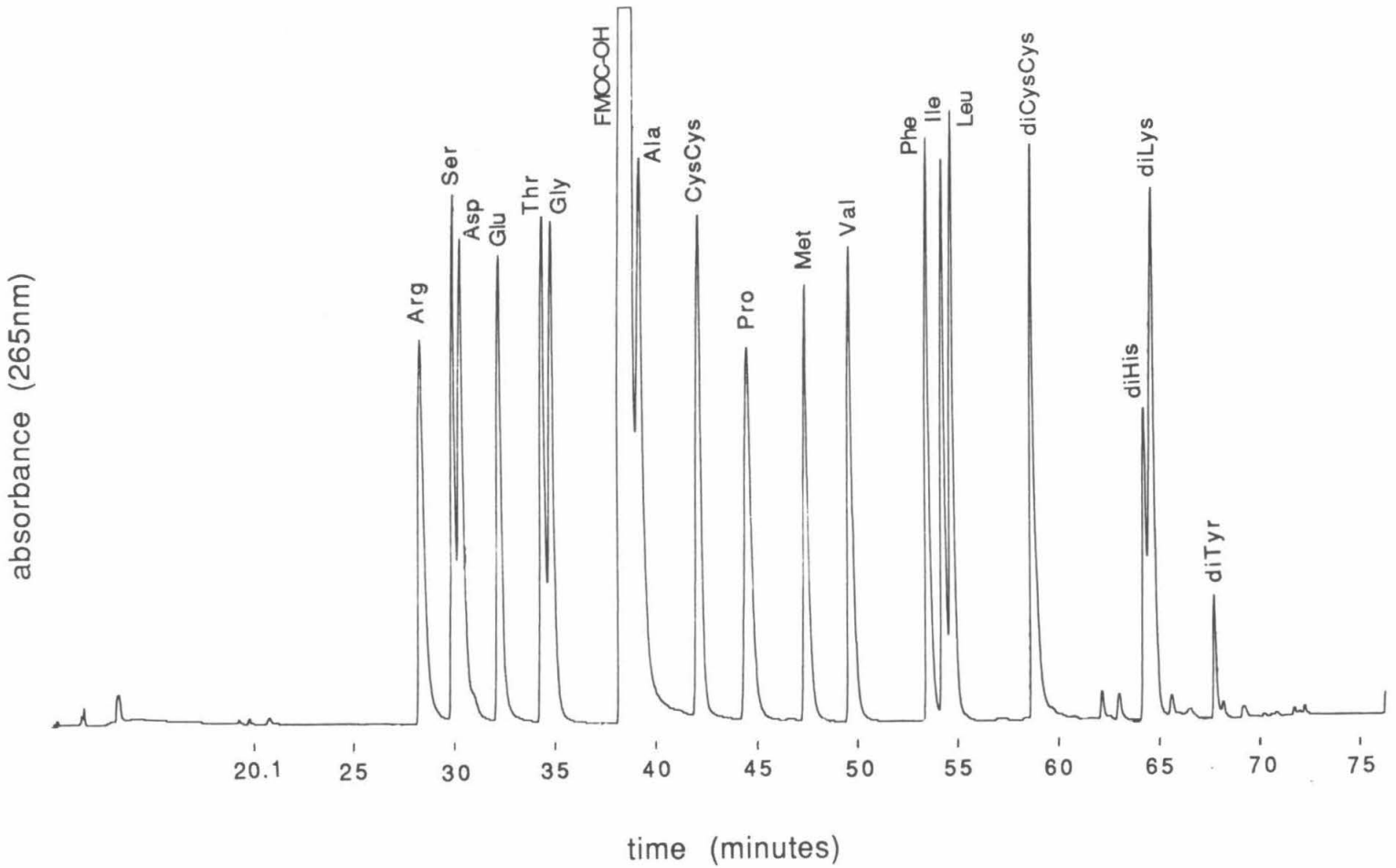

Figure A1.1. Elution profile for the derivatized amino acid standard (column is that used for actual analyses). The prefix di- refers to doubly-derivatized amino acids, *i.e.*, $(FMOC)_2AA$'s.

tinually changing mobile phase composition), and to some extent may be a result of variations in the period of column equilibration. In general, the greater the retention time of a derivative, the narrower was the range of elution volumes observed for it. Retention times for each derivative listed in table A1.2 are averages of at least 17 runs (data from calibration runs).

FMOC-Trp was found to coelute with FMOC-Phe. This should interfere minimally with peptide analysis, as tryptophan occurs infrequently (*C. krusei* cytochrome *c* contains one tryptophan residue per molecule), and when present, is expected to be destroyed in the course of acid hydrolysis.[10]

Determination of reaction conditions

Injection of the samples soon after the derivatization is essential, as histidine forms a disubstituted derivative which decays to the monosubstituted derivative with a half-life of ~5 days at pH 7.7.[11]

Initial work indicated that the phenolic oxygen atom of tyrosine also reacted with a second equivalent of FMOC-Cl, to form an ester. Both the singly and doubly derivatized tyrosine formed when the reaction was carried out in bicarbonate buffer in the pH 7-8 range. Conditions were sought which would result in reproducible analyses and complete derivatization.

The use of bicarbonate buffer was abandoned due to difficulties in maintaining it at constant pH and ionic strength. Borate buffer was

[10] Osterman, p. 465.

[11] Einarsson, Josefsson, and Lagerkvist, p. 609.

Table A1.2. Retention times and standard deviations for FMOC-AA derivatives

FMOC-AA	Retention time (minutes)	σ
Arg	28.76	0.92
Ser	30.19	0.83
Asp	30.59	0.80
Glu	32.68	1.06
Thr	34.87	0.96
Gly	35.33	0.95
Ala	39.89	0.82
CysCys	42.67	0.72
Pro	45.28	0.66
Met	48.18	0.71
Val	50.33	0.63
Phe	53.80	0.41
Ile	54.54	0.40
Leu	54.95	0.37
diCysCys	57.98	0.32
diHis	63.60	0.32
diLys	63.86	0.35
diTyr	67.05	0.30

selected as it is one of the few alkaline buffering agents lacking an amine functionality (which would react with the reagent).

The extraction was omitted in the study of pH and time dependence of the reaction to avoid complications arising from the lack of reproducibility this procedure introduces.

The data presented in table A1.3 and illustrated in figure A1.2 indicate that modest increases in peak area are observed for FMOC-AA derivatives as the reaction pH is increased from 8 to 9. Serine, aspartic acid, and glutamic acid showed anomalous behavior, which is attributed to column deterioration (doubling of peaks for these derivatives was observed). Dramatic increases in the formation of a disubstituted tyrosine derivative are seen with increasing pH. A concommitant decrease in the monotyrosine derivative is observed, but does not appear to be as dramatic.

An evaluation of the pH dependence of the rates of histidine and lysine derivative formation could be performed if a control study was done for the coeluting FMOC byproduct, but this was not pursued, as the results for tyrosine derivative formation demonstrated the advantage of performing the reaction at pH 9.

Data are presented in table A1.4 and plotted in figure A1.3 showing the time dependence of the derivatization reaction. The analytical results for many derivatives are constant for a range of reaction times spanning 5 to 40 minutes, indicating that the derivatization reaction is complete in minutes, and that the derivatives are stable. Formation of the disubstituted tyrosine derivative increases over the range of reaction time investigated, and for this reason 45 minutes was chosen as the reaction time for

Table A1.3. Area counts as a function of derivatization pH[a]

Amino Acid	pH 8	pH 8.4	pH 9
Arg	90558	90856	94881
Ser	90674	141154	153809
Asp	84318	41168	27703
Glu	82824	24051	44130
Thr	91198	90062	93400
Gly	95068	97720	104515
Tyr	50231	15272	21314
CysCys	111672	107875	112234
Pro	79643	84666	92130
Met	82621	95187	90950
Val	82647	86360	93266
Phe	70949	80443	91981
Ile	67937	77945	89049
Leu	75114	83106	91439
diTyr	11794	87808	180262

a. A quantitative evaluation of the histidine and lysine derivatives was not possible, as they coelute with an FMOC byproduct (which is completely removed in routine analyses by pentane extraction).

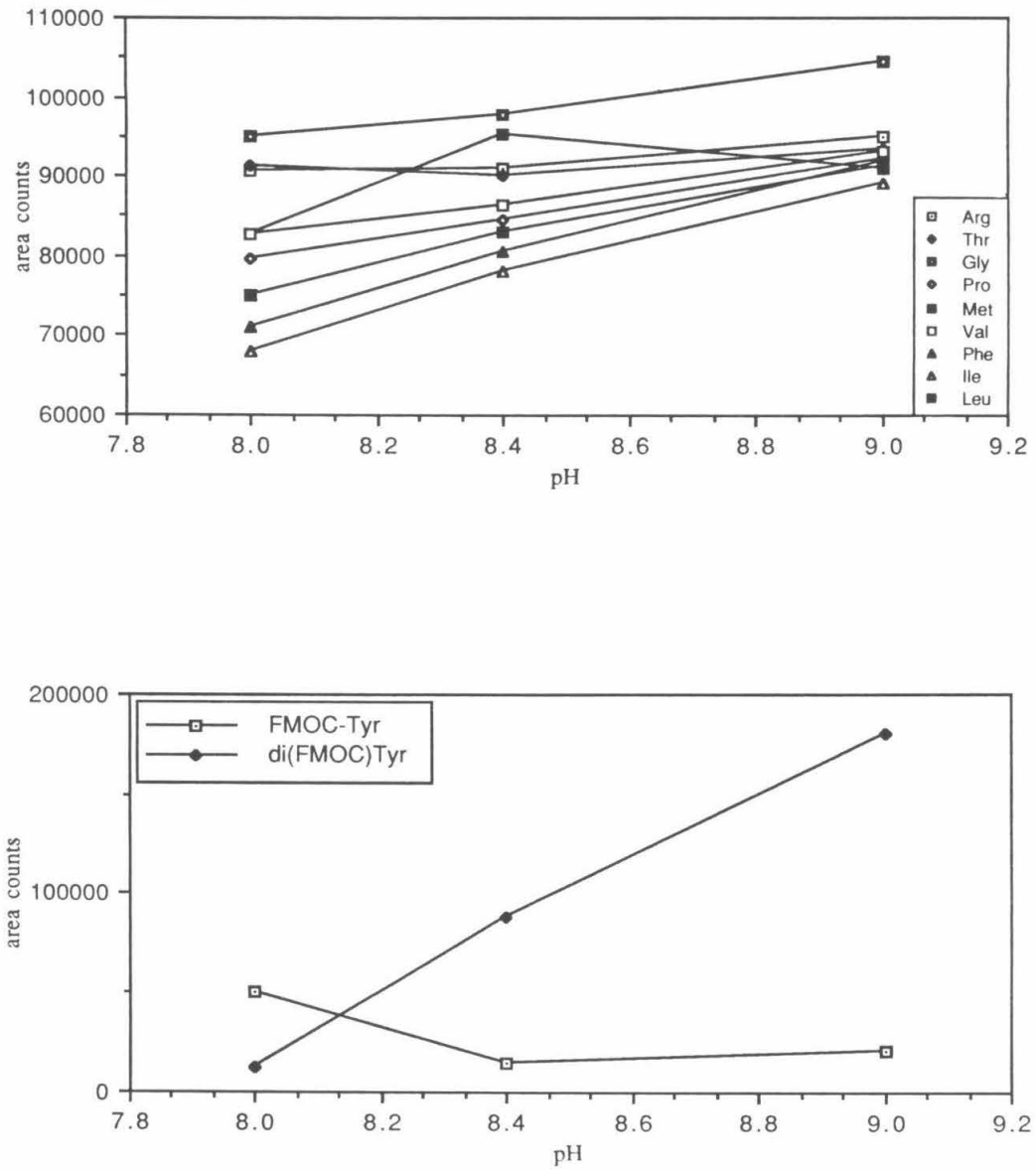

Figure A1.2. Peak area as a function of the pH of the derivatization reaction (20 minutes duration).

Table A1.4. Area counts as a function of derivatization reaction time[a]

Amino acid	5 min.	10 min.	20 min.	30 min.	40 min.
Arg	101126	92819	93442	92782	91697
Ser/Asp[b]	197625	171985	186823	173414	183925
Glu[c]	85080	84033	85587	85560	84884
Thr/Gly[b]	208917	199101	199855	200303	203166
CysCys	127906	107949	152789	128055	122541
Pro	95812	93945	94035	94362	96838
Met	107872	93380	92103	96070	92307
Val	102315	93159	93923	93646	93885
Phe	99468	93067	92389	92596	93247
Ile	100695	89877	89866	90378	89259
Leu	105770	97164	92717	93707	93353
diCysCys	115137	105322	146952	105852	90677
diHis	141728	129878	134642	131703	134939
diLys	180284[d]	183459	183208[e]	185924	180985
diTyr	128464	152135	179705	179193	190157

a. averages of four runs, unless specified otherwise
b. Due to column deterioration, resolution of the components of these pairs of fused peaks was poor. Hence, the sum of the areas for each pair only were considered.
c. Due to column deterioration, FMOC-Glu eluted as a doubled peak; the sum is reported here.
d. single run (unresolved from FMOC byproduct in other runs)
e. average of three runs

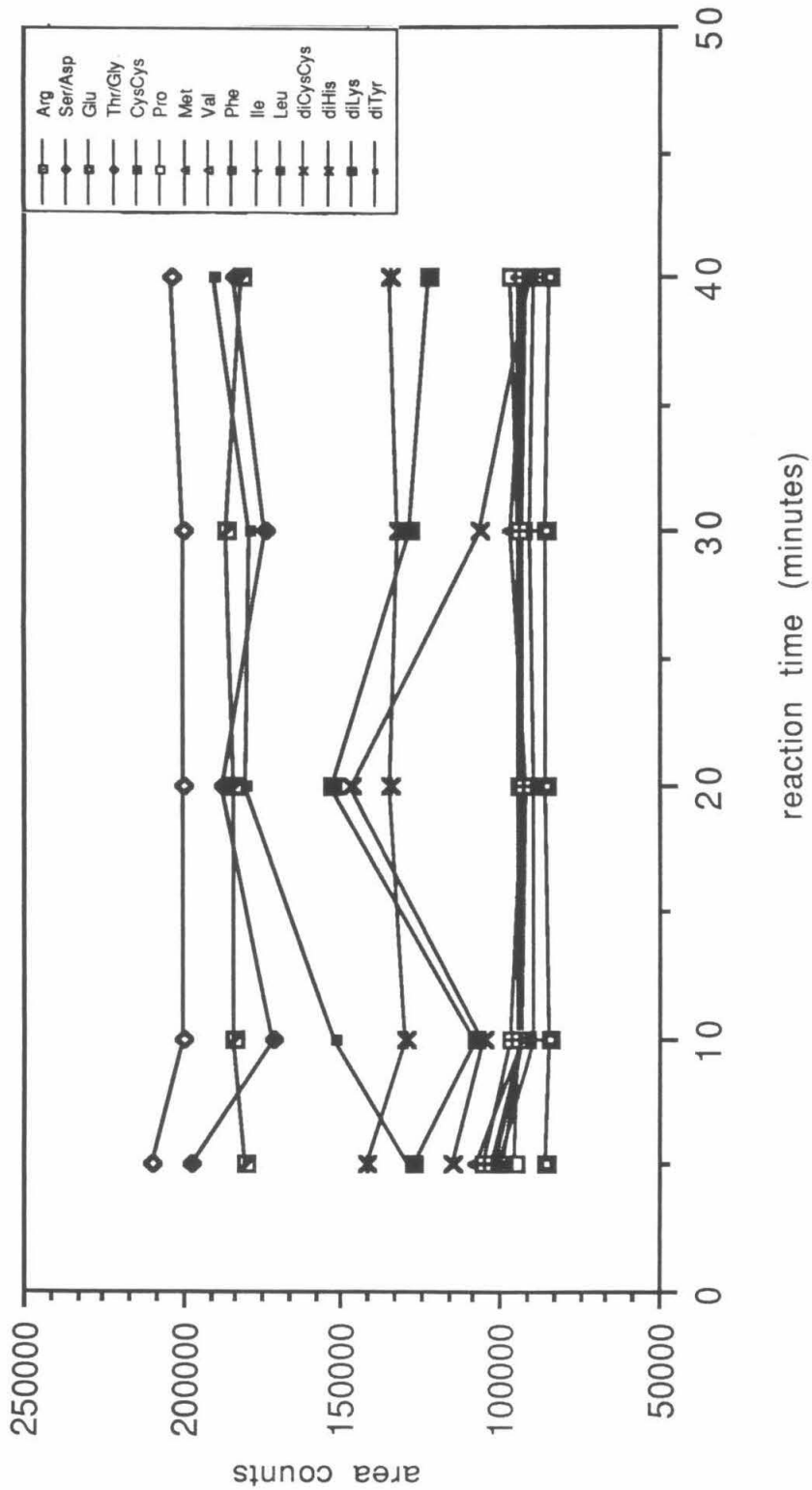

Figure A1.3. Area counts as a function of derivatization reaction time.

derivatization of real peptide hydrolysates.

Several amino acids were derivatized to a larger extent after 5 minutes than after 10 minutes, suggesting the derivatives are unstable. However, the peak areas were consistent for reaction times equal to or exceeding 10 minutes.

For both the time and pH dependence studies, some variability is expected for runs carried out under identical conditions, as the reaction was not stopped abruptly by reagent removal as with extraction, but rather was slowed considerably by dilution and exposure to ~pH 4 upon injection. Also, the method of integration for a particular derivative may vary from one run to the next, depending on the stability of the baseline and the extent of coelution of other compounds.

Alternatives to extraction

FMOC-Cl is readily hydrolyzed, and the hydrolysis product must be extracted from the reaction mixture to minimize its interference in the chromatography. Pentane has been reported to remove the hydrolysis product effectively with minimal extraction of the amino acid derivatives.[12] The pentane extraction was found to reduce significantly the peak area counts (a direct comparison was not possible, as the solution volume is changed by the extraction of CH_3CN, which is required in solution to solubilize the fluorenyl moiety; no data could be found on the partition coefficient of acetonitrile in *n*-pentane).

12 Cunico, R., Mayer, A., Dimson, P., Zimmerman, C. *Varian Instruments at Work Publication #163*, Varian Instrument Group (Walnut Creek, CA), 1986.

The extraction introduces error. Because of the high vapor pressure of pentane, it is difficult to pipet quantitatively; the high vapor pressure and the small volumes involved in the derivatization reaction make complete removal of the first pentane layer difficult. Hence, omission of the extraction step ought to lead to greater sensitivity and reproducibility. Also, it was thought that reduction of the FMOC-OH concentration might permit resolution of FMOC-Ala.

The possible use of an additional amine to scavenge the excess reagent[13] was investigated. 1-amino-adamantane was selected for its extreme hydrophobicity, so that elution of its FMOC derivative would not interfere with that of the FMOC-AA's.

Several problems were encountered with this approach, among them the solubility problems with FMOC-aminoadamantane and the inability of the scavenging reaction to compete with the hydrolysis of the reagent (once 45 minutes have elapsed for the derivatization reaction, little reagent is left to scavenge). Pentane extraction was found to be beneficial, as it removed impurities as well as excess reagent and hydrolysis product.

Calibration

Peak areas were found to increase linearly for all FMOC-AA derivatives, except diHis, diLys, and diTyr, with correlation coefficients of 0.9973 or greater (figure A1.4, tables A1.5 and A1.6).

A conservative estimate for the sensitivity of the method is ~250pmol, considering the concentrations used with the lowest

[13] Betnér, I., Földi, P. *Chromatographia* **22**, 381 (1986).

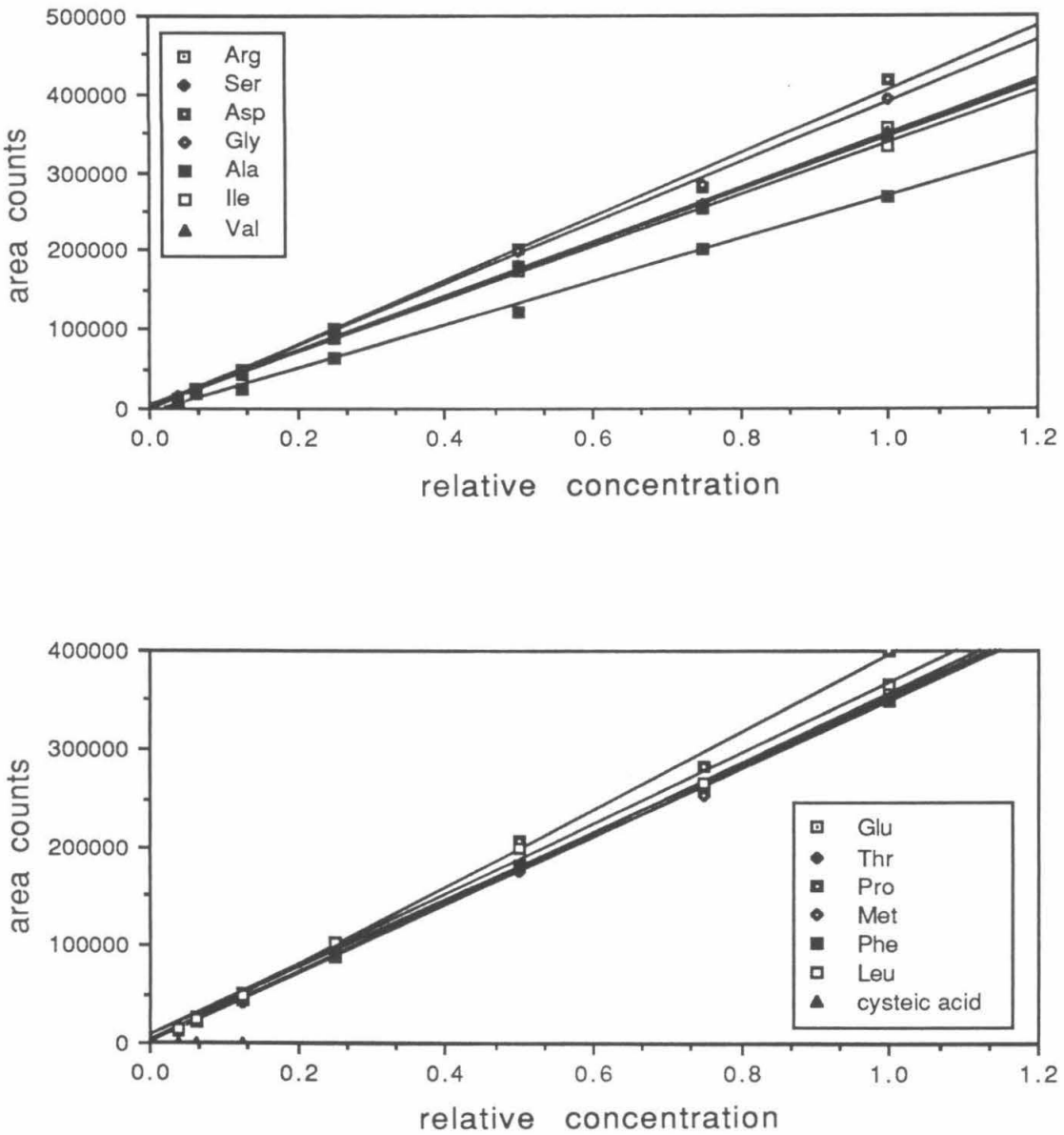

Figure A1.4. Calibration data for FMOC-amino acid derivatives. Solid lines indicate results of least squares fitting.

Table A1.5. Calibration data - peak area (average of at least 4 runs) as a function of concentration

Relative Concentration Amino Acid	**1.0x**	**0.75x**	**0.5x**	**0.25x**	**0.125x**	**0.0625x**	**0.0375x**
Arg	355470	252230	180217	90243	42558	22327	12711
Ser	340894	260433	179443	90759	45221	22087	12650
Asp	418708	281939	202017	99891	49663	23142	13246
Glu	356943	260554	180428	88552	43188	21223	12247
Thr	349891	259188	174867	90044	42199	22222	13263
Gly	393015	284026	198914	100391	49616	24617	14371
Ala	269276	202622	121036	64407	23738	18623	7290
Pro	399302	283050	208176	99423	51211	24106	14564
Met	350651	254482	179092	92834	44122	22619	13413
Val	350453	254842	179526	92127	44311	22572	13662
Phe	349247	266724	182624	97920	47858	27196	15383
Ile	331005	256216	174357	88229	43706	22330	13223
Leu	366826	265530	200384	102627	48880	25060	15789

Data for three single runs of cysteic acid: 0.45x (144929), 0.25x (87244), 0.135x (43733).

Table A1.6. Coefficients for calibration data analysis[a]

Amino acid	m ($\times 10^6$)	b	r^2
Arg	2.85	2.53 e-5	0.9983
Ser	2.92	-7.72 e-3	0.9993
Asp	2.44	9.62 e-3	0.9954
Glu	2.81	2.51 e-3	0.9996
Thr	2.87	-9.33 e-4	0.9998
Gly	2.57	-2.18 e-3	0.9992
Ala	3.67	1.90 e-2	0.9968
Pro	2.54	-1.81 e-3	0.9976
Met	2.89	-5.39 e-3	0.9990
Val	2.89	-5.50 e-3	0.9991
Phe	2.89	-1.77 e-2	0.9993
Ile	3.00	-8.99 e-3	0.9992
Leu	2.76	-1.55 e-2	0.9964
Cysteic acid	3.13	-9.67 e-3	0.9946

a. concentration = m(area counts) + b;
r = correlation coefficient

attenuation, and assuming no extraction of acetonitrile or the amino acid derivatives.

Internal standards

Norvaline, β-alanine, and norleucine were evaluated as potential internal standards.

FMOC-β-alanine elutes after FMOC-alanine, but before, and incompletely resolved from, FMOC-cystine. This region of the chromatogram is undesirable for elution of an internal standard, as it is crowded (the monosubstituted tyrosine derivative has similar retention characteristics) and dominated by the tailing peak of the reagent hydrolysis product.

FMOC-norleucine elutes immediately after FMOC-leucine, and the peaks of these two components are fused to about one-third the height of FMOC-leucine (for a ~4:1 ratio of norleucine to leucine). No attempt was made to improve the resolution by variations in the elution gradient due to the lack of success of this method in improving the resolution of the histidine and lysine derivatives.

FMOC-norvaline was found to elute immediately after FMOC-valine, with minimal fusion of the peaks (~5% of the FMOC-valine peak height). Provided it is stable under the conditions of acid hydrolysis, norvaline would be a good choice for an internal standard, as its FMOC derivative is well-resolved from the compounds of interest.

Evaluation

Data for total amino acid analyses of known peptides are compiled in table A1.7. The determinations agree quite well with the theore-

Table A1.7. Analyses of known peptides [a]

	Bradykinin [b]	Angiotensin II [b]	Insulin, chain B [b] (oxidized)	Sperm Whale Myoglobin [c] 155°C	110°C	Hen Egg Lysozyme [d]
Arg	1.98 (2)	1.02 (1)	0.98 (1)	3.36 (4)	3.94 (4)	10.8 (11)
Ser	1.06 (1)		0.95 (1)	5.91 (6)	5.10 (6)	11.0 (10)
Asp		0.94 (1)	1.00 (1)	8.11 (8)	7.67 (8)	22.5 (21)
Glu			3.34 (3)	19.1 (19)	19.0 (19)	5.53 (5)
Thr			0.90 (1)	4.05 (5)	4.70 (5)	7.10 (7)
Gly	0.97 (1)		2.91 (3)	11.6 (11)	10.8 (11)	12.2 (12)
Ala			2.37 (2)	19.8 (17)	18.6 (17)	11.8 (12)
Pro	3.02 (3)	1.02 (1)	0.94 (1)	3.85 (4)	3.82 (4)	1.89 (2)
Met				1.99 (2)	1.65 (2)	1.44 (2)
Val		1.00 (1)	2.90 (3)	5.08 (8)	8.07 (8)	4.09 (6)
Phe	2.03 (2)	1.01 (1)	2.74 (3)	6.38 (6)	6.55 (6)	5.23 (3)
Ile		0.93 (1)		5.42 (9)	8.15 (9)	3.69 (6)
Leu			3.65 (4)	15.1 (18)	17.4 (18)	6.79 (8)
His		+ (1)	+ (2)	+ (12)	+ (12)	+ (1)
Lys			+ (1)	+ (19)	+ (19)	+ (6)
Tyr		+ (1)	+ (2)	+ (3)	+ (3)	+ (3)
$CysO_3H$			2.21 (2)			
Trp				(2)	(2)	+ (6)

a. Found (theoretical); moles per mole of peptide
b. Theoretical values from the catalog of the Sigma Chemical Company, 1987.
c. Theoretical values: Edmundson, A. *Nature* **205,** 883 (1965).
d. Theoretical values: CRC Handbook of Biochemistry, 2nd edition, H. Sobert, ed., Chemical Rubber Co. (Cleveland), 1970, p. C-237.

tical values for small peptides. The deterioration of the quality of the analysis with increasing protein size is a puzzling trend also found for several other precolumn derivatization methods.[14]

The FMOC-amino acid analysis method is adequate for its intended purpose, *i.e.*, the identification of peptides from a protein of known sequence. Its shortcomings are a result of both the experimental method and the chemistry of the system. Another column or solvent system might better resolve the FMOC-AA derivatives, and the sensitivity would be greatly enhanced by the use of fluorescence detection. However, the problems of multiple sites of derivatization (Tyr, Lys, His) and derivative instability (especially $FMOC_2$His) cannot be readily eliminated.

[14] (a) Bergman, T., Carlquist, M., Jörnval, H. *Advances in Methods in Protein Microsequence Analysis*, B. Wittman-Liebold, *et al.*, eds., Springer-Verlag (New York), 1986; (b) Oray, B., Lu, H., Gracy, R. *J. Chrom.* **270**, 253 (1983).

Appendix 2

Tryptic Digestion of the Modified Derivative and Related Studies

INTRODUCTION

If SMP were to cleave *C. krusei* cytochrome *c* completely and specifically at peptide bonds whose carboxy moiety is contributed by arginine, five peptide products would result. His33 would occur on the fragment P2, Cys14-Arg38 (see figure 3.10). This stretch of the peptide chain includes Cys14 and Cys17, which provide the covalent linkage to the heme prosthetic group. Hence, should these bonds remain intact (as they are expected to do under the mild conditions of enzymatic digestion), the UV-visible spectrum of the His33-containing peptide would be dominated by the porphyrin bands, and the presence of $[A_5RuHis]^{3+}$ would be difficult to confirm by this technique.

In an effort to eliminate this problem, peptide mapping was also conducted using the protease trypsin, which cleaves peptide bonds whose carboxy moiety is contributed by lysine or arginine residues. Complete, specific digestion of *C. krusei* cytochrome *c* by trypsin is expected to result in 16 peptides (see figure A2.1), and His33 would reside on fragment T6, Val28-Arg38, independent of the heme fragment T5, Cys14-Lys27.

The results are reported here not as a confirmation of the SMP results, but rather to relate the occurrence of an unexpected side reaction, which may have important implications for temperature-dependent studies of all pentaammineruthenium-modified proteins in mildly basic solution.

MATERIALS AND INSTRUMENTATION

TPCK-treated trypsin was obtained from United States Biochemical Corporation and used as supplied. Digestion of native and modified *C.*

Figure A2.1. Peptides expected upon digestion of *C. krusei* cytochrome *c* with trypsin. The points of cleavage (after Lys and Arg residues) are indicated by vertical lines.

krusei cytochrome *c* was carried out as described by Mauk and Mauk.[1] Sources of HPLC solvent components and a description of the HPLC instrumentation can be found in Chapter 3. A Vydac 4.6mm x 250mm C18 column (model 218TP54, #755577) was utilized to resolve the peptide mixtures.

Na[CoEDTA] was synthesized as described in chapter 2. $[Ru(NH_3)_5Im]Cl_3 \cdot 2H_2O$ was synthesized by K. Yocom.[2] The synthesis of $[Ru(NH_3)_5His]Cl_3$ is described in chapter 3.

Control experiments were carried out in a manner identical to the digestion, without the use of trypsin. The $CoEDTA^-$ reaction products were analyzed by UV-visible spectroscopy and HPLC after separation on Biogel P-2 (BioRad, 200-400 mesh).

DPP studies were conducted as described in chapter 3.

METHODS

Peptides were resolved using the following mobile phase composition: A = 0.1%TFA in water; B = 0.1%TFA, 10%H_2O, in CH_3CN. The gradient program for peptide separation and column reequilibration is presented in table A2.1. The column was maintained at 27°C, and peptides were detected by their absorption of 220nm light.

RESULTS

In the course of concentrating HPLC fractions to recover peptides

[1] Mauk, M., Mauk, A. *J. Chrom.* **439**, 408 (1988).

[2] Sundberg, R., Bryan, R., Taylor, I., Taube, H. *J. Amer. Chem. Soc.* **96**, 381 (1974).

Table A2.1. *Gradient* program for the separation of tryptic peptides

time (minutes)	event
0	12.5%B; flow rate climbs to 1.0mL/min. in 0.5 min.
0.9	alarm
1.0	injection
6.0	%B climbs to 25 in 50 minutes
56	%B climbs to 50 in 50 minutes
106	%B climbs to 100 in 5 minutes
111	flow rate climbs to 2mL/min. in 1 minute
116	flow rate decreases to 1mL/min. in 1 minute; %B returns to 12.5 in 15 minutes
156	flow rate decreases to 0.3mL/min. in 1 minute

for possible analysis, it was noted that a peptide of ~30 minutes elution time from the digest of the modified cytochrome was purple in color. No such peptide was found in the native digest. The peptide eluted in a region where a peak(s) in the modified digest was shifted relative to one of the native digest, but due to lack of reproducibility in retention, it was not certain which peaks were correlated in the two digests. No other differences were observed between the elution profiles of the native and modified digests.

A UV-visible spectrum of the peptide (figure A2.2) revealed two visible bands with maxima at ~450nm and ~550nm, as well as an absorption band at 280nm. While the $[A_5RuHis]^{3+}$ complex has an absorbance maximum at ~450nm, it also has a more intense absorption centered at

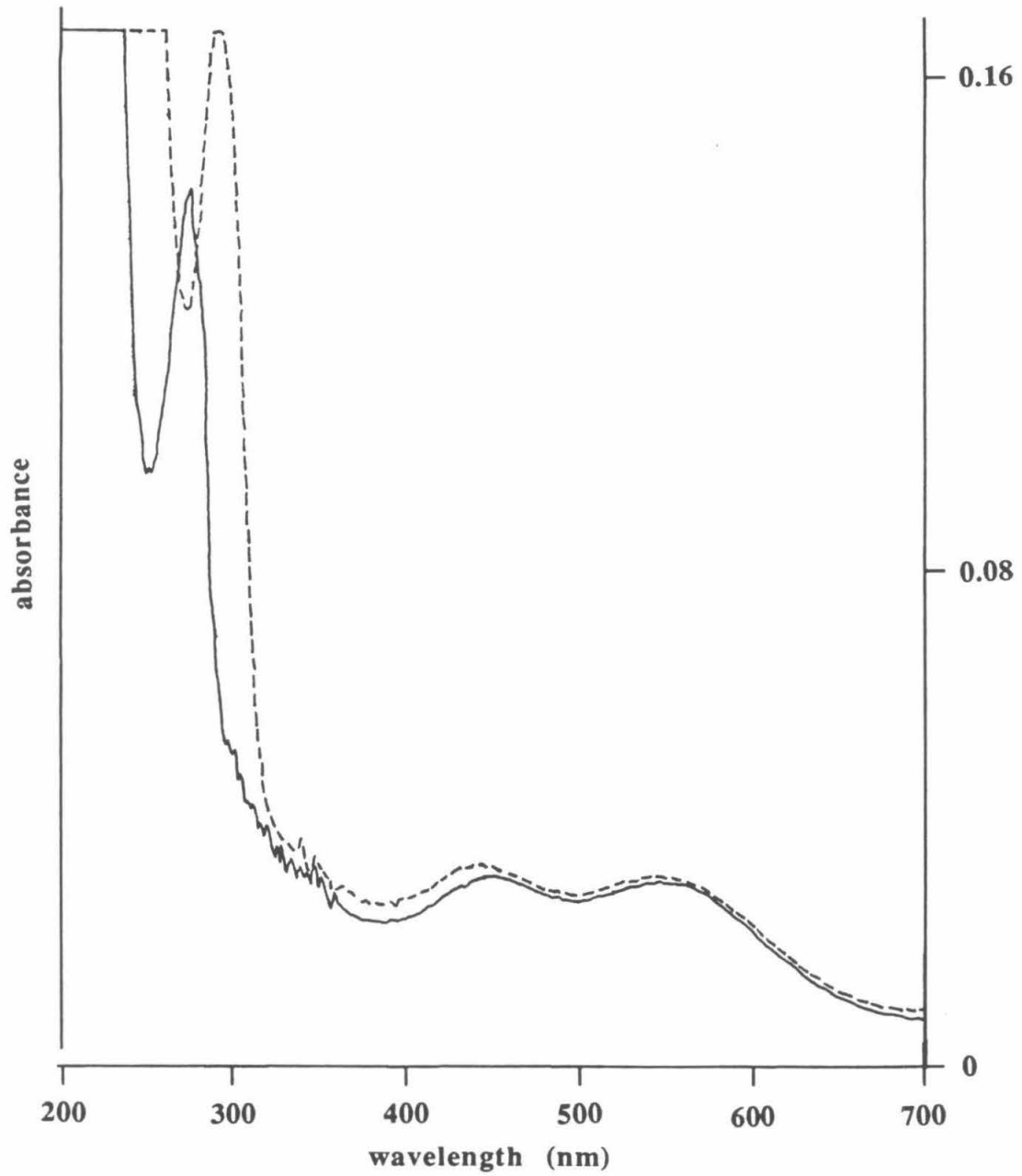

Figure A2.2. UV-visible spectrum of a modified peptide recovered from a tryptic digest of the A_5Ru(His39)-*C. krusei* cytochrome *c*: —— in 0.1M sodium phosphate; – – – after being made basic by the addition of sodium hydroxide.

300nm, which is lacking in the spectrum of the peptide.[1] A similar observation was made with a second tryptic digest of a different preparative batch of A_5Ru(His39)-*C. krusei* cytochrome *c*: the peptide spectrum had maxima at 275.6, 321, 450, and 550 nm. In that case, the peak was split, indicating that probably two peptides were present. No further purification of either peptide was attempted.

The 550nm absorption suggested that the oxidant, $CoEDTA^-$ (λ_{max}=384nm, 538nm), might be involved in a side reaction.[2] The presence of oxidant alone, or the presence of any product which might result from its reaction with the ruthenium reagent are unlikely, as such small, charged molecules are not expected to be retained by the hydrophobic column. Control studies were done to determine if the $CoEDTA^-$ complex might undergo substitution reactions analogous to those of the aquopentaammine complex:[3]

$$[A_5Co(OH_2)]^{3+} + RCOOH \rightarrow [A_5Co\text{-}OOCR]^{2+} + H_3O^+$$

Very small yields of products were obtained upon incubation of $CoEDTA^-$ in the presence of lysine, but none had spectral properties similar to those of the peptide.

Control studies were performed with ruthenium model complexes to confirm the inert nature of the ruthenium coordination sphere. $[A_5RuIm]^{3+}$ (Im=imidazole) was found to be quite robust by UV-visible absorption spectroscopy, while the $[A_5RuHis]^{3+}$ spectrum showed minor but noticeable changes. These changes included broadening of the

[1] Sundberg, R., Gupta, G. *Bioinorg. Chem.* **3**, 39 (1973).

[2] Seaman, G., Haim, A. *J. Am. Chem. Soc.* **106**, 1319 (1984).

[3] Hawkins, C., Lawson, P. *Inorg. Chem.* **9**, 6 (1970).

300nm band, but no features resembling those of the peptide were observed.

Differential pulse polarography studies of the peptide were conducted to determine the reduction potential of the metal site presumed to be associated with the peptide. The results are presented in figure A2.3. The intense anodic peak near 0.85V (*vs.* SCE) was thought to be due to redox processes of tyrosine, and this was confirmed by DPP studies of the free amino acid. Further evidence to indicate the presence of tyrosine is the pH dependence of the UV absorption (figure A2.2): the red shift of ~20nm in base is characteristic of tyrosine, and occurs as a result of ionization of the phenolic side chain.[4] The only features found in the DPP trace which are unique to the peptide (and not attributable to Tyr) are anodic maxima at -0.15V and 0.4V (*vs.* SCE). The -150mV peak is in the region expected for the $[A_5RuHis]^{3+/2+}$ couple, but the UV-visible spectra are inconsistent with its presence on the peptide. The undigested protein exhibited DPP behavior as described in chapter 3 (figure 3.18), demonstrating that the side reaction resulted from the digestion process, and that ruthenium was present on the protein as a pentaammine imidazole complex.

DISCUSSION

A literature survey of ruthenium ammine compounds suggested some possibilities as to the identity of the complex on the peptide. Rudd

[4] Cantor, C., Schimmel, P. *Biophysical Chemistry*, Part 2, W. H. Freeman (San Francisco), 1980, p. 377.

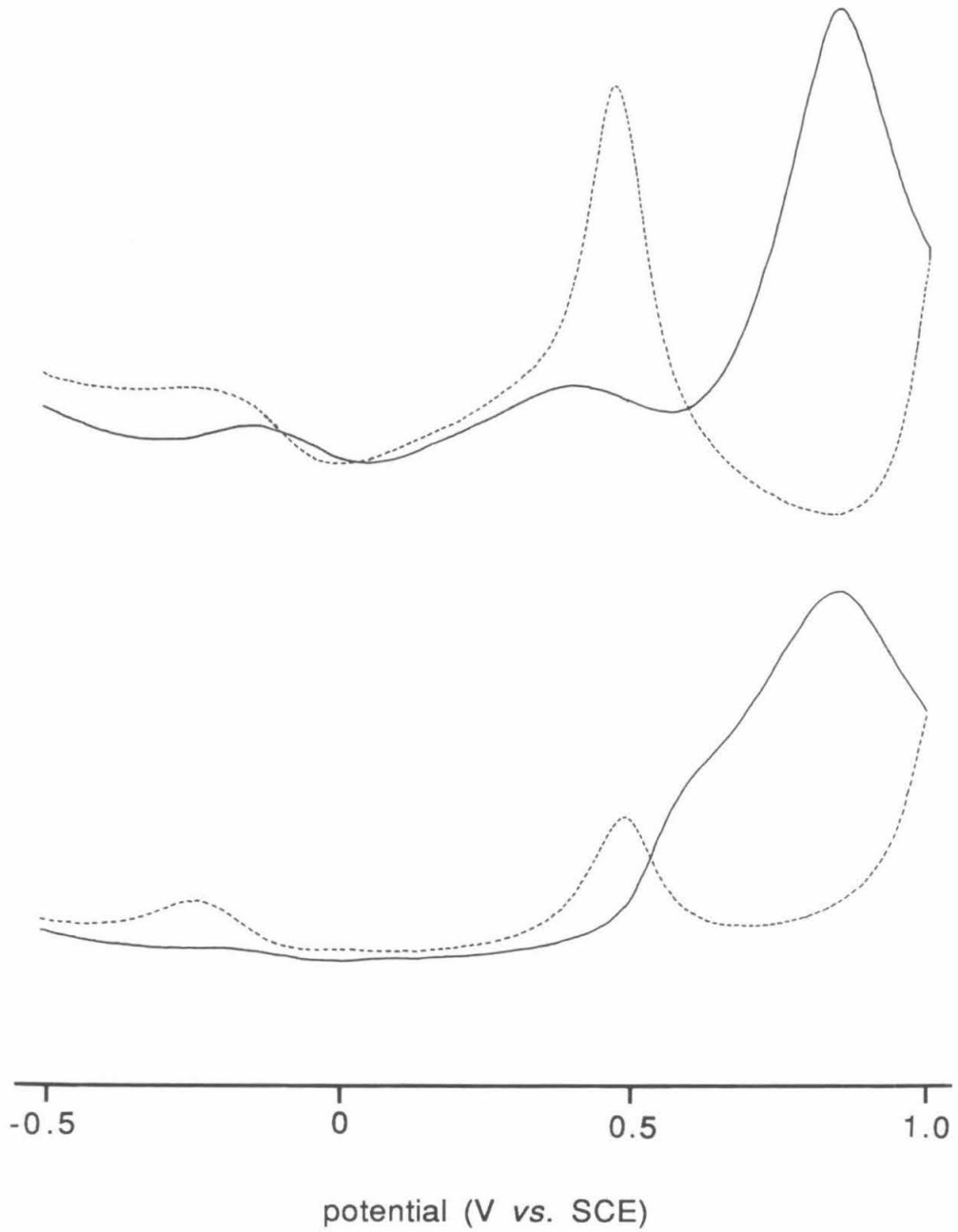

Figure A2.3. Differential pulse polarography traces for *(upper)* odd peptide recovered from A_5Ru(His39)-*C. krusei* cytochrome *c* tryptic digest and *(lower)* tyrosine; legend: — anodic and – – cathodic wave.

and Taube have reported that pentaammineruthenium(III) pyridine disproportionates in basic solution to give the ruthenium(II) compound, *i.e.*, isomer, and a ruthenium(IV) compound.[5] The latter exhibited an absorption maximum at 558nm in carbonate buffer. It was proposed that the disproportionation results from an initial deprotonation of an ammine ligand.

Aquation of an ammine ligand to yield $[A_4Ru(Im)(H_2O)]^{n+}$ can be ruled out, as the spectral features for the 3+ species are reported to be λ_{max}=297 and 385 nm,[6] and the 2+ complex has no visible absorption as well.[7] Aquation of an ammine ligand, followed by coordination of an amino acid carbonyl or nitrogen to form a peptide chelate is possible, and absorption bands in the region of 295nm and 555nm have been reported for such complexes.[8] It is difficult to rationalize, however, why these reactions might occur on the peptide but not with the histidine model complex.

The observed properties of the product recovered from the digest of the modified cytochrome indicate it is probably a ruthenium-containing peptide which includes His39, and which has undergone some reaction to alter the coordination sphere of the ruthenium complex. Why this is observed in the tryptic digestion and not that of the submaxillaris protease is puzzling, as the sole difference (aside from the

[5] Rudd, D., Taube, H. *Inorg. Chem.* **10**, 1543 (1971).

[6] Isied, S., Kuehn, C. *J. Amer. Chem. Soc.* **100**, 6754 (1978).

[7] Isied, S., Taube, H. *Inorg. Chem.* **15**, 3070 (1976).

[8] Kohata, S., Sagara, K., Takada, H., Ohyoshi, A. *Polyhedron* **4**, 1059 (1985).

identity of the protease) between the two procedures is the buffer used (NH_4CO_3 *vs.* $NaHCO_3$, respectively). An important conclusion that can be drawn from these results is that side reactions involving the ruthenium complex do occur at elevated temperatures in mild base, and this should be borne in mind when "recycling" of a modified protein after variable-temperature experiments is practiced.

Appendix 3

Spectroelectrochemical Data

Table A3.1. Native *Candida krusei* cytochrome *c* spectroelectrochemistry data[a]

T=9.1 (T_{SCE}=24.5)		T=15.2 (T_{SCE}=23.9)		T=19.8 (T_{SCE}=24.75)	
E	A_{548}	E	A_{548}	E	A_{548}
-231.0	0.815	232.3	0.287	-230.4	0.782
-25.2	0.785	109.6	0.314	-24.1	0.749
-4.4	0.755	80.4	0.371	-4.4	0.700
15.2	0.699	55.2	0.472	15.4	0.633
35.4	0.608	34.8	0.573	35.6	0.542
56.2	0.498	15.1	0.663	56.1	0.446
86.1	0.372	-5.1	0.724	81.1	0.359
115.0	0.318	-25.3	0.758	110.7	0.311
230.1	0.289	-230.6	0.791	230.3	0.288

T=24.4 (T_{SCE}=26.25)		T=29.6 (T_{SCE}=25.9)		T=34.2 (T_{SCE}=25.1)	
E	A_{548}	E	A_{548}	E	A_{548}
230.7	0.291	-230.9	0.768	229.9	0.309
109.8	0.314	-24.4	0.712	109.3	0.323
79.9	0.355	-4.3	0.660	79.8	0.353
55.0	0.431	15.2	0.589	54.6	0.418
34.8	0.519	30.5	0.523	34.2	0.498
14.0	0.618	51.9	0.432	14.8	0.587
-6.1	0.685	85.9	0.344	-5.9	0.665
-25.5	0.727	115.2	0.314	-25.6	0.715
-230.9	0.774	230.0	0.299	-229.6	0.769

T=39.8 (T_{SCE}=24.25)		T=44.8 (T_{SCE}=24.25)		T=50.2 (T_{SCE}=24.0)	
E	A_{548}	E	A_{548}	E	A_{548}
-229.7	0.769	242.6	0.320	-234.9	0.748
-23.8	0.685	109.8	0.331	-23.9	0.637
-4.5	0.627	79.3	0.353	-4.6	0.576
15.7	0.548	54.4	0.398	15.6	0.500
36.2	0.466	35.0	0.453	36.3	0.432
57.3	0.399	12.8	0.534	56.0	0.387
83.8	0.351	-6.9	0.608	81.7	0.352
113.2	0.328	-26.3	0.666	110.3	0.336
242.6	0.313	-234.9	0.754	239.9	0.328

a. Data is expressed as follows: potentials are given in mV *vs.* SCE, [O] and [R] are the concentrations of oxidized and reduced forms of the protein, respectively, and T and T_{SCE} are the temperatures of the working and reference electrodes, respectively, in degrees Celsius.

Table A3.1. Native *Candida krusei* cytochrome *c* spectroelectrochemistry data, continued

T=54.8 (T_{SCE}=24.0)	
E	A_{548}
239.8	0.343
75.4	0.361
54.9	0.379
34.3	0.409
14.8	0.452
-5.2	0.504
-25.5	0.552
-45.9	0.590
-85.0	0.629
-150.7	0.649
-231.1	0.656
-351.1	0.662

Table A3.2. Fitted parameters to spectroelectrochemical Nernst plots for native *Candida krusei* cytochrome *c*[a]

Temperature	b	m_{exptl}	m_{theor}	%error in m	r^2
9.1	45.44	56.7	56.0	1.25	0.9998
15.2	40.80	56.2	57.2	1.75	0.9998
19.8	37.21	55.9	58.1	3.79	0.9994
24.4	32.15	59.3	59.0	0.51	0.9999
29.6	27.55	59.6	60.1	0.75	0.9999
34.2	24.76	56.7	61.0	7.05	0.9999
39.8	17.41	64.4	62.1	3.74	0.9999
44.8	11.84	62.5	63.1	1.01	0.9998
50.2	5.34	62.3	64.1	2.80	0.9997
54.8	-18.48	96.2	65.1	48.0	0.9710

a. b, m_{exptl}, and r^2 are the intercept, slope, and correlation coefficient, respectively, of a plot of the potential (*vs*.SCE) *vs*. the log of the ratio of concentrations of oxidized to reduced forms of cytochrome *c*; m_{theor} is the theoretical value of the slope, and is equal to RT/ℱ, assuming a one electron reduction. The error in m is calculated as

$$\frac{|m_{theor} - m_{exptl}|}{m_{theor}} \times 100$$

Table A3.3. Modified $A_5Ru(His39)$-*Candida krusei* cytochrome *c* spectroelectrochemistry data (units and abbreviations as in Table A3.1)

Sample 1

T=7.6 (T_{SCE}=19.4)

E	A_{548}
299.8	0.201
129.4	0.223
97.4	0.278
71.8	0.369
46.9	0.484
29.4	0.552
12.1	0.598
-11.5	0.629
-40.8	0.643
-202.0	0.651

T=12.6 (T_{SCE}=21.0)

E	A_{548}
-202.0	0.643
-34.9	0.631
-6.4	0.608
19.6	0.558
43.8	0.468
64.5	0.375
87.1	0.292
110.8	0.241
299.4	0.202

T=19.6 (T_{SCE}=22.35)

E	A_{548}
299.6	0.207
112.9	0.236
87.0	0.280
62.5	0.356
41.4	0.443
20.0	0.521
-8.3	0.586
-35.4	0.611
-205.3	0.625

T=26.4 (T_{SCE}=22.5)

E	A_{548}
-205.4	0.611
-61.2	0.602
-34.9	0.591
-7.1	0.560
15.7	0.507
38.0	0.426
54.9	0.362
75.3	0.296
101.7	0.246
300.5	0.211

T=31.0 (T_{SCE}=22.0)

E	A_{548}
300.4	0.213
115.6	0.230
89.4	0.258
64.0	0.313
38.3	0.402
7.6	0.504
-16.1	0.552
-45.8	0.581
-246.1	0.598

T=36.6 (T_{SCE}=22.0)

E	A_{548}
-246.2	0.589
-78.8	0.579
-38.8	0.560
-13.3	0.528
8.9	0.477
34.1	0.394
50.6	0.338
97.8	0.242
299.7	0.212

Sample 2

T=6.8 (T_{SCE}=24.6)

E	A_{548}
295.8	0.284
111.8	0.333
88.9	0.392
70.8	0.468
49.0	0.574
29.0	0.659
6.1	0.716
-20.4	0.747
-241.4	0.761

T=36.6 (T_{SCE}=27.5)

E	A_{548}
-240.7	0.697
-70.6	0.688
-50.1	0.679
-18.2	0.646
7.0	0.587
31.2	0.511
54.9	0.416
73.0	0.367
145.5	0.300
298.6	0.296

T=40.6 (T_{SCE}=27.75)

E	A_{548}
298.7	0.303
122.4	0.314
90.9	0.337
70.5	0.368
47.4	0.428
23.9	0.509
-0.7	0.587
-30.8	0.644
-233.9	0.682

Table A3.3. Modified A_5Ru(His39)-*Candida krusei* cytochrome *c* spectroelectrochemistry data, continued

T=47.0 (T_{SCE}=26.5)	
E	A_{548}
-331.6	0.670
-78.5	0.658
-49.4	0.641
-19.5	0.601
7.1	0.536
31.9	0.455
56.2	0.387
84.8	0.338
298.4	0.320

Table A3.4. Fitted parameters to spectroelectrochemical Nernst plots for modified A_5Ru(His39)-*Candida krusei* cytochrome *c*[a]

Temperature	b	m_{exptl}	m_{theor}	%error in m	r^2
7.6	59.13	55.6	55.7	0.07	0.9993
12.6	53.80	56.6	56.7	0.10	0.9999
19.6	48.06	57.3	58.1	1.30	1.0000
26.4	41.48	60.6	59.4	1.95	0.9989
31.0	36.22	60.4	60.3	0.09	0.9997
36.6	30.81	66.3	61.4	7.91	0.9966
6.8	60.07	54.0	55.5	2.81	0.9996
36.6	30.95	59.7	61.4	2.86	0.9981
40.6	28.42	61.8	62.2	0.69	1.0000

a. b, m_{exptl}, and r^2 are the intercept, slope, and correlation coefficient, respectively, of a plot of the potential (*vs.* SCE) *vs.* the log of the ratio of concentrations of oxidized to reduced forms of cytochrome *c*; m_{theor} is the theoretical value of the slope, and is equal to RT/$\mathcal{F}$, assuming a one electron reduction. The error in m is calculated as

$$\frac{|m_{theor} - m_{exptl}|}{m_{theor}} \times 100$$

The blank line separates the results of two samples.

Appendix 4

Problems with the Flash Photolysis Instrumentation

"A wise sage has commented (in another context) 'One of the more serious disadvantages of this photometer is that it nearly always gives an answer.'."

J. Gunn, J. Westphal, *Soc. Photoopt. Instr. Eng. Proc.* **290**, 16 (1981).

Flash photolysis data were collected with two major flaws in the instrument design, (1) operation of the PMT in a region of possible nonlinear response, and, (2) flash breakthrough. These problems have existed for the past eighteen months, and hence are the reason for labeling other data presented in table 1.1 preliminary also. In addition to these problems, it was at one time common practice to turn off the air cooling the probe lamp immediately prior to flashing a sample. The resulting warming of the lamp alone gives rise to a measurable drift, which may have contributed error to some of those measurements as well (see figure A4.1). This problem does not apply to the *Candida* results, as the cooling air was left on throughout each experiment. A better solution to this problem is discussed in a review by Porter.[1]

The manufacturer specifications[2] for Hamamatsu photomultiplier tubes state that linear operation can be assured if the output current is maintained at or below the level of 1/20th the "bleeder chain" current.[3] The R928 PMT in the flash photolysis apparatus has been operated with a PMT housing containing ten stages, with voltage division provided by 200KΩ resistors. Typically, an applied voltage of 800V is used, hence the bleeder chain current would be

$$i = V/R = 800V/(2x10^6\Omega) = 0.4mA$$

The output current is passed through a 5KΩ resistor, and monitored by a voltmeter. Typically, a 3V signal is observed, with a 50mV change re-

[1] Porter, G. *Techniques of Organic Chemistry* **8**, 1055 (1963).

[2] Hamamatsu catalog no. SC-1-4-1, Hamamatsu TV Co., Ltd., Hamamatsu, Japan.

[3] "Bleeder chain" refers to the voltage divider circuit in the PMT housing which maintains the voltage difference between each dynode.

sulting after flashing the modified derivative. The output current is approximately

$$i = V/R = 3V/5000\Omega = 0.6mA$$

Therefore, the ratio of output to bleeder chain current is ~1.5 (0.6mA/0.4mA), significantly higher than the recommended maximum of 0.05 for linear operation. Hence, the possibility exists that the PMT output signal is not directly related to light intensity.

Figure A4.2 depicts the relationship of this current ratio to light intensity. Although a value of 1.5 for the current ratio definitely predicts nonlinearity of the PMT response for large intensity changes, small changes in light intensity may result in a linear response, as much, but not all, of the behavior for current ratios exceeding 0.05 is linear.

The second major problem relates to the PMT response to the flash event itself. With the 3-73 filters (~426nm cutoff) in use, flash light of almost the entire visible spectrum impinges on the sample. Because of the configuration of the flash lamp and cell holder, light from the flash is readily conducted down the optical fiber leading to the monochromator and PMT. A blank sample (water only) gives rise not only to the FWHM 10μs spike expected from the flash itself, but also to broader signals presumed to be related to PMT overload (figure A4.3). Approximately seven milliseconds are required before the signal returns to baseline. The 10mV+ signal cannot be ignored in relation to the typical 50mV signal observed in an electron transfer experiment, half of which is immediate, direct reduction of the iron site by $[Ru(bpy)_3]^{2+*}$. Subtraction of this signal from actual data is not possible, as the signal intensity was found to be dependent on the

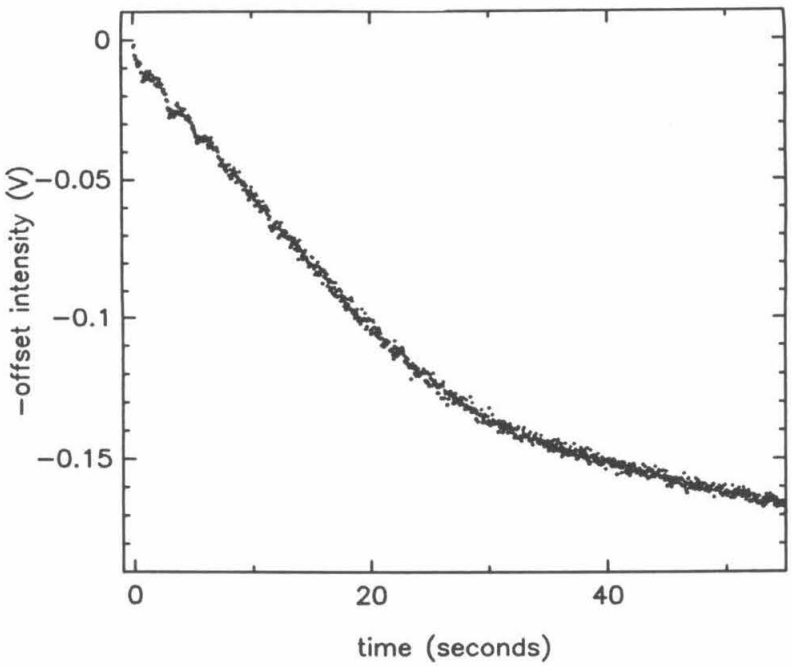

Figure A4.1. Signal resulting from cessation of air flow cooling probe lamp (no flash, water in cell, λ=549nm).

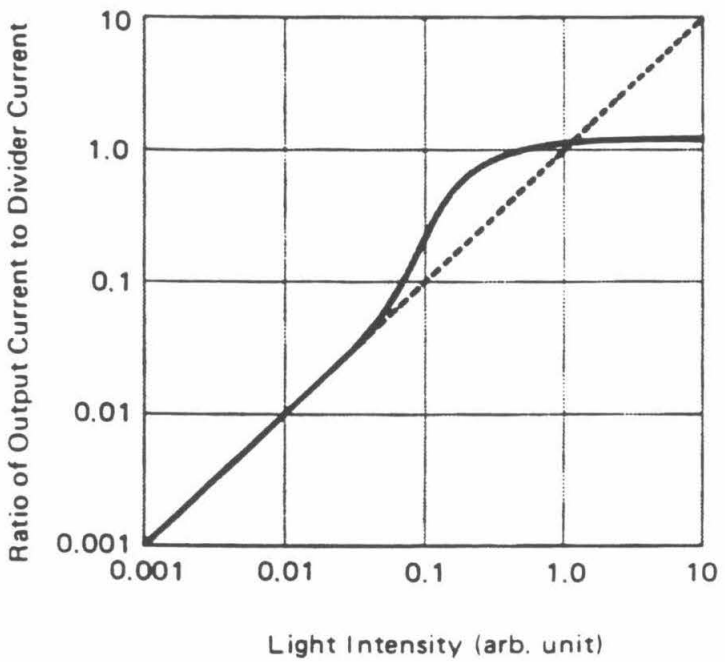

Figure A4.2. Relationship of output-to-bleeder chain current ratio and light intensity for a typical Hamamatsu photomultiplier tube (page 6 of reference 2).

sample absorbance, a property which is expected to change throughout an electron transfer experiment. Assuming one could "sacrifice" one half-life of data to this problem, *i.e.*, $t_{1/2}$=~7ms, a maximum rate of approximately $100s^{-1}$ could be measured with this instrument.

As recommended by the Hamamatsu Company,[2] capacitors were installed in the last four PMT housing stages to maintain the voltage division among the final dynodes, which tends to be lost when intense light is incident upon the PMT. This gave rise to a "ringing" of the signal, but no reduction in the time necessary for the return to baseline (figure A4.4).

In another effort to eliminate the problem of flash breakthrough, 450nm (±40nm) bandpass filters were obtained (Omega Optical, Brattleboro, VT) to reduce the ~549nm component of the flash light (~72% transmission at 452nm; 0.01% at 550nm). A definite improvement was noted, in that a lapse of ~5ms was required for the signal to return to baseline on a blank flash (figure A4.5). Therefore, it seems that the problem has been properly identified, but the flash intensity is so strong that whatever ~550nm light manages to pass through the filters is sufficient to overload the PMT (which, as discussed above, is already overloaded by the intense probe beam). Using these filters, and omitting the first half-life of data, *i.e.*, $t_{1/2}$=5ms, a maximum rate of $140s^{-1}$ could be measured.

A reduction in the flash intensity is not an option, as it is necessary to excite a sufficient population of $[Ru(bpy)_3]^{2+}$ molecules to reduce a sizeable portion of the cytochrome molecules. Increasing the concentration of the ruthenium complex (and decreasing the flash intensity) would result in a larger background absorbance (background

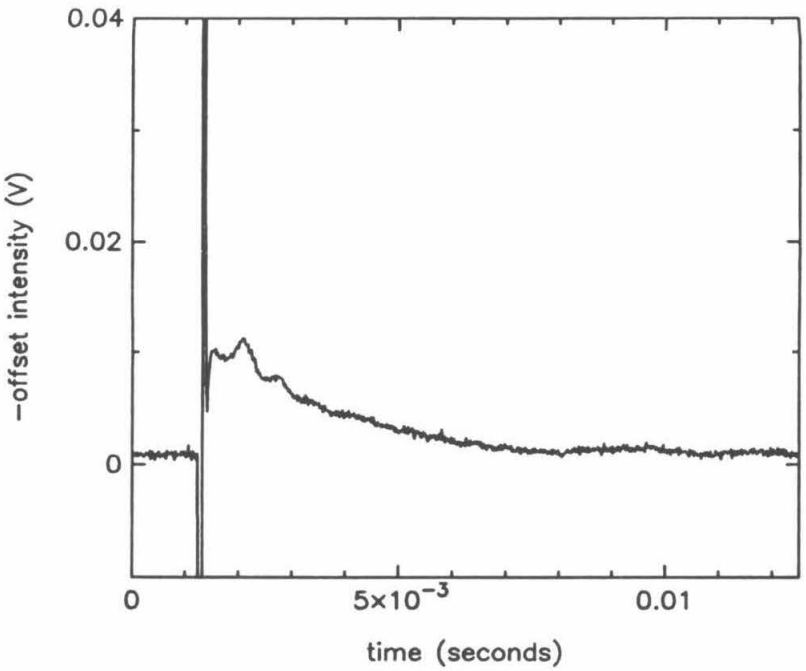

Figure A4.3. Signal resulting from flashing a blank (water) sample, with detection at 549nm.

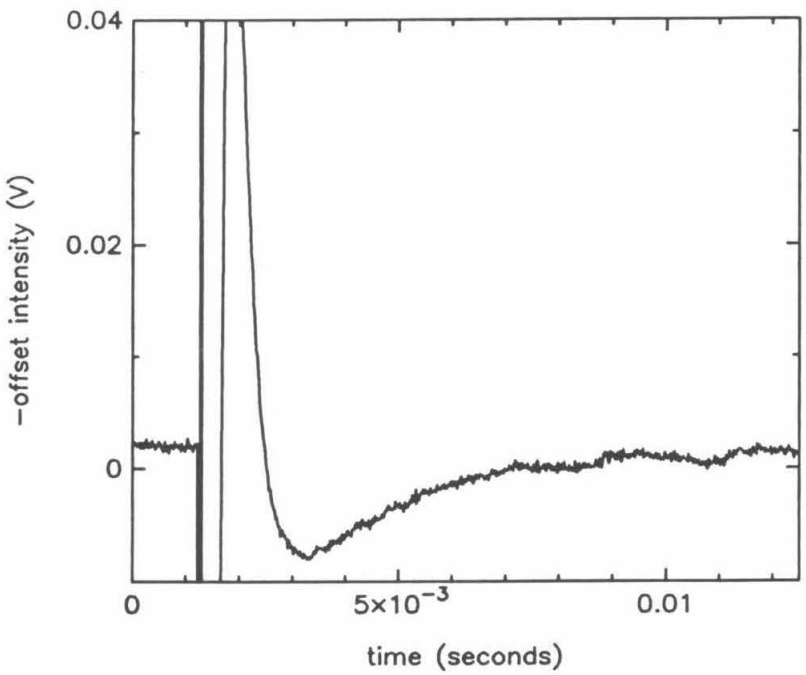

Figure A4.4. Signal resulting from flashing a blank sample after the installation of capacitors in the PMT housing to maintain the voltage difference between the final dynodes (λ=549nm).

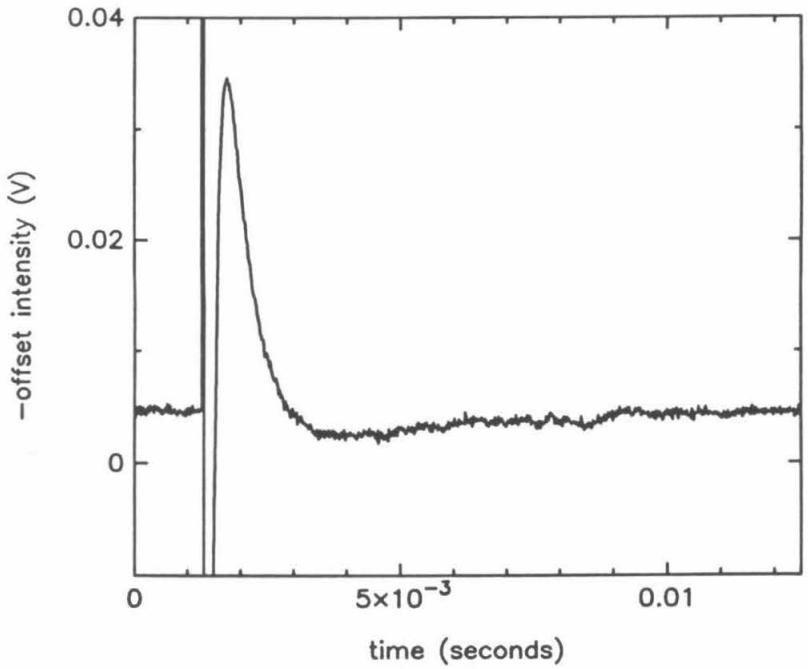

Figure A4.5. Signal resulting from flashing a blank sample using 450nm bandpass filters (λ=549nm).

absorbance is ~0.4 at 549nm for the 65μM $[Ru(bpy)_3]^{2+}$ routinely used).

The problems associated with the flash photolysis instrumentation may be rectified by the changes suggested below.

1. The probe beam light intensity should be reduced by a neutral density filter or iris so that the output current and output-to-bleeder chain current ratio is reduced. Simply operating the lamp at a reduced voltage was found to increase noise. Operation of the PMT at a current ratio below 0.05 may lead to larger signals, as the slope of the response curve is steeper here than on any linear portion above y=0.5.

2. The probe beam exiting the optical fiber and impinging on the face of the flash cell should be collimated and focused to a diameter less than that of the cell width. While it would seem that insufficient light is not a problem, and that losses could be tolerated, it is important to reduce the light impinging on the sample. The $[Ru(bpy)_3]^{2+}$ excitation band centered at 452nm extends as far as 580nm, so that the probe beam of $\lambda >$ 530nm does itself excite the complex somewhat, and will result in some loss of signal.[4]

[4] For a typical sample of 1.3μM cytochrome, the absorbance change occurring at 550nm upon reduction (through a pathlength of 15cm) is

$$(1.3\times10^{-6}M)(15cm)((29000 - 7800)M^{-1}cm^{-1}) = 0.41$$

Absorbance is defined as $\log(I_o/I)$, where I_o and I are the light intensities incident to and exiting from a sample, respectively. Hence, any absorbance change accompanying a reaction can be expressed as $\log(I_o/I_f) - \log(I_o/I_i)$, where I_f and I_i are the final and initial exiting light intensities, respectively:

3. Fittings which hold the cell in place and provide a means of connecting the optical fibers should be made of a black material to reduce light scatter. The fitting on the side of the cell where the probe beam exits should be made longer, to distance the optical fiber from the path of light rays originating from the flash lamp. Baffles within this connector would further discourage the propagation of flash light to the PMT.

These suggestions are but a few of the many possible changes which would improve the operation of the flash photolysis apparatus. Other possibilities, which would require changes in the basic components, include the use of a PMT with fewer stages (dynodes) to reduce the output current without changing the light intensity, or replacement of the PMT with a photodiode, a solid state device whose response is less likely to be perturbed by intense incident light.

$$\Delta A = \log(I_o/I_f) - \log(I_o/I_i) = \log[(I_o/I_f)/(I_o/I_i)] = \log (I_i/I_f)$$

For an absorbance change of 0.4, the ratio of initial and final light intensities is expected to be 2.51 ($=10^{0.4}$). Therefore, for a typical initial intensity reading of 3.0V, a final voltage of 1.20 (=3.0/2.51) is expected. However, a change of only ~50mV is observed. This is indicative of operation in the nonlinear portion of the PMT response curve (as predicted by the current ratio). It is important to note that probe light which bypasses the sample may also contribute to this behavior.

Appendix 5

Programs for Data Fitting

All programs included in this appendix were written by Fernando J. Selman.

Subroutines not explicitly written here can be found in *Numerical Recipes*, W. Press, B. Flannery, S. Teukolsky, W. Vettering, Cambridge University Press (New York), 1986.

```
      PROGRAM BLT2DAT
C*********************************************************
C                                                        |
C Used to reformat data from flash experiment (voltage   |
C readings) into a format understandable by the MEXPFIT_DP|
C program (relative absorbance values).                  |
C                                                        |
C*********************************************************
c
      IMPLICIT NONE
      REAL          TIME(2096),       !Time data vector (seconds)
     :              ABSORBA(2096),    !Absorbance vector
     :              SIGMA0,           !Estimate of error in absorbance
     :              VOLTAGE(2096),    !Offset amplified voltage data
                                      !vector
     :              RVOLT(2096),      !Raw voltage data vector
     :              SIGMAV,           !Estimate of error in voltage
     :              VI,               !Baseline raw voltage
     :              VHAT,             !Voltage offset constant
     :              V3I,              !Baseline offset amplified voltage
     :              GAIN,             !Gain (will divide offset voltage)
     :              TSPIKE,           !Time of flash
     :              T,                !Time (after flash)
     :              DUMR1,            !Dummy variable
     :              AVER,             !Moving average
     :              SUM,              !Sum of baseline voltages
     :              SIGMA,            !Moving standard deviation
     :              NXWIND,           !Length of window for AVER
     :              LOG10,            !ln(10)
     :              XFACTOR           !Number of standard deviations
C                                              to define flash spike.
      INTEGER       LEN,              !Fortran integer library function
     :              ISPIKE,           !Position of spike in data vector
     :              ISTART,           !Length of window for moving avg.
     :              NDATA,            !Number of data points
     :              NVALUES,          !Number of points after spike
     :              LENAME,           !Length of filename
     :              I,J               !Integer loop variables
      CHARACTER*16  FILE1,            !Filename of input (BINLOT output)
     :              FILE2,            !Filename of output
     :              DUMCH*1,          !Dummy character
     :              PREFIX            !Prefix of input filename
      LOGICAL       EOFIL,            !End of file
     :              FOUND
      PARAMETER   (LOG10=2.302585093)
C
C Initial values
C
      EOFIL=.FALSE.
      FOUND=.FALSE.
      XFACTOR=5.
C
C ---------------------------- INPUT ----------------------------|
C
```

```
      WRITE(6,100)
100   FORMAT(' Enter name of input file   --> ',$)
      READ(5,'(A)')FILE1
C
C If filename has an extension, use as is. If not, append .BLT.
C
      LENAME=LEN(FILE1)
      I=0
      DO WHILE ( (.NOT.FOUND) .AND. (I.LT.LENAME) )
        I=I+1
        DUMCH=FILE1(I:I)
        IF (DUMCH.EQ.'.') THEN
          FOUND=.TRUE.
          PREFIX=FILE1(:I-1)
        ENDIF
      ENDDO
      IF (.NOT.FOUND) THEN
        PREFIX=FILE1(:LENAME)
        FILE1=FILE1(:LENAME)//'.BLT'
      ENDIF
C
      WRITE(6,110)FILE1
110   FORMAT(' Opening file ',A16)
C
      OPEN (UNIT=11,FILE=FILE1,TYPE='OLD',FORM='FORMATTED')
C
C Get gain
C
      WRITE(6,120)
120   FORMAT(' Reading GAIN from first line and skipping 2 lines.. ')
c
      READ(11,125)   DUMCH,GAIN
125   FORMAT(A1,F3.0)
      WRITE(6,*)' GAIN = ',GAIN
      READ(11,'(A)') DUMCH
      READ(11,'(A)') DUMCH
C
C Reading rest of file
C
      WRITE(6,130)
130   FORMAT(' Reading rest of file.. ')
      I=0
      DO WHILE (.NOT.EOFIL)
        I=I+1
        READ(11,*,END=150) DUMR1 , TIME(I) , VOLTAGE(I) ,
     :                     DUMR1 , DUMR1 , DUMR1 , RVOLT(I)
      ENDDO
150   CONTINUE
      NDATA=I-1
      CLOSE(11)
C-------------------------------------------------------------------|
C------------------------ PREPARING DATA ---------------------------|
C
```

```
C Finding spike
C
      WRITE(6,160)
160   FORMAT(' Finding position of spike.. ')
c
      ISTART= 20
      NXWIND = FLOAT(ISTART)
C
      SUM=0.
      DO J=1,ISTART
        SUM=SUM+VOLTAGE(J)
      ENDDO
      AVER=SUM / NXWIND
C
      SIGMA=0.
      DO J=1,ISTART
        SIGMA=SIGMA+(VOLTAGE(J)-AVER)**2
      ENDDO
      SIGMA=SQRT(SIGMA)/SQRT( NXWIND -1. )
      I=ISTART
      DO WHILE (.NOT.FOUND .AND. I.LT.NDATA)
        I=I+1
        SIGMA = SIGMA - (VOLTAGE(I-ISTART)-AVER)**2 / (NXWIND-1.)
        AVER  = AVER  + (VOLTAGE(I)-VOLTAGE(I-ISTART)) / NXWIND
        SIGMA = SIGMA + (VOLTAGE(I)-AVER)**2 / ( NXWIND - 1. )
C
        IF ( ABS(VOLTAGE(I)-AVER).GT.XFACTOR*SIGMA) FOUND=.TRUE.
C
      ENDDO
      IF ( FOUND ) THEN
         ISPIKE=I
         WRITE(6,200) ISPIKE
200      FORMAT(' ..at data pair ',I4)
      ELSE
         WRITE(6,205) IFIX (XFACTOR)
205       FORMAT(' ..no ',I4,' sigma spike in data')
      ENDIF
      WRITE(6,206)
206    FORMAT(' Enter spike position --> ',$)
      READ (5,*) ISPIKE
C
C Calculating average and dispersion of baseline values.
C
C AVERAGE...
      WRITE(6,210)
210    FORMAT('Calculating average and dispersion of initial values.')
      V3I=0.
      VI=0.
      NXWIND=FLOAT(ISPIKE-2)
      DO I=1,ISPIKE-2
        V3I=V3I+VOLTAGE(I)
        VI=VI+RVOLT(I)
      ENDDO
```

```
      V3I= V3I/NXWIND
      VI = VI/NXWIND
C DISPERSION...
      SIGMAV=0.
      DO I=1,ISPIKE-2
        SIGMAV=SIGMAV+(VOLTAGE(I)-V3I)**2
      ENDDO
      SIGMAV=( SQRT(SIGMAV/GAIN ) / SQRT( NXWIND ) )
      VHAT=(V3I/GAIN-VI)
      SIGMA0=ABS( SIGMAV / ( VI * LOG10 ) )
C
C Calculating absorbances
C
      WRITE(6,220)
220   FORMAT(' Calculating absorbances..')
      DO I=1,NDATA
        VOLTAGE(I)=VOLTAGE(I)/GAIN-VHAT
C Offset amplified voltage variable redefined as a
C  raw voltage (dumb!).
      ENDDO
C
      DO I=1,ISPIKE
        ABSORBA(I)=0.
      ENDDO
      DO I=ISPIKE+1,NDATA
        IF ( VOLTAGE(I).LT. 0. ) THEN
          ABSORBA(I) = ALOG10(  ( VI/VOLTAGE(I) )  )
        ELSE
          ABSORBA(I) = 10.0
        ENDIF
      ENDDO
C
C-------------------------------------------------------------------|
C------------------------- OUTPUT ----------------------------------|
C Storing results
C
      FILE2=PREFIX(:LENAME)//'.DAT'
      OPEN(UNIT=12,STATUS='NEW',FILE=FILE2,FORM='FORMATTED')
C
      WRITE(6,300) FILE2
300   FORMAT(' Storing reformatted data in ',A16)
C
      NVALUES=NDATA-ISPIKE
      TSPIKE=TIME(ISPIKE)
      DO I=1,NVALUES
        T=TIME(I+ISPIKE)-TSPIKE
        WRITE(12,*) T,ABSORBA(I+ISPIKE),SIGMA0,VOLTAGE(I+ISPIKE)
      ENDDO
      CLOSE(12)
C
C Storing some useful information in file FILE1.HDR
c
      WRITE(6,350) PREFIX(:LENAME)//'.HDR'
```

```
350     FORMAT(' Storing useful information in ',A16)
        OPEN (UNIT=13,STATUS='NEW',FILE=PREFIX(:LENAME)//'.HDR')
        WRITE(13,400)GAIN,VI,VHAT,ISPIKE,TSPIKE,NVALUES,SIGMA0,SIGMAV,
     :     TIME(ISPIKE+1)-TSPIKE,ABSORBA(ISPIKE+1),VOLTAGE(ISPIKE+1),
     :     TIME(NDATA)-TSPIKE,ABSORBA(NDATA),VOLTAGE(NDATA)
400     FORMAT('1',T11,'  GAIN = ',F9.2/
     :            T11,'    VI = ',F9.3/
     :            T11,'OFFSET = ',F9.3/
     :            T11,'ISPIKE = ',I9/
     :            T11,'TSPIKE = ',F9.3/
     :            T11,' NDATA = ',I9/
     :            T11,'SIGMA0 = ',E9.3/
     :            T11,'SIGMAV = ',E9.3/
     :            T11,'    TO = ',F9.3,' A0 = ',F11.4,' V0 = ',F9.3/
     :            T11,'    TF = ',F9.3,' AF = ',F11.4,' VF = ',F9.3 )
        STOP
        END
```

```
      PROGRAM MEXPFIT_DP
C
C-------------------------------------------------------------\
C  DOUBLE PRECISION VERSION.                                  |
C  This program is used to calculate the fitting parameters   |
C  of a nonlinear model; written after subroutine func_fit to|
C  specify physical sizes of arrays, as required by FORTRAN. |
C-------------------------------------------------------------
C
                    IMPLICIT     NONE
C
      INTEGER       NMAX,                !max. no. of data points
     :              NPMAX                !max. no. of parameters
      PARAMETER   ( NMAX=2096,
     :              NPMAX=20    )
C
      REAL*8        X(NMAX),
     :              Y(NMAX),
     :              SIG(NMAX),
     :              XO,                  !initial x value for fit
     :              XE,                  !final x value for fit
     :              XDUM,
     :              YY
C
      REAL*8        A(NPMAX),            !initial values for parameters
     :              DYDA(NPMAX),
     :              ALPHA(NPMAX,NPMAX),
     :              CHISQ,
     :              COVAR(NPMAX,NPMAX),
     :              EPS,
     :              Q,
     :              SIGMA_A(NPMAX)
C
      INTEGER       LISTA(NPMAX),        !parameters to be varied
     :              MA,                  !no. of parameters in model
     :              MFIT,                !no. of variable parameters
     :              NDATA,
     :              NVALUES,
     :              NMIN_COUNTS,
     :              NMAX_STEPS
C
      INTEGER       LENAME,
     :              ICH_LEN              !Integer function.
C
      INTEGER       IO,                  !index for data pair at start of
C                                         fitting window
     :              IE,                  !index for data pair at end of
C                                         fitting window
     :              I,
     :              J
C
      CHARACTER*64 FILE1,                !data filename
     :              FILE2                !parameter filename
```

```
      CHARACTER*64 FILE3,              !filename for fitted parameters
     :             FILE4,              !filename for theor. y values
     :             PREFIX
C
      LOGICAL      NOTEOF,             !not end of file
     :             FOUND
C
C------------------------- INPUT ---------------------------------|
C
      WRITE (6,100)
100   FORMAT(' Enter file with (x,y,sig) data [.DAT] --> ',$)
      READ(5,'(A)') FILE1
C
C Determining if file has extension; if not, .dat appended.
C
      LENAME=ICH_LEN(FILE1)
C      Ich_len is a subroutine which determines the length of
C      a filename.
      I=0
      DO WHILE ( (.NOT.FOUND) .AND. (I.LT.LENAME) )
        I=I+1
        IF (FILE1(I:I).EQ.'.') THEN
          FOUND=.TRUE.
          PREFIX=FILE1(:I-1)
        END IF
      ENDDO
      IF (.NOT.FOUND) THEN
        PREFIX = FILE1(:LENAME)
        FILE1  = FILE1(:LENAME)//'.DAT'
      ENDIF
C
      OPEN (UNIT=10,FILE=FILE1,STATUS='OLD')
      NOTEOF=.TRUE.
      I=0
      DO WHILE (NOTEOF)
              I=I+1
              READ(10,*,END=200) X(I),Y(I),SIG(I)
      ENDDO
200   CONTINUE
      NDATA=I-1
      CLOSE(UNIT=10)
C
C Reading parameters for fit
C
      FILE2=PREFIX(:LENAME)//'.PAR'
      WRITE(6,210) FILE2
210   FORMAT(' Reading parameters from ',A16)
C
      OPEN(UNIT=11,FILE=FILE2,STATUS='OLD')
C
      READ (11,*)  MA          !Number of parameters in model
      READ (11,*)  MFIT        !Number of free parameters
      DO I=1,MA
```

```
      READ(11,*) A(I)          !Initial guesses for parameters
      ENDDO
      DO I=1,MFIT
        READ(11,*) LISTA(I)    !List of parameters to be varied
      ENDDO
      READ(11,*)   XO          !Starting x-value for fitting window.
      READ(11,*)   XE          !Ending x-value for fitting window.
      CLOSE(UNIT=11)
C
C----------------------- PERFORMING FIT -----------------------------
C
      WRITE(6,*)' Performing fit..'
      CALL FUNCT_FIT(X,Y,SIG,NDATA,XO,XE,MA,MFIT,A,LISTA,
     :              COVAR,ALPHA,NPMAX,Q,CHISQ,SIGMA_A)
      WRITE(6,*)' OK. '
C
C-----------------------    OUTPUT     -----------------------------
C
C Storing fitting parameters
C
      FILE3=PREFIX(:LENAME)//'.FIT'
      WRITE(6,300)FILE3
300   FORMAT(' Storing fit results in ',A16)
C
      OPEN(UNIT=12,STATUS='NEW',FILE=FILE3,FORM='FORMATTED')
C
      DO I=1,MA
      DO J=1,MA
            WRITE(12,400)I,J,COVAR(I,J),I,J,ALPHA(I,J)
      ENDDO
      ENDDO
400   FORMAT(' COVAR(',I2,',',I2,') = ',D12.6,
     :' ALPHA(',I2,',',I2,') = ',D12.6)
      WRITE(12,500) Q,CHISQ
500   FORMAT(' Goodness of fit = ',D12.6,' chi-square = ',D12.6)
      DO I=1,MA
            WRITE(12,600) I,A(I),SIGMA_A(I)
      ENDDO
600   FORMAT(' A(',I2,') = ',D12.5,' SIGMA_A = ',D12.6)
      CLOSE(12)
C
C Storing a tabulation of the fitting function
C
      FILE4=PREFIX(:LENAME)//'.THE'
      WRITE(6,650) FILE4
650   FORMAT(' Storing fitting curve (x,y pairs) in ',A16)
c
      OPEN(UNIT=12,STATUS='NEW',FILE=FILE4,FORM='FORMATTED')
c
      WRITE(12,*)' OK. '
      WRITE(12,710)
710   FORMAT(5X,'     X     ',5X,'     Y     ')
      CALL LOCATE(X,NDATA,XO,IO)
```

```
        CALL LOCATE(X,NDATA,XE,IE)
C
C LOCATE is a subroutine (Numerical Recipes) which finds the indices
C of the data pairs most closely matching the desired fitting window.
C
       IF (IO.LE.1)      IO=1
       IF (IE.GE.NDATA) IE=NDATA
       NVALUES=IE-IO+1
       DO I=1,NVALUES
           XDUM=X(IO+I-1)
           CALL FUNCT(XDUM,A,YY,DYDA,MA)
C
C FUNCT subroutine calculates theoretical y values for each x
C  value using specified parameters.
C
           WRITE(12,*) XDUM,YY
       ENDDO
       CLOSE(12)
       STOP
       END
c
       SUBROUTINE FUNCT_FIT(X,Y,SIG,NDATA,XO,XE,MA,MFIT,A,LISTA,
     :                      COVAR,ALPHA,NP,Q,CHISQ,SIGMA_A)
C+
C-------------------------------------------------------------------|
C  DOUBLE PRECISION VERSION.                                        |
C  Determines indices of data pairs most closely matching desired   |
C   fitting window.  Calls subroutines FUNCT, LOCATE, and           |
C   NONLINFIT (the last itself calls many subroutines from          |
C   Numerical Recipes).                                             |
C                                                                   |
C INPUT:                                                            :
C                                                                   :
C     > X           Vector of dimensions NDATA containing the     :
C                    independent, error free abscissas.           :
C     > Y            Vector of dimensions NDATA containing the    :
C                    dependent variable.                          :
C     > SIG          Vector of dimensions NDATA containing the    :
C                    standard deviations of the Y's.              :
C     > NDATA        INTEGER*4 number of data points              :
C     > XO           REAL*4 The starting value of the X coordinate:
C                    to be used for the fitting.                  :
C     > XE           REAL*4 The last value of the X coordinate    :
C                    to be used for the fit.                      :
C     > MA           INTEGER*4 The number of parameters for the   :
C                    fit                                          :
C     > MFIT         INTEGER*4 The number of parameters to be     :
C                    varied during the fit.                       :
C     > A(MA)        REAL*4 Vector of dimension MA, containing    :
C                    the initial guesses for the parameters. It   :
C                    will contain the final values                :
C     > LISTA(MA)    INTEGER*4 Vector containing the list of      :
C                    parameters to be varied in its first MFIT    :
```

```
C                    slots.                                                :
C     > NP           INTEGER*4 Physical dimensions of arrays              :
C                    COVAR and ALPHA.                                     |
C                                                                         :
C OUTPUT:                                                                 :
C                                                                         :
C     < A(MA)            REAL*4 Vector containing the desired            :
C                        best fit parameters in its first MA             :
C                        slots.                                          :
C     < SIGMA_A(MA)      REAL*4 Vector containing the standard           :
C                        deviations of the calculated parameters         :
C     < COVAR(NP,NP)     REAL*4 Covariance Matrix                        :
C     < ALPHA(NP,NP)     REAL*4 Curvature Matrix                         :
C     < Q                REAL*4 Goodness of fit                          :
C     < CHISQ            REAL*4 Chi-square                               :
C                                                                         :
C-------------------------------------------------------------------------'
C+
      IMPLICIT          NONE
C
      INTEGER           NMAX_STEPS,NMIN_COUNTS,
     :                  NDATA,MA,MFIT,NP,
     :                  I,J,IO,IE,NVALUES
C
      REAL*8            EPS,
     :                  X(NDATA),Y(NDATA),SIG(NDATA),
     :                  A(MA),SIGMA_A(MA),LISTA(MA),
     :                  XO,XE,
     :                  ALPHA(NP,NP),COVAR(NP,NP),
     :                  Q,CHISQ,
     :                  X1(2096),Y1(2096),S1(2096)
C
      PARAMETER         (NMAX_STEPS=1000,NMIN_COUNTS=4,EPS=1.00E-04)
C    (Default values for max. and min. no. of iterations, epsilon.)
C
      EXTERNAL          FUNCT
C
C Determining indices of array marking position of window to
C be used for fitting.
C
      IF ( (XO.GT.X(1)) .AND. (XE.LT.X(NDATA)) ) THEN
        CALL LOCATE(X,NDATA,XO,IO)
        CALL LOCATE(X,NDATA,XE,IE)
      ELSE IF ( (XO.GT.X(1)) .AND. (XE.GT.X(NDATA)) ) THEN
        CALL LOCATE(X,NDATA,XO,IO)
        XE=X(NDATA)
        IE=NDATA
      ELSE IF ( (XO.LE.X(1)) .AND. (XE.LT.X(NDATA)) ) THEN
        CALL LOCATE(X,NDATA,XE,IE)
        XO=X(1)
        IO=1
      ELSE
        IO=1
```

```
          IE=NDATA
          XO=X(1)
          XE=X(NDATA)
        ENDIF
        NVALUES=IE-IO+1
c
        WRITE(5,100) NVALUES,X(IO),X(IE),IO,IE
100     FORMAT(' Using ',I3,' values for fit.'//
     *          ' From  X = ',D10.4,' to  X= ',D10.4,'.'//
     *          ' From IO = ',   I3,' to IE= ',I4)
c
        DO I=1,NVALUES
         X1(I)=X(IO+I-1)
         Y1(I)=Y(IO+I-1)
         S1(I)=SIG(IO+I-1)
        ENDDO
C
        CALL NONLINFIT(X1,Y1,S1,NVALUES,A,MA,LISTA,MFIT,
     :    COVAR,ALPHA,NP,CHISQ,FUNCT,Q,NMAX_STEPS,NMIN_COUNTS,EPS)
C        (Summons actual fitting routine)
C
        DO I=1,MA
         SIGMA_A(I)=DSQRT(ABS(COVAR(I,I)))
        END DO
        RETURN
        END
c
        SUBROUTINE NONLINFIT ( X,Y,SIG,NDATA,A,MA,LISTA,MFIT,
     :                         COVAR,ALPHA,NCA,CHISQ,FUNCS,
     :                         Q,NMAX_STEPS,NMIN_COUNT,EPS)
C-----------------------------------------------------------------------
C DOUBLE PRECISION VERSION.                                            |
C This subroutine does a nonlinear fitting of the function FUNCS to    |
C the data X,Y,SIG. The parameters of the fit are in the array A(MA).  |
C The list of MFIT parameters to be varied are in the first MFIT slots |
C of LISTA(MA). The remaining MA-MFIT parameters are held fixed at     |
C their input values. The method used is the Levenberg-Marquardt       |
C method as implemented in Numerical Recipes.  The user also supplies  |
C the maximum number of iterations allowed in the variable NMAX_STEPS, |
C the minimum number of iterations with a negligible change in CHISQ   |
C required to stop the iteration in the variable NMIN_COUNT, and the   |
C meaning of 'negligible change in CHISQ' in the variable EPS, it      |
C being the maximum allowable percentual change in CHISQ(e.g., 0.001). |
C The user must supply the first guess at A(MA), the parameters of     |
C the fit.  The output is the optimal set of parameters A(MA),         |
C the covariance matrix COVAR(NCA,NCA), the curvature matrix           |
C ALPHA(NCA,NCA), the goodness of the fit Q, and chi-square CHISQ.     |
C-----------------------------------------------------------------------|
C                                                    FJS // CIT 1988   |
C======================================================================='
C
        IMPLICIT NONE
C
```

```
C  SUBROUTINE VARIABLES DECLARATIONS
C
      INTEGER          NDATA,MA,NCA,
     :                 LISTA(MA),MFIT,
     :                 NMAX_STEPS,NMIN_COUNT
C
      REAL*8           X(NDATA),Y(NDATA),SIG(NDATA),A(MA),
     :                 COVAR(NCA,NCA),ALPHA(NCA,NCA),
     :                 Q,EPS,FUNCS,CHISQ
C
C GENERAL VARIABLES DECLARATIONS
C
      REAL*8           DCHISQ,PREV_CHISQ,ALAMBDA,GAMMQ
C
      INTEGER          NSTEPS,ICOUNT
C
C Initialization call to MRQMIN
C
      ALAMBDA=-1.0
      CALL MRQMIN(X,Y,SIG,NDATA,A,MA,LISTA,MFIT,COVAR,ALPHA,
     :            NCA,CHISQ,FUNCS,ALAMBDA)
C
C Iterative procedure for optimization
C
      NSTEPS=0
      ICOUNT=0
      DO WHILE (ICOUNT.LT.NMIN_COUNT)
            PREV_CHISQ=CHISQ
            CALL MRQMIN ( X,Y,SIG,NDATA,A,MA,LISTA,MFIT,
     :                    COVAR,ALPHA,NCA,CHISQ,FUNCS,ALAMBDA)
            DCHISQ=DABS(CHISQ-PREV_CHISQ)/CHISQ
            IF (DCHISQ.LT.EPS) THEN
                  ICOUNT=ICOUNT+1
            WRITE(6,*)' Iteration #',ICOUNT,' going for ',NMIN_COUNT
            ELSE
                  ICOUNT=0
            END IF
            NSTEPS=NSTEPS+1
            IF (NSTEPS.GT.NMAX_STEPS) PAUSE ' NO CONVERGENCE '
      END DO
C
C FINAL CALL TO MRQMIN WITH ALAMBDA=0.
C
      ALAMBDA=0.0
      CALL MRQMIN(X,Y,SIG,NDATA,A,MA,LISTA,MFIT,COVAR,ALPHA,
     :            NCA,CHISQ,FUNCS,ALAMBDA)
C
C OBTAINING GOODNESS OF FIT
C
      Q=GAMMQ( (FLOAT(NDATA)-2.)/2. , CHISQ/2. )
      RETURN
      END
c
```

```
      SUBROUTINE FUNCT(X,A,Y,DYDA,NA)
C-----------------------------------------------------------------|
C DOUBLE PRECISION VERSION.                                       |
C Given an independent variable x and parameters for a multiexponen-|
C tial fit, calculates theoretical values for the dependent variable|
C y and dy/d[A(NA)].  Function is of the form                      |
C      y = A(1) + A(2){1-exp[-A(3)t]} + A(4){1-exp[-A(5)t]} etc.  |
C To be called from subroutine FUNC_FIT or NONLINFIT.             |
C-----------------------------------------------------------------'
C
      IMPLICIT NONE
      INTEGER NA,                       !Number of parameters
     *        NEXP                       !Number of exp. components
      INTEGER I
      DIMENSION A(NA),DYDA(NA)
      REAL*8    X,A,Y,DYDA,SUM,EXPARG
      LOGICAL LARGE
C
      LARGE=.FALSE.
      NEXP = ( NA-1 ) / 2
      DO I=1,NEXP
        EXPARG = A(2*I+1)*X
        IF ( EXPARG .GT. 20.) THEN
          LARGE=.TRUE.
        ENDIF
      ENDDO
C
C FOR LARGE ARGUMENT (to prevent underflow)
C
      IF (LARGE) THEN
        SUM=0.
        DO I=1,NEXP
          SUM=SUM+A(2*I)
          DYDA(2*I)=1.
          DYDA(2*I+1)=0.
        ENDDO
        DYDA(1)=1.
        Y=A(1)+SUM
        RETURN
      ENDIF
C
C FOR REGULAR SIZE ARGUMENT
C
      SUM=0.
      DO I=1,NEXP
        SUM=SUM+A(2*I)*( 1. - DEXP( -A(2*I+1)*X ) )
      ENDDO
      Y = A(1)+SUM
      DYDA(1)=1.
      DO I=1,NEXP
        DYDA(2*I)   = 1. - DEXP( -A(2*I+1)*X )
        DYDA(2*I+1) =  A(2*I)*X*DEXP( -A(2*I+1)*X )
      ENDDO
```

```
RETURN
END
```

Appendix 6

Characterization of the Second Derivatization Product

Introduction

Described here are data relating to the preliminary characterization of the second product resolved on CM-52 of the reaction of aquopentaammineruthenium(II) and *C. krusei* cytochrome *c*. This species will be referred to as "product 2".

All instrumentation, materials, and methods used are identical to those described in chapters 2 and 3 for the preparation and characterization of A_5Ru(His39)-*C. krusei* cytochrome *c*.

Purification

Because of the slow mobility of the third band resolved from the modification reaction mixture on CM-52, it was often eluted with a high ionic strength buffer (made so by the addition of NaCl). Although there was no indication of inhomogeneity of this product from its band shape,[1] it was known from electrophoresis that several modified products formed at long reaction times (figure 2.2b). Therefore, attempts were made to resolve any constituent components by FPLC. It should be noted that the second product of mobility higher than that of native seems to be formed at the expense of product 1, which is known to be A_5Ru(His39)-cytochrome *c*, indicating there is at least one site modified in addition to His39 in product 2.

Product 2 was eluted from an analytical MonoS cation-exchange FPLC column with a variety of gradients. In each case, a single major product was observed, which eluted on top of a broad band. Using the

[1] The shoulder on the tail of the third band seen in figure 2.3 is likely to be a result of the abrupt switch to a higher ionic strength elution buffer.

method described in chapter 2, retention of this broad band ranged from 12.8 to 26.4 mL, with the peak occurring at 19.2-19.3mL (figure A6.1). The broad band preceding the major component is likely to include native and singly-modified cytochrome redox isomers, as well as those of the major component, which is itself presumed to be a fully oxidized species (reduced native cytochrome elutes at 12.8mL). Such products may have formed from degradation of the major component, as evidence from FPLC studies of the A_5Ru(His39)-cytochrome *c* indicates that the ruthenium label is much more labile in the reduced state. Components of higher retention may be products of double modification at sites other than His33 and His39 (*vide infra*), *e.g.*, His26, or higher modifications, *i.e.*, ≥3 ruthenium ions per cytochrome molecule.

Samples utilized for NMR were purified using this FPLC method. All other experiments were conducted on the product as it eluted from the CM-52 column, after desalting and the appropriate buffer change.

Results

EPR spectra for the native and two modified products are presented in figure A6.2. As seen in the spectrum of A_5Ru(His39)-cytochrome *c*, signals indicative of a histidine complex are evident in the spectrum of product 2. Since the spectra of both modified products were recorded at identical temperature, a comparison of the intensities of the signals from the iron and ruthenium centers is appropriate. The greater apparent ratio of the intensity of the ruthenium signal as compared to the iron signal in product 2 *vs.* A_5Ru(His39)-cytochrome *c* suggests more than one histidine has been modified.

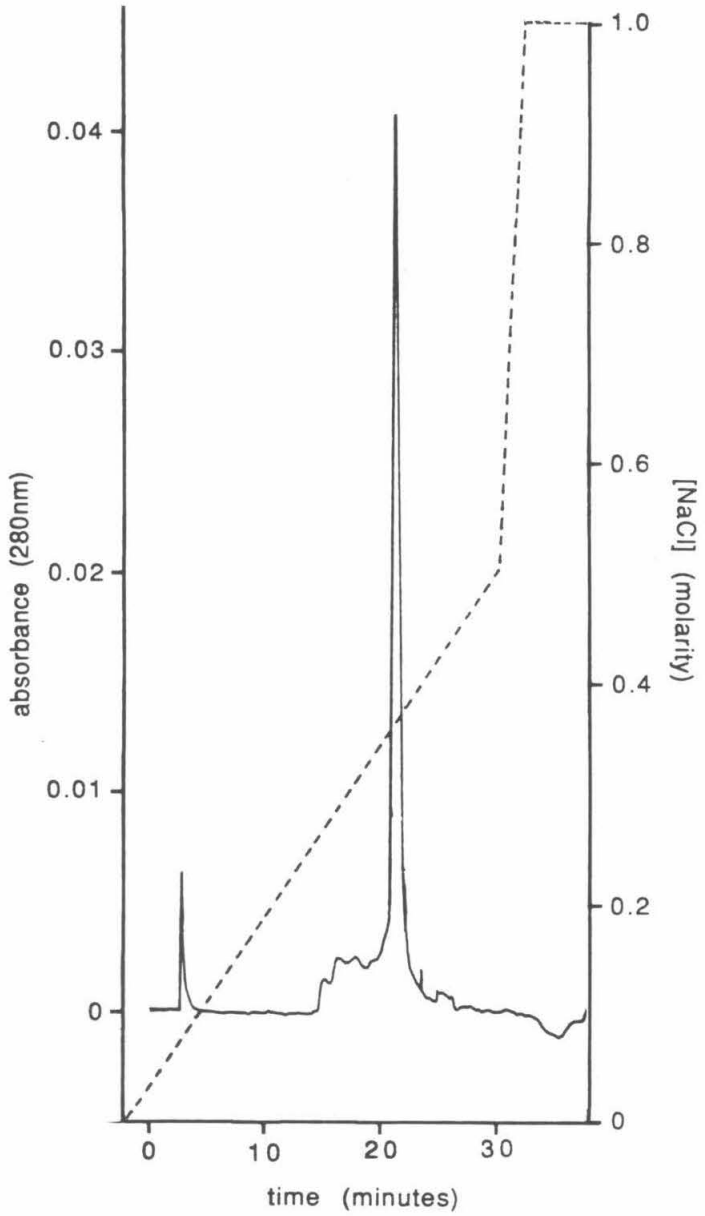

Figure A6.1. Chromatogram for the analytical FPLC elution of the oxidized product 2, the third band eluting from a CM-52 separation of the modification reaction mixture (--- gradient, 0-50%B in 32 minutes at 1mL/min; injection at 2 minutes; unretained product is $CoEDTA^-$).

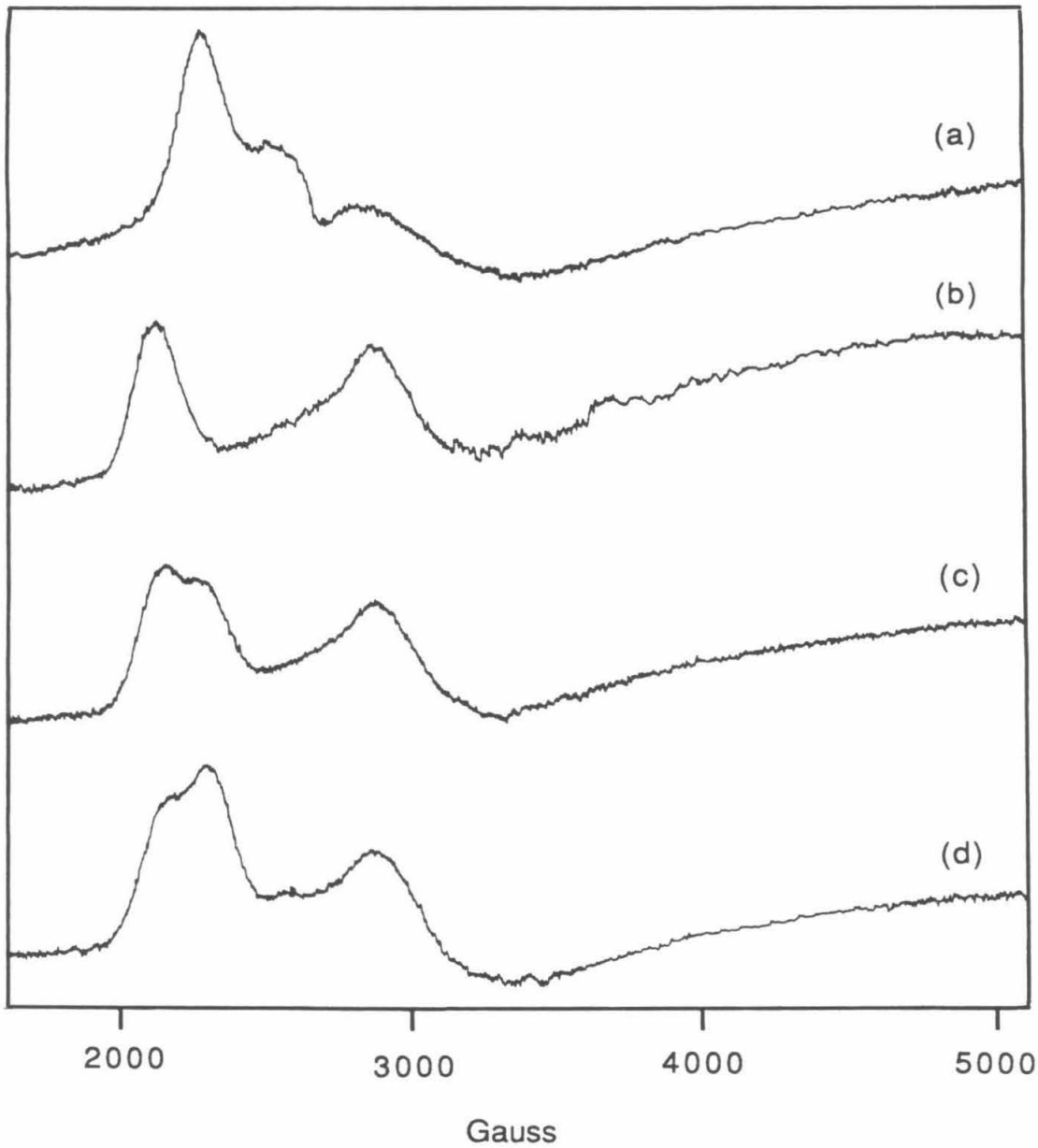

Figure A6.2. EPR spectra of (a) 7.73mM $[A_5RuHis]Cl_3$, (b) 2mM native *C. krusei* cytochrome *c*, (c) 1.85mM A_5Ru(His39)-*C. krusei* cytochrome *c*, (d) 2.1mM A_5Ru-cytochrome modification product 2. Protein samples in μ=0.1M pH 7 NaP_i, complex in 0.1M NaAc, pH 5. Initial sample temperatures (rose as much as 0.5K during a run): (a) 12.8K, (b) 12.6K, (c) & (d) 13.3K. Other conditions: modulation amplitude, 16G; power, 0.2mW; gain 1.6 x 10^4; frequency: (a) 9.25GHz, (b) 9.245GHz, (c) 9.247GHz, (d) 9.2485GHz.

NMR spectra for the native cytochrome and two modified products are presented in figure A6.3 (δ6-10ppm) and A6.4 (δ-22 to -38 ppm). Both sharp histidine C-2 ^{1}H resonances in the δ8.7ppm region are absent in the spectrum of product 2, confirming the suspicion that His39 is modified, and indicating His33 is modified as well. A new resonance is evident at ~δ-31ppm (in addition to the δ-32.5ppm signal observed for A_5Ru(His39)-cytochrome), which may be a histidine proton resonance contact-shifted by a proximal ruthenium complex.

A UV-visible difference spectrum for product 2 minus native *C. krusei* cytochrome is shown in figure A6.5. The features of the spectrum are those expected for a pentaammineruthenium(III) histidine complex, and the intensity of the 300nm absorbance (corrected for differences in redox state concentrations) is such that a 2:1 ruthenium-to-cytochrome ratio is indicated.

Discussion and Conclusion

The UV-visible spectrum and NMR spectrum of product 2 together indicate that both His33 and His39 have been modified. Electrochemical experiments (DPP) should be performed on this derivative to verify that no other (non-histidine) sites have been modified.

The production of this derivative, together with the fact that native protein is recovered from the A_5Ru-modification reaction mixture, suggest that some product, singly-modified at His33, should also be present. No evidence was found for such a product, but it is possible that it exists as a minor contaminant to the A_5Ru(His39)-cytochrome product. NMR,[2] EPR, and UV-visible difference spectra

Figure A6.3. NMR ^{1}H spectra for (a) native, (b) A_5Ru(His39)-modified, and (c) A_5Ru-modified (product 2) *C. krusei* ferricytochromes *c*, δ6-10ppm *vs.* DSS.

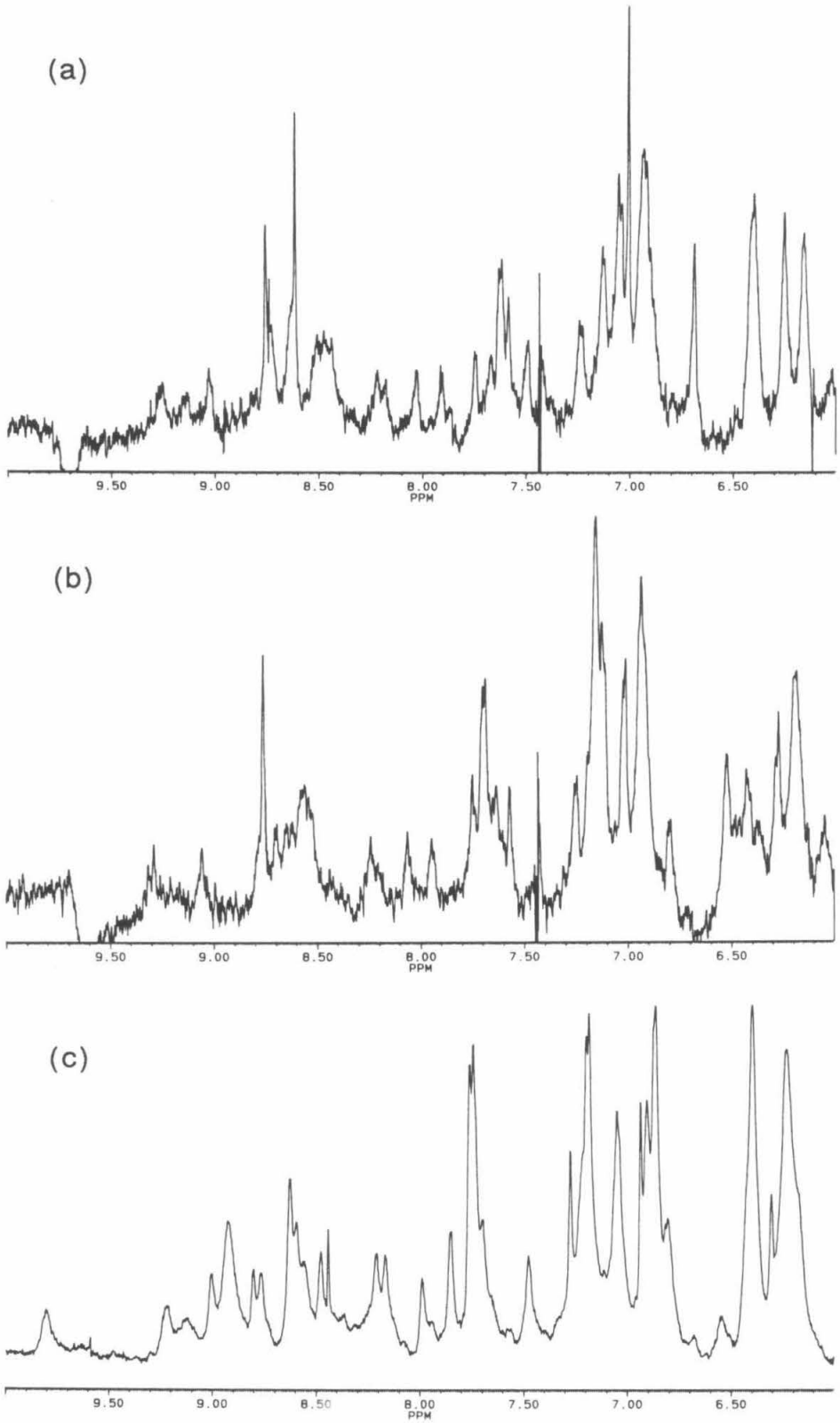
(a)
9.50
9.00
8.50
8.00
PPM
7.50
7.00
6.50
(b)
9.50
9.00
8.50
8.00
PPM
7.50
7.00
6.50
(c)
9.50
9.00
8.50
8.00
PPM
7.50
7.00
6.50

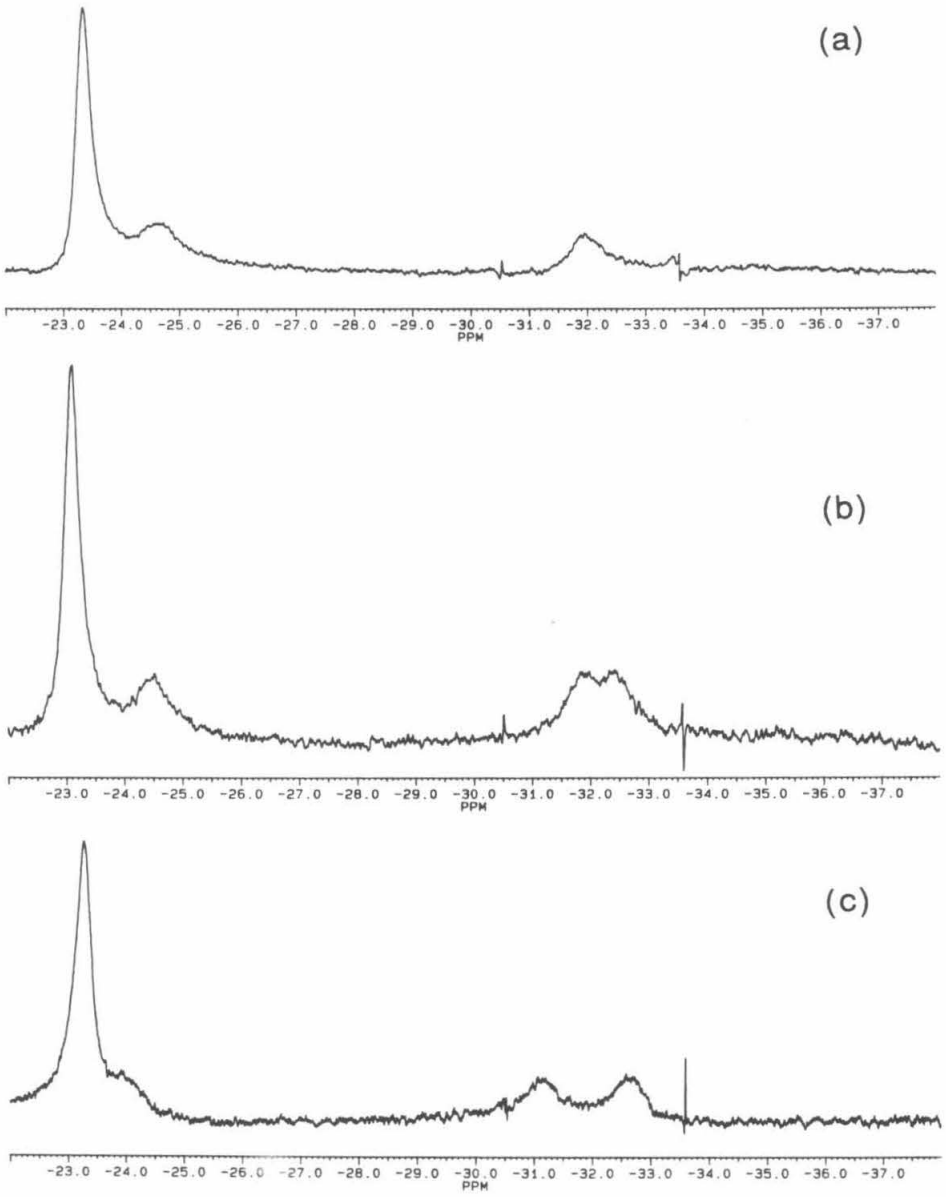

Figure A6.4. NMR ^{1}H spectra for (a) native, (b) A_5Ru(His39)-modified, and (c) A_5Ru-modified (product 2) *C. krusei* ferricytochromes *c*, δ-22 to -38 ppm *vs.* DSS.

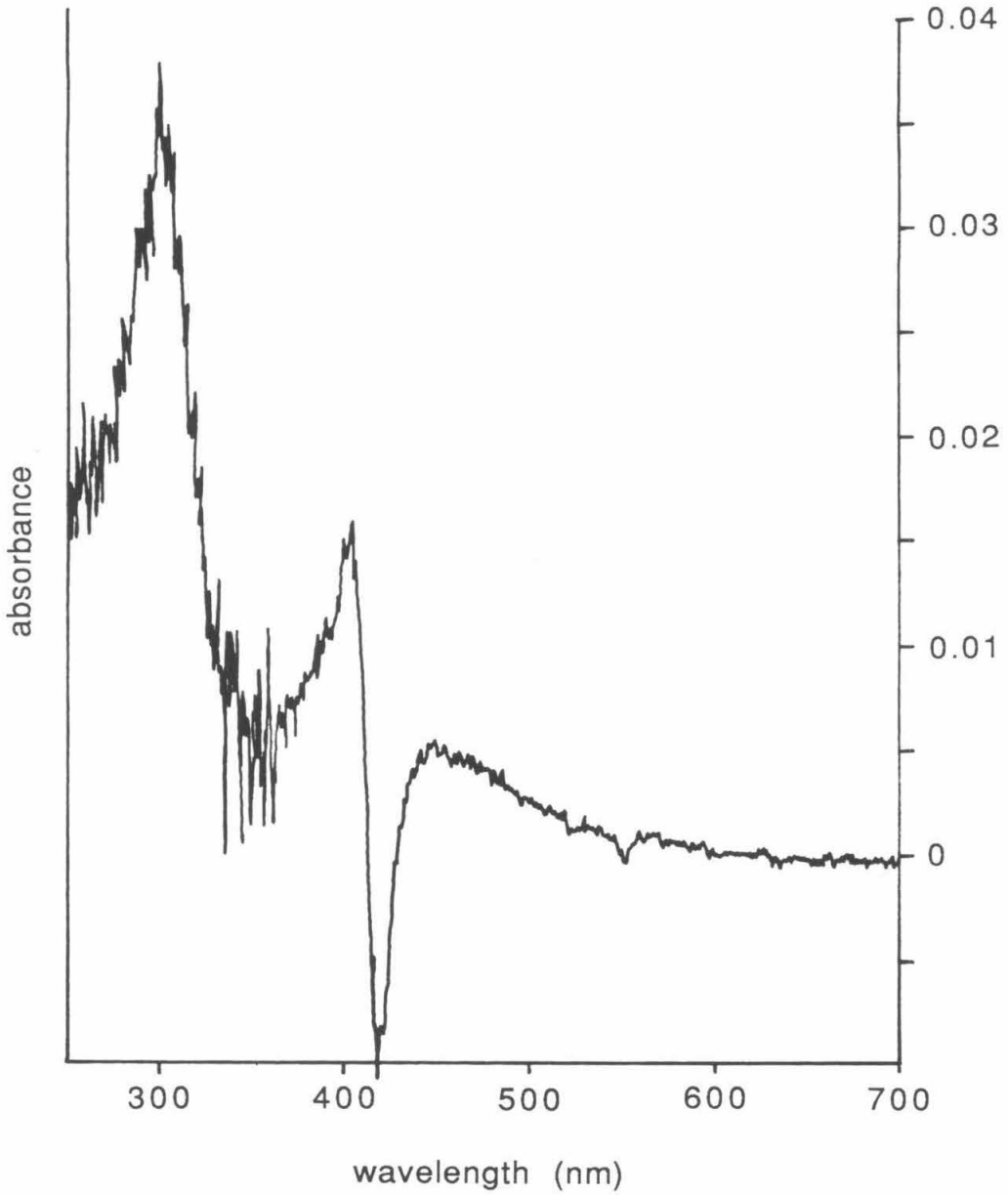

Figure A6.5. UV-visible difference spectrum: 8.74μM A_5Ru-modified *C. krusei* cytochrome *c* (product 2) minus native *C. krusei* cytochrome *c*; absorption of ~0.038 at 300nm indicates two histidine side chains have been modified.

would not necessarily reveal the presence of a mixture of singly-modified derivatives, but such a situation should be evident from peptide mapping. No such evidence was found.

The reaction of the *C. krusei* cytochrome His33 within one half hour (pH 7.5, 30 equivalents of ruthenium, ≥12% modified) can be compared with the reactivity of this same residue in horse cytochrome *c* (pH 7, 50 equivalents of ruthenium, 24 hours, 10-30% modified). As discussed in chapter 3, computer-modeling of these proteins suggests that His33 is less accessible in the horse cytochrome, and in both cytochromes its reaction with a bulky reagent such as aquopentaammineruthenium(II) is expected to be severely hindered.

[2] provided the concentration of one component is minor; an equimolar mixture of singly-modified products might not appear to be modified at all unless quantitative comparisons with native spectra were made.